Maximizing Expression and Detergent Stability of a GPCR by Directed Evolution.

Dissertation

zur

Erlangung der naturwissenschaftlichen Doktorwürde

(Dr. sc. nat.)

vorgelegt der

Mathematisch-naturwissenschaftlichen Fakultät

der Universität Zürich

von

Karola Schlinkmann

aus Deutschland

Promotionskomittee

Prof. Andreas Plückthun (Vorsitz)

Prof. Raimund Dutzler

Prof. Donald Hilvert

Prof. Wolfram Welte

Zürich, 2012

Die vorliegende Arbeit wurde von der Mathematisch-naturwissenschaftlichen Fakultät der Universität Zürich im Herbstsemester 2012 auf Antrag von Prof. Andreas Plückthun und Prof. Raimund Dutzler als Dissertation angenommen.

Inmitten der Schwierigkeiten liegt die Möglichkeit!

– Albert Einstein –

Erklärung

Diese Dissertation wurde selbständig und ohne unerlaubte Hilfe im Sinne von §3 und §5 der Promotionsordnung der MNF vom 08.Juli 2002 angefertigt. Zur Abfassung der Dissertation wurden keine anderen als die darin angegebenen Hilfsmittel benutzt.

Zürich, 02. Oktober 2012

Karola Schlinkmann

Contents

Publications

1: Schlinkmann, K.M. and Plückthun, A. (2012) Directed evolution of G protein-coupled receptors for high functional expression and stability. *Methods Enzymol.* **in press.**

2: Schlinkmann, K.M., Honegger, A., Türeci, E., Robison, K.E., Lipovsek, D., Plückthun, A. (2012). Critical features for biosynthesis, stability, and functionality of a G protein-coupled receptor uncovered by all-versus-all mutations. *Proc. Natl. Acad. Sci. USA* **109**, 9810-9815.

3: Schlinkmann, K.M., Hillenbrand, M., Rittner, A., Künz, M., Strohner, R., Plückthun, A. (2012). Maximizing detergent stability and functional expression of a GPCR by exhaustive recombination and evolution. *J. Mol. Biol.* **422**, 414-428.

4: Schlinkmann, K.M, Honegger, A., Plückthun, A. (2012). Directed evolution of proteins: Analysis of a comprehensive mutagenic randomization study of a GPCR by deep sequencing. *CSHL press, New York.* ***manuscript in preparation****.*

Summary

G protein-coupled receptors (GPCRs) are 7-helical transmembrane receptors holding a pivotal position in many cellular signal transduction processes. GPCRs act as molecular switches to transfer extracellular signals into the cell by conformational rearrangements within the protein, and to eventually evoke a cellular response. Deregulation or dysfunction of GPCRs is the cause of many pathophysiological conditions. Hence, GPCRs are not only essential to cell survival, but also represent a major drug target covering about 40% of all marketed drugs.

However, GPCR research is as challenging as it is interesting. *In vitro* studies, covering mechanistic studies, structure determination and drug screening approaches, are necessary to better characterize GPCR function and regulation, but are severely limited due to the difficulties in obtaining high quantities of detergent-solubilized and stable protein. Hence, GPCR research is far behind its expectations and significance.

The low expression levels and detergent-stability of GPCRs are the major roadblocks that need to be solved in order to expand and simplify GPCR research. By means of a previously developed FACS-based selection system, several GPCRs were efficiently evolved for higher expression and detergent-stability by introduction of only a few amino acid substitutions. Obviously, the limitations are directly related to their poor biophysical properties, i.e. the amino acid sequence.

Despite its success, the random mutagenesis approaches did not suffice to conclude why certain sequences were selected, and how every single amino acid contributes to the restraints in expression and stability. This question was the basis for the work presented here.

The first project of this work describes the saturation mutagenesis of every receptor position of the neurotensin receptor 1, with subsequent selection for high functional expression. The evolved pools of 380 position-specific libraries were analyzed by ultra deep sequencing, revealing which residues are preferred, tolerated and not accepted for every single position of the receptor. Thirty shift mutants, carrying one selected point mutation, were found to increase expression levels of D03. The detailed analysis of these shift mutants revealed that many of them also ameliorate detergent stability of the receptor.

In a subsequent project, the identified mutations with advantageous effect on the biophysical protein properties were shuffled by *in vitro* DNA recombination and by DNA assembly of a synthetic binary library to generate combinatorial libraries. From these libraries, receptor variants with unprecedented expression levels and detergent stability could be evolved, showing a strong coevolution of both properties. The best variants express more than 25,000 functional receptors per *E. coli* cell, are highly stable in short-chain detergents and retain their receptor-typical ligand binding profile and signaling ability.

The final study describes the selection of DARPin binders to the final evolved NTR1 variants for later co-crystallization purposes. The GPCR-surface available for protein-protein interactions is constrained to the solvent-accessible areas that are mainly

composed of helix ends and flexible loops. Despite highest detergent-stability, these limitations are obviously critical.

In summary, this work has provided detailed and exhaustive insight into the contribution of every receptor position to expression and detergent-stability, allowing us to better understand the concepts and limitations of natural versus directed evolution. The results of this study enabled us to evolve combinatorial NTR1-variants with maximal effects, which are of high interest for drug discovery, *in vitro* functional and structural studies.

Zusammenfassung

G Protein-gekoppelte Rezeptoren (GPCRs) sind Zelloberflächenrezeptoren mit einer bedeutenden Funktion in der Signaltransduktion. GPCRs sind gekennzeichnet durch sieben Helices, welche die Lipidmembran senkrecht durchspannen. Sie agieren als molekulare Schalter, indem sie extrazelluläre Information in Form von Ligandenbindung durch eine Konformationsänderung des Proteins in die Zelle übertragen, und so eine zelluläre Reaktion auslösen. Funktionsstörungen von GPCRs und Fehlregulation von GPCR-basierten zellulären Prozessen sind die Ursache vieler Erkrankungen. Aufgrund dieser Relevanz stellen GPCRs ein bedeutendes Zielmolekül für die pharmakologische Intervention dar, mit einem Marktanteil von geschätzten 40% an allen verschriebenen Medikamenten.

Die Erforschung von GPCRs ist daher äusserst interessant, jedoch ebenso schwierig. Viele Forschungsansätze zum besseren Verständnis der GPCRs, vor allem *in vitro*-basierte Studien wie die funktionelle Charakterisierung von GPCRs sowie die Strukturbestimmung als auch innovative *drug screening*-Methoden werden durch die schlechten biophysikalischen Eigenschaften der GPCRs erschwert. Eines der Hauptprobleme ist dabei die Herstellung von hohen Mengen an detergens-gelöstem und aufgereinigtem Rezeptor.

Um die Arbeit an GPCRs zu vereinfachen und intensivieren, ist es notwendig, das allgemein sehr niedrige Expressionsniveau von GPCRs und ihre begrenzte Stabilität in Detergensmicellen zu verstehen und zu optimieren. Die gerichtete Evolution von Proteinen stellt eine elegante Methode dar, um Proteine auf einen gewünschten Phänotyp hin zu evolvieren, und ist mit der Entwicklung eines FACS-basierten Selektionssystems inzwischen auch auf GPCRs anwendbar. Mithilfe dieses Verfahrens konnten bereits einige Rezeptoren erfolgreich evolviert werden. In allen Fällen waren nur wenige Mutationen notwendig, um hohe Expression und robuste Detergensstabilität zu erreichen. Offensichtlich ist der Phänotyp des GPCRs direkt auf die biophysikalischen Eigenschaften und demnach auf die Aminosäuresequenz zurückzuführen.

Der Erfolg der zufälligen Mutagenese und Selektion ist unbestritten, jedoch generiert diese Methode nicht genügend Daten, um zu verstehen, warum bestimmte Sequenzen selektiert werden und wie jede einzelne Position des GPCRs seine Expression und Stabilität beeinflusst.

Die erste Studie dieser Arbeit beschreibt daher die vollständige Mutagenese des Neurotensinrezeptors 1 (rNTR1), in der jede Aminosäure des Rezeptors separat und vollständig randomisiert wurde. Die 380 positionsspezifischen Bibliotheken wurden auf hohe Expression hin selektiert, und die evolvierten *pools* wurden mittels *ultra-deep sequencing* analysiert. Diese Analyse machte deutlich, welche Aminosäuren bevorzugt, toleriert und inakzeptabel für die jeweilige Rezeptorposition sind. So wurden dreissig Shift-Mutanten, die je eine Mutation in der Rezeptorsequenz tragen, identifiziert, die das Expressionsniveau von D03 erhöhen. Die detaillierte Analyse dieser Mutanten zeigte, dass einige dieser Mutationen auch die Detergensstabilität des Rezeptors verbessern.

In der folgenden Studie wurden kombinatorische Bibliotheken der bereits charakterisierten Einzelmutationen hergestellt. Hier wurden einerseits *in vitro* DNA-

Rekombination als auch die synthetische Assemblierung einer binären Bibliothek angewendet. Aus diesen Bibliotheken konnten Rezeptorvarianten mit beispielloser Expression und Detergensstabilität, unter offensichtlicher Korrelation beider Faktoren, evolviert werden. Die besten Varianten zeigten mehr als 25,000 funktionelle Rezeptoren pro Zelle, sind hochstabil auch in kurzkettigen Detergenzien, erhalten aber auch ihre rezeptortypische Ligandenbindung als auch Signalfähigkeit.

Die finale Studie beschreibt die Selektion von DARPin Bindeproteinen an die evolvierten Varianten, um diese für Co-Kristallisationsstudien einzusetzen. Die Oberfläche des GPCRs, welche für Protein-Protein-Wechselwirkungen zur Verfügung steht, ist beschränkt auf den extra- und intrazellulär orientierten Bereich, der hauptsächlich aus *loops* (unstrukturierter Abschnitt zwischen zwei Helices) und den Helixenden besteht. Trotz hoher Detergensstabilität der evolvierten Varianten scheinen diese Einschränkungen limitierend für die Selektion zu sein.

Zusammenfassend lässt sich sagen, dass diese Arbeit einen detaillierten und gründlichen Einblick in die Bedeutung jeder Rezeptorposition für Expression und Stabilität des Rezeptors erreicht hat. Diese Daten ermöglichen ein besseres Verständnis und Vergleich der natürlichen gegenüber der *in vitro*-Evolution. Das Ergebnis dieser Arbeit sind hochexprimierte und stabile Rezeptorvarianten von enormer Relevanz für zukünftige Studien im Bereich des *drug screenings*, sowie für Funktions- und Strukturanalysen.

Aim of the thesis

By means of directed evolution, this study aims to first identify, and subsequently to overcome the constraints within the primary sequence of a GPCR that determine its poor biophysical properties, and to generate receptor variants with high functional expression levels and high detergent-stability that facilitate subsequent *in vitro* studies, such as functional studies, drug screening approaches and crystallization studies. The D03-variant of the rat neurotensin receptor 1 (rNTR1) is used as a model receptor.

Chapter 1 provides the theoretical background to this work. Chapter 2 (article in press) introduces GPCRs as targets for directed evolution, and explains the methods covering library generation and selection that are used throughout the study. The experimental results are divided in two parts: The first part (Chapter 3-A, published article) focuses on the elucidation of the critical residues in the receptor sequence which determine and limit functional expression and detergent stability of GPCRs. One by one, every receptor position is turned into an NNN-library that is subsequently selected for the variants with highest expression levels and analyzed by ultra deep sequencing. Chapter 3-B is a separate manuscript highlighting the theoretical background and statistical corrections applied to analyze the ultra deep sequencing data. The second part (Chapter 4, published article) aims to maximize receptor expression and stability by combining the advantageous shift mutations identified in part one. Shuffled libraries of shift and D03 residues are generated by two different approaches, and selected for high functional expression. The best variants are characterized in detail with respect to expression, detergent stability and signaling activity. The highest evolved receptor variants are used as targets for selection of DARPin binders by ribosome display for cocrystallization purposes (Chapter 5). Chapter 6 draws general conclusions and shows future perspectives for this study.

Chapter 1

General Introduction

1.1 Membrane proteins

Integral membrane proteins (IMPs) are found in all organisms from bacteria to man. Many fundamental physiological processes rely on the proper functioning of IMPs, among which transport mechanisms (ranging from ions to nutrients) and signaling processes are essential for cell survival. In signaling processes, IMPs transfer information across the lipid bilayer and evoke a cellular response to adapt to environmental changes.

Gram-negative bacteria are surrounded by two membranes, differing in their composition and function. The inner membrane is a symmetric lipid bilayer composed of phospholipids, functioning as a major permeability barrier, whereas the outer membrane is asymmetric with phospholipids on the inside and lipopolysaccharides on the outside. Both membranes are populated by integral membrane proteins that optionally contain soluble domain(s) located within the cell or outside, but that differ substantially in their transmembrane architecture: In contrast to soluble proteins, IMPs populate only two protein folds, namely α-helices and β-barrels (Minetti and Remeta, 2006). The α-helical fold comprises proteins with single-spanning transmembrane helices to proteins composed of helix bundles of 2 to up to 12 individual helices. The α-helical fold is highly abundant, and is found from inner membranes of bacteria to plasma membranes of mammalian cells. In contrast to that, β-barrels, composed of 8 to 22 β-sheets building a closed barrel, are exclusively found in the outer membrane of gram-negative bacteria, mitochondria and chloroplasts (Tamm *et al.*, 2004). The α-helical and β-barrel membrane proteins differ in their hydrophobicity, which is larger for α-helical membrane proteins and smaller for β-barrels which, to the inside, form a rather hydrophilic pore for the selective transport of cargo across the outer membrane.

Biosynthesis of IMP requires correct targeting to and folding and insertion into the membrane. Not surprisingly, α-helical and β-barrel membrane proteins are characterized by individual protein targeting, folding and insertion pathways. All IMPs are targeted from the translating ribosome to the translocon pore (SecYEG in bacteria, Sec61 in eukaryotes) located in the inner bacterial membrane (plasma membrane in eukaroytes). The α-helical proteins designated for the inner membrane (or plasma membrane) attain secondary structure during this process, and the α-helices are subsequently and laterally released from the translocon pore into the lipid bilayer (Rapoport, 2007; Shan and Walter, 2005). The fact that backbone hydrogen bonding is satisfied within the entity of a single helix sufficiently compensates for the cost of helix insertion into the hydrophobic lipid bilayer, hence facilitating simultaneous folding and insertion, with tertiary interactions formed between individual helices in a later stage within the membrane. Fully denatured α-helical IMPs do not spontaneously refold *in vitro*, further highlighting the complex nature of the *in vivo* folding and insertion process.

In contrast to that, proteins with a signal sequence for the outer membrane are translocated into the periplasmatic space in an unfolded state, where these polypeptides are bound by specific chaperones that prevent aggregation and assist folding of β-barrels. A unique feature of β-barrels is that they fold form a fully unfolded polypeptide sequence,

both in *vivo* in the bacterial periplasm as well as *in vitro* (Huysmans *et al.*, 2010; Tamm *et al.*, 2001). The intramolecular hydrogen bonding pattern of β-folds and β-barrels in particular is established on the tertiary structure level, requiring at least a partially formed barrel before insertion into the hydrophobic outer membrane can occur (tilted folding-insertion mechanism). This, in turn, also explains the relative high hydrophility of β-barrel proteins in order to facilitate folding in the periplasm. Insertion of the β-barrel into the outer membrane is believed to be a spontaneous process (Tamm *et al.*, 2001).

Positioning and anchoring of α-helical IMP within the lipid bilayer is enhanced by the presence of an "aromatic belt", in which aromatic amino acids anchor the protein in the lipid bilayer (Kelkar and Chattopadhyay, 2006), and basic residues at the intracellular helix ends interact with the phospho-moiety of the lipid head groups (Heijne, 1986). The hydrophobic shell of IMPs is both imperative *in vivo* and disadvantageous *in vitro* (see Section 1.4). The α-helical membrane proteins are compactly folded, and relay signals into the cell rather than cargo, as achieved by pumps.

1.2 G protein-coupled receptors

Eukaryotic signaling processes are primarily mediated by G protein-coupled receptors (GPCRs), the largest group of IMPs that is characterized by seven membrane-spanning helices (TMs) with differences in the (optional) soluble N-terminal domain, located on the extracellular side (Figure 1-1).

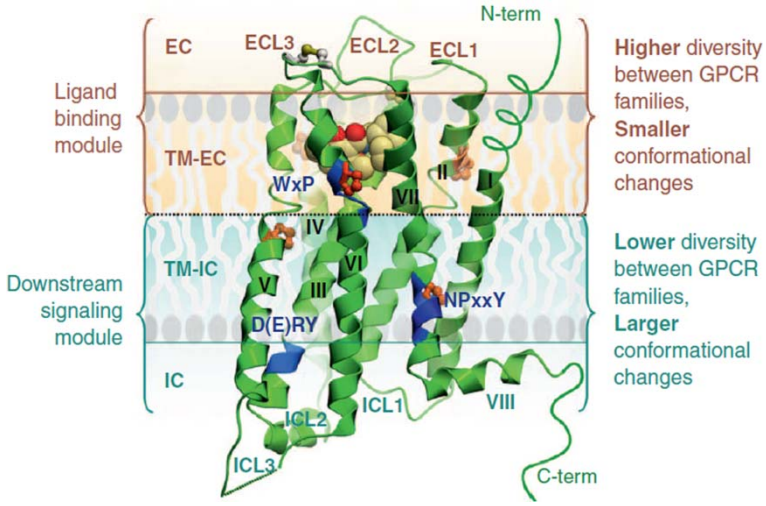

Figure 1-1. GPCR architecture in the lipid bilayer (dopamine receptor D3, PDB ID 3PBL). The 7 transmembrane helices (I-VII) are connected by three extracellular (ECL1-ECL3) and three intracellular loops (ICL1-ICL3). Ligand binding occurs at the extracellular surface (EC), and coupling with G proteins on the intracellular surface (IC). Adapted from Katritch *et al.*, 2012.

The human genome comprises approximately 1000 GPCRs, grouped according to sequence homology, function and nature of the ligand (groups A-F, (Lefkowitz, 2004; Pierce *et al.*, 2002)). Class A comprises the large group of rhodopsin-like receptors,

including the diverse set of olfactory receptors (~400) as well as receptors activated by endogenous ligands. Class A receptors are distinguished from the other classes by their short and flexible N-terminus, and their endogenous ligands which bind in a groove between the C-terminal helices and loops (depending on the nature and size of the ligand). Recently, an alternative classification system has been proposed, following the results of a new and strict phylogenetic analysis (GRAFS-system, "R" stands for the rhodopsin family which is roughly equivalent to class A (Bjarnadottir *et al.*, 2006)). GPCRs share common and unique sequence motifs in every helix (Table 1-1), exhibiting a functional or structural role (Mirzadegan *et al.*, 2003). Consensus motifs are conserved for functional or structural reasons. The Ballesteros-Weinstein nomenclature refers to the most conserved position of a helix as x.50, with x denoting the helix in sequential order, and the second number counting downwards to the N-terminus and upwards to the C-terminus (Ballesteros and Weinstein, 1995). The E/DRY motif in TM3 is a highly conserved motif in GPCRs, and involved in receptor activation (Rovati *et al.*, 2007).

Table 1-1. GPCR consensus motifs.

	Consensus	Position	rNTR1
TM 1	GNxxV	$81^{1.49}$-$85^{1.53}$	GNSVT
TM 2	LxxxD	$109^{2.46}$-$113^{2.50}$	LALSD
TM 3	DRY	$166^{3.49}$-$168^{3.51}$	ERY, D03: ELY
TM 4	W	$194^{4.50}$	W
TM 5	FxxP	$246^{5.47}$-$249^{5.50}$	FLFP
TM 6	CWxP	$320^{6.47}$-$323^{6.50}$	CWLP
TM 7	NPxxY	$365^{7.49}$-$369^{7.53}$	NPILY

GPCRs show enormous diversity with respect to the nature and the size of the ligand molecule, ranging for example from photons (rhodopsin) to odorants (olfactory receptors) and peptide hormones (e.g. angiotensin) to nucleotides (e. g. ATP) and ions (e.g. Ca^{2+}) (e.g. (Kobilka, 2007)). Despite their broad ligand diversity, all GPCRs share a common activation and signaling mechanism upon ligand binding: Binding of an extracellular receptor agonist induces conformational rearrangement of the helices, bringing the receptor into the activated state R*, in which the receptor can bind and activate the downstream heterotrimeric G proteins (Deupi and Kobilka, 2007). While the detailed mechanism of receptor activation is not fully elucidated yet, there is structural evidence that agonist binding induces "collapsing" of the TM helices, resulting in a more constrained agonist binding site. The necessary conformational rearrangements are enabled by movement of the helices, and it is assumed that movement of TM5 and TM6 reveal the G-protein interaction surface on the intracellular side of the membrane (Ye *et al.*, 2010).

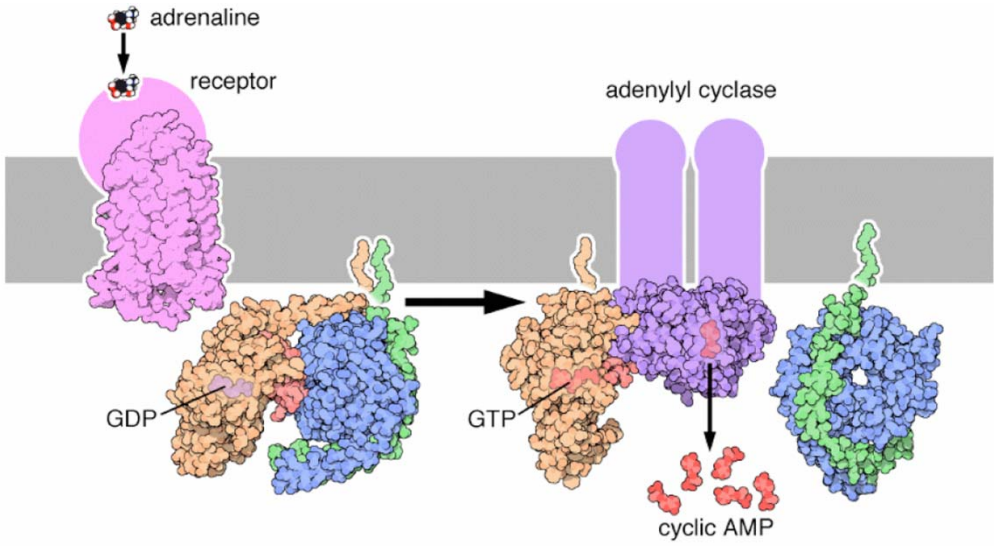

Figure 1-2. Illustration of the GPCR-G-protein interaction. Agonist binding to the GPCR induces GDP for GTP exchange at the Gα subunit, resulting in dissociation of Gα from Gβγ and further downstream signaling. Picture adapted from www.rcsb.org, molecule of the month October, 2004.

Binding of the G protein to the activated GPCR induces exchange of GDP for GTP at the Gα subunit, and signal transduction is continued by the dissociation of the Gα-subunit from the Gβγ-subunits after nucleotide hydrolysis (Figure 1-2). At this step, signal transduction to downstream effectors includes strong signal amplification, thus ensuring fast and efficient signal propagation (Figure 1-3), eventually resulting in a cellular response and adaptation to environmental changes. The downstream signaling pathways are highly diverse and not necessarily dependent on G proteins (Lefkowitz, 2004; Pierce *et al.*, 2002). Phosphorylation of the GPCR by G protein-coupled receptor kinases (GRKs) and subsequent binding of β-arrestins was assumed for a long time to mainly drive receptor desensitization, recycling and degradation (Ferguson, 2001). Recently, it emerged that β-arrestins are multifunctional, with an additional role in signal transduction (Lefkowitz and Shenoy, 2005).

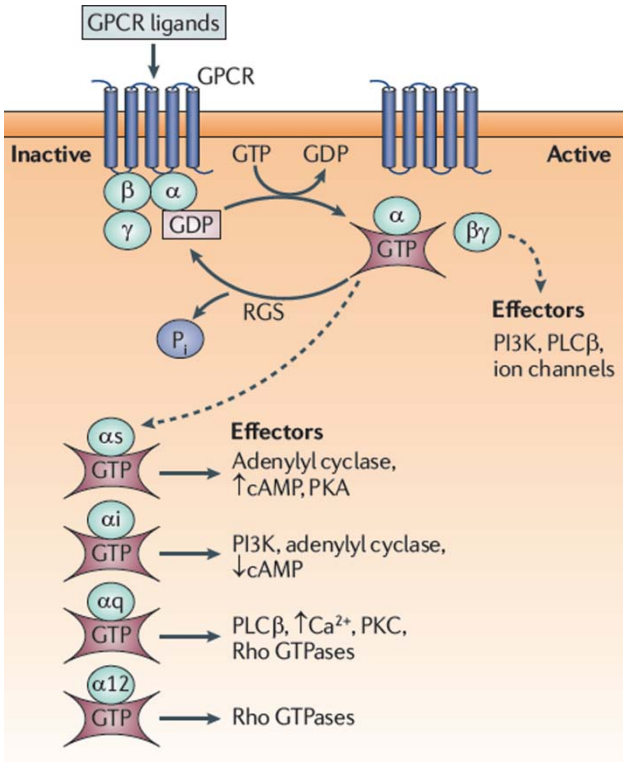

Figure 1-3. Overview of GPCR downstream signaling. The GPCR is activated by its ligand, inducing recruitment of the heterotrimeric G protein and exchange of GDP for GTP at the Gα subunit, followed by nucleotide hydrolysis and dissociation of the Gα from the Gβγ subunits. Both Gα and Gβγ can activate downstream effectors, depending on the G protein isoform. Picture adapted from Lappano and Maggiolini, 2011.

1.3 G protein-coupled receptors as drug targets

GPCRs act as bridges between extracellular information and intracellular reaction, and this key switch position in signal transduction makes them essential for cell survival. GPCR deregulation and dysfunction causes many pathophysiological conditions, including diseases such as cardiovascular conditions (β_1-adrenergic receptor (Drake *et al.*, 2006)) and asthma (β_2-adrenergic receptor (Kawakami *et al.*, 2004)); while some diseases are the consequence of alterations at the genetic level, ranging from retinitis pigmentosa (RP) to female infertility (follicle-stimulating hormone receptor (Insel *et al.*, 2007; Schöneberg *et al.*, 2004)) or cancer (Lappano and Maggiolini, 2011). Furthermore, perception and treatment of pain is conveyed via GPCRs (Stone and Molliver, 2009), a major target of pharmaceutical intervention. As a direct consequence, GPCRs represent highly prevalent drug targets, covering about 40% of all currently marketed drugs (Overington *et al.*, 2006).

GPCR drug discovery has long been based on screening large compound libraries in cellular ligand-displacement studies. Such studies rely on the availability of a high-affinity radiolabelled ligand, and are hence not applicable to “orphan” receptors, for which no ligand has been identified. Additionally, they also produce considerable waste disposal

costs (Eglen and Reisine, 2009) and do not allow agonists, antagonists or partial agonists/antagonists to be distinguished (Eglen *et al.*, 2007). Consequently, the last decade observed a shift in drug discovery towards more cell-based functional assays, allowing the study of orphan receptors as well as directly differentiation between agonistic or antagonistic compounds (Salon *et al.*, 2011). Such assays monitor, for example, the ability of a compound to recruit G proteins, measured as GTPγS binding to Gα, or the increase in second messengers such as Ca^{2+} or inositolphoshate. However, such indirect assays are highly susceptible to assay conditions, cell viability issues and interference with other cellular signaling processes resulting in difficult-to-interprete data (Salon *et al.*, 2011). Hence, none of these methods has achieved the hit rate of ligand-based methods (Eglen *et al.*, 2007; Macarron, 2006).

Recently, fragment-screening approaches (Congreve *et al.*, 2011) and *in vitro* screening approaches became more prevalent in drug discovery. *In vitro* biochemical and biophysical assays circumvent the described limitations of cell-based assays, allowing direct and unequivocal measurement of G protein recruitment to purified receptor and specific targeting of receptor transition states or interaction surfaces, a promising approach in drug development (Alkhalfioui *et al.*, 2009). An interesting method in this respect is the use of surface plasmon resonance (SPR) employing detergent-solubilized and purified GPCRs. These bimolecular assays are advantageous as they are label-free and allow simultaneous acquisition of kinetic binding data (Navratilova *et al.*, 2005).

Similar to *in vitro* studies using conventional small-molecule compound libraries, recent advances in drug development making use of binding proteins such as antibodies (e.g. (Chan and Carter, 2010) and others) or alternative scaffolds such as DARPins (for recent review, see Tamaskovic *et al.*, 2012) as therapeutics can only become applicable to GPCRs if suitably solubilized and purified GPCR targets are available (Hutchings *et al.*, 2010).

In addition to these innovative screening approaches opening new ways for development of GPCR-targeting drugs, a detailed understanding of the molecular mechanisms driving GPCR activation is fundamental to decipher the basis of GPCR-derived pathophysiological conditions. Recently, Kobilka and coworkers have shown that receptor activation and G-protein interaction can be monitored *in vitro* by attaching fluorescence probes to the β_2-adrenergic receptor (Swaminath *et al.*, 2005; Yao *et al.*, 2006), providing insights into conformational receptor rearrangements upon ligand binding. Eventually, these results will help to advance treatments by tailored drug design.

1.4 Caveats in G protein-coupled receptor research

Seen its pivotal role for pharmacology, GPCR research is far behind what is needed, despite enormous efforts. *In vitro*-based studies of GPCR function have great potential for pharmacology and for gaining mechanistic insight into GPCR activation. However, GPCRs have evolved to function efficiently *in vivo* in a lipid bilayer, and their adapted characteristic features are often contrary to what is desirable for *in vitro* studies.

When isolated from the membrane, GPCRs necessarily require the presence of a detergent micelle to substitute for the lipid bilayer and to shield the hydrophobic outer surface. The availability of a suitable detergent for membrane protein extraction and retention of protein activity may constitute the main bottlenecks and challenges in GPCR research. While membrane proteins in general can be remarkably stable in the lipid bilayer (Haltia and Freire, 1995), they are inevitably more prone to protein denaturation over time when solubilized in detergent, since no detergent can fully compensate for the stabilizing effect of the lipid bilayer (Figure 1-4 for illustration). Moreover, conformational flexibility is inherent to GPCR function, allowing both antagonists and agonists to be accommodated, and to respond to this binding with individual receptor conformations representing different and intermediate activity states. In a detergent micelle, the sampling of conformational states is detrimental to protein stability.

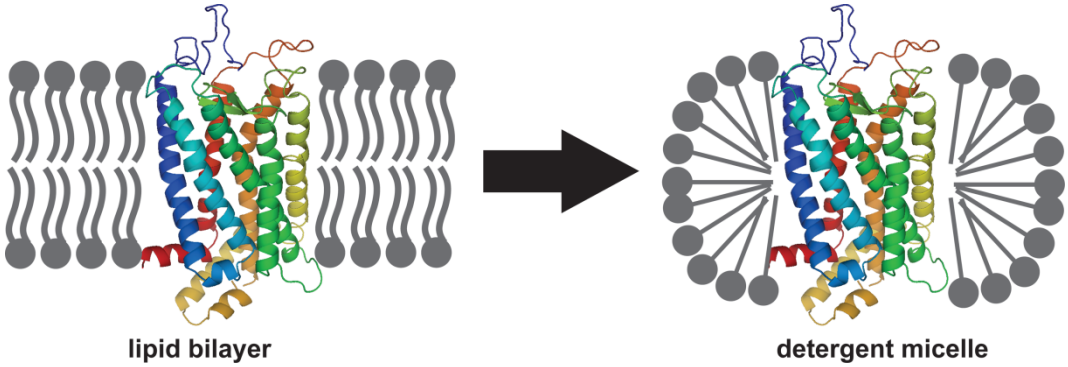

Figure 1-4. Scematic illustration of the lipid bilayer and detergent micelle environment. GPCR, homology model of rNTR1 (homology model by A. Honegger).

In particular, GPCR research is further plagued by low expression levels. The exception is rhodopsin, which can be directly isolated from its natural source due to its high abundance (isolation from bovine eye tissue (Palczewski *et al.*, 2000)). *In vivo*, low expression levels account for low basal signaling activity, compensated by fast and strong signal amplification in the case of receptor activation, and both expression and stability have evolved to facilitate appropriate signal termination by receptor recycling and degradation. Recombinant expression of GPCRs requires laborious and often costly large-scale setups to obtain milligram amounts of purified protein. Many GPCRs are difficult to express in *Escherichia coli*, further impeding the process of obtaining recombinant and purified GPCR protein. More complex expression hosts such as yeast, mammalian cells or *Spodoptera frugiperda* (*Sf9*)-insect cells might prove successful for the expression of a specific target GPCR, but are not only slower and more expensive, but importantly cannot overcome the limitations imposed by the protein sequence itself, e.g. low detergent-stability.

These major roadblocks to produce large amounts of detergent-solubilized, purified and detergent-stable GPCR dramatically restrict drug development, functional studies and structural biology of GPCRs.

1.5 Structural studies on GPCRs

Structural biology of GPCRs suffers from the above described caveats, and is further aggravated by limited options for crystal contact formation, since most of the receptor is shielded by the detergent micelle, and only the extra- and intracellular receptor surfaces composed of flexible loops are solvent-accessible. Detergents with a small micelle size (short-chain detergents) are preferred for crystallization, but are strongly protein-denaturating (le Maire *et al.*, 2000; Ostermeier and Michel, 1997). Addition of cholesteryl hemisuccinate (CHS) has been shown to aid in GPCR crystallization (Lebon *et al.*, 2011), pointing to the modulation of GPCR stability by lipid-like molecules. Recent advances in GPCR crystallization have been facilitated by the development of new methodologies: Replacement of the large and flexible intracellular loop 3 (IL3), connecting transmembrane helices (TM) 5 and 6, by the soluble and rigid protein T4 lysozyme (T4L) has proven successful for crystallization of various GPCRs. In addition to replacing unstructured regions, this approach increases the protein surface available for crystal contact formation (see (Katritch *et al.*, 2012) for review). The inherent conformational flexibility of GPCRs is reduced by ligand binding to the receptor, and indeed, all currently solved GPCR structures except for opsin have been solved as ligand-receptor complexes. Antagonist binding is preferred, since the inactive state R of the receptor is inherently more stable than the activated state R* (Gether *et al.*, 1997). From the first structure of a non-rhodopsin GPCR in 2007, it took another four years for the first agonist-bound receptor structure to be solved (Rasmussen *et al.*, 2011a). Combined with the lipidic-cubic phase-methodology for crystallization of membrane proteins (LCP, for review see Cherezov, 2011), it seems that a main bottleneck of GPCR crystallography has been solved. However, the T4 lysozyme strategy comes with a major drawback: Replacement of IL3 by T4L masks the G-protein interaction surface, thus precluding any conclusions on downstream signaling mechanisms. Recently, the structure of the β_2-adrenergic receptor in complex with $G_{\alpha s}$ provided some information (Rasmussen *et al.*, 2011b), but it represents only one snapshot of the myriad of possible GPCR-G protein interactions (Figure 1-5).

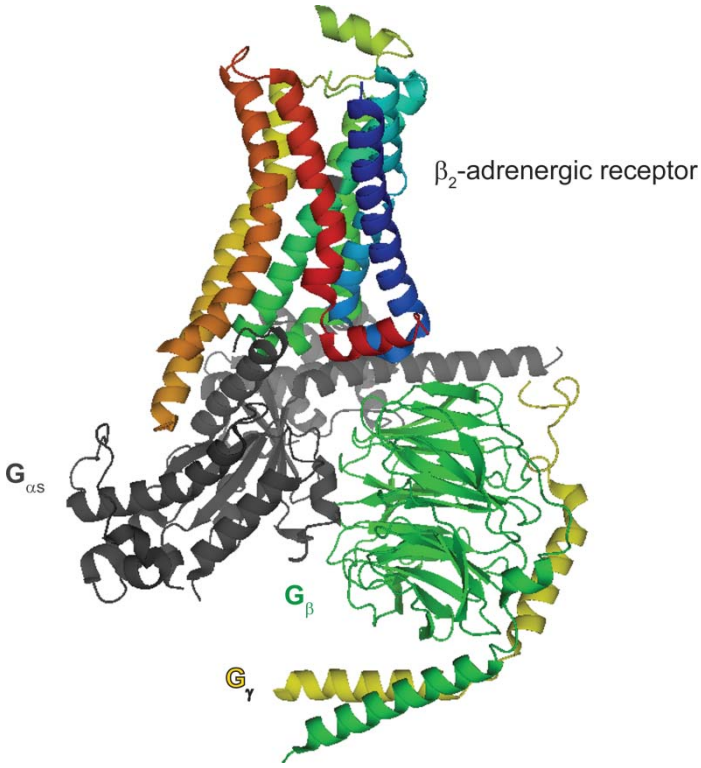

Figure 1-5. Crystal structure of the β_2-adrenergic receptor in complex with $G_{\alpha s}$ (PDB ID 3SN6). The GPCR is depicted in rainbow colours, $G_{\alpha s}$ in grey, G_β in green and G_γ in yellow. The C-terminus of $G_{\alpha s}$ is responsible for interaction with the GPCR, and protrudes into the GPCR helix bundle upon binding. Picture generated with PyMOL (http://www.pymol.org/).

While at the beginning of this thesis work no structure of a GPCR other than rhodopsin had been solved, more than 15 GPCR structures are now solved, and hence commonalities and differences between individual receptors start to emerge. Obviously, the receptor part oriented towards the extracellular space accounts for ligand binding, with a high diversity between individual receptors, but only small conformational changes (see Figure 1-1 for illustration). The more intracellular half of the receptor interacts with downstream effector proteins, and is thus more conserved to maintain functional coupling, but includes larger conformational changes that can be distinguished between signaling-inactive and signaling-active states of the receptor (for review, see Katritch *et al.*, 2012).

Rather unclear from a structural point of view is the prevalence and role of the "ionic lock" between the arginine (position 3.50) of the E/DRY motif in TM3 and the glutamate in TM6 (position 6.30) for the inactive receptor state, which was observed to be in the locked conformation in the first structure of rhodopsin (Palczewski *et al.*, 2000), but could not be confirmed in many of the subsequent structures of GPCRs (e.g. Cherezov *et al.*, 2007), hence questioning a functional role for this motif. Subsequent studies revealed that the ionic lock exists in solution, and is compromised in the crystal as a consequence of the presence of T4 lysozyme and crystal lattice restraints (Dror *et al.*, 2009; Romo *et al.*, 2010). The structure of the dopamine receptor D3 fused with T4L displays the ionic lock (Chien *et al.*, 2010), showing that formation of the ionic lock is not generally precluded in the presence of T4L, but is rather dependent on the receptor conformational

state that is populated in the T4L-fusion protein. Despite its unchallenged relevance, these studies show that current GPCR structural biology, especially the use of protein fusions, nonetheless has its limitations.

1.6 Requirement of new GPCR engineering approaches

Structure determination alone will not suffice to fully understand GPCR function, drug binding and activity. Such data need to be complemented with functional data for the soluble protein. During the last few years, the model of GPCRs exhibiting a simple on/off-mode of action has been expanded tremendously, revealing that GPCRs rather populate several intermediate receptor states during the activation process (Deupi and Standfuss, 2011). While this observation opens new intervention possibilities for drug development (see Section 1.3), it also highlights that any single structure can not tell the entire story. Additionally, despite the broad applicability of the T4 lysozyme strategy, structure determination is still restricted to GPCRs which can be recombinantly expressed, solubilized and purified and which retain their integrity in detergent micelles. Many GPCRs that exhibit poor recombinant expression and detergent stability, among them receptors of utmost pharmacological relevance, fail already during earlier steps of the protein production pipeline.

The necessity for functional characterization and *in vitro* drug screening methods demand innovative approaches to broaden the spectrum of GPCRs that become accessible to *in vitro* studies. Process engineering aims at maximizing protein yield by optimization of external parameters such as expression conditions, expression host, detergent used for solubilization and the purification process itself. However, such parameters have to be individually tested and optimized for each target protein, making it a cumbersome undertaking. Also, process engineering alone cannot overcome the limitations imposed by the primary protein sequence itself, hence restricting its implications.

1.7 Directed evolution of proteins

Natural evolution has shaped protein function over millions of years. According to Darwin, natural selection drives evolution, and "*survival of the fittest*" leads to continuous adaptation of the species to the environment, thus shaping the gene pool. A very important principle in adaptive evolution is the occurrence of neutral mutations, that remain silent with respect to protein function as they occur but have potential effects when combined with other mutations. Furthermore, natural evolution is shaped by the preference for single base exchanges and the conserved nature of the genetic code. As a consequence, only 7 of 19 possible amino acid substitutions are typically assessed and these usually have similar biophysical properties (Miyazaki and Arnold, 1999). The

consequences of this limitation on natural evolution are difficult to assess, but certainly contribute to making natural evolution a slow process.

Directed evolution of proteins is a very elegant and efficient approach to engineer a given target protein for a desired phenotype. Basically, the process of natural evolution is mimicked *in vitro* in a condensed form, allowing a target protein to be evolved for a desired phenotype in a short time, typically weeks to months. Genetic diversity is most commonly introduced by random mutagenesis of the target DNA sequence, providing control over mutagenic load and bias. Very similar to natural evolution, however, random mutagenesis is biased towards substitutions encoded by single base changes. Different from natural evolution, *in vitro* evolution allows the product of evolution to be directed by adjustment of selection pressure, while iterative randomization and selection rounds allow enrichment of protein variants with a new phenotype within a short time. By means of random mutagenesis and selection, protein properties such as enzyme selectivity (Chen and Arnold, 1993) or thermal stability (Liao *et al.*, 1986) have been efficiently evolved.

Natural evolution of membrane proteins, and GPCRs in particular, is a comparably slow process. However, the high conservation of GPCRs over time is not neccessarily a result of low mutagenic tolerance, but represent strong conservation of GPCR function in a finely-tuned network, keeping *in vivo*-expression and stability at an acceptable level.

Indeed, it has been shown by Bowie and coworkers that stabilizing mutations are not rare in membrane proteins (Bowie, 2001), which are rather unused in natural evolution due to contrary or absent selection pressure. Likewise, it can be assumed that mutations can be found that improve expression level and detergent stability, thereby facilitating *in vitro* studies. Until recently, such methods could not be applied to GPCRs, mainly because of the lack of an appropriate selection system. This deficit could recently be overcome with the development of a FACS (fluorescence activated cell sorting)-based screening and selection method that enables application of directed evolution to GPCRs (Sarkar *et al.*, 2008) (Figure 1-6). Briefly, the target GPCR sequence is diversified by random mutagenesis, allowing isolation — under the applied selection pressure — near-target like receptor variants with improved phenotype, specifically increased expression and detergent stability. Most importantly, receptor functionality is retained as a consequence of employing a fluorescence-labeled agonist for selection. This methodology has proven successful to render the tachykinin receptor NK_1 accessible to downstream studies (Dodevski and Plückthun, 2011). In its wild-type state, NK_1 expresses at very low levels, but more critically, cannot be functionally solubilized from the membrane, thus precluding any functional or structural studies. In other words, most GPCR studies so far have concentrated on receptors with reasonable expression and stability that are amenable to the above described methodologies. Obviously, the biophysical properties of receptors such as NK_1 are different and, for that reason, highly interesting for characterization, since especially the comparison of differences in GPCR function and architecture can broaden our understanding of this protein class.

Several receptors could be efficiently evolved for high expression, accompanied by increased detergent stability. The apparent coevolution suggests that there are at least partially overlapping forces driving expression and detergent stability, since detergent stability is never under direct selection pressure. A possible explanation for this

coevolution could be improved protein folding and packing, resulting in more efficient targeting to and protein folding within the membrane, and simultaneously resulting in higher detergent resistance due to more compact protein folding and decreased conformational flexibility.

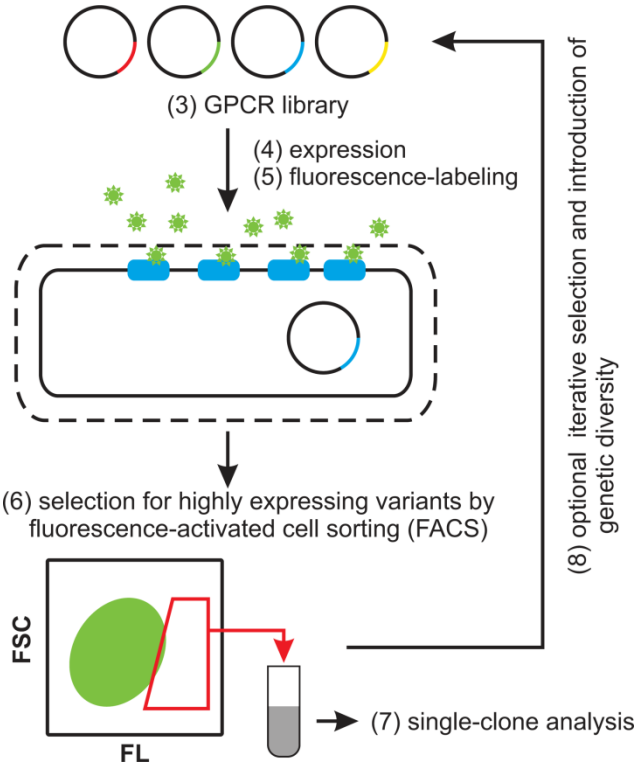

Figure 1-6. FACS-based selection for high functional expression. The randomized GPCR library is expressed in *E. coli* (4), and subsequently incubated with a fluorescence-ligand to label the cells relative to their expression level (5). The highest expressing cells are then selected by fluorescence-activated cell sorting (6). The selected receptor variants are analyzed (7) or alternatively, iterative expression and selection rounds are performed to further enrich the best receptor variants (8).

While it is not entirely clear yet how the observed amelioration of the biophysical protein properties is achieved at the molecular level, FACS-based selection is obviously successful for quick and efficient evolution of receptors for expression and stability, rendering GPCRs amenable to *in vitro* study which had not been previously possible. As suggested by Bowie in 2001, we found that stabilizing mutations were frequent and easy to identify by random mutagenesis, and as few as 4-10 mutations were needed to substantially increase expression and detergent stability (Dodevski and Plückthun, 2011; Sarkar *et al.*, 2008). With an average length of 300-400 amino acids for a GPCR, these mutants retain very high sequence homology, usually greater than 95%, giving these evolved variants high relevance for functional and structural investigations.

Expression and selection in *E. coli* is preferred over other systems for its technical ease and its efficiency to produce high amounts of recombinant protein in a time- and cost-saving manner. At the same time, removal of the target receptor from its native environment might be valuable and even mission-critical. Although the evolved receptor variants also exhibit higher expression in eukaryotic expression systems, selection in the

context of natural signaling networks could constrain the product of directed evolution and could limit expression and stability in order to avoid deregulation of GPCR-related cellular processes. Overexpression of certain GPCRs can itself be the cause of a pathophysiological condition, as observed for the β_2-adrenergic receptor when overexpressed in mouse heart (Liggett *et al.*, 2000). With the absence of any GPCR signaling networks in *E. coli*, selection for high functional expression is only restricted by the limitations imposed by the protein itself.

D03, the product of directed evolution of the neurotensin receptor 1 (rNTR1), revealed that a 10-fold increase in functional expression is achieved by only nine amino acid substitutions (Sarkar *et al.*, 2008). Interestingly, the directed evolution of further GPCRs plateaued at a similar expression level per cell, raising the question whether an upper limit intrinsic to GPCRs or intrinsic to the expression host *E. coli* had been reached, or whether this rather represents a hurdle that has to and can be cleared to proceed to new grounds. Despite its potential, random mutagenesis using error prone PCR is limited in its depth (mutational spectrum) and breadth (sequence coverage). The bias towards amino acid exchanges encoded by single nucleotide exchanges (Wong *et al.*, 2006) constrains especially the fraction of non-similar mutations, for example hydrophobic to charged residues. Furthermore, random mutagenesis stochastically samples the receptor sequence, but is far from exhaustive regarding sequence coverage.

To assess the existence and contribution of internal (GPCR) and external (random mutagenesis) limitations for GPCR expression and stability, a systematic mutagenic analysis is required. Alanine-scanning mutagenesis is commonly used to screen a target protein for phenotype-critical residues (Clackson and Wells, 1995; Wells, 1991). Every position is replaced one-by-one by alanine, and the effect on protein function is assayed. Alanine is characterized by a small and inert side chain with helical propensities, making it a good candidate to identify positions with side chains involved in protein activity. With respect to GPCRs, alanine is a likely tolerated substitution, and might even be favorable for helix folding and packing. Alanine-scanning mutagenesis has been applied to three GPCRs, the β_1-adrenergic receptor (Serrano-Vega *et al.*, 2008), the adenosine A_{2A} receptor (Magnani *et al.*, 2008) and the neurotensin receptor (Shibata *et al.*, 2009). However, this analysis is incomplete, missing all advantageous mutations other than alanine. Full randomization of every position can overcome these constraints, and such approaches recently became feasible with the availability of a suitable selection for GPCRs.

The analysis of such a saturating mutagenesis and the evolved receptor variants can help to shed light on protein activity, to elucidate activation mechanisms and to decipher the constraints of protein stability.

1.8 The rat neurotensin receptor as target GPCR

The neurotensin receptor is a typical class A GPCR, liganded by the 13-amino acid peptide neurotensin (ELYENKPRRPYIL; active fragment RRPYIL). Neurotensin receptors

are predominantly found in the brain, where they regulate neurotransmitting processes such as analgesia, hypothermia and hormone secretion, and to a lesser degree in the gut, regulating colon motility, respectively (Vincent *et al.*, 1999). More interesting from a directed evolution-point of view is that the wild-type rat neurotensin receptor 1 (rNTR1) shows low, but detectable expression in *E. coli* with approximately 500 receptors per cell when expressed as a fusion protein with N-terminal MBP and C-terminal thioredoxin (Grisshammer *et al.*, 1993; Tucker and Grisshammer, 1996). While the periplasmatic MBP efficiently directs the GPCR to the inner membrane, the C-terminal thioredoxin is assumed to function as a “folding chaperone” to increase the fraction of functional receptor (Kern *et al.*, 2003). Its expression profile in *E. coli* makes rNTR1 an optimal candidate for directed evolution. By means of directed evolution using random mutagenesis and FACS-based selection, rNTR1-D03 was evolved from the wild type, displaying a 10-fold increase in expression and higher detergent stability, and the effects are conveyed by nine amino acid substitutions (Sarkar *et al.*, 2008). The expression levels of D03 is the basis for the full saturation mutagenesis performed here, since only the robust expression of D03 allows reliable detection of small changes.

References

Alkhalfioui, F., Magnin, T., Wagner, R. (2009). From purified GPCRs to drug discovery: the promise of protein-based methodologies. *Curr. Opin. Pharm.* **9**, 629-635.

Ballesteros, J.A., Weinstein, H. (1995). Integrated methods for the construction of three dimensional models and computational probing of structure function relations in G protein-coupled receptors. *Meth. Neurosci.* **25**, 63.

Bjarnadottir, T.K., Gloriam, D.E., Hellstrand, S.H., Kristiansson, H., Fredriksson, R., Schiöth, H.B. (2006). Comprehensive repertoire and phylogenetic analysis of the G protein-coupled receptors in human and mouse. *Genomics* **88**, 263-273.

Bowie, J.U. (2001). Stabilizing membrane proteins. *Curr. Opin. Struct. Biol.* **11**, 397-402.

Chan, A.C., Carter, P.J. (2010). Therapeutic antibodies for autoimmunity and inflammation. *Nat. Rev. Immunol.* **10**, 301-316.

Chen, K., Arnold, F.H. (1993). Tuning the activity of an enzyme for unusual environments: sequential random mutagenesis of subtilisin E for catalysis in dimethylformamide. *Proc. Natl. Acad. Sci. USA* **90**, 5618-5622.

Cherezov, V. (2011). Lipidic cubic phase technologies for membrane protein structural studies. *Curr. Opin. Struct. Biol.* **21**, 559-566.

Cherezov, V., Rosenbaum, D.M., Hanson, M.A., Rasmussen, S.G., Thian, F.S., Kobilka, T.S., Choi, H.J., Kuhn, P., Weis, W.I., Kobilka, B.K., Stevens, R.C. (2007). High-resolution crystal structure of an engineered human β_2-adrenergic G protein-coupled receptor. *Science* **318**, 1258-1265.

Chien, E.Y., Liu, W., Zhao, Q., Katritch, V., Han, G.W., Hanson, M.A., Shi, L., Newman, A.H., Javitch, J.A., Cherezov, V., Stevens, R.C. (2010). Structure of the human dopamine D3 receptor in complex with a D2/D3 selective antagonist. *Science* **330**, 1091-1095.

Clackson, T., Wells, J.A. (1995). A hot spot of binding energy in a hormone-receptor interface. *Science* **267**, 383-386.

Congreve, M., Rich, R.L., Myszka, D.G., Figaroa, F., Siegal, G., Marshall, F.H. (2011). Fragment screening of stabilized G-protein-coupled receptors using biophysical methods. *Methods Enzymol.* **493**, 115-136.

Deupi, X., Kobilka, B. (2007). Activation of G protein-coupled receptors. *Adv. Protein Chem.* **74**, 137-166.

Deupi, X., Standfuss, J. (2011). Structural insights into agonist-induced activation of G-protein-coupled receptors. *Curr. Opin. Struct. Biol.* **21**, 541-551.

Dodevski, I., Plückthun, A. (2011). Evolution of three human GPCRs for higher expression and stability. *J. Mol. Biol.* **408**, 599-615.

Drake, M.T., Shenoy, S.K., Lefkowitz, R.J. (2006). Trafficking of G protein-coupled receptors. *Circul. Res.* **99**, 570-582.

Dror, R.O., Arlow, D.H., Borhani, D.W., Jensen, M.O., Piana, S., Shaw, D.E. (2009). Identification of two distinct inactive conformations of the β_2-adrenergic receptor reconciles structural and biochemical observations. *Proc. Natl. Acad. Sci. USA* **106**, 4689-4694.

Eglen, R.M., Bosse, R., Reisine, T. (2007). Emerging concepts of guanine nucleotide-binding protein-coupled receptor (GPCR) function and implications for high throughput screening. *Assay Drug Dev. Technol.* **5**, 425-451.

Eglen, R.M., Reisine, T. (2009). New insights into GPCR function: implications for HTS. *Methods Mol. Biol.* **552**, 1-13.

Ferguson, S.S. (2001). Evolving concepts in G protein-coupled receptor endocytosis: the role in receptor desensitization and signaling. *Pharmacol. Rev.* **53**, 1-24.

Gether, U., Ballesteros, J.A., Seifert, R., Sanders-Bush, E., Weinstein, H., Kobilka, B.K. (1997). Structural instability of a constitutively active G protein-coupled receptor. Agonist-independent activation due to conformational flexibility. *J. Biol. Chem.* **272**, 2587-2590.

Grisshammer, R., Duckworth, R., Henderson, R. (1993). Expression of a rat neurotensin receptor in *Escherichia coli*. *Biochem. J.* **295** 571-576.

Haltia, T., Freire, E. (1995). Forces and factors that contribute to the structural stability of membrane proteins. *Biochim. Biophys. Acta* **1241**, 295-322.

Heijne, G. (1986). The distribution of positively charged residues in bacterial inner membrane proteins correlates with the trans-membrane topology. *EMBO J.* **5**, 3021-3027.

Hutchings, C.J., Koglin, M., Marshall, F.H. (2010). Therapeutic antibodies directed at G protein-coupled receptors. *mAbs* **2**, 594-606.

Huysmans, G.H., Baldwin, S.A., Brockwell, D.J., Radford, S.E. (2010). The transition state for folding of an outer membrane protein. *Proc. Natl. Acad. Sci. USA* **107**, 4099-4104.

Insel, P.A., Tang, C.M., Hahntow, I., Michel, M.C. (2007). Impact of GPCRs in clinical medicine: monogenic diseases, genetic variants and drug targets. *Biochim. Biophys. Acta* **1768**, 994-1005.

Katritch, V., Cherezov, V., Stevens, R.C. (2012). Diversity and modularity of G protein-coupled receptor structures. *Trends Pharmacol. Sci.* **33**, 17-27.

Kawakami, N., Miyoshi, K., Horio, S., Fukui, H. (2004). β_2-adrenergic receptor-mediated histamine H_1 receptor down-regulation: another possible advantage of β_2 agonists in asthmatic therapy. *Journal of Pharmacological Sciences* **94**, 449-458.

Kelkar, D.A., Chattopadhyay, A. (2006). Membrane interfacial localization of aromatic amino acids and membrane protein function. *J. Biosci.* **31**, 297-302.

Kern, R., Malki, A., Holmgren, A., Richarme, G. (2003). Chaperone properties of *Escherichia coli* thioredoxin and thioredoxin reductase. *Biochem. J.* **371**, 965-972.

Kobilka, B.K. (2007). G protein coupled receptor structure and activation. *Biochim. Biophys. Acta* **1768**, 794-807.

Lappano, R., Maggiolini, M. (2011). G protein-coupled receptors: novel targets for drug discovery in cancer. *Nat. Rev. Drug Discov.* **10**, 47-60.

le Maire, M., Champeil, P., Moller, J.V. (2000). Interaction of membrane proteins and lipids with solubilizing detergents. *Biochim. Biophys. Acta* **1508**, 86-111.

Lebon, G., Warne, T., Edwards, P.C., Bennett, K., Langmead, C.J., Leslie, A.G., Tate, C.G. (2011). Agonist-bound adenosine A_{2A} receptor structures reveal common features of GPCR activation. *Nature* **474**, 521-525.

Lefkowitz, R.J. (2004). Historical review: a brief history and personal retrospective of seven-transmembrane receptors. *Trends Pharmacol. Sci.* **25**, 413-422.

Lefkowitz, R.J., Shenoy, S.K. (2005). Transduction of receptor signals by β-arrestins. *Science* **308**, 512-517.

Liao, H., McKenzie, T., Hageman, R. (1986). Isolation of a thermostable enzyme variant by cloning and selection in a thermophile. *Proc. Natl. Acad. Sci. USA* **83**, 576-580.

Liggett, S.B., Tepe, N.M., Lorenz, J.N., Canning, A.M., Jantz, T.D., Mitarai, S., Yatani, A., Dorn, G.W., 2nd (2000). Early and delayed consequences of β_2-adrenergic receptor overexpression in mouse hearts: critical role for expression level. *Circulation* **101**, 1707-1714.

Macarron, R. (2006). Critical review of the role of HTS in drug discovery. *Drug Discov. Today* **11**, 277-279.

Magnani, F., Shibata, Y., Serrano-Vega, M.J., Tate, C.G. (2008). Co-evolving stability and conformational homogeneity of the human adenosine A_{2A} receptor. *Proc. Natl. Acad. Sci. USA* **105**, 10744-10749.

Minetti, C.A., Remeta, D.P. (2006). Energetics of membrane protein folding and stability. *Arch. Biochem. Biophys.* **453**, 32-53.

Mirzadegan, T., Benko, G., Filipek, S., Palczewski, K. (2003). Sequence analyses of G-protein-coupled receptors: similarities to rhodopsin. *Biochemistry* **42**, 2759-2767.

Miyazaki, K., Arnold, F.H. (1999). Exploring nonnatural evolutionary pathways by saturation mutagenesis: rapid improvement of protein function. *J. Mol. Evol.* **49**, 716-720.

Navratilova, I., Sodroski, J., Myszka, D.G. (2005). Solubilization, stabilization, and purification of chemokine receptors using biosensor technology. *Anal. Biochem.* **339**, 271-281.

Ostermeier, C., Michel, H. (1997). Crystallization of membrane proteins. *Curr. Opin. Struct. Biol.* **7**, 697-701.

Overington, J.P., Al-Lazikani, B., Hopkins, A.L. (2006). How many drug targets are there? *Nat. Rev. Drug Discov.* **5**, 993-996.

Palczewski, K., Kumasaka, T., Hori, T., Behnke, C.A., Motoshima, H., Fox, B.A., Le Trong, I., Teller, D.C., Okada, T., Stenkamp, R.E., Yamamoto, M., Miyano, M. (2000). Crystal structure of rhodopsin: A G protein-coupled receptor. *Science* **289**, 739-745.

Pierce, K.L., Premont, R.T., Lefkowitz, R.J. (2002). Seven-transmembrane receptors. *Nat. Rev. Mol. Cell Biol.* **3**, 639-650.

Rapoport, T.A. (2007). Protein translocation across the eukaryotic endoplasmic reticulum and bacterial plasma membranes. *Nature* **450**, 663-669.

Rasmussen, S.G., Choi, H.J., Fung, J.J., Pardon, E., Casarosa, P., Chae, P.S., Devree, B.T., Rosenbaum, D.M., Thian, F.S., Kobilka, T.S., Schnapp, A., Konetzki, I., Sunahara, R.K., Gellman, S.H., Pautsch, A., Steyaert, J., Weis, W.I., Kobilka, B.K. (2011a). Structure of a nanobody-stabilized active state of the β_2 adrenoceptor. *Nature* **469**, 175-180.

Rasmussen, S.G., DeVree, B.T., Zou, Y., Kruse, A.C., Chung, K.Y., Kobilka, T.S., Thian, F.S., Chae, P.S., Pardon, E., Calinski, D., Mathiesen, J.M., Shah, S.T., Lyons, J.A., Caffrey, M., Gellman, S.H., Steyaert, J., Skiniotis, G., Weis, W.I., Sunahara, R.K., Kobilka, B.K. (2011b). Crystal structure of the β_2 adrenergic receptor-G_s protein complex. *Nature* **477**, 549-555.

Romo, T.D., Grossfield, A., Pitman, M.C. (2010). Concerted interconversion between ionic lock substates of the β_2 adrenergic receptor revealed by microsecond timescale molecular dynamics. *Biophys. J.* **98**, 76-84.

Rovati, G.E., Capra, V., Neubig, R.R. (2007). The highly conserved DRY motif of class A G protein-coupled receptors: beyond the ground state. *Mol. Pharmacol.* **71**, 959-964.

Salon, J.A., Lodowski, D.T., Palczewski, K. (2011). The significance of G protein-coupled receptor crystallography for drug discovery. *Pharmacol. Rev.* **63**, 901-937.

Sarkar, C.A., Dodevski, I., Kenig, M., Dudli, S., Mohr, A., Hermans, E., Plückthun, A. (2008). Directed evolution of a G protein-coupled receptor for expression, stability, and binding selectivity. *Proc. Natl. Acad. Sci. USA* **105**, 14808-14813.

Schöneberg, T., Schulz, A., Biebermann, H., Hermsdorf, T., Rompler, H., Sangkuhl, K. (2004). Mutant G-protein-coupled receptors as a cause of human diseases. *Pharmacol. Ther.* **104**, 173-206.

Serrano-Vega, M.J., Magnani, F., Shibata, Y., Tate, C.G. (2008). Conformational thermostabilization of the β_1-adrenergic receptor in a detergent-resistant form. *Proc. Natl. Acad. Sci. USA* **105**, 877-882.

Shan, S.O., Walter, P. (2005). Co-translational protein targeting by the signal recognition particle. *FEBS Lett.* **579**, 921-926.

Shibata, Y., White, J.F., Serrano-Vega, M.J., Magnani, F., Aloia, A.L., Grisshammer, R., Tate, C.G. (2009). Thermostabilization of the neurotensin receptor NTS1. *J. Mol. Biol.* **390**, 262-277.

Stone, L.S., Molliver, D.C. (2009). In search of analgesia: emerging roles of GPCRs in pain. *Mol. Interventions* **9**, 234-251.

Swaminath, G., Deupi, X., Lee, T.W., Zhu, W., Thian, F.S., Kobilka, T.S., Kobilka, B. (2005). Probing the β_2 adrenoceptor binding site with catechol reveals differences in binding and activation by agonists and partial agonists. *J. Biol. Chem.* **280**, 22165-22171.

Tamaskovic, R., Simon, M., Stefan, N., Schwill, M., Plückthun, A. (2012). Designed ankyrin repeat proteins (DARPins) from research to therapy. *Methods Enzymol.* **503**, 101-134.

Tamm, L.K., Arora, A., Kleinschmidt, J.H. (2001). Structure and assembly of beta-barrel membrane proteins. *The Journal of biological chemistry* **276**, 32399-32402.

Tamm, L.K., Hong, H., Liang, B. (2004). Folding and assembly of β-barrel membrane proteins. *Biochim. Biophys. Acta* **1666**, 250-263.

Tucker, J., Grisshammer, R. (1996). Purification of a rat neurotensin receptor expressed in *Escherichia coli*. *Biochem. J.* **317** 891-899.

Vincent, J.P., Mazella, J., Kitabgi, P. (1999). Neurotensin and neurotensin receptors. *Trends Pharmacol. Sci.* **20**, 302-309.

Wells, J.A. (1991). Systematic mutational analyses of protein-protein interfaces. *Methods Enzymol.* **202**, 390-411.

Wong, T.S., Zhurina, D., Schwaneberg, U. (2006). The diversity challenge in directed protein evolution. *Combinatorial Chem. High Throughput Screening* **9**, 271-288.

Yao, X., Parnot, C., Deupi, X., Ratnala, V.R., Swaminath, G., Farrens, D., Kobilka, B. (2006). Coupling ligand structure to specific conformational switches in the β_2-adrenoceptor. *Nat. Chem. Biol.* **2**, 417-422.

Ye, S., Zaitseva, E., Caltabiano, G., Schertler, G.F., Sakmar, T.P., Deupi, X., Vogel, R. (2010). Tracking G-protein-coupled receptor activation using genetically encoded infrared probes. *Nature* **464**, 1386-1389.

Chapter 2

Directed evolution of G protein-coupled receptors for high functional expression and stability

2.1 Article in press

2.1 Article in press

Directed evolution of G protein-coupled receptors for high functional expression and detergent stability.

Karola M. Schlinkmann[§] and Andreas Plückthun[§*]
[§]Department of Biochemistry, University of Zurich, Winterthurerstrasse 190, 8057 Zürich, Switzerland

*corresponding author: Andreas Plückthun, plueckthun@bioc.uzh.ch, telephone 0041 (0) 44 6355570, fax 0041 (0) 44 6355712

Running title: Directed evolution of G protein-coupled receptors

Abstract

G protein-coupled receptors (GPCRs) are cell-surface receptors exhibiting a key role in cellular signal transduction processes, thus making them pharmacologically highly relevant target proteins. However, the molecular mechanisms driving receptor activation by ligand binding and signal transduction are poorly understood, since as integral membrane proteins, most GPCRs are very challenging for functional and structural studies. The biophysical properties of natural GPCRs, usually required by the cell in only low amounts, support their functionality in the lipid bilayer, but are insufficient for high-level recombinant overexpression and stability in detergent-solution. Current structural information about GPCRs is thus limited to a subset of GPCRs with either intrinsically favorable or properly improved biophysical behavior. Recently, directed protein evolution techniques for functional expression and detergent stability have been developed to increase the accessibility of GPCRs for functional and structural studies. Directed evolution does not rely on any preconceived notion of what might be limiting biophysical properties. By random mutagenesis combined with a high-throughput screening and selection system, directed protein evolution has the power to efficiently isolate rare phenotypes and thus contribute to the elucidation of the stability-determining factors, in addition to solving the practical problem of creating stable GPCRs. In the current chapter, protocols for generation of genetic diversity within GPCRs and selection are provided and discussed.

1. Introduction

1.1 G protein coupled receptors

Natural evolution has designed G protein-coupled receptors (GPCRs) for functionality in a cellular context: As integral membrane proteins they are adapted to the lipid bilayer, and most of them are needed only in very small amounts by the cell. Their mode of action requires a considerable conformational change, transmitting the information of a ligand binding on the extracellular side to the inside of the cell, where a heterotrimeric G protein binds to the activated receptor (Rosenbaum *et al.*, 2009). After activation, the GPCR is often phosphorylated, internalized and degraded to avoid continuous signaling (Ferguson, 2001). The biophysical protein properties of GPCRs are thus evolved to fulfill their key role in signal transduction processes, allowing for efficient and sensitive activation of signaling pathways upon changes in the extracellular environment. Nature has evolved GPCRs to fulfill these requirements *in vivo*, which are almost antithetic to what is desired for *in vitro* characterization purposes.

About 1% of open reading frames in vertebrates code for GPCRs (Bjarnadottir *et al.*, 2006) and the number of class A GPCRs is estimated to cover about 800 different receptors in humans, of which 50% are olfactory receptors (Bjarnadottir *et al.*, 2006; Foord *et al.*, 2005). The remaining 400 GPCRs play key roles in many signal transduction processes making non-olfactory GPCRs important pharmaceutical targets, and it is estimated that about 30% of all currently marketed drugs target GPCRs (Lagerström and Schiöth, 2008; Overington *et al.*, 2006). Almost certainly, among the 400 GPCRs of potential interest, there are many valid targets that have not even been explored.

Although GPCRs are physiologically expressed at low levels, high ligand affinities and strong amplification of downstream signals guarantee specific and efficient signal transduction. Moreover, the low expression levels further account for minimal background signaling activity. Similar to expression levels, the biophysical protein properties have evolved for functionality, and the limited stability of GPCRs might even be a desired feature in the cellular context to facilitate fast turnover and degradation.

I*n vitro*, however, the protein properties of GPCRs desired and evolved *in vivo* turn out to be a biochemist's nightmare. Many GPCRs cannot be expressed in *E. coli*, representing the easiest, fastest and cheapest system to produce high quantities of recombinant protein. Some of them are poorly expressed even in mammalian cells.

Receptor solubilization from membranes to obtain functional and stable receptor in detergent solution is a further crucial challenge along the purification process. Moreover, the intrinsic conformational flexibility of GPCRs, enabling activation of the receptor by conformational changes upon ligand binding, hinders structure determination.

Consequently, our understanding of GPCR architecture and mechanism has remained limited, and the design features of agonists and antagonists for the diverse set of receptors have remained mostly enigmatic. The evident discrepancy between the high pharmacological relevance and the poor status of GPCR characterization accounts for the enormous scientific effort in GPCR research. The effort of decades started to pay off only recently with the crystal structure determination of a handful of GPCR receptors.

1.2 GPCR structures

The first crystal structure of a GPCR, bovine rhodopsin, was solved in the year 2000 (Palczewski *et al.*, 2000), and remained unchallenged for several years until 2007. The pioneer position of rhodopsin in GPCR structural research is a result of its extraordinary and unique features, namely its high natural abundance and high conformational stability and homogeneity as a result of its covalently bound ligand 11 cis-retinal, acting as a potent antagonist. However, its uniqueness limits implications for other GPCRs.

Recent GPCR structures, including the inactive states of the human adenosine receptor A_{2A} (Jaakola *et al.*, 2008), human β2-adrenergic receptor (Cherezov *et al.*, 2007; Rosenbaum *et al.*, 2007), turkey β1-adrenergic receptor (Warne *et al.*, 2008), CXCR4 and the human dopamine D3 receptor (Chien *et al.*, 2010), pointed out differences between rhodopsin and the remaining class A GPCRs, which, different from rhodopsin, are liganded by diffusible molecules (reviewed for example in (Katritch *et al.*, 2012)). The recent determination of the β2-adrenergic receptor structure in complex with a heterotrimeric G-protein (Katritch *et al.*, 2012; Rasmussen *et al.*, 2011b) depicts a landmark in the understanding of the signaling process itself.

Except for rhodopsin, most GPCR structure determination required changes within the protein sequence, including loop deletions, engineered domain insertions and/or trial-and-error optimization of the protein sequence.

Domain insertions (for example T4-lysozyme (Rosenbaum *et al.*, 2007)) or deletions of flexible loops (for example (Cherezov *et al.*, 2007)) and the use of binding proteins such as a specific camelid VHH antibody domain (Rasmussen *et al.*, 2011a) or a conventional antibody F_{ab} fragment (Rasmussen *et al.*, 2007) were used to successfully facilitate crystal contact formation for the above described receptors. The binding proteins, however, cannot overcome intrinsic limitations in biophysical properties, and the domain insertions and loop deletions mask functional information about receptor activation mechanisms in the resulting structures. Trial an error stabilization in detergents using alanine scanning has been used as well (Serrano-Vega *et al.*, 2008; Warne *et al.*, 2008).

Despite these efforts, the limited number of receptor structures and the redundancy of the datasets do not reflect the functional diversity of GPCRs, and thus general conclusions about their activation mechanism remain limited as well. Most importantly, fundamental rules for agonist and antagonist design have not yet emerged. So far, structure determination is limited to a subset of GPCRs that can be well-expressed and purified and requires already detergent-stable GPCRs. Most GPCRs are not amenable to functional and structural studies, as the bottleneck lies in earlier steps, namely expression and purification, which involves detergent stability as well.

To increase the spectrum of GPCRs accessible for functional and structural analysis and to gain detailed understanding of the GPCR activation and inactivation mechanisms, two main parameters have to be optimized, the recombinant functional expression of a target GPCR and its biophysical protein properties. Improved biophysical

properties, mainly stability in detergents, increase the chances of crystal formation, particularly when conformational homogeneity is achieved.

1.3 Engineering of GPCRs

Process engineering

Two different and orthogonal engineering strategies can be distinguished: First and conventionally, alterations are made to the "external" conditions of GPCR expression and purification. Here, we focus on heterologous expression of GPCRs in *E. coli*. This can be subsumed under process engineering, as opposed to protein engineering.

Empiric optimization of expression host, temperature and medium of expression and plasmid copy number can substantially influence functional expression levels (for example (Tucker and Grisshammer, 1996)). For example, GPCRs are typically expressed from low copy plasmids to reduce toxicity of GPCR expression in *E. coli*. We showed in several of our studies that low copy numbers are essential for non-optimized receptors (Sarkar *et al.*, 2008), while GPCRs with improved biophysical properties can be expressed from higher copy number plasmids without toxic effects (Sarkar *et al.*, 2008; Schlinkmann *et al.*, 2012a).

GPCR overexpression in yeast cells, mammalian cells or the baculovirus expression system using *Spodoptera frugiperda (Sf9)* cells is an alternative. We observed, in the analysis of numerous mutants, a strong correlation between the relative expression levels in all these hosts (Sarkar *et al.*, 2008; Schlinkmann *et al.*, 2012a). Thus, changes in the protein sequence that have been found to improve expression in *E. coli* have also been found to improve expression levels in eukaryotic hosts, including mammalian cells where the receptors came from.

As a production host, these alternative systems are more time-consuming, laborious and expensive, but need to be used of course when the posttranslational modifications are studied. Yet, for most GPCRs, posttranslational modifications, mainly glycosylation, are not imperative, and the respective site can be mutated or the flexible N-terminus can be deleted for expression in *E. coli*, even though a small subset of GPCRs might potentially remain non-expressible.

Optimization of GPCR overexpression in eukaryotic hosts is further hampered by the fact that high GPCR levels can lead to increased basal signaling activity, which often interferes with cellular signaling pathways, also leading to high toxicity after overexpression.

Similar to the expression conditions, detergent solubilization from membranes has to be optimized for a given target protein. Many detergents are available, differing in solubilization efficiency and capability to retain the membrane protein in a functional state (see for example (Duquesne and Sturgis, 2010; le Maire *et al.*, 2000; Seddon *et al.*, 2004)).

While probably every GPCR will require some kind of process optimization, it currently appears that most members of the family cannot be studied with process optimization alone. Furthermore, most processes are not transferable, as the above

laborious empiric optimization process has to be specifically optimized for each given target receptor. Moreover, in many cases, no feasible conditions at all will be found. Thus, with this conventional approach alone, most GPCRs would remain inaccessible, since the biophysical protein properties itself are limiting.

Protein engineering

The second strategy thus focuses on identifying a related protein sequence with improved biophysical properties. A commonly used strategy is to screen the "homology space" for target homologs with similar function, but better protein behavior with respect to expression and biophysical properties. It is commonly found that homologous proteins of bacterial origin, notably from thermophilic bacteria, have more favorable properties than proteins from eukaryotes, and this has been observed for membrane proteins as well (Granseth *et al.*, 2007).

Unfortunately, the above strategy cannot be applied to GPCRs, as it appears that prokaryotes do not contain such proteins. Despite the fact that this strategy is popular in current structural biology, the homologs used often share only very low sequence identity, thus potentially limiting the relevance of homolog characterization.

In this situation, protein engineering techniques provide a valuable alternative to the classical (but limited) homology search to identify near-target like GPCR variants with a desired phenotype, which are first of all functional, stable and show high expression. Many protein engineering strategies are routinely applied to soluble proteins, but cannot easily be transferred to integral membrane proteins. Rational design of a protein sequence relies on sufficient structural and functional information about the target protein in order to design a favorable phenotype — the very reason of writing this chapter is that this information is not available yet. For GPCRs, rational design is thus not an alternative, at least not yet, since the limited structural information and the difficulties of protein expression and purification constitute major roadblocks in the application of this strategy. Furthermore, using classical trial and error approaches, many variants would have to be individually designed and tested for a given target protein.

Directed evolution and selection for the desired phenotype provides a more attractive methodology, and the availability of a screening and selection technique would render sampling of highly diverse libraries possible in order to identify a rare mutant with the envisaged phenotype. A main focus in GPCR research is to improve receptor expression levels and stability, in order to increase the diversity of receptors that are accessible to functional and structural studies. It has been shown by Bowie and coworkers (Bowie, 2001) that stabilizing mutations are not rare in membrane proteins, emphasizing the great potential of membrane proteins as a target for directed protein evolution.

In our laboratory, we had previously developed an *E. coli*-based selection system to evolve and engineer GPCRs for high functional expression and stability in detergent (Dodevski and Plückthun, 2011; Sarkar *et al.*, 2008; Schlinkmann *et al.*, 2012a; Schlinkmann *et al.*, 2012b). The lack of GPCR-homologs in *E. coli* turns out as an advantage here, as these receptors cannot interfere with any cellular signaling pathway,

as opposed to when using eukaryotic expression systems. By multiple and iterative rounds of gene randomization followed by selection for high functional expression using a FACS-based approach, functional and highly expressed receptor variants can be efficiently identified within less than a month time.

The main prerequisite for this approach is the availability of a functional ligand: The FACS-selection is based on positive selection using a fluorescence-labeled ligand, thereby ensuring functionality of the receptor. No further functional or structural information other than the primary protein sequence is needed, since unfavorable variants are efficiently selected against. Furthermore, library sizes of $>10^7$ can be easily transformed in *E. coli* and efficiently be screened by the FACS-based selection system (screening of approximately 10^7 single cells per hour in yield mode). High-efficiency transformation of yeast cells or mammalian cells is not as straightforward and thus less suitable for highly diverse libraries.

The robustness of our method allows application of stringent selection conditions on receptor libraries with high diversity, as only the coverage of a large mutational space increases the chances to identify rare receptor variants with the desired phenotype. We have successfully applied this methodology to substantially improve the expression levels of several GPCRs from hardly detectable (<500 receptors per cell) to well expressed (6,000 - 25,000 receptors per cell) receptors (Dodevski and Plückthun, 2011; Sarkar *et al.*, 2008; Schlinkmann *et al.*, 2012a; Schlinkmann *et al.*, 2012b).

In the above studies we further observed an inherent coevolution of detergent stability with functional expression levels, the latter one never being under direct selection pressure. During selection, pressure is applied on functional receptor expression, which is a result of the efficiency of correct protein folding, insertion into the lipid bilayer and stability within the lipid bilayer (Jungnickel *et al.*, 1994). It is thus an indirect selection for biophysical properties, emphasized by the fact that mutants selected in *E. coli* also express better in eukaryotic cells (Dodevski and Plückthun, 2011; Schlinkmann *et al.*, 2012a). Nonetheless, functional expression and detergent stability are not directly linked as we find residue substitutions influencing one property but not the other (Dodevski and Plückthun, 2011; Sarkar *et al.*, 2008; Schlinkmann *et al.*, 2012a; Schlinkmann *et al.*, 2012b). Different from our selection technique, *in vitro* alanine-scanning solely for detergent stability leads to uncoupling of receptor expression and stability, and coevolution is thus unlikely to be detected (Shibata *et al.*, 2009).

The selected receptor variants display very high sequence identity to their original target (usually above 95%). Only a few amino acid changes are necessary to significantly improve the expression and biophysical behavior of the target protein, clearly illustrating that GPCRs maintain a delicate balance between stability in the membrane, flexibility required for signaling and the subsequent steps of receptor inactivation and degradation or recycling (Deupi and Kobilka, 2007). These constraints limit stability and at least partly explain the paucity of structural information from this large family, despite herculean efforts.

2. Methods

2.1 Generation of genetic diversity

The described diversification methodologies are applicable to all GPCRs for which the coding sequence is known and which can be successfully cloned into an *E. coli* -expression vector. If the below described FACS-based selection method is applied, a respective receptor ligand has to be available (see above).

Error-prone PCR to randomize GPCR sequences

By default, random mutagenesis is a stochastic process, without any external influence on the distribution of the introduced mutations. This assumption-free process is an easy and fast method to create genetically diverse receptor libraries on DNA level. Random alterations are introduced to the receptor coding sequence by error-prone PCR, and the mutational load per receptor sequence can be controlled by adaptation of the reaction conditions. Error-prone PCR amplification should be limited to the receptor coding sequence to keep the fusion protein tags intact and functional. Evidently, diversification can be further restricted to a specific receptor region, if desired.

The obtained mutational load is a product of the number of base misincorporations per amplification round and the number of amplification rounds. Both factors need to be adjusted to ensure optimal results since the optimal mutational load highly depends on the target protein and the desired phenotype. From our experience, in the case of GPCRs under functional selection of ligand binding a low mutational load of 1-5 amino acid substitutions per randomization round is suitable. The argument for choosing a low error rate and rather more selection cycles are as follows: The 7 transmembrane helices of the GPCR are long stretches where the introduction of even one charged residue would render protein non-functional. Such a substitution would therefore mask the beneficial effect of other mutations, and the clone would be lost. Thus, we have to treat carefully and add the mutations slowly, "purifying" the population by selection rounds after mutagenesis. Error-prone PCR mainly introduces single-base changes, and a subset of substitutions will hence remain silent on the amino acid level, but they can become non-silent with further diversifications rounds. Even some mutations on the amino acid level will only show their beneficial effect in the presence of existing mutations. These beneficial "neutral drift" phenomena are an inherent property of the evolutionary process.

Different alternatives exist for gene diversification: First, a low fidelity DNA polymerase such as *Taq* DNA polymerase can be employed. To support base misincorporations, Mg^{2+}-concentrations, Mn^{2+} or the amount of polymerase are elevated to increase the likelihood of continuous strand synthesis after mismatches, and unbalanced nucleotide mixtures or nucleotide analogues can be used to favor mismatches (Cadwell and Joyce, 1994; Spee *et al.*, 1993). However, the obtained diversification is highly nonrandom, since *Taq* DNA polymerase favors AT to GC substitutions over others

(Wilson and Keefe, 2001). A different mutational bias (GC to AT) can be obtained by using Mutazyme® DNA polymerase (Stratagene GeneMorph Kit). The need for random diversification led to the development of a new and optimized enzyme blend, Mutazyme II® (Stratagene GeneMorph Kit II), a DNA polymerase with reduced mutational bias by combination of the Mutazyme® with a novel *Taq* DNA polymerase (for example (Vanhercke *et al.*, 2005)). A routinely used method in our laboratory employs the Mutazyme II® DNA polymerase.

The GPCR coding sequence of interest is used for error prone PCR, and 10 ng of template DNA are used as input. Flanking PCR primers should include suitable restriction sites for subcloning into the expression vector. Low template DNA input decreases the final fraction of wild-type sequence in the diversified sequence pool, and increases the likelihood that amplification and diversification in further GPCR rounds starts from a previously diversified template. Thirty cycles of PCR amplification are routinely used for error-prone PCR, and the diversified PCR product is treated with DpnI to digest template sequences, as it is specific for methylated DNA as produced in *E. coli* in the form of the starting plasmid. A subsequent PCR amplification with a high fidelity polymerase, for example Phusion® Polymerase (Finnzyme), is used to obtain sufficient quantities for the subsequent cloning steps. The diversified PCR product is then purified, if necessary from a preparative agarose gel to avoid carryover of PCR side products, and is subsequently digested with the flanking restriction enzymes. A further purification step is used to obtain the final PCR product for subcloning, typically, 2-3 µg of DNA.

Despite optimization of error-prone PCR conditions to minimize mutagenic bias, it has to be considered that error-prone PCR will still favor certain amino acid substitutions over others, as some substitutions would require two consecutive base changes, which are statistically unlikely to happen.

Random mutagenesis using error-prone PCR was successfully applied to create genetic diversity within the rNTR1 (Sarkar *et al.*, 2008), the adrenergic receptors α_{1a} and α_{1b} and the tachykinin receptor NK_1 (Dodevski and Plückthun, 2011) for selection for high functional expression and stability. Notably, the tachykinin receptor NK_1 did not only evolve to higher expression levels, but could also be evolved for functional extraction from the lipid bilayer by detergent treatment, which is not possible for the wild type (Dodevski and Plückthun, 2011). For all receptors, increase in expression levels was associated with improvement of biophysical protein properties.

Single amino acid scanning-mutagenesis approaches

Alanine-scanning mutagenesis is a common approach to identify positions of a target protein that are crucial for a desired phenotype (Clackson and Wells, 1995; Wells, 1991). Every amino acid position of a given target protein is sequentially and separately replaced by alanine and every mutant is analyzed for the desired phenotype.

With respect to GPCRs, the high helical propensities, the small side chain size and the relative inertness of alanine make it a most likely tolerated substitution in most receptor positions, and might in principle improve the biophysical properties of the receptor by improving helix propensities and packing. Yet in a comprehensive all-versus-all screen (Schlinkmann *et al.*, 2012b), almost no alanines were the most preferred amino

acid type. By alanine scanning alone, mutational space is only minimally covered, and the relevance of a specific position for detergent-stability may not be identified if the favorable effect would not be conveyed by Ala, but only by a different amino acid substitution.

Nonetheless, alanine-scanning mutagenesis has been successfully applied to two GPCRs, rNTR1 (Shibata *et al.*, 2009) and the human β1-adrenergic receptor (Serrano-Vega *et al.*, 2008). Recently, leucine-scanning mutagenesis of the human β1-adrenergic receptor was performed and revealed further beneficial substitutions (Miller and Tate, 2011).

Technical aspects of mutant construction

The production of a collection of single mutants is a straightforward point mutagenesis, albeit becoming laborious with the number of mutants to be generated. For each mutant to be constructed, a mutagenic and complementary primer pair covering the codon of interest and introducing the mutation is required. Two cloning strategies can be applied: First, the mutagenic primer pair can be used for PCR amplification of the entire expression vector, for which only the mutagenic primer pair is needed. The PCR reaction is performed for 15-18 cycles using a high fidelity DNA polymerase such as *Pfu* DNA polymerase (Promega). For elongation, 2-2.5 min per 1000 base pairs (bp) are recommended for optimal performance of the reaction. Digestion of the input template DNA is achieved by DpnI treatment, followed by transformation of the amplified expression vector into *E. coli*. With complete digestion of the input DNA, only mutant clones should be obtained. Plasmid DNA from a single colony is then isolated, the sequence is recloned into a fresh vector (to eliminate any spurious introduction of backbone mutations in the vector which could mask the true phenotype), and the sequence of the final construct is verified by sequencing.

Second, a two-step assembly PCR strategy (Fig.1A) can be alternatively used. In a first PCR amplification round, the two following PCR fragments are generated: A flanking forward primer, introducing the 5' restriction site, and the reverse mutagenic primer are used to obtain a PCR fragment covering the 5'-half of the receptor sequence, including the desired mutation. Similarly, the 3'- half fragment including the desired mutation is obtained from a PCR reaction using the forward mutagenic primer and the reverse flanking primer, introducing the 3'- restriction site. The quality of the two PCR products is analyzed on an analytical agarose gel, and PCR products are purified from a preparative agarose gel in case of additional side products. If large numbers of mutants have to be generated, it is worth to optimize PCR conditions such that a pure and single PCR product of correct length is obtained every time. In this case, the output of the first PCR amplification round can be directly used as input for the second PCR assembly step. 20-100 ng of each purified PCR fragment or 1-2 µl of each unpurified PCR reaction are used for extension of the two fragments and assembly of the full-length mutagenized receptor sequence. Both PCR products overlap in the mutagenized region, and the mutagenic primer pair should be designed such that the overlap is 25-30 base pairs. The flanking PCR primers are used for PCR amplification of the full-length mutagenic sequence.

For fragments of similar length, a standard amplification PCR protocol is working well. However, particularly for fragments with larger differences in length, the extension of the two fragments from the overlap region before assembling them is beneficial for obtaining the specific PCR product. For this purpose, 5-10 PCR cycles are performed in the absence of the flanking primers, and 25-30 amplification rounds are subsequently performed after addition of the flanking primers. If the position to be mutagenized is close to one end of the receptor sequence, the corresponding flanking primer can be elongated to include the target position and introduce the desired mutation. In this case, only one PCR amplification step is necessary. Primers of approximately 100 nucleotides have been successfully used by the authors to introduce mutations.

The assembly strategy can be easily employed for fast generation of multiple defined mutants by generation of multiple mutagenic and overlapping fragments that are assembled to the full-length construct in the second PCR step. A triple mutant can be successfully obtained within one round of assembly (Fig. 1B). For this purpose, mutagenic primer pairs covering the target positions, denoted X, Y and Z here in sequential order, are designed to introduce the desired mutations. In the first PCR amplification, four fragments are generated: The first fragment covers the region from the 5' end to the most upstream mutation X (obtained with the 5'- flanking primer and the reverse mutagenic primer X), the second fragment reaches from mutation X to mutation Y, and corresponding fragments are amplified for Y to Z and Z to the 3' end. Individual fragment lengths should be 200 bp at minimum for optimal results. All fragments are then combined in a second PCR step for assembly of the full-length sequence by amplification with the flanking primers as described above. If the assembly of four fragments is inefficient or results in PCR side products, it is recommend to assemble two overlapping fragments in two separate reactions and to assemble the full-length sequence from these intermediate fragments.

The full-length mutagenic fragment is then purified, if necessary from a preparative agarose gel, and the flanking restriction sites are digested by the respective restriction enzymes. The purified mutagenic fragment is then ligated into the expression vector and transformed into *E. coli*. The DNA of a single colony is isolated and sequence-verified.

The second strategy seems to be more work-intensive at first sight. However, it contains only one cloning step, as every sequence is cloned directly into a fresh expression vector. In contrast, amplification of the entire expression vector by PCR can easily accumulate mutations in the vector backbone, affecting origin of replication or the promotor, for example. In order to avoid any spurious mutation, the mutagenized receptor sequence has to be cut and ligated into a fresh vector backbone by restriction digest, hence making this strategy actually more time-consuming than the second strategy.

Comprehensive mutagenesis

A more integrative method is to explore the entire mutational space by full randomization of a specific receptor position with selection for the amino acid variant conveying the desired phenotype. With our FACS-based selection system, a powerful and

efficient selection method exists to select for high functional expression and stability (Sarkar *et al.*, 2008).

Because of the incomplete coverage of mutational space as well as target sequence space by random mutagenesis, we recently performed a saturating and exhaustive mutagenesis on rNTR1-D03 to determine for every position the residue types that are not permitted, permitted and preferred (Schlinkmann *et al.*, 2012b). Importantly, the already improved mutant rNTR1-D03 was used as framework, since rNTR1-wt expression levels were too low for these experiments.

A full coverage of mutational space should ideally include the full codon diversity, to ensure phenotype selection and exclude any bias from variable tRNA levels, mRNA secondary structure or other undesired influences. The occurrence of several or all codons of a preferred amino acid after selection internally verifies the selection outcome.

Generally, the strategy to fully randomize a specific amino acid position, that is to create a position-specific library, is based on the generation of a single point mutagenesis (Fig. 1A). The mutagenic primers contain an NNN sequence at the target codon, where N denotes an equimolar mixture of all four nucleotides. An NNN mixture also includes stop codons, and depending on the screening and selection technique that is employed, the primer design may have to be adapted to exclude stop codons. However, with FACS-based selection for functional expression using fluorescent ligands, stop-codon mutants are counter-selected, as most of these mutants do not contain a functional ligand binding site (unless the stop codon occurs after TM7). Thus, the counter-selection of stop codons is a useful internal quality control of the selection success.

Primers should be designed such that the hybridization temperature with the template is between 55 to 65°C so that differences in specific primer sequences are negligible. Two overlapping half fragments of the target sequence are then generated similar to the approach described above, extended and amplified. Very importantly, throughout all steps of library generation, care must be taken to preserve library diversity. Thus, DNA amounts equivalent to 10-20 fold of the library diversity should be used as input in every PCR step. The expression vector for subcloning of the position specific library should not contain a wild-type receptor sequence in order to avoid wild-type overrepresentation due to incomplete vector digest (for details, see (Schlinkmann *et al.*, 2012a)).

In vitro DNA shuffling of GPCR sequences to generate highly diverse chimeric receptor libraries

In vitro DNA shuffling is used to generate chimeras from two receptor sequences. We have recently adapted and optimized the staggered extension process (StEP) (Fig. 2A) for generation of chimeric libraries starting from the rNTR1-D03 and a mutagenized artificial receptor sequence, rNTR1-M30 or rNTR1-M303 (Schlinkmann *et al.*, 2012a). StEP is a PCR-based approach (Aguinaldo and Arnold, 2002; Zhao and Zha, 2006), in which two or more different sequences are used as input templates. By using a very short combined annealing and extension step at a suboptimal DNA polymerase elongation

temperature, the amplification primers are only extended by a few nucleotides per StEP PCR cycle. After the subsequent denaturation step, the primers are further extended, until eventually a full-length receptor sequence is obtained. Most importantly, by using two or more different input templates, the growing primer fragment can switch templates between two PCR cycles, and thus accumulates mutations from two different templates in one chimeric receptor sequence.

For shuffling of two GPCR variants of approximately 1200 base pairs (bp), 10 ng of each plasmid template DNA is mixed per 50 µl PCR reaction using 2 units $Vent_R$® DNA Polymerase (NEB) and 30 pmol each of the two flanking primers, introducing a restriction site. The choice of DNA polymerase greatly affects shuffling efficiency, and the following aspects should be considered: High fidelity is desired to avoid undesired mutations as a result of high number of StEP PCR cycles. To yield short recombination distances, a slower DNA polymerase is preferred, for example $Vent_R$® (NEB, approx. 1000 bp per minute) over Phusion® DNA polymerase (Finnzymes, 1000 bp per 15 seconds).

The amplification yield in a StEP reaction is comparably low, and further PCR amplification of a single StEP reaction should be avoided, as it does not increase diversity. With a theoretical diversity of about 10^7, twelve reactions are set up in parallel to increase the product amount while simultaneously generating high diversity. StEP shuffling is performed for 125 PCR cycles on a Biometra T3 thermocycler (heating rate of 2°C/s) with 30 seconds denaturation at 94°C and 6 seconds annealing/ elongation at 50°C per cycle and 2 minutes of initial denaturation. A final and extended elongation step should be omitted, as it could lead to amplification of the template sequences without shuffling.

StEP is a delicate PCR-based process, reacting strongly to small changes in reaction conditions. The most important parameters for optimization and troubleshooting are as follows: Duration and temperature of annealing and elongation are key determinants of shuffling efficiency. Under these conditions, recombination events within 30 bp distance are obtained. Importantly, the differences in heating and cooling rates between thermocyclers strongly influence the recombination efficiency and yield of the StEP process, and should be controlled and adjusted together with the elongation conditions. With slow heating and cooling rates (2°C/s), the actual window of DNA polymerase activity is longer than defined by the annealing and elongation cycle (here 6 seconds per cycle),compared to thermocyclers with fast heating rates (up to 6°C/s). Under these conditions, elongation times might have to be extended to allow sufficient product formation.

VentR® and Phusion DNA polymerases both exhibit 3’ to 5’- proofreading exonuclease activity, which, for the case that an incorporated mutation locates at the 3’-end of the growing fragment, could lead to correction by the polymerase proofreading activity after template switching. Here, a DNA polymerase lacking 3’ to 5’- proofreading exonuclease activity, for example Deep VentR™ (exo -) (NEB), might be compared with respect to recombination efficiency, but resulted in high amounts of PCR side products in our experiments and was thus not used.

Further, despite the presence of 2 mM $MgSO_4$ in the PCR reaction buffer, we observed that the use of additional 2 mM $MgSO_4$ positively affected the reaction yield, probably by stabilizing DNA-polymerase complexes after mismatches.

The shuffled StEP product is digested with DpnI to minimize the carryover of input templates. The StEP product should be purified from a preparative agarose gel, as PCR side products are common to StEP reactions. The purified product is digested with the corresponding restriction enzymes and purified. At least 3 µg of final StEP-product should be obtained for subcloning of a product with a theoretical diversity of 10^7.

Shuffling by StEP is an easy and fast technique to generate a chimeric library from two or more target sequences. However, mutations close in sequence (3 to 30 bp) are inefficiently separated by StEP, and sequences with coupled mutations are overrepresented, compared to the recombined sequences. If more than two templates are shuffled, the apparent recombination efficiency can suffer from a "dilution effect" (Fig. 2B): If 10 individual point mutants of a given receptor are used as input templates for StEP shuffling, one sequence will contain a particular mutation, while 9 templates contain the wild-type codon in the respective position. Statistically, 8 of 9 recombination events will shuffle wild type against wild type and the accumulation of mutations in one shuffled sequence is consequently low.

Alternatively, an artificial receptor sequence combining all mutations of interest can be synthesized and shuffled against the wild-type sequence for an mutant to wild type ratio of 1:1 (for example (Schlinkmann *et al.*, 2012a)). Evidently, the above effect can be easily exploited to direct and influence recombination by adjustment of template ratios and template design.

The selection output from a diverse StEP-library can be easily subjected to a further StEP-shuffling by plasmid DNA isolation from the selected cell pool.

Cloning and transformation of GPCR libraries with high diversity

Cloning and transformation of single point mutants, i.e. single plasmids, is straightforward and explained elsewhere (Sambrook and Russel, 2001).

Library cloning and transformation is technically more demanding, and care must be taken to ensure full library diversity throughout all cloning steps. In case of random mutagenesis, library diversity can be estimated by multiplying the number of substitutions per sequence with the number of molecules in the reaction. For a StEP shuffling of two sequences, the theoretical diversity can be calculated from the mutational load of the input templates. In a StEP reaction from two templates, which differ in 30 amino acid positions, the theoretical diversity is given as 2^{30} (~ 10^9).

For a theoretical diversity of 10^7 and a 1200 bp StEP product to be subcloned, 3 µg of purified product DNA is ligated into the expression vector with a 3-fold molar excess of insert DNA over vector DNA and 10 units of T4 DNA ligase per µg of DNA in the ligation mix in a total volume of 500 µl. Ligation is performed for 12-16 h at 16°C. Ligation products are then purified using, for example, Qiagen MinElute columns. Column purifications are quick, the final concentration of the ligated product can be controlled by the elution volume and the product is quantitatively recovered. Other methods such as DNA precipitation or purification from agarose gels can be alternatively used, but are more time consuming and less quantitative.

Usually, the limiting step in keeping library diversity is transformation of *E. coli*. Electrocompetent *E. coli* cells are superior to chemocompetent cells with regard to transformation rates and should be routinely used for library transformations (for protocols, see for example (Chuang *et al.*, 1995; Dower *et al.*, 1988)). The amount of DNA per electroporation reaction has to be optimized with respect to the cell density of electrocompetent cells. Routinely, a maximum of 1 µg ligation product in a 5 µl volume, preferably water or a 5 mM Tris-buffered solution, is transformed per 100 µl of electrocompetent cells. DNA and cells are premixed on ice, and transferred to a prechilled electroporation cuvette (2 mm, for example Eurogentec electroporation cuvettes). A Gene Pulser® II electroporator (Biorad) is used to electroporate the DNA-cell mixture at 2500 V with a capacitance of 25 µF and 200 Ω resistance. Time constants should be above 4 ms, ideally 4.5 to 5 ms to ensure high efficiency of transformation. The given protocol is found to give optimal electroporation efficiency, which is particularly affected by changes in the electroporation volume, and larger volumes per electroporation cuvette will dramatically decrease electroporation efficiency.

Electroporated cells are directly recovered in 1 ml SOC medium for 1 h at 37°C in a shaking incubator. Directly after the 1 hour recovery of the transformed cells, dilution series are plated on agar dishes to determine electroporation efficiency (10 µl, 10^1 to 10^7-fold dilutions). Typically, $5 \cdot 10^7$ to $3 \cdot 10^8$ colonies can be obtained using the described procedure. The recovered cells are subsequently diluted into in 500 ml 2YT medium, supplemented with 1% glucose and antibiotic selection marker and grown for 12-16 h at 28°C in a shaking incubator. Growth temperature should be low to minimize possible growth differences between mutants. The final cell density should be approximately 10^9 per ml of culture volume (OD_{600} of 1). For long-term storage, aliquots of > 10^9 cells are supplemented with 20% glycerol, snap-frozen in liquid N_2 and stored at -80°C until further use.

Optimally, single colonies of the naïve library should be analyzed by sequencing of the receptor sequence to ensure library quality and analyze randomization or shuffling efficiency. In case of high genetic diversity, 48-96 colonies should by assayed at minimum.

2.2 Expression and selection

Design of expression vector and GPCR fusion construct

As discussed above, the expression vector and the receptor construct have to be empirically optimized for a given target receptor, for which the following general considerations apply:

First, depending on the expression host, GPCRs are often expressed as fusion proteins to allow efficient targeting of the receptor to the lipid bilayer. For expression of the wild-type rat neurotensin receptor in *E. coli*, expression levels were highest when expressed with an N-terminal maltose binding protein (MBP) and a C-terminal thioredoxin fusion (Tucker and Grisshammer, 1996).

For receptors that do not contain any N-terminal domain that is directly involved in ligand binding and that does not contain critical modifications, the flexible N-terminus can often been truncated. For some receptors, however, the N-terminal domain is large, and involved in ligand binding and GPCR activation (see for example (Pin *et al.*, 2004)).The rNTR1 receptor for example is expressed with deletion of the first 42 N-terminal amino acids (Grisshammer *et al.*, 1993). All solved non-rhodopsin GPCR structures have truncated or modified N- and C-termini (Katritch *et al.*, 2012).

MBP is connected to the GPCR target by a flexible linker including a protease cleavage site, for example tobacco etch virus (TEV) protease. MBP is efficiently targeted to the periplasmatic space by its signal sequence, thereby directing the GPCR to the inner membrane. Even though the GPCR can be incorporated into the membrane without this fusion and without a native signal sequence, the use of this MBP fusion system may better guide the receptor to the Sec translocon in *E. coli*.

C-terminally, thioredoxin is fused to the GPCR, again via a flexible linker and protease cleavage site, and is followed by a His_{10}-tag for purification purposes. Whether thioredoxin, a small well-folding and soluble protein, really serves as a "folding chaperone" (Tucker and Grisshammer, 1996) will require further investigations, and it might suffice that it provides a defined soluble folded domain that helps correct positioning of the C-terminal end on the cytoplasmic side. In any event, thioredoxin considerably affects the functional expression level of a GPCR in *E. coli*

Different fusion protein tags and purification tags might be tested for optimal expression of a specific target GPCR. We have replaced the C-terminal His_{10}-tag by an AviTag sequence (GLNDIFEAQKIEWHE, biotinylation on K) for enzymatic *in vivo* biotinylation of the receptor fusion construct (Dodevski and Plückthun, 2011) by the *E. coli* biotin protein ligase (BirA). *In vivo* biotinylation using an AviTag sequence is simple, stoichiometric, specific and quantitative, and hence superior to chemical biotinylation of the purified receptor. While quantitative biotinylation of a highly expressed recombinant protein requires coexpression of BirA ligase and addition of free biotin, these measures are not necessary for *in vivo* biotinylation of GPCRs expressed at only about 500 – 6000 receptors per *E. coli* cell.

Second, promotor strength and plasmid copy number are critical determinants of GPCR expression, as has already been mentioned above, and have to be adapted to avoid toxicity of GPCR expression in *E. coli*. A low copy plasmid should be used for difficult-to-express target receptors, combined with a tunable and tight promotor. For expression of wild type rNTR1, a pBR322-derived origin of replication and the *lac*-promotor is used (Tucker and Grisshammer, 1996). As discussed above, with improvement of the biophysical receptor properties (rNTR1-D03, see (Sarkar *et al.*, 2008)), higher plasmid copy numbers are tolerated, and plasmid copy number can even limit expression levels of superior receptor variants (Schlinkmann *et al.*, 2012a).

Expression of highly diverse GPCR libraries in *E. coli*

GPCRs are generally expressed at low temperatures in *E. coli*, leading to decreased protein synthesis rates, probably positively affecting targeting efficiency to and insertion efficiency into the lipid bilayer. The rNTR1 is expressed in the *E. coli* strain DH5α. A given volume of 2YT medium, supplemented with 0.2% glucose and selection marker, is inoculated to a cell density of OD_{600}= 0.05, and grown at 37°C in a shaking incubator to OD_{600}= 0.5. Expression is then induced by addition of 250 µM IPTG (isopropyl-β-D-thiogalactopyranoside), and expression is continued for 18-24 hours at 20°C. Receptor variants with improved biophysical properties tolerate higher expression temperatures up to 30°C (Schlinkmann *et al.*, 2012a).

For high-diversity libraries, inoculation density has to be controlled to sustain library diversity at this step. Expression temperatures should be kept low, i. e. 20°C, for the naïve library and optionally for the first rounds of selection to minimize possible differences in growth behavior of individual receptor variants.

If the cell density of the glycerol stock is known, the cell number needed for an inoculation density of OD_{600}= 0.05 can be calculated on the assumption that 10^9 cells per ml in a cuvette with 1 cm pathlength equal 1 OD_{600}.The cell number used for inoculation should again cover 10-20 fold the library diversity. It is recommended to increase expression culture volumes, and not inoculation density, if the above recommendation does not hold for a given expression volume. A library with a diversity of 10^7-10^8 variants is expressed in 60 ml culture volume in a 300 ml Erlenmeyer flask. To reach an inoculation density of OD_{600}= 0.05 in a volume of 60 ml, 3 OD units of cells, equaling $3 \cdot 10^9$ cells, are needed, thus oversampling library diversity 30-300 fold.

Fluorescence-labeling of GPCR-expressing *E. coli* cells

FACS-selection is applicable to any receptor for which a known ligand with reasonable affinity exists that can be fluorescence-labeled. Peptide ligands and many small molecules are known to work well, whereas ligands that are too hydrophobic tend to bind nonspecifically to the cells, thus making their use more difficult with respect to receptors with low basal expression levels, as the ratio specific : nonspecific signal is low. The size of the labeled ligand affects permeability and labeling efficiency, and small ligands of approximately 1 kilodalton (kDa) diffuse well through the permeabilized outer membrane, while also larger ligands of up to 10 kDa in size were shown to penetrate the outer membrane (Chen *et al.*, 2001) after suitable permeabilization. However, for selection by FACS sorting, cell viability after recovery from FACS selection is a relevant parameter that might suffer from harsh permeabilization conditions and should be tested for a specific buffer.

The fluorescence label has to be compatible with excitation wavelengths and emission filter wavelengths on the respective FACS machine, which are most commonly equipped with a 488 nm laser and a 633 nm laser (for example BD FACS Aria Series). Depending on the machine configuration, a 355 nm or 405 nm UV laser, or a 561 nm laser might be available for excitation.

For selection of well-expressed receptor variants by FACS, cells are labeled relative to their expression levels by use of a fluorescence-labeled receptor ligand. In case of rNTR1, a BOPIPY-labeled neurotensin peptide is used (BODIPY-neurotensin(8-12), BP-NT) (Sarkar *et al.*, 2008). The outer membrane of *E. coli* is gently permeabilized to allow diffusion of the BP-NT to the inner membrane, where the receptor is located. A Tris-salt buffer (50 mM Tris·HCl pH 7.4, 150 mM KCl, abbreviated TKCl buffer) is found optimal for permeabilization of *E. coli* DH5α cells expressing rNTR1 (Sarkar *et al.*, 2008), but might differ for a specific target receptor and receptor ligand (Dodevski and Plückthun, 2011). Sodium salts should be avoided when working with rNTR1, since the receptor is sodium-sensitive (Martin *et al.*, 1999). Depending on the library diversity, an aliquot of cells covering 10-fold library diversity should be used for selection. The volume for permeabilization and labeling should be adjusted accordingly to ensure efficient labeling, and can be concentrated during later washing steps if necessary. Cell densities of $5 \cdot 10^7$ to $2 \cdot 10^8$ are suitable under these conditions. Cells are collected by centrifugation for 3 minutes at 6000 g, washed once in TKCl buffer and resuspended in the appropriate volume of TKCl buffer. 20 nM BP-NT is added, and permeabilization and labeling is performed for 1-2 hours on ice in the dark. The optimal ligand concentration should be at least 10-fold above K_D, to ensure quantitative binding to receptors. The apparent K_D needs to be tested in a saturation binding experiment before selections, since the ligand diffusion across the permeabilized outer membrane might cause the system not be at full equilibrium. Furthermore, if receptor expression levels per cell are expected to be high, the ligand concentration might have to be increased to prevent ligand depletion. Nonspecific binding is assayed in the presence of 10 µM unlabeled neurotensin peptide (AnaSpec). Cells are then washed twice in 1 ml TKCl buffer, and resuspended in 1-2 ml TKCl buffer and directly subjected to FACS sorting.

Selection for high functional GPCR expression using FACS

The labeled and washed receptor-expressing cells are subjected to selection by FACS (Fig. 3). We routinely work with a BD FACS Aria I. Unlabeled cells are used to gate for the viable cell population. For selection for high functional expression, the fluorescence signal of the viable cells is used to gate for highest cell fluorescence, hence functional expression. If applicable, multiple fluorescence parameters can be analyzed and gated in parallel or consecutively. The 1% highest fluorescent cells are gated and selected. Selection stringency can be adjusted by the gate size and the selection mode. Gate sizes of 0.5-2% are recommended, with higher stringency in subsequent rounds of selection. The purity of selection is adjusted by the sorting mode, where yield mode should be used for naïve libraries to recover any positive cell within the gate, while purity mode is routinely used for subsequent rounds to avoid carry-over of non-gated cells (refer to the manufacturer's FACS manual for further detail). On a BD FACS Aria I, flow rates of 5,000-20,000 cells are working well. The most fluorescent cells, usually 10^6 cells for the naïve library and 10^5 cells for subsequent rounds, are then directly sorted into 2 ml recovery medium, 2YT medium supplemented with 1-2% glucose and selection marker. If cell

viability is low, the selection marker should be decreased in the recovery medium or even omitted.

To screen and select very large libraries, a “fluorescence-threshold selection” can be performed. For that purpose, the labeled cells are highly concentrated to allow flow rates of about 500,000 cells per second. Note that not every FACS machine technically supports this application.

Next, a threshold is set to the fluorescence signal, until only the most highest fluorescent cells are recorded by the machine and the apparent flow rate is reduced to 20,000-30,000 cells per second. Finally, the most fluorescent cells of this population are gated and selected. By this approach, very high cell numbers can be screened, but the sort is of low purity, since the true flow rate, i.e. cell density, is much higher. Under these conditions, many non-relevant cells, which are close to a cell falling within the sorting gate, are co-sorted, because they fall below the fluorescence and are not detected by the FACS machine, so that the sorting mask (purity or yield) does not apply. The output can be directly resorted, if a sufficient number of cells are isolated, or subjected to purity selection in the subsequent round.

Cells are recovered for 1 hour at 28-37°C, then diluted into 5-20 ml of 2YT medium supplemented with 1-2% glucose and selection marker and grown at 25-28°C to $OD_{600} < 1$. Aliquots of $> 10^9$ cells are supplemented with 20% glycerol, snap frozen and stored at -80°C until further use. Expression for subsequent selection rounds can directly be inoculated from a glycerol stock.

2.3 Characterization of selected GPCR variants

Sequence analysis of selected GPCR variants

First of all, the sequence diversity, mutational load and sequence distribution of mutations in the selected cell pool is analyzed by sequencing. Either the plasmid DNA of single colonies is isolated and the receptor sequence is sequenced, or the receptor sequence is directly amplified from a single colony by colony PCR for subsequent sequencing of the PCR product. Colony PCR (cPCR) is much faster than plasmid DNA isolation and suitable to analyze large numbers of different variants, since it can be easily adapted to a 96-well format. For this purpose, a 20 µl PCR reaction is set up containing 0.1 µM of each flanking primer, 0.8 mM dNTP mix in PCR buffer with 2 mM $MgCl_2$ and 1-2 units of DNA polymerase. *Taq* DNA polymerase is sufficient for sequences up to 1000 bp, while a DNA polymerase with higher fidelity should be used to amplify longer sequences, for example $Vent_R$™ (NEB) or Phusion® (Finnzymes) DNA polymerase. A 10 µl-pipette tip is used to gently pick a single colony from an agar plate and transfer it in into one well of a 96-well PCR plate. During transfer of cells, any carryover of agar should be avoided, since it inhibits the cPCR reaction. For very large colonies, a small sample from the colony boundary should be used. Cells are resuspended by repeated pipetting, and the pipette tip is then transferred to the corresponding well on a 96 deep-well plate containing 1 ml 2YT medium supplemented with 1% glucose (to suppress expression) and selection marker. The mini-cultures are then grown at 37°C for 6-12 hours in a shaking

incubator and either stored at 4°C for a few days, or as glycerol stocks at -80°C. Receptor variants of interest can thus be easily regrown from a stock culture for further analysis or storage.

The cPCR reaction includes a 10 min initial denaturation step which ensures cell disruption, while PCR amplification conditions have to be adjusted to primer sequence, product length and DNA polymerase.

The PCR products are then purified, using for example MultiScreen PCR□96 Filter Plate (Millipore) and subsequently sequenced.

Expression levels of individual selected GPCR variants

The final selected pool of cells is plated on agar plates to obtain single colonies, which can then be individually analyzed. Single colonies are grown and expressed in 24-well plates in 3-5 ml of 2YT medium with 0.2% glucose and selection marker each, sealed with gas-permeable seals, and expression is performed as for the library expression.

Analytical flow cytometry can then be used to analyze the relative expression level, using the fluorescence-labeled receptor ligand. The assay is performed as described for the FACS sorting, except that smaller expression volumes and number of cells for analysis can be used (10^6-10^7 cells for flow cytometry analysis).

For quantification of functional receptor expression, a radioligand-binding assay (RLBA) can be used, with the assumption that 1 OD_{600} in a cuvette of 1 cm pathlength equals 10^9 cells per ml. RLBAs are high-throughout compatible and hence suitable for the screening of large variant numbers. For rNTR1, a [^{3}H]-labeled neurotensin peptide is used (PerkinElmer). All steps are performed in 96-well plates. For one measurement, $2 \cdot 10^7$ cells are collected by centrifugation, washed once in ligand binding buffer (LBB, 50 mM Tris·HCl pH 7.4, 1 mM EDTA, 0.1% BSA and 40 µg/ ml bacitracin) and resuspended in 100 µl LBB buffer. 100 µl of LBB containing 20 nM [^{3}H]-neurotensin are added to a final concentration of 10 nM and incubated for 2-3 h at 4°C to allow for ligand saturation. Nonspecific binding is determined in the presence of 5 µM unlabeled neurotensin peptide (Anaspec). Unbound and free [^{3}H]-neurotensin is separated from the cell-bound ligand by vacuum filtration using 96-well glass fiber filter plates (Millipore MultiScreen-FB plates MAFBN0B50, pretreated with 100 µl of 0.01% polyethylenimine (PEI)), on a 96-well vacuum filtration device (for example Millipore MultiScreen Vacuum Manifold). The sample volume is applied to a well of the filter plate, and filtrated by application of vacuum, and the filters are washed 4-5 times with 200 µl of LBB buffer. Filters are dried for 30-60 minutes at 60°C, and the filter- and cell-bound radioactivity is then quantified by liquid scintillation. For this, filters are transferred to scintillation plates (IsoPlate 96, PerkinElmer) containing 200 µl of OptiPhase SuperMix scintillation cocktail (Perkin Elmer). Filters are allowed to dissolve for 3-12 hours and quantified for 2 minutes in a Wallac 1450 Microbeta plus liquid scintillation counter.

Detergent stability of selected variants in the presence and absence of receptor ligand

To assess the detergent stability of the selected variants, we have previously reported a fast and efficient method to screen large numbers of variants, which is explained in detail elsewhere (Dodevski and Plückthun, 2011). Briefly, receptor variants are *in vivo* biotinylated using the AviTag sequence, detergent-solubilized and immobilized on magnetic, streptavidin-coated beads (MyOne Streptavidin T1 beads, Invitrogen). Detergents can be efficiently exchanged after immobilization by repetitive washing in the detergent of choice (Fig. 4). According to our experiments, stability measurements in a particular detergent are not affected by the choice of detergent used for solubilization or the rebuffering process (Fig. 4).

The solubilized and immobilized receptor is then thermally challenged, and the remaining receptor activity is quantified by RLBA. In this experimental setup, the apparent detergent-stability in the absence of ligand is determined. The assay is easily adapted to study apparent detergent-stability in the presence of ligand: For this purpose, the immobilized receptor is first saturated with [^{3}H]-neurotensin for 2 hours, free ligand is washed away, and the receptor is then thermally challenged. Depending on the sample volume, the concentration of [^{3}H]-neurotensin has to be adjusted to allow ligand saturation under these conditions. LBB buffer containing 3-5 nM [^{3}H]-neurotensin is then added and incubated for 1 hour before remaining receptor activity is quantified by liquid scintillation counting.

Acknowledgements

We thank Drs. Christoph Klenk and Erik Sedlak for critical reading of the manuscript. Work in the author's laboratory was supported by the Swiss National Science Foundation through the NCCR Structural Biology.

References

Aguinaldo, A.M., Arnold, F. (2002). Staggered extension process (StEP) in vitro recombination. *Methods Mol. Biol.* **192**, 235-239.

Bjarnadottir, T.K., Gloriam, D.E., Hellstrand, S.H., Kristiansson, H., Fredriksson, R., Schiöth, H.B. (2006). Comprehensive repertoire and phylogenetic analysis of the G protein-coupled receptors in human and mouse. *Genomics* **88**, 263-273.

Bowie, J.U. (2001). Stabilizing membrane proteins. *Curr. Opin. Struct. Biol.* **11**, 397-402.

Cadwell, R.C., Joyce, G.F. (1994). Mutagenic PCR. *PCR Methods Appl.* **3**, S136-140.

Chen, G., Hayhurst, A., Thomas, J.G., Harvey, B.R., Iverson, B.L., Georgiou, G. (2001). Isolation of high-affinity ligand-binding proteins by periplasmic expression with cytometric screening (PECS). *Nat. Biotechnol.* **19**, 537-542.

Cherezov, V., Rosenbaum, D.M., Hanson, M.A., Rasmussen, S.G., Thian, F.S., Kobilka, T.S., Choi, H.J., Kuhn, P., Weis, W.I., Kobilka, B.K., Stevens, R.C. (2007). High-resolution crystal structure of an engineered human beta2-adrenergic G protein-coupled receptor. *Science* **318**, 1258-1265.

Chien, E.Y., Liu, W., Zhao, Q., Katritch, V., Han, G.W., Hanson, M.A., Shi, L., Newman, A.H., Javitch, J.A., Cherezov, V., Stevens, R.C. (2010). Structure of the human dopamine D3 receptor in complex with a D2/D3 selective antagonist. *Science* **330**, 1091-1095.

Chuang, S.E., Chen, A.L., Chao, C.C. (1995). Growth of E. coli at low temperature dramatically increases the transformation frequency by electroporation. *Nucleic Acids Res.* **23**, 1641.

Clackson, T., Wells, J.A. (1995). A hot spot of binding energy in a hormone-receptor interface. *Science* **267**, 383-386.

Deupi, X., Kobilka, B. (2007). Activation of G protein-coupled receptors. *Adv. Protein Chem.* **74**, 137-166.

Dodevski, I., Plückthun, A. (2011). Evolution of three human GPCRs for higher expression and stability. *J. Mol. Biol.* **408**, 599-615.

Dower, W.J., Miller, J.F., Ragsdale, C.W. (1988). High efficiency transformation of *E. coli* by high voltage electroporation. *Nucleic Acids Res.* **16**, 6127-6145.

Duquesne, K., Sturgis, J.N. (2010). Membrane protein solubilization. *Methods Mol. Biol.* **601**, 205-217.

Ferguson, S.S. (2001). Evolving concepts in G protein-coupled receptor endocytosis: the role in receptor desensitization and signaling. *Pharmacol. Rev.* **53**, 1-24.

Foord, S.M., Bonner, T.I., Neubig, R.R., Rosser, E.M., Pin, J.P., Davenport, A.P., Spedding, M., Harmar, A.J. (2005). International Union of Pharmacology. XLVI. G protein-coupled receptor list. *Pharmacol. Rev.* **57**, 279-288.

Granseth, E., Seppala, S., Rapp, M., Daley, D.O., Von Heijne, G. (2007). Membrane protein structural biology--how far can the bugs take us? *Mol. Membr. Biol.* **24**, 329-332.

Grisshammer, R., Duckworth, R., Henderson, R. (1993). Expression of a rat neurotensin receptor in *Escherichia coli*. *Biochem. J.* **295** 571-576.

Jaakola, V.P., Griffith, M.T., Hanson, M.A., Cherezov, V., Chien, E.Y., Lane, J.R., Ijzerman, A.P., Stevens, R.C. (2008). The 2.6 angstrom crystal structure of a human A2A adenosine receptor bound to an antagonist. *Science* **322**, 1211-1217.

Jungnickel, B., Rapoport, T.A., Hartmann, E. (1994). Protein translocation: common themes from bacteria to man. *FEBS Lett.* **346**, 73-77.

Katritch, V., Cherezov, V., Stevens, R.C. (2012). Diversity and modularity of G protein-coupled receptor structures. *Trends Pharmacol. Sci.* **33**, 17-27.

Lagerström, M.C., Schiöth, H.B. (2008). Structural diversity of G protein-coupled receptors and significance for drug discovery. *Nat. Rev. Drug Discov.* **7**, 339-357.

le Maire, M., Champeil, P., Moller, J.V. (2000). Interaction of membrane proteins and lipids with solubilizing detergents. *Biochim. Biophys. Acta* **1508**, 86-111.

Martin, S., Botto, J.M., Vincent, J.P., Mazella, J. (1999). Pivotal role of an aspartate residue in sodium sensitivity and coupling to G proteins of neurotensin receptors. *Mol. Pharmacol.* **55**, 210-215.

Miller, J.L., Tate, C.G. (2011). Engineering an ultra-thermostable beta(1)-adrenoceptor. *J. Mol. Biol.* **413**, 628-638.

Overington, J.P., Al-Lazikani, B., Hopkins, A.L. (2006). How many drug targets are there? *Nat. Rev. Drug Discov.* **5**, 993-996.

Palczewski, K., Kumasaka, T., Hori, T., Behnke, C.A., Motoshima, H., Fox, B.A., Le Trong, I., Teller, D.C., Okada, T., Stenkamp, R.E., Yamamoto, M., Miyano, M. (2000). Crystal structure of rhodopsin: A G protein-coupled receptor. *Science* **289**, 739-745.

Pin, J.P., Kniazeff, J., Goudet, C., Bessis, A.S., Liu, J., Galvez, T., Acher, F., Rondard, P., Prezeau, L. (2004). The activation mechanism of class-C G-protein coupled receptors. *Biol. Cell.* **96**, 335-342.

Rasmussen, S.G., Choi, H.J., Fung, J.J., Pardon, E., Casarosa, P., Chae, P.S., Devree, B.T., Rosenbaum, D.M., Thian, F.S., Kobilka, T.S., Schnapp, A., Konetzki, I., Sunahara, R.K., Gellman, S.H., Pautsch, A., Steyaert, J., Weis, W.I., Kobilka, B.K. (2011a). Structure of a nanobody-stabilized active state of the β_2-adrenoceptor. *Nature* **469**, 175-180.

Rasmussen, S.G., Choi, H.J., Rosenbaum, D.M., Kobilka, T.S., Thian, F.S., Edwards, P.C., Burghammer, M., Ratnala, V.R., Sanishvili, R., Fischetti, R.F., Schertler, G.F., Weis, W.I., Kobilka, B.K. (2007). Crystal structure of the human β_2-adrenergic G-protein-coupled receptor. *Nature* **450**, 383-387.

Rasmussen, S.G., DeVree, B.T., Zou, Y., Kruse, A.C., Chung, K.Y., Kobilka, T.S., Thian, F.S., Chae, P.S., Pardon, E., Calinski, D., Mathiesen, J.M., Shah, S.T., Lyons, J.A., Caffrey, M., Gellman, S.H., Steyaert, J., Skiniotis, G., Weis, W.I., Sunahara, R.K., Kobilka, B.K. (2011b). Crystal structure of the β_2-adrenergic receptor-Gs protein complex. *Nature* **477**, 549-555.

Rosenbaum, D.M., Cherezov, V., Hanson, M.A., Rasmussen, S.G., Thian, F.S., Kobilka, T.S., Choi, H.J., Yao, X.J., Weis, W.I., Stevens, R.C., Kobilka, B.K. (2007). GPCR engineering yields high-resolution structural insights into β_2-adrenergic receptor function. *Science* **318**, 1266-1273.

Rosenbaum, D.M., Rasmussen, S.G., Kobilka, B.K. (2009). The structure and function of G-protein-coupled receptors. *Nature* **459**, 356-363.

Sambrook, J.F., Russel, D.W., (2001). Molecular Cloning: A Laboratory Manual, 3 Volumes, Third Edition ed. Cold Spring Harbor Laboratory Press.

Sarkar, C.A., Dodevski, I., Kenig, M., Dudli, S., Mohr, A., Hermans, E., Plückthun, A. (2008). Directed evolution of a G protein-coupled receptor for expression, stability, and binding selectivity. *Proc. Natl. Acad. Sci. USA* **105**, 14808-14813.

Schlinkmann, K.M., Hillenbrand, M., Rittner, A., Künz, M., Strohner, R., Plückthun, A. (2012a). Maximizing detergent stability and functional expression of a GPCR by exhaustive recombination and evolution. *J. Mol. Biol.*

Schlinkmann, K.M., Honegger, A., Türeci, E., Robison, K.E., Lipovsek, D., Plückthun, A. (2012b). Critical features for biosynthesis and functionality of a GPCR uncovered by all-versus-all mutations *Proceedings of the National Academy of Sciences USA* **109**, 9810-9815.

Seddon, A.M., Curnow, P., Booth, P.J. (2004). Membrane proteins, lipids and detergents: not just a soap opera. *Biochim. Biophys. Acta* **1666**, 105-117.

Serrano-Vega, M.J., Magnani, F., Shibata, Y., Tate, C.G. (2008). Conformational thermostabilization of the β_1-adrenergic receptor in a detergent-resistant form. *Proc. Natl. Acad. Sci. USA* **105**, 877-882.

Shibata, Y., White, J.F., Serrano-Vega, M.J., Magnani, F., Aloia, A.L., Grisshammer, R., Tate, C.G. (2009). Thermostabilization of the neurotensin receptor NTS1. *J. Mol. Biol.* **390**, 262-277.

Spee, J.H., de Vos, W.M., Kuipers, O.P. (1993). Efficient random mutagenesis method with adjustable mutation frequency by use of PCR and dITP. *Nucleic Acids Res.* **21**, 777-778.

Tucker, J., Grisshammer, R. (1996). Purification of a rat neurotensin receptor expressed in *Escherichia coli*. *Biochem. J.* **317** 891-899.

Vanhercke, T., Ampe, C., Tirry, L., Denolf, P. (2005). Reducing mutational bias in random protein libraries. *Anal. Biochem.* **339**, 9-14.

Warne, T., Serrano-Vega, M.J., Baker, J.G., Moukhametzianov, R., Edwards, P.C., Henderson, R., Leslie, A.G., Tate, C.G., Schertler, G.F. (2008). Structure of a β_1-adrenergic G-protein-coupled receptor. *Nature* **454**, 486-491.

Wells, J.A. (1991). Systematic mutational analyses of protein-protein interfaces. *Methods Enzymol.* **202**, 390-411.

Wilson, D.S., Keefe, A.D. (2001). Random mutagenesis by PCR. *Curr. Protoc. Mol. Biol.* **Chapter 8**, Unit8 3.

Zhao, H., Zha, W. (2006). In vitro 'sexual' evolution through the PCR-based staggered extension process (StEP). *Nature protocols* **1**, 1865-1871.

Figure legends

Figure 1. Generation of position-specific randomized GPCR libraries (A) and multiple GPCR mutants (B). (A) Fully randomized position-specific libraries are generated by a 2-step PCR assembly strategy. First, two separate PCR reactions are performed with the GPCR coding sequence (1) as template: With primers p1fw and pNre (2a), the 5'-end of the library N is generated. Primer pNre and pNfw are NNN-randomized in the codon of library position N, thus introducing the desired randomization. For a specific point mutation, primer pNfw and pNre have a defined sequence at the target position. Primer p1fw and p2re introduce restriction sites for subcloning into the expression vector (blue ends). With primers pNfw and p2re (2b), the 3'-end of library N is generated. The resulting PCR products (3a, 3b) are isolated and purified, and used as template for the subsequent assembly PCR (4). Primers p1fw and p2re are used to generate and amplify the full-length library PCR product from the two fragments. The full-length library is purified and subsequently cloned into the expression vector. (B) A triple mutant is assembled from four separate fragment PCRs similar to the position-specific library in (A).

Figure 2. Generation of shuffled GPCR libraries using StEP-PCR. (A) Two (or more) different GPCR templates are used for in vitro DNA shuffling, denoted as seq.1 and seq 2 here (1). By using high numbers of very short StEP-PCR cycles, the flanking primers are only extended by a few nucleotides (3a- 3c) until eventually, a full-length and chimeric GPCR sequence is generated (3d). By template switches between the StEP-PCR cylces, mutations from two templates are combined in one StEP-PCR product (3c). The StEP-PCR product is then purified from an agarose gel (4) and the flanking restriction sites are digested (5) for ligation into the expression vector (6). (B) Recombination efficiency of a StEP-reaction on 10 individual point mutants will suffer from «dilution» of a given mutation with wildtype (wt) from other mutant sequences, and the observed recombination efficiency is much lower than the actual efficiency, since many recombination events will not result in sequence changes.

Figure 3. Selection for high functional expression. Here, a GPCR library is generated from two GPCR templates, denoted as seq. 1 and seq. 2 here, (1) using StEP shuffling (2). The resulting library (3) is electroporated and expressed in *E. coli* DH5α cells (4).The fluorescence-labeled agonist BP-NT (BODIPY-neurotensin(8-13)) is used to label the cells relative to their functional expression levels (5). Highly expressing cells are identified and isolated by fluorescence-activated cell sorting (FACS) (6). Individual selected clones are either grown for single clone analysis (7), or the selected cell pool is subjected to iterative selection rounds with optional reshuffling by StEP (8).

Figure 4. Influence of detergent exchange on thermostability measurements. GPCR variants are solubilized from *E. coli* membranes by DDM (n-dodecyl-β-D-maltopyranoside, black) or DM (n-decyl-β-D-maltopyranoside, grey) and immobilized on

streptavidin-coated magnetic beads. Detergents are exchange by repeated washing and pull-down of the beads in the final detergent buffer. Final detergents are DDM (open circles), UM (n-undecyl-β-D-maltopyranoside, diamonds) or DM (squares). Aliquots of solubilized and rebuffered GPCR are thermally challenged and the remaining ligand binding affinity is analyzed by radioligand binding assay.

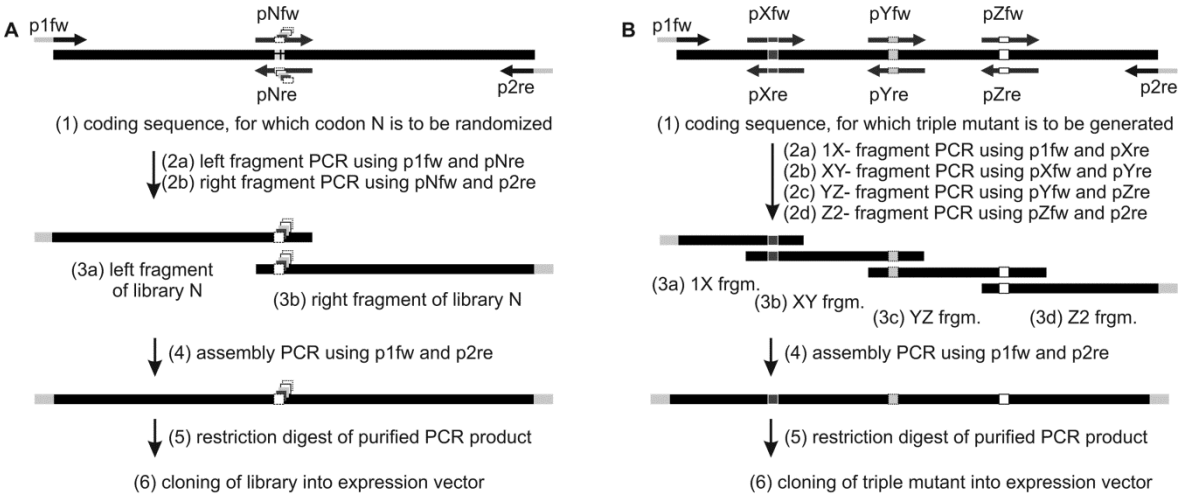
A
p1fw
pNfw
pNre
p2re
(1) coding sequence, for which codon N is to be randomized
(2a) left fragment PCR using p1fw and pNre
(2b) right fragment PCR using pNfw and p2re
(3a) left fragment of library N
(3b) right fragment of library N
(4) assembly PCR using p1fw and p2re
(5) restriction digest of purified PCR product
(6) cloning of library into expression vector
B
p1fw
pXfw
pYfw
pZfw
pXre
pYre
pZre
p2re
(1) coding sequence, for which triple mutant is to be generated
(2a) 1X- fragment PCR using p1fw and pXre
(2b) XY- fragment PCR using pXfw and pYre
(2c) YZ- fragment PCR using pYfw and pZre
(2d) Z2- fragment PCR using pZfw and p2re
(3a) 1X frgm.
(3b) XY frgm.
(3c) YZ frgm.
(3d) Z2 frgm.
(4) assembly PCR using p1fw and p2re
(5) restriction digest of purified PCR product
(6) cloning of triple mutant into expression vector

Figure 1.

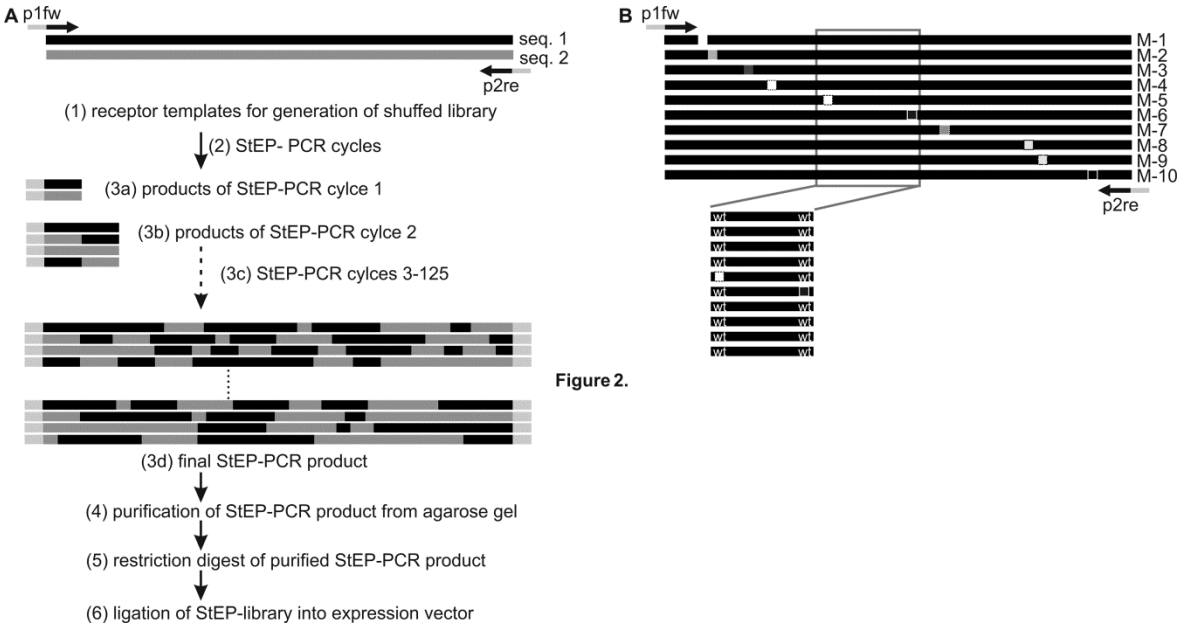

Figure 2.

Figure 2.

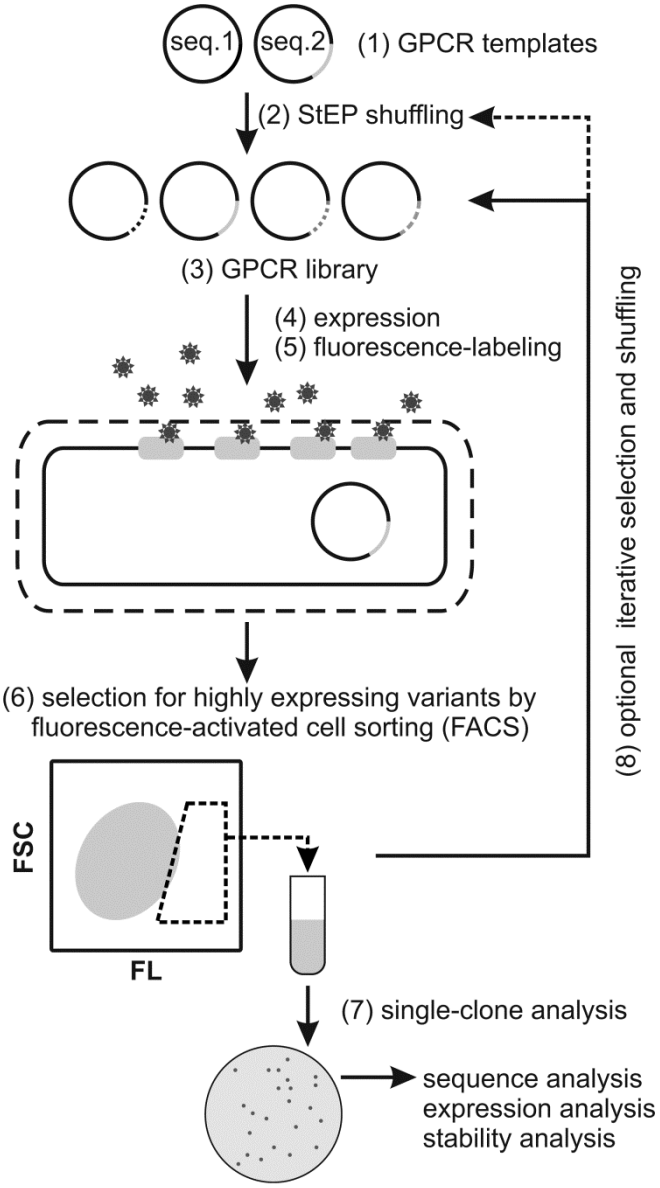
seq.1
seq.2
(1) GPCR templates
(2) StEP shuffling
(3) GPCR library
(4) expression
(5) fluorescence-labeling
(6) selection for highly expressing variants by fluorescence-activated cell sorting (FACS)
FSC
FL
(7) single-clone analysis
sequence analysis
expression analysis
stability analysis
(8) optional iterative selection and shuffling

Figure 3.

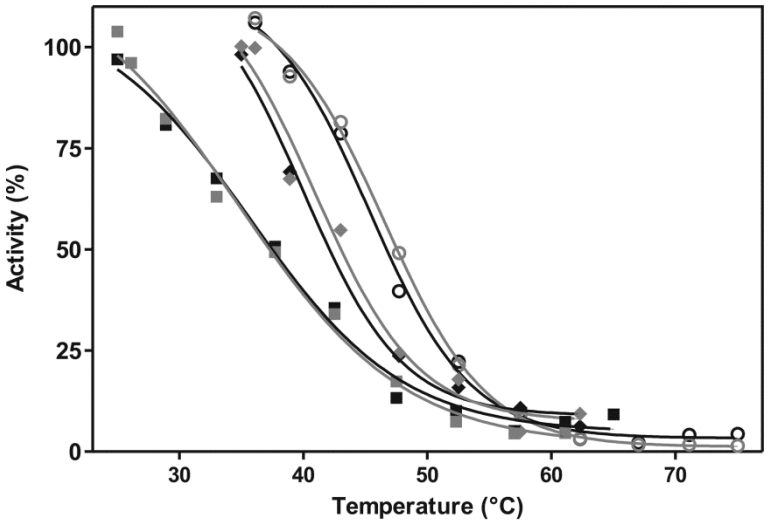

Figure 4.

Chapter 3-A

Critical features for biosynthesis, stability and functionality of a G protein-coupled receptor uncovered by all-versus-all mutations

3-A.1 Published article

PNAS

Critical features for biosynthesis, stability, and functionality of a G protein-coupled receptor uncovered by all-versus-all mutations

Karola M. Schlinkmann[a], Annemarie Honegger[a], Esin Türeci[a], Keith E. Robison[b,1], Daša Lipovšek[b,2], and Andreas Plückthun[a,3]

[a]Department of Biochemistry, University of Zurich, 8057 Zurich, Switzerland; and [b]Codon Devices, Inc., Cambridge, MA 02139

Edited by David Baker, University of Washington, Seattle, WA, and approved May 1, 2012 (received for review February 8, 2012)

The structural features determining efficient biosynthesis, stability in the membrane and, after solubilization, in detergents are not well understood for integral membrane proteins such as G protein-coupled receptors (GPCRs). Starting from the rat neurotensin receptor 1, a class A GPCR, we generated a separate library comprising all 64 codons for each amino acid position. By combining a previously developed FACS-based selection system for functional expression [Sarkar C, et al. (2009) *Proc Natl Acad Sci USA* 105:14808–14813] with ultradeep 454 sequencing, we determined the amino acid preference in every position and identified several positions in the natural sequence that restrict functional expression. A strong accumulation of shifts, i.e., a residue preference different from wild type, is detected for helix 1, suggesting a key role in receptor biosynthesis. Furthermore, under selective pressure we observe a shift of the most conserved residues of the N-terminal helices. This unique data set allows us to compare the in vitro evolution of a GPCR to the natural evolution of the GPCR family and to observe how selective pressure shapes the sequence space covered by functional molecules. Under the applied selective pressure, several positions shift away from the wild-type sequence, and these improve the biophysical properties. We discuss possible structural reasons for conserved and shifted residues.

deep sequencing | directed evolution | protein stability | stability in detergents

Very few residues are strictly conserved in the family of G protein-coupled receptors (GPCRs), the eukaryotic seven-transmembrane (TM) receptors that regulate many cellular events in response to chemically diverse ligands. GPCRs undergo conformational changes in response to agonist binding, and need to maintain a delicate balance between stability in the membrane, flexibility required for signaling, and the subsequent steps of receptor inactivation and degradation or recycling (1). These constraints limit stability and at least partly explain the paucity of structural information from this large family, despite herculean efforts.

Structural studies have been reported only recently (2–4), mostly for naturally stable receptors or including engineered domain insertions and/or trial-and-error optimization of the protein sequence (5, 6; summarized and reviewed in ref. 7). The limited number of solved receptor structures and the redundancy of the datasets do not reflect the functional diversity of GPCRs and still limit general conclusions about their activation mechanism, and thus about fundamental rules for agonist and antagonist design.

Most GPCRs are not amenable to functional and structural studies, because their biophysical properties are imposing major roadblocks to earlier steps in the characterization process, expression, purification, and detergent stability.

We wished to determine the critical information content in the GPCR sequence and structure for their biophysical properties and compare this to the conserved sequence features of the whole family and to experimentally test and expand previously proposed architectural rules about membrane proteins. Here, rat neurotensin receptor 1 (rNTR1)-D03 (termed here D03) was used as a model. D03 is a variant of rNTR1 that had been obtained previously by in vitro evolution of the wild type (8). D03 displays higher functional expression and detergent stability than wild type (5,000 vs. 500 receptors per cell), thus allowing reliable detection and interpretation of small changes in expression levels and detergent stability. However, despite increased expression level of D03 and improved detergent stability of the evolved variant D03 (8) or the engineered variant NTS1-7m (9), the critical structural features might not yet have been identified, requiring an in-depth and comprehensive mutagenic analysis.

Previous mutagenesis studies have relied on either error-prone PCR (8, 10) or spiked oligonucleotides (11) and could thus not cover the complete mutant space. More importantly, the studies using reporter genes have not quantitated stability or expression level (8, 10, 11). We have therefore undertaken a complete analysis of mutant space to explore the biosynthesis and biophysical properties of a GPCR.

Results and Discussion

Directed Evolution System for GPCRs. A total of 376 DNA libraries were generated by separately randomizing amino acid positions 43–418 of rNTR1-D03 (8) into all 64 codons. Sequencing of individual clones from every second library was performed before selection to confirm the library design and quality. This analysis of about half of all libraries showed an even distribution of the four bases in all codon positions (Table S1), consistent with full randomization. Libraries were expressed in *Escherichia coli*, exposed to a fluorescence-labeled agonist of rNTR1, BODIPY-neurotensin, in a buffer facilitating ligand penetration through the outer membrane (8). After ligand binding to the native GPCR located in the inner membrane, the 1% highest-binding cells were selected by FACS. This selection for ligand binding directly selects for efficient production, insertion, and correct folding of the GPCR in the inner membrane of *E. coli*. The system was tested and adjusted in a proof-of-principle experiment using the 64-codon library of residue $Y347^{7.31}$ that is critical for binding of the agonist neurotensin (12) (Figs. S1 and S2). We use the sequential numbering in plain text and the Ballesteros–Weinstein numbering as a superscript; here, the first number denotes the helix in sequential order, and the second number defines the position within the helix, where the most conserved position of a

Author contributions: K.M.S., K.E.R., D.L., and A.P. designed research; K.M.S., E.T., and K.E.R. performed research; K.M.S. and A.H. analyzed data; and K.M.S., A.H., and A.P. wrote the paper.

The authors declare no conflict of interest.

This article is a PNAS Direct Submission.

[1]Present address: Warp Drive Bio, Cambridge, MA 02142.

[2]Present address: Adnexus, a Bristol-Myers Squibb R&D Company, Waltham, MA 02453.

[3]To whom correspondence should be addressed. E-mail: plueckthun@bioc.uzh.ch.

This article contains supporting information online at www.pnas.org/lookup/suppl/doi:10.1073/pnas.1202107109/-/DCSupplemental.

helix is denoted as x.50, counting downward toward the N terminus and upwards to the C terminus (13).

Standard Sanger full-length sequencing of 6–20 selected clones per randomized position ensured that no spurious additional mutations influenced the phenotype (4,298 sequences; Fig. S3). Very few mutations were found outside the randomized positions. Ultradeep 454 sequencing yielded 890,381 high-quality reads, each covering about 180–250 bp (*SI Text*, Figs. S4 and S5, and Table S2). After processing, 518,228 sequences deviating from the wild type by exactly one codon in a randomized position remained, covering 363 of the 376 positions of rNTR1-D03 at an average of 1,428 independent sequences per randomized position.

Because libraries randomized in different positions had to be combined for 454 sequencing, only 63 of the 64 codons could be quantified. The frequency of the wild-type codon was obscured (Fig. S5). However, we could determine the wild-type codon conservation from the frequencies of synonymous codons. Based on these results, the mutational tolerance in each position was addressed by calculation of rmsd (Fig. 1). The rmsd (see *SI Text* and Eq. **S1** for detailed description) compares the observed amino acid frequency distribution after selection with

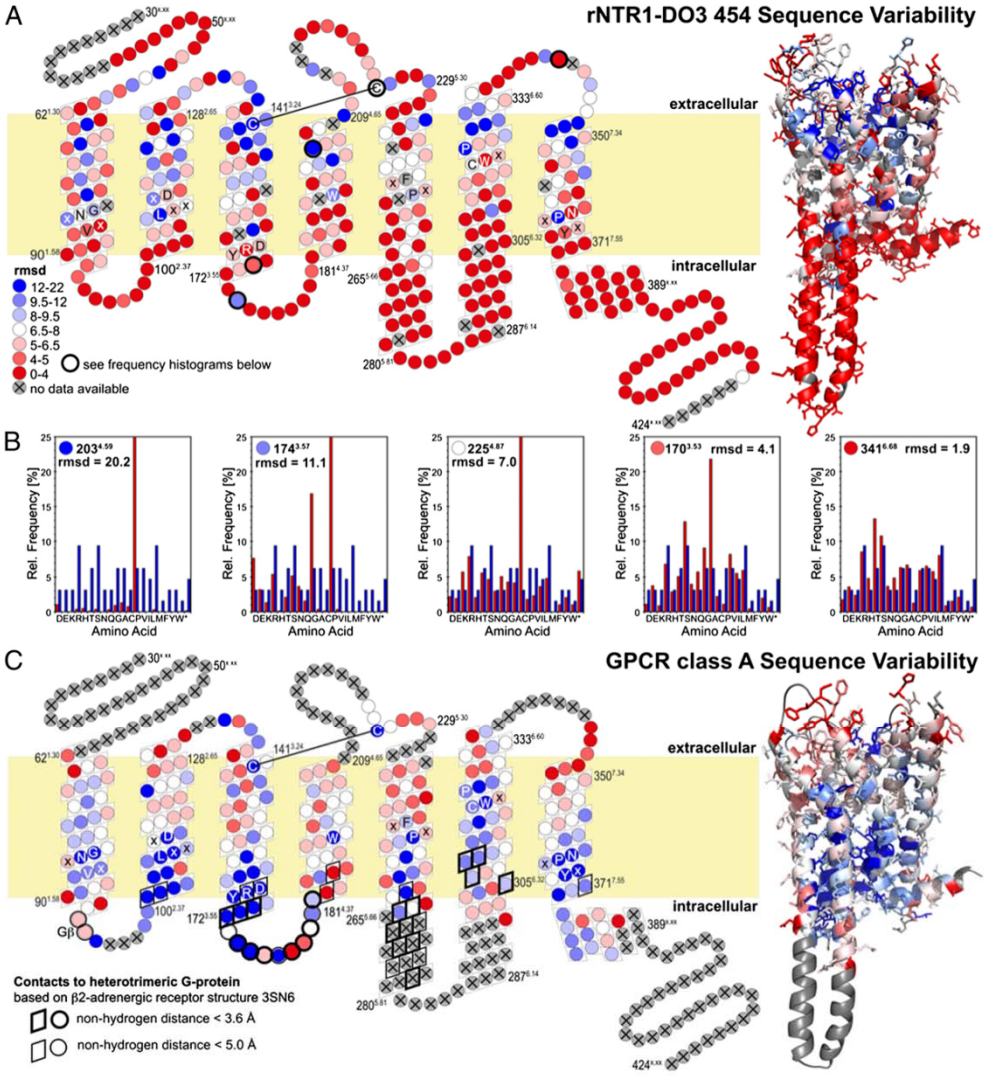

Fig. 1. Sequence variability of rNTR1-D03 (*A*) and GPCR class A consensus (*C*). Positions in a snake plot (*Left*) and homology model of rNTR1-D03 (*Right*) are color coded in a gradient from red for high mutational tolerance to blue for low tolerance (see *SI Text* for details). Letters indicate conserved sequence motifs in each helix. Positions that were not randomized (flexible N terminus and C terminus) or for which no 454 data were obtained (13 transmembrane positions) are coded in gray. (*B*) Histograms of observed amino acid frequencies (red) compared with the amino acid frequency distribution expected for an unbiased library (blue) illustrate the significance of the different rmsd levels.

the input amino acid frequency distribution (that of an unbiased NNN codon randomization). The rmsd reflects the selective pressure shaping the amino acid distribution in a given position. Sanger and 454 datasets agree well. On average, synonymous codons were used with equal frequency (Fig. S6), indicating a purely phenotypic selection at the protein level, e.g., membrane insertion, folding, and stability within the membrane and deleterious effects of misfolded proteins on the host organism. Thus, we did not detect any effects of rare codons.

According to the ultradeep sequencing analysis after selection, positions are classified as conserved, as shift positions, or as not significant, the latter describing a broad amino acid distribution. A shift position focuses the selection on an amino acid (or very few) *different* from the wild type. Both conserved and shift position are subclassified as robust or weak, where weak effects are observed only after correction for codon bias, and robust effects under any condition (details are given in *SI Text*).

Very few amino acids are globally conserved within the GPCR family, and amino acid distributions are broad for most positions in the 454 results (Fig. S7). Structurally relevant glycines and prolines, the conserved disulfide bond and very few other residues are immutable in rNTR1 and GPCRs in general (Fig. 2 and Fig. S8). The different selection pressures, toward efficient biosynthesis, membrane insertion, and folding to form a functional ligand binding site in *E. coli* (rNTR1-D03 libraries), or toward finely regulated signaling competence in response to different ligands (in the case of the GPCR family evolved in nature), are reflected in different patterns of sequence constraints. In general, the GPCR class A consensus shows a strong conservation of the intracellular helix ends, pointing to their importance for downstream signaling interactions. G protein contact residues, conserved in the GPCR family, are variable in our results, whereas residues involved in ligand contact are conserved in our dataset. Residues equally conserved in both systems and those shifting away from the rNTR1 sequence presumably reflect the constraints of efficient folding and stability. The statistically robust 454 data set provides a unique opportunity to assess the relevance of structural rules (14–16), deduced from early membrane protein structures and statistical analysis of primary sequences (Fig. S9). Aromatic residues are often found to contact the periphery of the membrane, whereas aliphatics contact the hydrophobic interior or the bilayer. Basic residues are found at the cytoplasmic ends of transmembrane helices. rNTR1 obeys this last rule, displaying a strong accumulation and preference of basic amino acids at the cytoplasmic helix ends, especially at TM1/IL1 and TM5. TM5 is connected to TM6 by a long intracellular loop, and the increase in basic amino acids in TM5 might help to define the helix length and position the helix within the lipid bilayer through interactions with the phospholipid head groups.

Of particular interest are the shift positions (Fig. 3). Strong shift positions are exclusively located within the TMs. Both lipid-exposed side chains and those pointing into the helical interspace are observed to shift. Shifted residues form clusters, defining specific locations important for protein folding and stability, with the shift mutations releasing a previous constraint present in the wild-type sequence. Clustered mutations represent different solutions to the same problem, and may thus not be additive.

We find an accumulation of shifts in TM1 and TM2, whereas TM3, known to be involved in structural rearrangements upon activation (1, 17), remains highly conserved. TM1 shows three independent gains of aromatic amino acids pointing toward the lipid interface at the N terminus, at V65W$^{1.33}$, L66F$^{1.34}$, or A69F$^{1.37}$. This gain of aromatic side chains might enhance protein integration into the lipid bilayer during positioning of the first TM helix in the lipid bilayer. Considering that membrane protein biosynthesis is crucially dependent on correct helix folding, targeting, and insertion into the lipid bilayer, we hypothesize that the accumulation of shifts in the N terminus and the most N-terminal helices is an adaptation to that process, and this effect might be highly

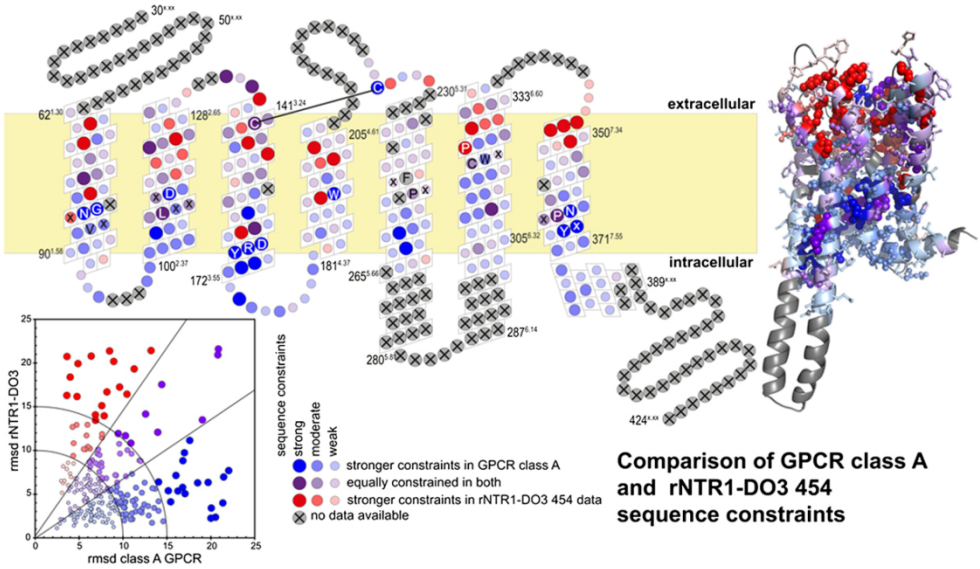

Fig. 2. Correlation between sequence constraints in natural GPCRs and in the rNTR1-D03 454 sequencing experiment. Colors indicate whether the amino acid distribution in a given position is equally constrained in both systems (purple), more constrained in natural class A GPCR sequences (blue), or in the deep sequencing from rNTR1-D03 (red). The size of the circles indicates the constraints imposed by the respective system; large circles indicate positions with high constraints.

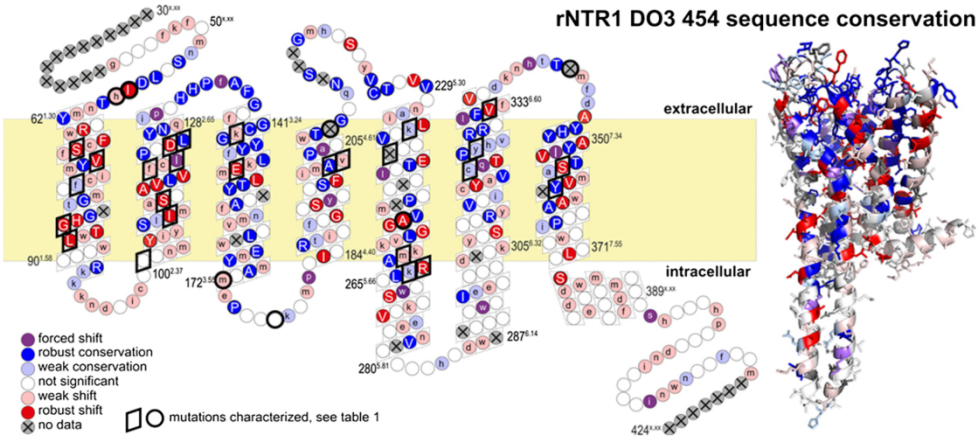

Fig. 3. Sequence shifts. Positions are colored according to conservation (blue) or shift (red) away from the rNTR1-D03 sequence. Uppercase letters refer to robust effects and lowercase letters to effects obscured by codon bias in the raw amino acid consensus. The strength of the conservation or shift is given by the rmsd of the amino acid distribution from the input distribution as shown in Fig. 1*A* and listed in Fig. S7. For the highlighted positions, the influence of mutations on the performance of the receptor has been further characterized (Table 1).

relevant for increased GPCR expression levels (Fig. 3). This particular importance of the N-terminal helices was not apparent from previous analyses of residue preferences in membrane proteins.

In TM7, we find a loss of aromatic residues at positions F346A$^{7.26}$, F350A$^{7.34}$, and F358V$^{7.42}$, approximately within two helical turns from each other. According to our model of rNTR1, F358$^{7.42}$ is located close in space to the proline-induced kink in TM6, and the shift F358V$^{7.42}$ might relieve a steric constraint and lead to optimized helix packing. Because TM7 contributes specifically to ligand binding, a comparison with the GPCR consensus is more difficult. Y347$^{7.31}$, for example, is crucial for ligand binding in rNTR1 (12). The GPCR consensus shows an additional proline at position 362$^{7.46}$ that will substantially influence the structural architecture of TM7, but is absent in rNTR1.

GPCRs share high conservation of key signature motifs in every helix (highlighted in Fig. 2; Table S3) that are common to the GPCR family and reflect structural features (e.g., proline-determined helical architecture) or the common signaling process [E/DRY motif in TM3 (E166$^{3.49}$, R167$^{3.50}$, and Y168$^{3.51}$ in rNTR1) for receptor activation] (18). As explained above, the Ballesteros–Weinstein nomenclature (added in superscript) refers to 50 as the most conserved position of a helix. Unexpectedly, we find that the key residues of the first three helices are shift positions, i.e., N82H$^{1.50}$, D113S$^{2.50}$, and R167L$^{3.50}$. N82H$^{1.50}$ and D113S$^{2.50}$ are close in space according to our homology model, and these mutations might be alternative solutions to the same problem of an unsatisfied salt bridge. D113$^{2.50}$ was shown to be responsible for the sodium-sensitivity of the rNTR1 receptor (19). R167L$^{3.50}$ is part of the E/DRY motif for which a crucial role, the "ionic lock," in receptor activation has been proposed (17). The fact that we find GPCR signature residues shift is rather surprising, and suggests that functionally required conformational flexibility of the receptor may limit its biophysical stability. In vivo, these signature residues might be required to maintain the delicate balance of receptor-signaling networks, and even facilitate GPCR degradation after endocytosis. When studied in an isolated system, however, these residues are identified as roadblocks for recombinant overexpression and detergent stability. The phenotype of rNTR1-D03 is determined by nine mutations, originating from random mutagenesis on the wild type (8). Among these mutations, we find R167L$^{3.50}$ to improve functional expression but to decrease signaling competence (8). Interestingly, we find the D03 mutations to be mostly confirmed after full randomization (Figs. S3 and S7). For R167$^{3.50}$, we find only mild preference of aliphatic residues over R, allowing us to reintroduce R167$^{3.50}$ and thus to restore signaling capability without compromising functional expression levels, as shown for D03 (8).

Several mutations, based on the D03 background, were selected for further characterization (Table 1). For all mutants tested, expression levels were as high as or higher than rNTR1-D03, indicating that no false-positive selection result was observed. A86L$^{1.54}$, I253A$^{5.54}$, and F358V$^{7.42}$ significantly increase the stability of the receptor in n-dodecyl-β-D-maltopyranoside (DDM), a mild detergent used for solubilization and functional studies of many GPCRs, increasing the apparent T_m by 7.5, 3.5, and 4°, respectively, in the absence of ligand (Table 1). F358A$^{7.42}$, a nonenriched negative control, had no effect on receptor stability, clearly showing the specific effect of the valine substitution. These results clearly demonstrate the power of the full randomization and selection applied here, in contrast to an alanine scan (9); the latter would only have investigated I253A$^{5.54}$, but discarded F358A$^{7.42}$ as unfavorable, and thus would not have discovered F358V$^{7.42}$.

For these three shifts, we find a correlation between increased functional expression levels, which report on the biophysical properties in the bilayer, and stability in detergents. This overlap is intriguing regarding the fact that selection for functional expression reflects the sum of correct biosynthesis; efficient and functional membrane integration; stability in the lipid bilayer; resistance to degradation; and the potential influence of misfolded species on survival and growth of the host organism, whereas stability within a detergent micelle is governed by the influence of the small detergent molecules on the structure, potentially penetrating into the core, or allowing some access to solvent molecules. The chemical nature of the detergent, protein packing, and helical stability will all influence the observed stability, and some of the selected mutations have improved stability in detergents and functional expression.

I253A$^{5.54}$ is located in the core of TM5, facing TM3 and TM6. Previous functional and structural studies on GPCRs have shown an important role for TM5 in receptor activation (1), because TM5 contains crucial residues that, upon binding of agonist, induce local structural rearrangements that presumably lock the receptor in the activated state (1, 20). I253A$^{5.54}$, located one

Table 1. Detergent stability in DDM and expression levels of single-shift mutants

Mutation	Conservation	Rmsd 454	T_m, °C (n = 2)*	T_m, ΔD03, °C	Receptors per cell relative to D03, % (n = 3)
T68S	Robust shift	16.7	28.6	−2.5	99 ± 43
E124D	Robust shift	15.1	28.0	−3.2	
V57I	Robust shift	11.9	31.2	0.1	
S83G	Robust shift	10.2	32.0	0.9	144 ± 9
T354S	Robust shift	8.6	28.7	−2.4	129 ± 1
C332V	Robust shift	7.2	28.7	−2.5	174 ± 7
N262R	Robust shift	6.5	28.8	−2.4	
D113A	Robust shift	6.4	28.1	−3.0	116 ± 8
D113S	Robust shift	6.4	29.6	−1.5	145 ± 19
D150E	Robust shift	6.4	30.5	−0.6	
I70V	Robust shift	6.3	28.7	−2.4	114 ± 26
A110L	Robust shift	5.7	28.4	−2.7	82 ± 17
I253A	Robust shift	5.2	34.4	3.3	175 ± 19
A86L	Robust shift	4.9	38.4	7.3	149 ± 25
R143K	Weak shift	12.9	30.8	−0.4	
L119F	Weak shift	10.1	31.9	0.8	134 ± 21
I260A	Weak shift	7.1	28.8	−2.4	
I202L	Weak shift	5.3	28.0	−3.1	121 ± 10
I202S	Weak shift	5.3	30.8	−0.3	75 ± 27
N58R	Weak shift	4.2	30.9	−0.3	
C172R	Weak shift	2.9	28.6	−2.5	
T101R	Not significant	3.4	29.4	−1.8	131 ± 5
A177H	Not significant	3.1	29.2	−1.9	123 ± 13
K263R	Weak conservation	4.7	30.8	−0.4	152 ± 17
Y324L	Weak conservation	6.3	24.6	−6.6	164 ± 21
C320L	Weak conservation	7.0	26.8	−4.4	152 ± 10
K235R	Weak conservation	8.7	30.8	−0.4	148 ± 21
F75L	Weak conservation	10.8	27.5	−3.6	108 ± 7
F358V	Robust conservation	4.8	34.8	3.7	179 ± 23
F358A	Robust conservation	4.8	29.7	−1.5	
L125V	Robust conservation	7.2	28.1	−3.1	143 ± 14
A201S	Robust conservation	14.0	27.2	−4.0	180 ± 26
M121L	Forced shift	11.7	29.5	−1.7	158 ± 10
M208V	No data		29.6	−1.5	139 ± 7
V240L	No data		28.4	−2.7	
F342A	No data		30.1	−1.0	
D03			31†		100 ± 13

*Average error, 2 °C.
†n = 8.

helical turn away from the structurally conserved proline in TM5, might reduce conformational flexibility of the receptor, thereby increasing stability. In contrast to that, we assume that $A86L^{1.54}$ and $F358V^{7.42}$ improve detergent stability by addressing helix packing. Based on our homology model, $A86L^{1.54}$ and $F358V^{7.42}$ are solvent accessible, and a compact helix fold might reduce the susceptibility toward detergent penetration into the helical core.

Both conformational stabilization and optimized helix interactions reduce the susceptibility of the receptor toward denaturation by detergents, and these effects are certainly not rNTR1 specific, but of general importance for membrane protein stabilization. However, not all of the mutations that increase functional expression also affect stability, or the reverse (Table 1). We thus hypothesize that a large number of shift residues improve interactions within the receptor that are critical for efficient and correct biosynthesis, thus increasing functional expression in the lipid bilayer, whereas only a subset of shift residues affect interactions within the folded receptor, thus leading to higher detergent resistance.

The combination of saturation mutagenesis, FACS selection, and analysis by 454 sequencing has produced unprecedented insight into the contribution of every receptor position on receptor functionality, stability in the natural bilayer, and in detergents. Membrane proteins maintain a delicate balance between expression, function, and stability. In vivo evolution of GPCRs and membrane proteins in general shows strong selective and functional pressure (21). The high tolerance toward randomization, and especially the high frequency of shifts observed in this study, including signature residues in helices, is intriguing and of utmost importance for our understanding of membrane proteins. Though our in vitro evolutionary approach covers the full mutant space in one library, in vivo evolution would require neutral intermediates, some of which might not be tolerated in case of integral membrane proteins. Our results show that rNTR1, and presumably other GPCRs, offer ample opportunity for engineering, without compromising protein activity.

Several trends uncovered here might be of general applicability: clusters that evolve toward the class A consensus indicate the validity of the rules of preferential location of aromatic amino acids (16) and positive charges (14). These trends might be easily transferable to other GPCRs. Furthermore, the importance of the N-terminal helices had not previously been highlighted: the location of some of the most prominent shifts within TM1 indicates that functional expression may be at least

partially limited by cotranslational membrane insertion via the SecYEG translocon in *E. coli*.

Some receptor residues, among them key GPCR signature residues, might be conserved mainly to maintain a fine-tunable receptor-signaling network, because the receptor needs to be able to exist in two conformational states: signaling active and inactive. Though the mutations investigated, even when combined, maintain signaling at high agonist concentration, they show higher levels of activity at low agonist concentrations than wild type (22). Thus, selection may have favored mutants that shift the balance toward the activated state, because selection was carried out in the presence of agonist. This selection for biophysical behavior maintained receptor-activated nucleotide exchange at the G proteins (22), but not the ability of the GPCR to fully turn off in the absence of agonist.

It is interesting to note that mutations selected in *E. coli* also lead to improved expression in eukaryotic hosts (8, 22). Some shift mutations significantly increase the stability of rNTR1 in short-chain detergents, presumably by controlling access of detergent molecules (22).

We believe that this systematic and evolutionary approach to the biophysical properties of the GPCR family will greatly help equally systematic structure determination efforts across this important family, and also delineate the biophysical constraints on the natural evolution of this family. These results may be thus of interest for other membrane proteins, and could be the basis for rational design of membrane proteins for higher stability in detergent solution for more efficient drug screening and structural studies.

Methods

Library Design and Synthesis. A total of 376 different libraries were generated for receptor positions 43–418 by a PCR approach using oligos with NNN-diversified codons, generating a position-specific 64-codon library with at least 10- to 20-fold oversampling. Each library was subcloned into the expression vector pRGD03 (8, 23). The absence of any bias in the randomized library was confirmed by sequencing individual variants before selection.

Library Expression and Selection. Each library was separately expressed in *E. coli* DH5α for 20 h at 20 °C. After expression, cells were labeled using BODIPY-neurotensin, a fluorescence-labeled ligand of rNTR1. The outer membrane was permeabilized by a Tris·HCl salt buffer to allow for ligand binding (1–2 h at 4 °C). The 1% highest fluorescent cells were selected using FACS and recovered for sequence analysis.

Sequencing Analysis and Characterization. Per library, 6–20 single selected clones were analyzed by Sanger sequencing. The plasmid DNA of the selected variant pool was isolated and analyzed by ultradeep 454 sequencing. Expression levels were determined by radioligand binding assays, and detergent stability was assessed with protein variants isolated from the *E. coli* membrane according to Sarkar et al. (8).

ACKNOWLEDGMENTS. We thank Anette Schütz and Malgorzata Kisielow [Flow Cytometry Laboratory, Swiss Federal Institute of Technology Zurich (ETHZ)/University of Zurich (UZH)] for valuable technical support during FACS selections, and Jan Furrer and Michael Hohl for help during the selections for high functional expression. We also thank the following former Codon Devices, Inc., employees: Patti Aha, Subhayu Basu, Katie Black, Brad Chapman, Eric Devroe, Chris Emig, David Rappolli, and Shervin Riahi for method development and for assembling the position-specific libraries; Kathy Galle for project management; and Brian Baynes for support of this collaboration. Further, we thank the Codon Devices DNA assembly, automation, and sequencing teams for technical support of library construction and validation, which were funded by the Codon Devices, Inc., research and development budget. ET was supported by a postdoctoral fellowship by the Roche Research Foundation. This work was supported by grants from the National Center of Competence in Research Structural Biology funded by the Swiss National Science Foundation (A.P.).

1. Deupi X, Kobilka B (2007) Activation of G protein-coupled receptors. *Adv Protein Chem* 74:137–166.
2. Chien EY, et al. (2010) Structure of the human dopamine D3 receptor in complex with a D2/D3 selective antagonist. *Science* 330:1091–1095.
3. Wu B, et al. (2010) Structures of the CXCR4 chemokine GPCR with small-molecule and cyclic peptide antagonists. *Science* 330:1066–1071.
4. Jaakola VP, et al. (2008) The 2.6 Ångstrom crystal structure of a human A2A adenosine receptor bound to an antagonist. *Science* 322:1211–1217.
5. Rosenbaum DM, et al. (2007) GPCR engineering yields high-resolution structural insights into beta2-adrenergic receptor function. *Science* 318:1266–1273.
6. Cherezov V, et al. (2007) High-resolution crystal structure of an engineered human beta2-adrenergic G protein-coupled receptor. *Science* 318:1258–1265.
7. Katritch V, Cherezov V, Stevens RC (2012) Diversity and modularity of G protein-coupled receptor structures. *Trends Pharmacol Sci* 33:17–27.
8. Sarkar CA, et al. (2008) Directed evolution of a G protein-coupled receptor for expression, stability, and binding selectivity. *Proc Natl Acad Sci USA* 105:14808–14813.
9. Shibata Y, et al. (2009) Thermostabilization of the neurotensin receptor NTS1. *J Mol Biol* 390:262–277.
10. Li B, et al. (2007) Rapid identification of functionally critical amino acids in a G protein-coupled receptor. *Nat Methods* 4:169–174.
11. Sommers CM, Dumont ME (1997) Genetic interactions among the transmembrane segments of the G protein coupled receptor encoded by the yeast STE2 gene. *J Mol Biol* 266:559–575.
12. Barroso S, et al. (2000) Identification of residues involved in neurotensin binding and modeling of the agonist binding site in neurotensin receptor 1. *J Biol Chem* 275:328–336.
13. Ballesteros JA, Weinstein H (1995) Integrated methods for the construction of three-dimensional models and computational probing of structure function relations in G protein-coupled receptors. *Meth Neurosci* 25:366–428.
14. von Heijne G (1994) Membrane proteins: From sequence to structure. *Annu Rev Biophys Biomol Struct* 23:167–192.
15. Heijne G (1986) The distribution of positively charged residues in bacterial inner membrane proteins correlates with the trans-membrane topology. *EMBO J* 5: 3021–3027.
16. Kelkar DA, Chattopadhyay A (2006) Membrane interfacial localization of aromatic amino acids and membrane protein function. *J Biosci* 31:297–302.
17. Kobilka BK (2007) G protein coupled receptor structure and activation. *Biochim Biophys Acta* 1768:794–807.
18. Rovati GE, Capra V, Neubig RR (2007) The highly conserved DRY motif of class A G protein-coupled receptors: Beyond the ground state. *Mol Pharmacol* 71:959–964.
19. Martin S, Botto JM, Vincent JP, Mazella J (1999) Pivotal role of an aspartate residue in sodium sensitivity and coupling to G proteins of neurotensin receptors. *Mol Pharmacol* 55:210–215.
20. Kobilka BK, Deupi X (2007) Conformational complexity of G-protein-coupled receptors. *Trends Pharmacol Sci* 28:397–406.
21. Schöneberg T, Hofreiter M, Schulz A, Römpler H (2007) Learning from the past: Evolution of GPCR functions. *Trends Pharmacol Sci* 28:117–121.
22. Schlinkmann KM, et al. (2012) Maximizing detergent stability and functional expression of a GPCR by exhaustive recombination and evolution. *J Mol Biol*, in press.
23. Tucker J, Grisshammer R (1996) Purification of a rat neurotensin receptor expressed in *Escherichia coli*. *Biochem J* 317:891–899.

3-A.2 Supporting Information

Supporting Information

Schlinkmann et al. 10.1073/pnas.1202107109

SI Text

Position Nomenclature. Positions of rat neurotensin receptor 1 (rNTR1) are identified by their residue type, using the one-letter amino acid code, and by their sequential rNTR1-position (e.g., N82). The Ballesteros–Weinstein nomenclature is given as a superscript, in this example $N82^{1.50}$, with the first number (before the period) identifying the transmembrane helix (1–7), and the second number (after the period) describing the position within the helix, where 1.50 is assigned to the most conserved position of helix 1. See Ballesteros and Weinstein (1) for details. Thus, $N82A^{1.50}$ denotes a mutation from Asn to Ala in position 82, located in helix 1, very conserved, and located near the middle of the helix.

Starting Construct. The starting construct NTR1-D03 (abbreviated D03) comprises amino acids 43–424 of rNTR1 (UniProtKB release no. P20789) fused between the C terminus of maltose binding protein and the N terminus of thioredoxin to enhance expression in *Escherichia coli*. The fusion protein contains tobacco etch virus protease cleavage sites on both ends of the receptor and a C-terminal His_{10} tag. Through multiple rounds of error-prone PCR followed by FACS selection, wild-type rNTR1 had acquired nine mutations ($H103D^{2.40}$, $H105Y^{2.42}$, $A161V^{3.44}$, $R167L^{3.50}$, $R213L^{4.69}$, $V234L^{5.35}$, $H305R^{6.32}$, $S362A^{7.46}$, and $S417C^{8.01}$) that enhanced expression in *E. coli* from 500 to 5,000 receptors per cell (2). This enhanced expression level was needed for robust selection, and thus for the experiments reported here.

The results of the full randomization and selection applied here are especially interesting for the D03-specific mutations, because for each position the D03 residue and the wild-type residue are compared side by side, and are in direct competition. Interestingly, Sanger and 454 sequencing results verified the selection of these mutations: $R213L^{4.69}$, $V234L^{5.35}$, and $S362A^{7.46}$ were confirmed as robust shifts, and $A161V^{3.44}$ and $H105Y^{2.42}$ as weak shifts. $H305R^{6.32}$ preferred K after correcting for codon bias, and $H103D^{2.40}$ preferred either D or N. $R167L^{3.50}$ significantly decreased the signaling capability of the receptor, because $R167^{3.50}$ is the key position of the E/DRY motif conserved throughout all G protein-coupled receptors (GPCRs). As discussed in the main text, we found only a mild preference of aliphatic residues over Arg, which allowed us to reconstitute the E/DRY motif and signaling competence in the evolved mutants without compromising stability or functional expression levels. S417 was found to be a promiscuous position.

Library Design and Cloning. To construct the 376 libraries used in this study, the codons encoding NTR1-D03 residues 43–418 were randomized by replacing them, one at a time, with the diversified trinucleotide NNN, where N stands for an equimolar mixture of A, G, C, and T. Depending on the position of the diversified codon relative to the 5′ and 3′ ends of the gene, one of two PCR-based methods was used.

To randomize codons distant from the two ends, two mutagenic oligonucleotides per diversified codon were designed. The first mutagenic oligonucleotide contained the diversified NNN sequence at the targeted codon, but still hybridized with the wild-type D03 sequence with a T_m of 55–65 °C. A second oligonucleotide was designed to hybridize to either the region 5′ of the NNN on the first oligonucleotide, or else form the reverse complement of the first oligonucleotide, including the NNN region (Fig. S1*A*). Each of these oligonucleotides was paired with the appropriate amplification oligonucleotide hybridizing at the end of the gene and encoding one of the two cloning sites (p1fw and p2re; see Table S2 for primer sequences), resulting in PCR amplification of half of the D03 gene. The PCR products of the two separate amplification reactions were then combined and extended to generate the full-length D03 gene containing a single diversified codon. The full-length product was amplified further using 5′-biotinylated primers, which contained recognition sites for the type IIS endonuclease BsmBI, the cleavage with which would generate sticky ends compatible with BamHI and XmaI restriction site overhangs.

The amplification product was digested with BsmBI, any remaining undigested fragment and cleaved overhangs were removed by adding streptavidin and filtering the mixture, and the digested and purified DNA fragments were ligated into the acceptor vector, pRG-del. This acceptor vector is a derivative of pRGD03 (2) in which the BamHI-XmaI fragment encoding D03 has been replaced with a stuffer sequence containing multiple restriction sites (Fig. S1*B*). To clone each amplified full-length library into the acceptor vector, the acceptor vector was first digested with NotI, XmaI, and BamHI, and dephosphorylated with calf intestine alkaline phosphatase (all from New England Biolabs), then purified. The cutting with NotI would destroy intact stuffer fragment and thus prevent it from religation.

To randomize codons 43–50 and 418, all of which are close to one of the two cloning sites, a mutagenic oligonucleotide was designed to contain both the cloning site and an NNN sequence at the targeted site. A second, nonmutagenic oligonucleotide was designed to hybridize to the opposite terminus of the gene. In addition, both oligonucleotides contained the recognition site for BsmBI, the cleavage which would generate sticky ends compatible with overhangs produced by BamHI and XmaI. The two oligonucleotides were used to amplify full-length D03 from wild-type template; the resulting diversified fragment was further amplified using primers that also contained 5′ biotin. As described above, the amplification product was digested with BsmBI, purified, and ligated into pRG-del.

To confirm that library diversity conformed to the design and was free of bias, a representative subset of library variants was sequenced by Sanger sequencing. On average, every second naïve library was further analyzed by sequencing of individual clones (219 libraries). Sequences of a total of 2,170 clones from naïve (unselected) libraries (on average, 13 clones per library) were shown to contain an even distribution of the four bases in all codon positions (Table S1), consistent with full randomization. The observed codon distribution was found to be consistent with unbiased randomization. No bias toward any codon, especially the wild-type codon, was detected. Also after selection, the frequencies of synonymous codons were very similar, with one exception. In the data derived from 454 sequencing, the use of the CCC codon appears low (Fig. S6); in fact, this is an artifact of sequence evaluation, because 12 of 19 prolines in rNTR1 are encoded by CCC. Because the wild-type codon (here CCC) is obscured in our evaluation of the 454 sequencing reaction and, additionally, substitutions to proline are tolerated only at very few positions, proline codons are rarely found, and thus other positions do not contribute additional CCC codons.

For ligation, 33 ng digested and purified DNA library PCR product was mixed with 55 ng digested and purified vector pRG-del and ligated for 16 h at 16 °C in the presence of 0.25 units of T4 DNA Ligase (Invitrogen). The ligation mix was purified using StrataClean Resin (Stratagene), and *E. coli* DH5alpha cells were transformed by electroporation (GenePulser II; Bio-Rad). Cells were recovered in 1 mL super optimal broth with catabolite re-

pression medium for 1 h, centrifuged at 6,000 × *g* for 3 min and cells were plated on four 12- × 12-cm LB agar dishes (LB/1% glucose/100 μg/mL ampicillin). Colonies were scraped off the plates and resuspended in LB medium (1% glucose and 100 μg/mL ampicillin), adjusted to 20% final glycerol, and aliquots were snap-frozen and stored at −80 °C until further use.

Proof-of-Principle Experiment. Position $Y347^{7.31}$ is a crucial residue for ligand binding of rNTR1, and its mutation decreases ligand binding (3). $Y347^{7.31}$ was thus chosen for a proof-of-principle experiment to test selection pressure during FACS selections. The randomized library was generated and subjected to one round of FACS selection as above, and different selection stringencies were analyzed. Clones recovered from selection of the top 1% of receptor-expressing cells exclusively contained the two tyrosine codons, indicating both appropriate selection pressure and selection based on phenotype, i.e., the protein sequence. All libraries were selected accordingly.

Library Expression and Selection. Sixty milliliters 2YT medium (0.2% glucose, 100 μg/mL ampicillin) were inoculated to OD_{600} = 0.05 and grown at 37 °C for ∼2 h to OD_{600} = 0.5. Protein expression is under control of the *lac* promotor, and expression was induced by addition of 250 μM isopropyl-β-D-thiogalactopyranoside and continued for 20 h at 20 °C. Expression cultures were cooled to 4 °C, and an aliquot corresponding to 10^7 cells was centrifuged for 3 min at 6,000 × *g* in a table-top centrifuge, washed in 1 mL TKCl buffer [50 mM Tris (pH 7.4), 150 mM KCl] and resuspended in 1 mL TKCl buffer with 20 nM BODIPY-labeled neurotensin (BP-NT; residues 8–13; neurotensin was obtained from AnaSpec, BODIPY-FL from Molecular Probes, Invitrogen). Samples were kept in the dark at 4 °C for 1–2 h to allow for agonist binding. Cells were washed twice in 1 mL TKCl buffer filtrated through a 50-μm mesh to avoid cell aggregates that could clog the FACS tubings (Becton Dickinson). Washed and singularized cells were applied to selection for high expression using the fluorescence-activated cell sorting approach essentially as described in Sarkar et al. (2). Here, 2,500 cells with expression levels corresponding to the top 1% of a D03 control were collected for each library. Selected cells were plated overnight on LB agar dishes (1% glucose, 100 μg/mL ampicillin; see Fig. S2 for a schematic overview of the selection process).

Selected libraries were analyzed both by Sanger sequencing of the full-length gene and by 454 sequencing of segments carrying the respective mutation.

In preparation for Sanger sequencing, for each library, DNA from 24 single clones was amplified by colony PCR (cPCR) and analyzed by Sanger sequencing of the PCR product, resulting in a sequence covering the whole GPCR. Colonies were scraped off the agar plates, and glycerol stocks were prepared as described for the naïve libraries to conserve the selected libraries.

For 454 sequencing analysis, the glycerol stocks were used for DNA isolation of each of the selected cell pools (see below). The obtained DNA library was prepared for ultradeep sequencing as summarized in Fig. S4 *A* and *B*. How the different PCR products covering different mutant positions were mixed and prepared for 454 sequencing is detailed in Fig. S4*C*.

cPCR and Sequencing. A 20-μL PCR mix containing 1× PCR buffer (Invitrogen 10× PCR buffer without $MgCl_2$), 2 mM $MgCl_2$, 0.8 mM dNTP mix, 100 nM primer NTR1longfw, 100 nM primer NTR1longre (see Table S2 for primer sequences), and 1 μL Taq polymerase was set up per well of a 96-well PCR plate. A single colony was picked gently, using a small pipette tip, and cells were resuspended in the PCR mix by repetitive pipetting. Cells were broken by a 10-min incubation step at 96 °C, following by 35 cycles of 95 °C for 15 s, 54 °C for 15 s, and 72 °C for 100 s, followed by a final elongation step of 5 min. PCR products were purified and sequenced at Synergene Biotech. A total of 6–20 sequencing reactions were performed per library.

Preparation of 454 Sequencing Samples. A glycerol stock of the selected library pools was used to inoculate a 5-mL 2YT culture (1% glucose, 100 μg/mL ampicillin) and grown at 37 °C for 16 h. Cells were centrifuged, and DNA was isolated using a Qiagen BioRobot 8000 with Macherey-Nagel NucleoSpin 96 Plasmid Kits. A 100-ng template DNA was used per amplicon PCR. At the time of the experiment, the read length performance of the 454 technology typically reached 250 bp. Amplicons were thus designed as 250-bp overlapping fragments to fully cover the receptor sequence (Fig. S4*A*; see Table S2 for primer sequences). By design, each library contains only one diversified codon, allowing us to sequence only a small region of the gene (because the Sanger sequencing of the whole gene had already confirmed the absence of other mutations outside of the designed ones). By using the appropriate amplicon primer pair, an amplicon (PCR product) containing the diversified codon was generated (Fig. S4*B*). The PCR products were purified by ultrafiltration (NucleoFast 96 PCR; Macherey-Nagel), and the DNA concentration was quantified using Quant-iT PicoGreen (Invitrogen). The DNA amount corresponding to $2{\cdot}10^{11}$ DNA molecules was used as input material for 454 sequencing (Functional Genomics Center Zürich). DNA from different libraries was mixed in one reaction (Fig. S4*C*), and later assigned to its original library by sequence reference alignment (Fig. S5).

We decided to not sequence all randomized positions falling within one amplicon (typically 50) in the same pool, but rather distribute them over eight aliquots, such that each amplicon is pooled from only 6–8 randomized positions, for the following reason: in a mixed sample of 50 different PCR products coming from the 50 different randomized positions within one amplicon, for each codon 2% of sequence reads would be assignable as mutations within this codon. However, for each position, the remaining 98% of sequence reads would be wild type in a given position and thus align perfectly to D03 in that specific codon, because their diversified codon is at a different position. This high frequency of wild type would make the accurate determination of mutant frequencies rather difficult. From a pilot experiment, we learned that the noise of our 454 sequencing reaction is ∼0.1%, meaning that 0.1% of sequence reads contain one or more mismatches in the nonrandomized gene regions. The observed error frequency here is a sum of base-pair mismatches introduced during amplicon PCRs as well as sequencing errors during the 454 sequencing reaction. The 454 sequencing reaction accuracy is mostly limited by shortcomings in the identification of homopolymer length by pyrosequencing (4, 5), and the noise of 0.1% observed here is mainly observed in homopolymeric sequence stretches. Here, all sequences showing miscalled bases in addition to the randomized codon were excluded from analysis. In the given example, an assignment of 2% of sequences per library and 0.1% noise would have resulted in a signal-to-noise ratio of only 20.

To obtain a higher ratio of assignment percentage over noise percentage (i.e., signal over noise), we have prepared the samples as follows (Fig. S4*C*): 376 different libraries were grouped into eight individual 454 sequencing reactions, run separately on one-eighth of a 454 picotiterplate. Every reaction contains 45–52 individual PCR products in total, of which 6–8 fall within each amplicon (denoted as amplicons 1–7). Alignments of 454 sequence reads to D03 (i.e., assignment of 454 sequence reads to a specific library origin) were later run independently for each 454 sequencing reaction and amplicon. One alignment of 454 sequence reads to D03 thus contains sequence reads of 6–8 individual amplicon PCR products, meaning that sequences from this pool are randomized in one of these 6–8 positions. Thus, 12.5–16% of sequences are assigned per library (i.e., for a given

codon that was randomized in this set, this is the percentage of sequences actually carrying an altered codon in this codon), resulting in an improved signal-to-noise ratio of at least 125 (12.5% over 0.1%). Nonetheless, sequence reads of an amplicon fully identical to the D03 reference sequence could not be assigned to which (maintained) position it came from, requiring a statistical correction during data processing (Fig. S5).

Analysis of 454 Sequencing Data. The raw sequences were transferred from the 454 system as large FASTA-format text files. B0.fastA, the pilot experiment, contained 206,405 sequences, all read in forward direction. B1.fastA to B8.fastA contained a total of 638,976 sequences, read in forward or reverse direction. The sequences were imported into EXCEL and processed using a set of custom Visual Basic macros. For our experiment, it was crucial to keep the background of sequencing errors as low as possible. Therefore, we stringently eliminated unreliable parts of the sequence. The 454 sequences tend to acquire insertions and deletions in runs of the same nucleotide, and indeed most sequences eventually went out of frame. Because we did not expect any frameshifts from the original sequences (because functional receptors were selected), we took the occurrence of frame shifts in the sequence as a sign that the sequence quality had deteriorated and truncated the shifted part of the sequence.

To identify the amplicon and the reading frame, we searched for the first 12 base exact match between each sequence and the D03 sequence (forward and reverse), and cut off all nucleotides before the start of the first in-frame codon match. The sequence was aligned without gaps and cut into in-frame nucleotide triplets. Mismatched codons were trimmed back from the end of the sequence until a four-codon (12 base) exact match was found. The truncated sequences were compared with the D03 sequence. Only those sequences that differed by exactly one codon from the D03 sequence were used for further analysis; for B0, these were 86,734 of 206,405 sequences (42%), covering 48 randomized positions. For each randomized position, an average of 1,800 sequences differed from the consensus; for unrandomized positions, 7.6 sequences (noise <0.5%). For B1–B8, 476,322 sequences (69.6%) showed exactly one deviation from D03, covering 331 positions with 771 forward and 737 reverse sequences (total 1,400 sequences) per randomized position, against a background of 4.4 mutations in nonrandomized positions.

Codon and Amino Acid Frequency Distribution. For each amplicon, comprising 3–8 randomized positions, the frequency distribution of the 64 codons was determined for each position in the sequence. The frequency of the wild-type codon in the randomized positions could not be determined directly, because it could not be distinguished from the wild-type codon originating from the sequences randomized in a different position. For amino acids encoded by several synonymous codons, the frequency of the wild-type codon was estimated as the average of the frequencies of synonymous codons. This correction could not be applied for the two amino acids encoded by a unique codon, Met (ATG) and Trp (TGG). The codon frequency distribution was normalized to give a sum over all 64 codons of 100%. The amino acid frequency distribution was derived as the sum of the frequencies of synonymous codons and renormalized to a sum of 100%. For further analysis, we evaluated the effects of selection on the width of the frequency distribution (sequence variability) and the peak of the distribution (sequence consensus). The amino acid distributions demonstrated a high tolerance of the rNTR1-D03 toward randomization: The positional variability of the sequences recovered from the top 1% neurotensin-binding *E. coli* clones isolated by FACS was comparable to that of all class A (rhodopsin-like) GPCR sequences.

Unbiased NNN randomization, combined with the degeneracy of the genetic code, introduces a bias in the amino acid distribution. Ser, Arg, and Leu, encoded by six codons each, are sixfold overrepresented over Trp and Met, encoded by a single codon; other amino acids lie between the two extremes. For most positions, the selection pressure was not strong enough to overcome this intrinsic bias: between amino acids with similar properties, the amino acid sequence consensus frequently went to the one encoded by the highest number of codons, e.g., to Leu in membrane-embedded positions that tolerated Leu, Val, Ile, and Met, or to Arg in positions that required a positively charged amino acid. Usual metrics of sequence variability [e.g., Shannon sequence entropy (6, 7) or Kabat sequence variability (8)] and sequence consensus did not perform well in this context, as they usually assume all amino acids to be equally probable and therefore bias the results in favor of the amino acids overrepresented in the original library, due to the degeneracy of the genetic code. The amino acid consensus sequence therefore differed significantly from the translation of the codon consensus (Fig. S8), and amino acids encoded by a larger number of codons on average appeared more conserved than amino acids encoded by fewer codons.

To avoid this bias, the rmsd of the observed amino acid distribution from the input amino acid distribution generated by unbiased NNN codon randomization was chosen as a measure of the selective pressure shaping the amino acid distribution in a given position. The rmsd for a given position is calculated according to Eq. **S1**:

$$rmsd = 2\sqrt{\frac{\sum_{i=1}^{20}\left(f_i - f_{s_i}\right)^2}{20}}, \qquad \textbf{[S1]}$$

where f_{1_i} is the frequency of amino acid i in the library before selection and f_{s_i} is the frequency after selection. The frequency of amino acid i before selection is deduced from the theoretical distribution of a NNN library, which is justified by the Sanger sequencing results of the naïve libraries, which was found to be not biased (Table S1), and the high oversampling of the library diversity throughout all experimental steps. A low rmsd denotes a permissive position, where the selection process had little or no effect on the observed amino acid frequency distribution, whereas a high rmsd is a sign of a restrictive position with a clear amino acid preference. Intermediate rmsds frequently denote positions where the general character of the amino acid is preserved (e.g., aliphatic), but not the exact type (e.g., valine).

This distinction between permissive (low rmsd) and restrictive positions (high rmsd) does not depend on whether the wild-type sequence is conserved or not—a position can be restrictive, but shift away from the wild-type sequence to a new focus, or be permissive and still include and partially preserve the wild-type sequence (e.g., by only selecting for the aliphatic character of the amino acid).

Fig. 1 compares the rmsds obtained from the sequences of the selected members of the rNTR1-D03–based libraries to those derived from more than 20,000 aligned class A GPCR sequences obtained from the GPCR database (GPCRDB; http://www.gpcr.org/7tm/). The ratio of the rNTR1-D03 rmsds to the class A rmsds indicates in which of the two systems a given position is more highly conserved (Fig. 2).

The assessment of sequence conservation and sequence shifts was based on the comparison of the wild-type sequence to the selected consensus, generated from a normalized table of the observed amino acid frequencies divided by the number of synonymous codons for each amino acid. This normalized consensus better reflects the influence of the applied selection pressure on the amino acid distribution than the classical amino acid consensus (Fig. S8). A position was considered robustly conserved if the two consensus sequences (not normalized and normalized by codon frequency) both agreed with the wild-type sequence; it was considered weakly conserved if only the normalized consensus

agreed. A robust shift meant that both consensus sequences agreed, but differed from the wild-type sequence. If the normalized consensus differed both from the wild type and the classical consensus, two classifications are possible: the result was classified as not significant if the average codon frequency for the consensus amino acid did not differ significantly from that of the wild-type amino acid, whereas it was termed a weak shift if the wild-type amino acid was clearly underrepresented. A robust shift or conservation can be the result of strong selective pressure, but it is not necessarily so. It can also be a mild selection of an amino acid additionally favored by the codon bias.

Homology Modeling. To visualize the positions and potential interactions of the different mutations, homology models of the ground state and the activated state were built. A structural alignment of all available GPCR structures was used to verify the sequence alignments and identify irregularities in the transmembrane helices in individual structures. Because selection was based on agonist binding, the model of the active state is shown in all figures. Because the first structures of a GPCR in complex with an agonist became available only very recently (9) (PDB ID code 3SN6), the model shown in Figs. 1–3 was based on the structures of opsin in complex with a C-terminal peptide of transducing alpha (PDB ID code: 3DQB; 3.2 Å resolution) and of squid rhodopsin (PDB ID code: 2Z73; 2.5 Å). Due to unresolvable clashes, the N-terminal side of the first helix had to be tilted further away from the axis of the helix bundle, its orientation was taken from a structure of the β2 adrenergic receptor (PDB ID code: 2RH1; 2.4 Å). Various templates and loop generation methods were used to model the loops connecting the helices. Comparison with aligned GPCR structures combined with hydrophobicity and sequence conservation pattern within the NTR lineage (GPCRDB 001_002_015) helped to choose between different loop conformations that satisfied the steric constraints. The conformation of the large third intracellular loop of rNTR1, which in most GPCR structures is replaced by T4 lysozyme, was patterned after the loop conformation observed in squid rhodopsin (PDB ID code: 2Z73), extending transmembrane helices 5 and 6 from PDB ID code 3DQB and connecting them in a helix-turn-helix motif. This loop conformation allowed fitting a Gα or Gαβγ structure to the Gα-derived peptide in template PDB ID code 3DQB without clashing with the loop. Insight II (Accelrys Inc.) and the Rosetta suite of programs (http://www.rosettacommons.org/) (10) were used for modeling; figures were generated using PyMol (Schrödinger, LLC).

Analysis of Single Mutants. Thirty-two shift mutations, based on the D03 background, were selected for further characterization from evaluation of the Sanger sequencing results (Table 1). The Sanger sequencing and the 454 sequencing results are in good agreement. However, the 454 sequencing results allow more robust statistical analysis, because on average 1,428 sequences were analyzed per individual position. Furthermore, statistical corrections were applied (see 454 data analysis above). Thus, for a few positions, the 454 sequencing proposes a different consensus amino acid than the Sanger sequencing results (e.g., position $L119^{2.56}$). We find a $L119F^{2.56}$ shift according to the Sanger sequencing results, whereas according to the 454 sequencing results, $L119F^{2.56}$ is the second preferred residue for $L119^{2.56}$, after Leu, suggesting that it is primarily conserved. The expression levels of $L119F^{2.56}$ show the feasibility of the substitution with respect to expression levels (Table 1), and thus that both residues behave very similarly.

Analysis of Stability in Detergents. Thermostability of selected mutants was analyzed essentially as described in Dodevski and Plückthun (11). A gradient PCR machine was used to incubate receptor aliquots at increasing temperatures (TProfessional Gradient; Biometra). Data were analyzed by a nonlinear fitting using GraphPad Prism 5. The apparent T_m is defined as the temperature at which 50% of receptor molecules retain ligand binding activity after 20 min of incubation.

1. Ballesteros JA, Weinstein H (1995) Integrated methods for the construction of three dimensional models and computational probing of structure function relations in G protein-coupled receptors. *Meth Neurosci* 25:366–428.
2. Sarkar CA, et al. (2008) Directed evolution of a G protein-coupled receptor for expression, stability, and binding selectivity. *Proc Natl Acad Sci USA* 105:14808–14813.
3. Barroso S, et al. (2000) Identification of residues involved in neurotensin binding and modeling of the agonist binding site in neurotensin receptor 1. *J Biol Chem* 275:328–336.
4. Chan EY (2009) Next-generation sequencing methods: Impact of sequencing accuracy on SNP discovery. *Methods Mol Biol* 578:95–111.
5. Ronaghi M, Uhlén M, Nyrén P (1998) A sequencing method based on real-time pyrophosphate. *Science* 281:363–365, 365.
6. Shannon CE (1997) The mathematical theory of communication. 1963. *MD Comput* 14:306–317.
7. Strait BJ, Dewey TG (1996) The Shannon information entropy of protein sequences. *Biophys J* 71:148–155.
8. Kabat EA, Wu TT, Bilofsky H (1977) Unusual distributions of amino acids in complementarity-determining (hypervariable) segments of heavy and light chains of immunoglobulins and their possible roles in specificity of antibody-combining sites. *J Biol Chem* 252:6609–6616.
9. Rasmussen SG, et al. (2011) Crystal structure of the β_2 adrenergic receptor-Gs protein complex. *Nature* 477:549–555.
10. Leaver-Fay A, et al. (2011) ROSETTA3: An object-oriented software suite for the simulation and design of macromolecules. *Methods Enzymol* 487: 545–574.
11. Dodevski I, Plückthun A (2011) Evolution of three human GPCRs for higher expression and stability. *J Mol Biol* 408:599–615.

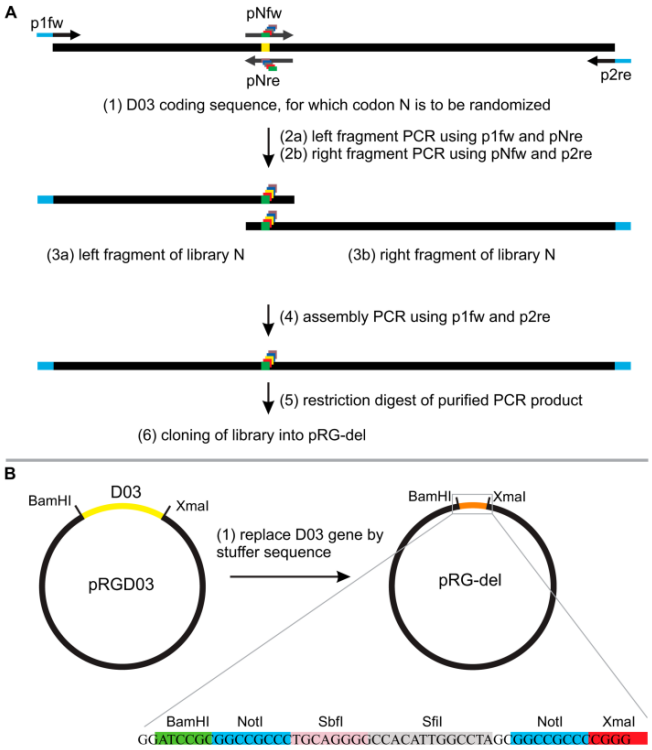

Fig. S1. Library generation and cloning. (*A*) Libraries are generated by a two-step PCR assembly strategy. First, two separate PCR reactions are performed with the D03 coding sequence as template: With primers p1fw and pNre (2a), the 5′-end of the library N is generated. Primer pNre and pNfw are NNN randomized in the codon of library position N, thus introducing the desired randomization. Primer p1fw introduces a BsmBI site with BamHI-compatible overhangs, whereas primer p2re introduces a BsmBI site with XmaI-compatible overhangs (blue ends). With primers pNfw and p2re (2b), the 3′-end of library N is generated. The resulting PCR products (3a, 3b) are isolated and purified, and used as template for the subsequent assembly PCR (4). Primers p1fw and p2re are used to generate and amplify the full-length library PCR product from the two fragments. Primers p1fw and p2re introduce BsmBI restriction sites and BamHI (p1fw)- and XmaI (p2re)-compatible overhangs. The full-length library is purified and subsequently cloned into the acceptor plasmid pRG-del. (*B*) The acceptor plasmid pRG-del is generated from pRGD03 by exchange of the D03-coding sequence by a stuffer sequence using BamHI and XmaI.

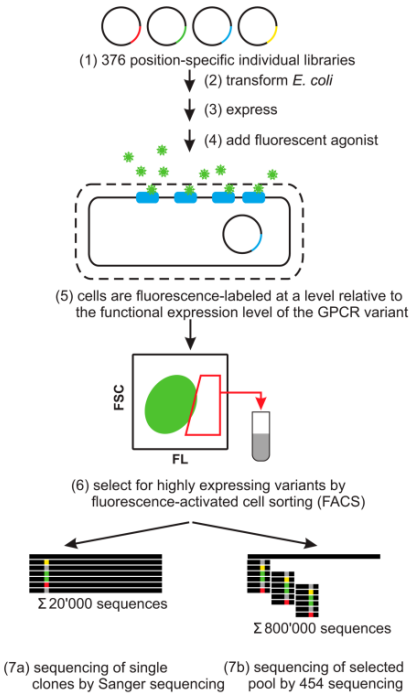

Fig. S2. Selections for high functional expression. A total of 376 individual, position-specific libraries are transformed and expressed in *E. coli* DH5alpha cells (2, 3). The fluorescence-labeled agonist BP-NT (residues 8–13) is used to label the cells according to their functional expression levels (4, 5). Highly expressing cells are identified and isolated by FACS (6). Individual selected cells are grown and then analyzed by Sanger sequencing of the complete gene (7a), and the pool of selected cells is also analyzed by 454 sequencing of a gene segment containing the mutation (7b).

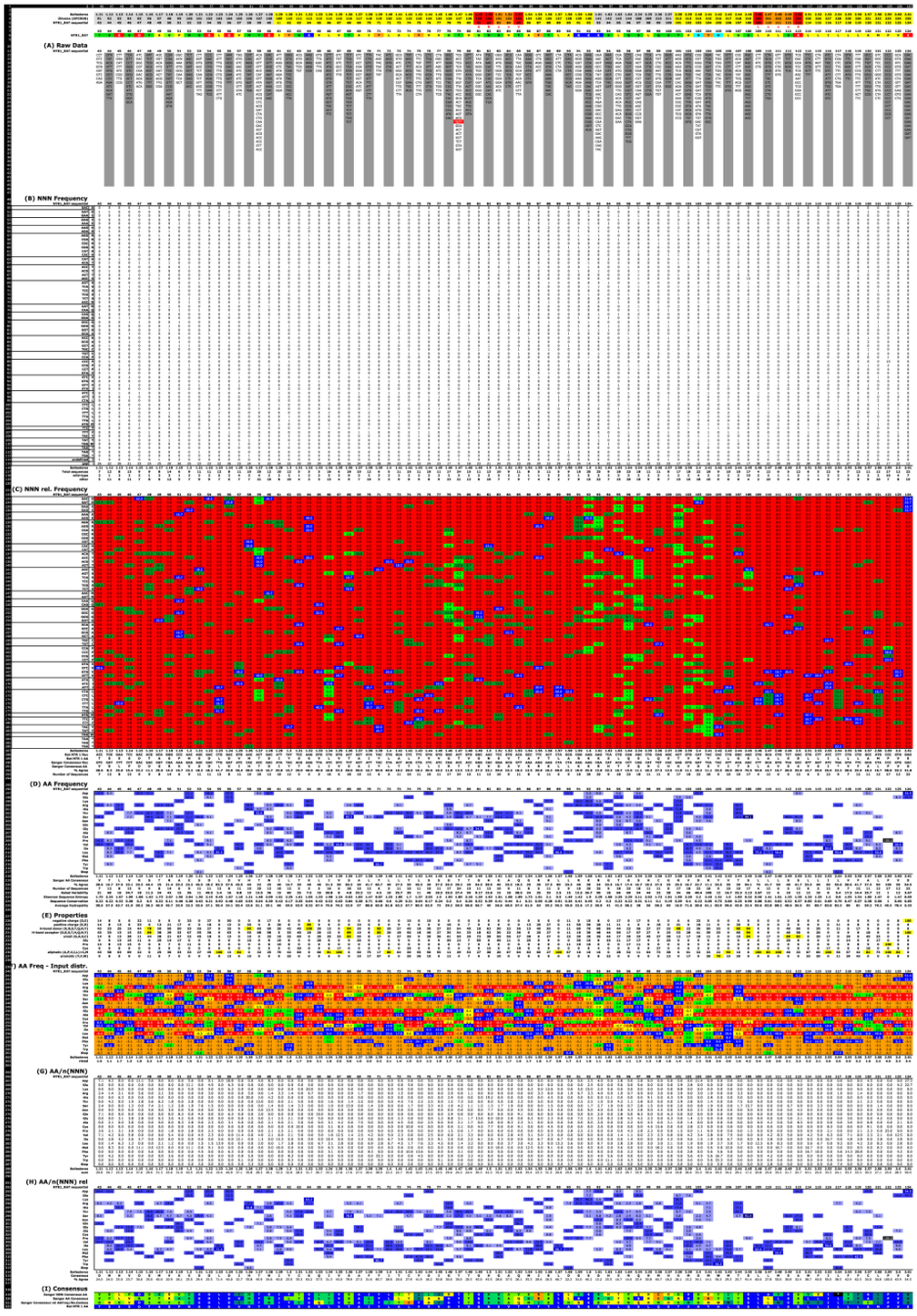

Fig. S3. (Continued)

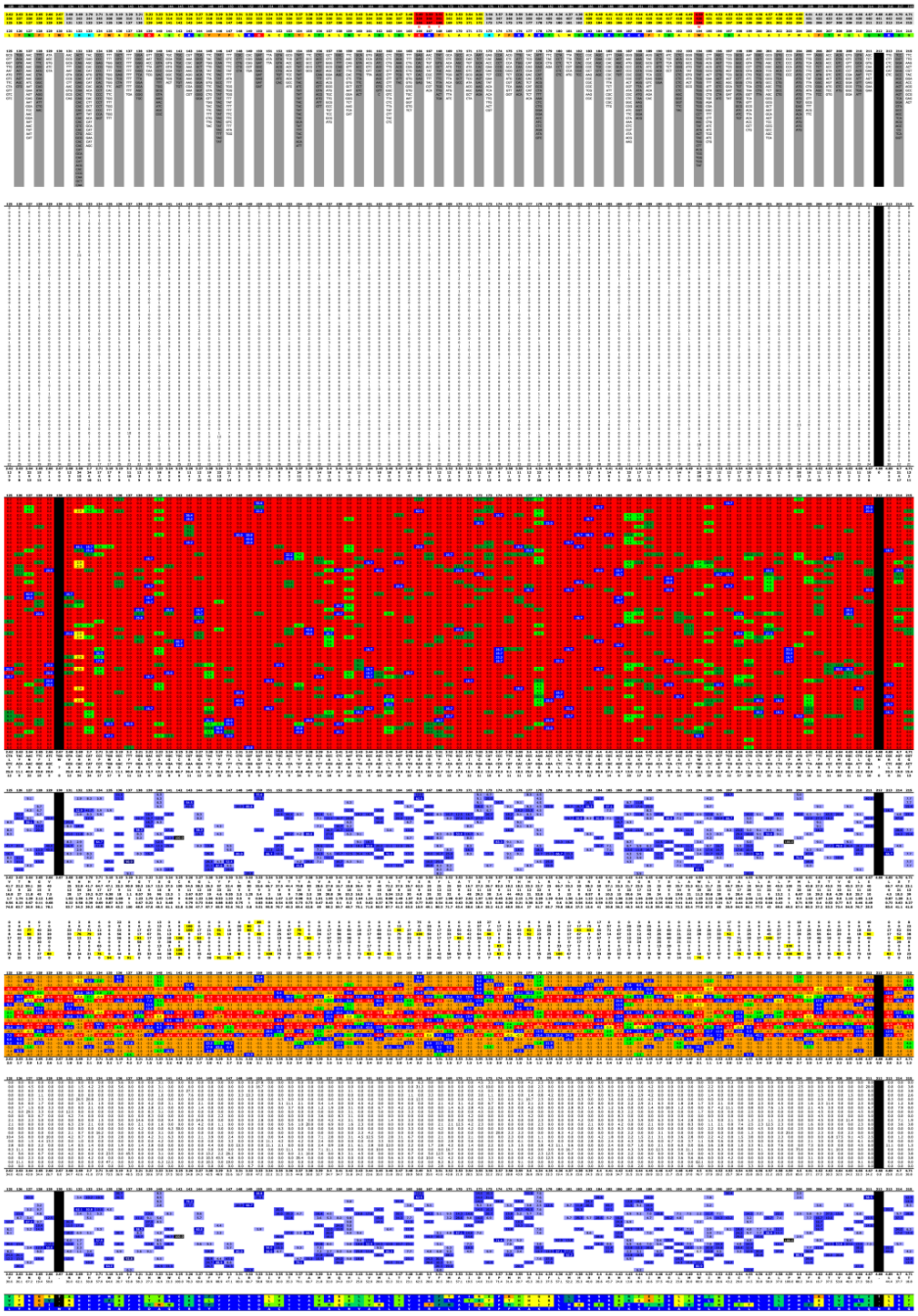

Fig. S3. (Continued)

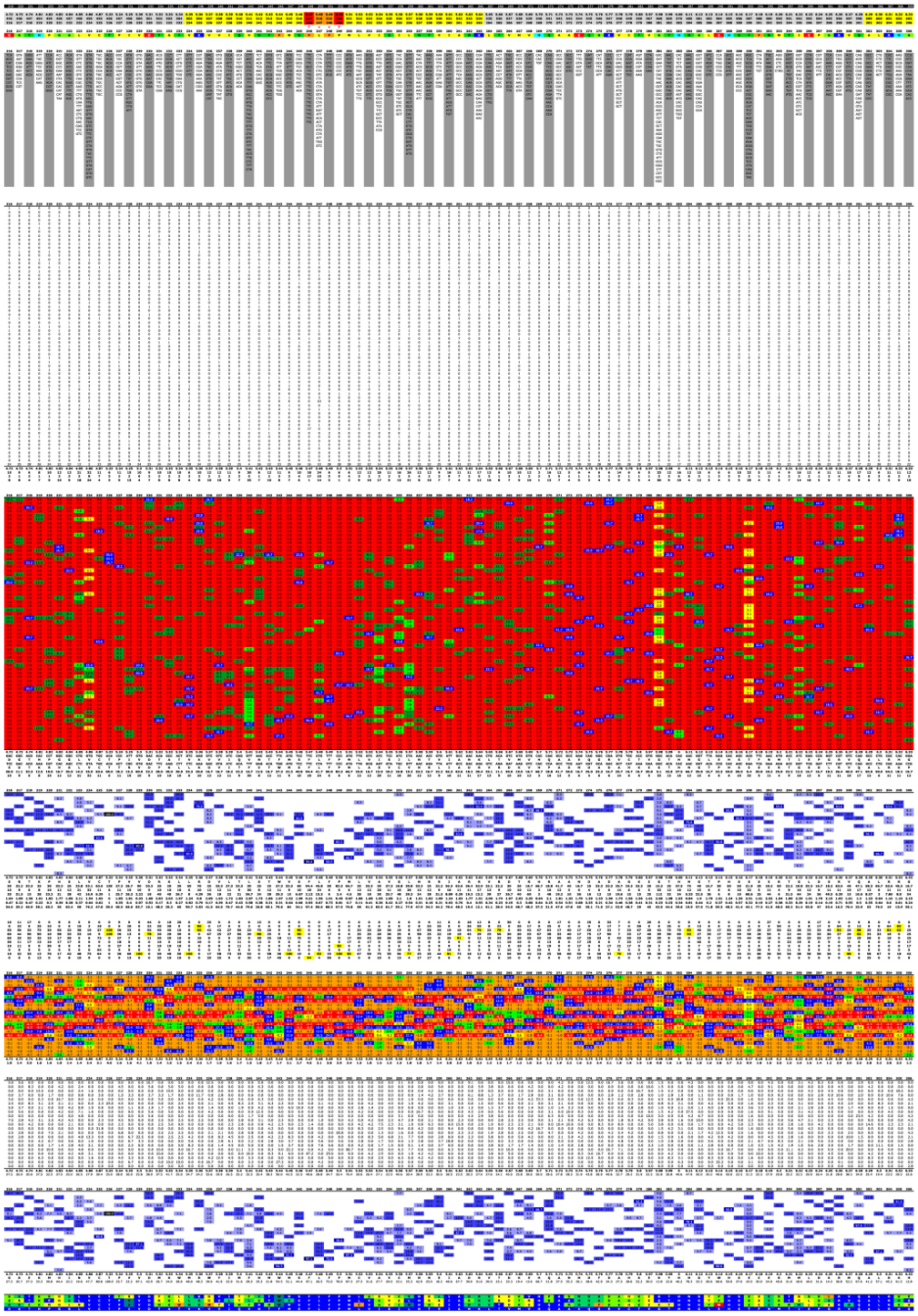

Fig. S3. (Continued)

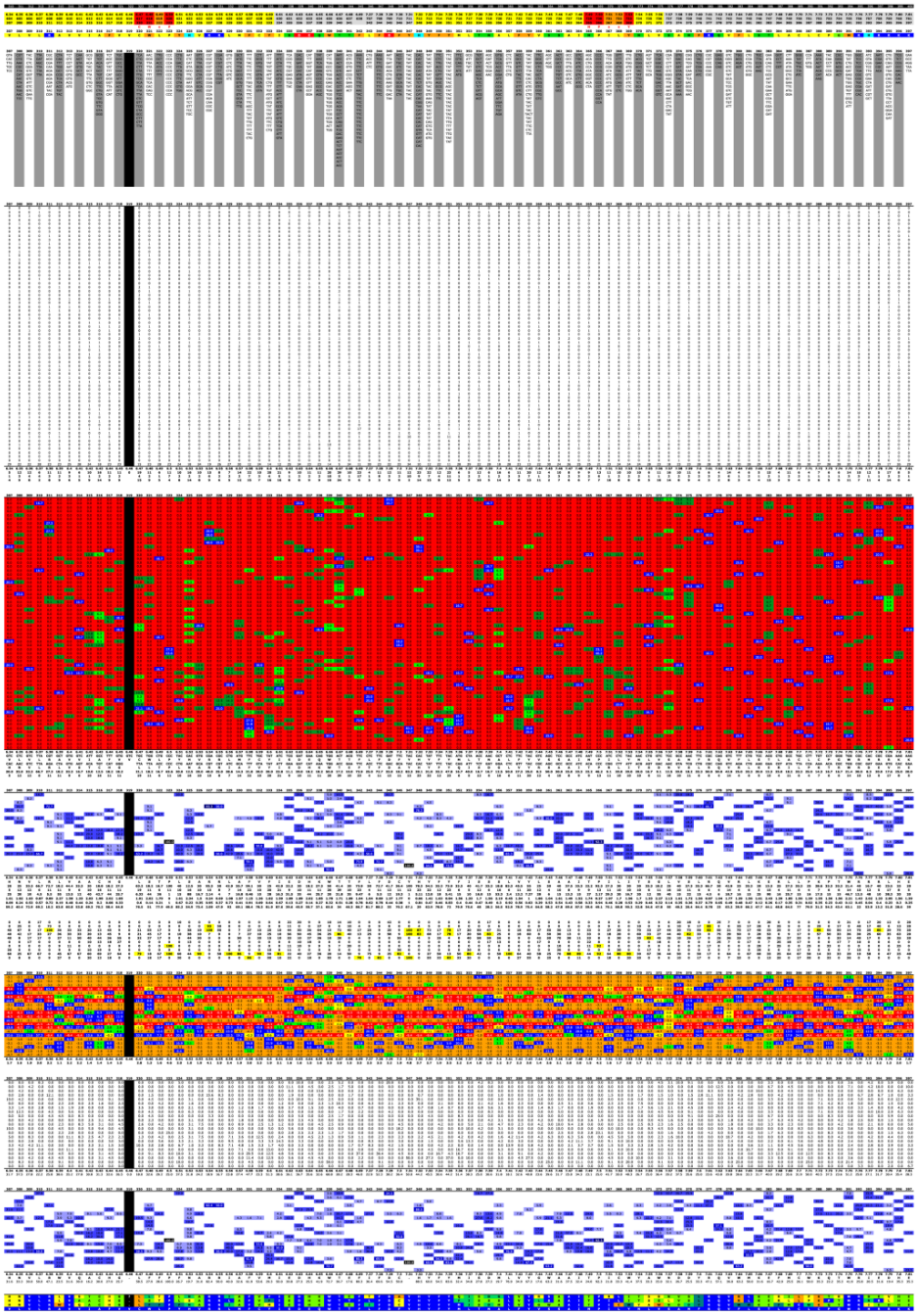

Fig. S3. (Continued)

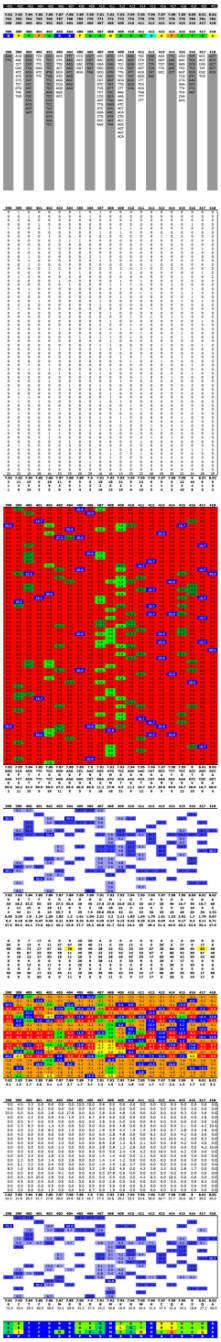

Fig. S3. Sanger sequencing data. (*A*) Raw data enumerates the nucleotide triplets observed in the randomized positions of a total of 4,310 selected clones analyzed by Sanger sequencing, 1,152 of which showed the wild-type codon and 3,158 a different codon. (*B*) NNN frequency lists how often each of the 64 triplets has been observed in a given position. (*C*) NNN relative frequency normalizes this distribution to a sum of 100%. (*D*) AA frequency. The amino acid frequencies were derived from the relative codon frequencies in *C* by summing up the contributions of synonymous codons. Shades of blue indicate the prevalence of the different amino acids, from white for not observed at all to dark blue for highly enriched amino acids. Note that the rNTR1 sequence is given at the top. (*E*) Properties sums up the percentage of amino acids with similar properties, e.g., charged, hydrophilic, small, hydrophobic, aliphatic, and aromatic.
Legend continued on following page

Because an amino acid can belong to more than one group, the sum can be larger than 100%. (*F*) AA Freq-Input distr: the difference between the input amino acid distribution and the distribution after selection is given, which highlights the effect of selection. The number represents the rmsd between the two distributions, which was calculated according to Eq. **S1** (*SI Text*). Amino acids colored blue are strongly enriched; green, mildly enriched; yellow, no significant change; orange, mildly deselected; and red, strongly deselected. (*G*) AA/n(NNN): amino acid frequencies corrected for the bias of the input library by dividing the observed frequencies by the number of synonymous codons. (*H*) AA/n(NNN) rel.: normalizes the corrected distribution to a sum of 100%. The color code is the same as in *D*. (*I*) Consensus compares the consensus sequences derived from the most frequently observed codon, the most frequently observed amino acid, and the most frequently observed amino acid after correcting for the number of synonymous codons to the wild-type sequence of rNTR1. The color code indicates the level of conservation of the substitution in a spectrum from dark blue for sequence identity to red for the least-conservative substitution possible.

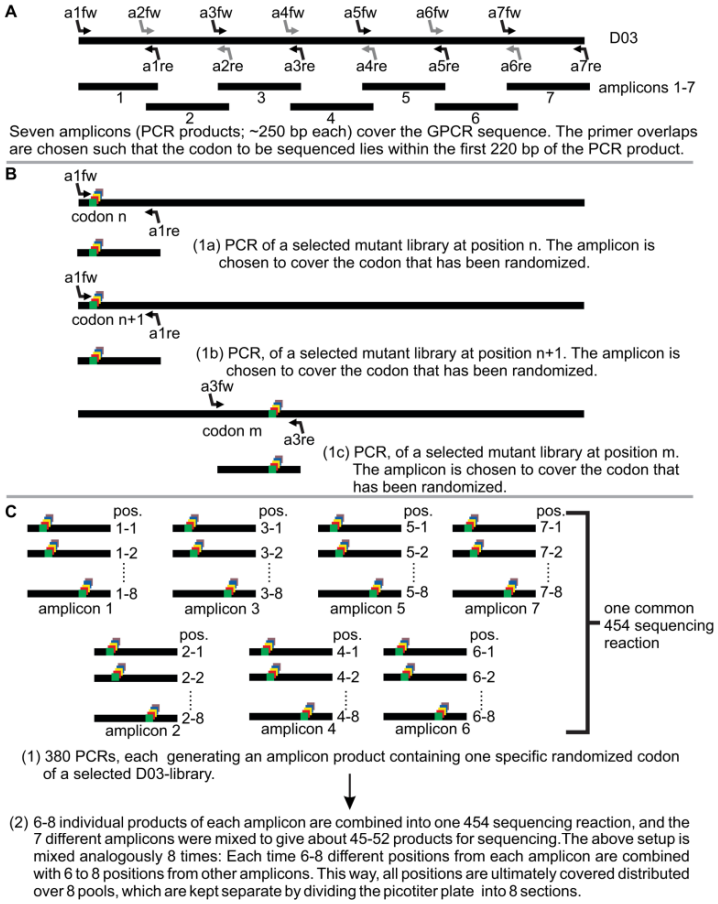

Fig. S4. The 454 sequencing setup. (*A*) Seven amplicon PCR products (amplicons) of ~250 bp are designed to cover the GPCR gene. (*B*) For each selected library pool, an amplicon PCR containing the diversified codon is generated (1a–1d). (*C*) One 454 sequencing reaction contains 6–8 members of each amplicon. Eight individual 454 sequencing reactions are performed to analyze all 380 amplicon PCR products (2), kept separately on a subdivided picotiter plate.

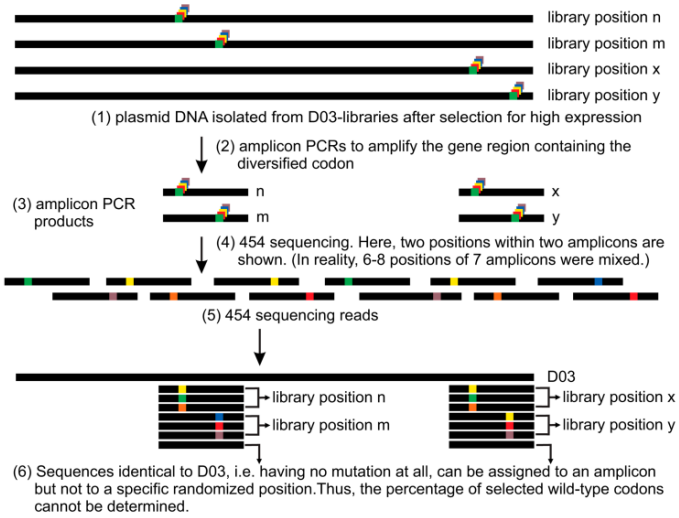

Fig. S5. The 454 sequencing read assignment. After amplification of the gene region containing the diversified codon (1–3), various amplicon PCR products are analyzed in one 454 sequencing reaction (4). The resulting 454 sequencing reads (5) are assigned by alignment to D03 (6). The diversified codon unambiguously identifies the library origin (6; library positions n, m, x, and y). However, 454 sequence reads with perfect alignment to D03 cannot be assigned to a particular randomized codon and statistical correction is applied for compensation.

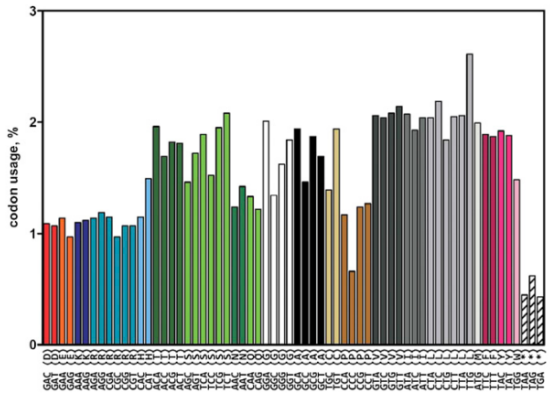

Fig. S6. Codon use at randomized positions was calculated from all 454 sequencing results. Synonymous codons are used at similar frequencies.

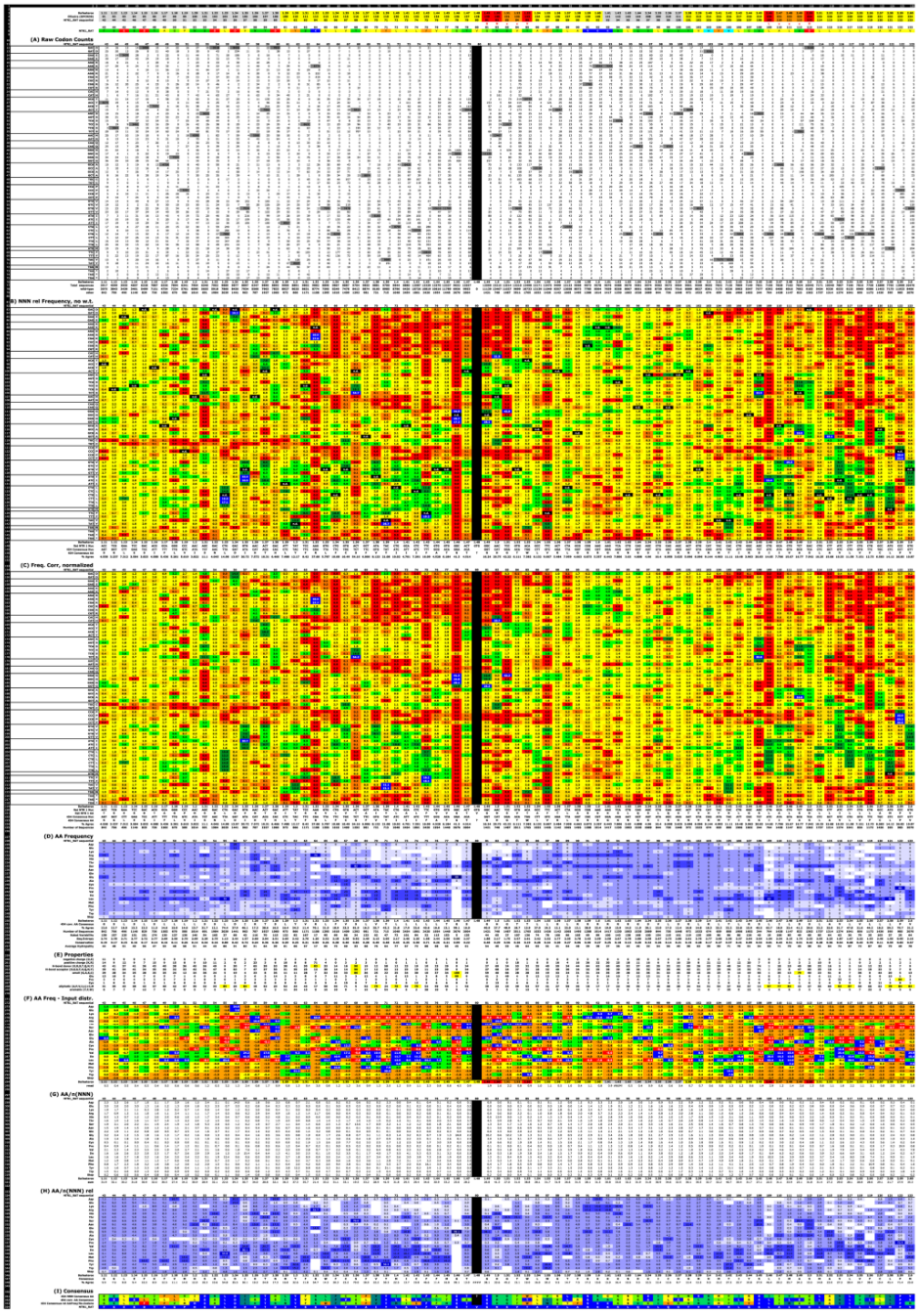

Fig. S7. (Continued)

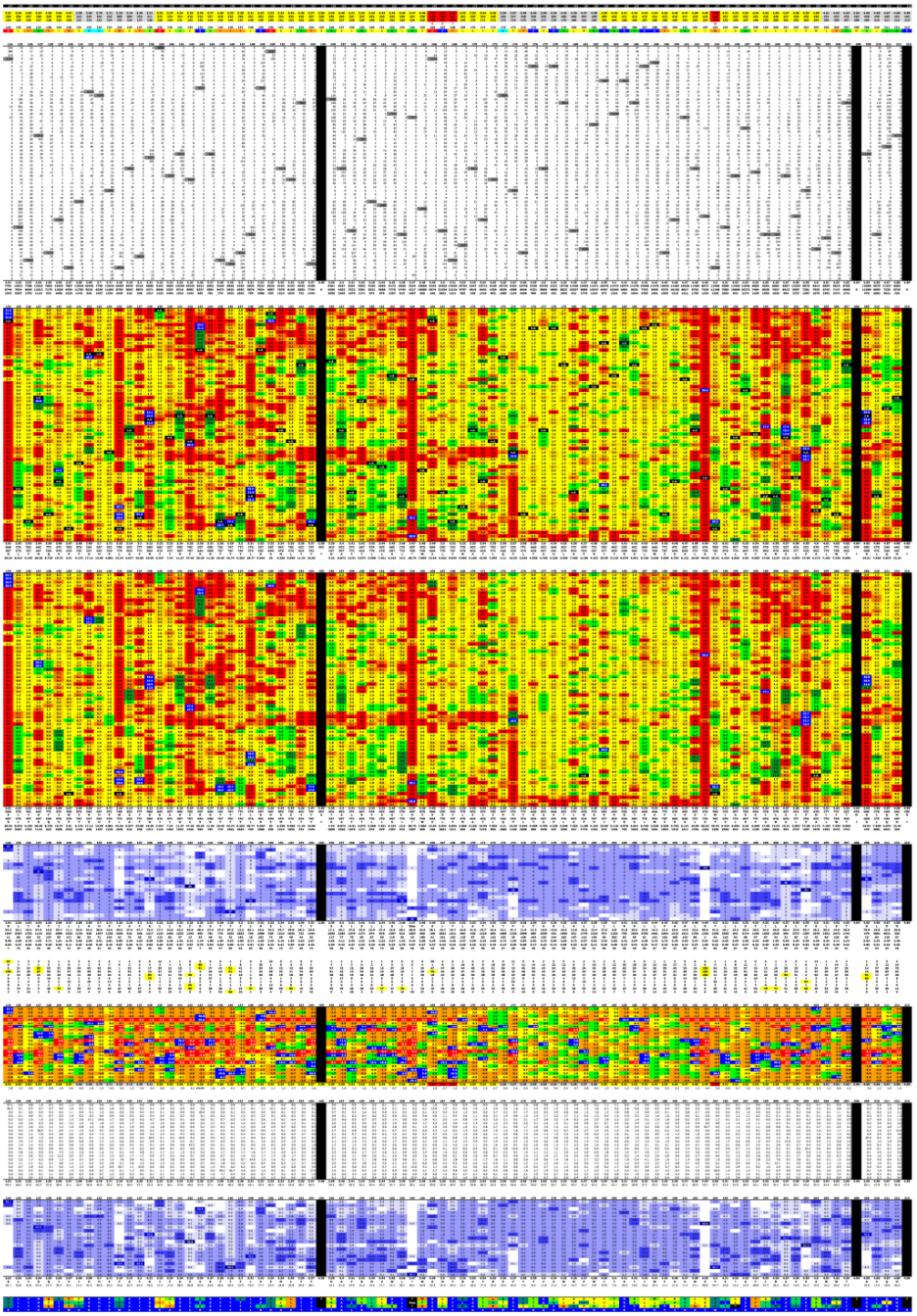

Fig. S7. (Continued)

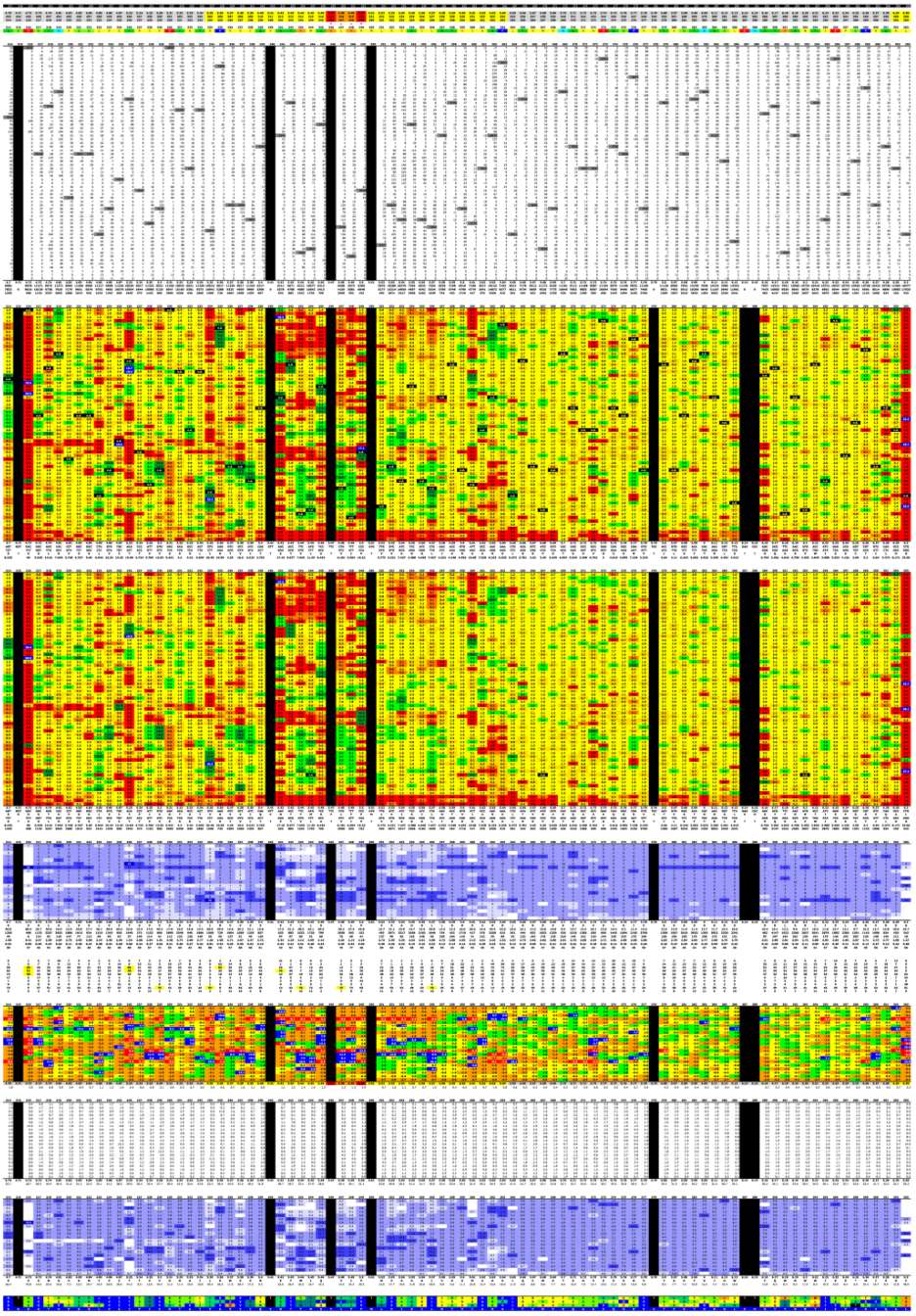

Fig. S7. (Continued)

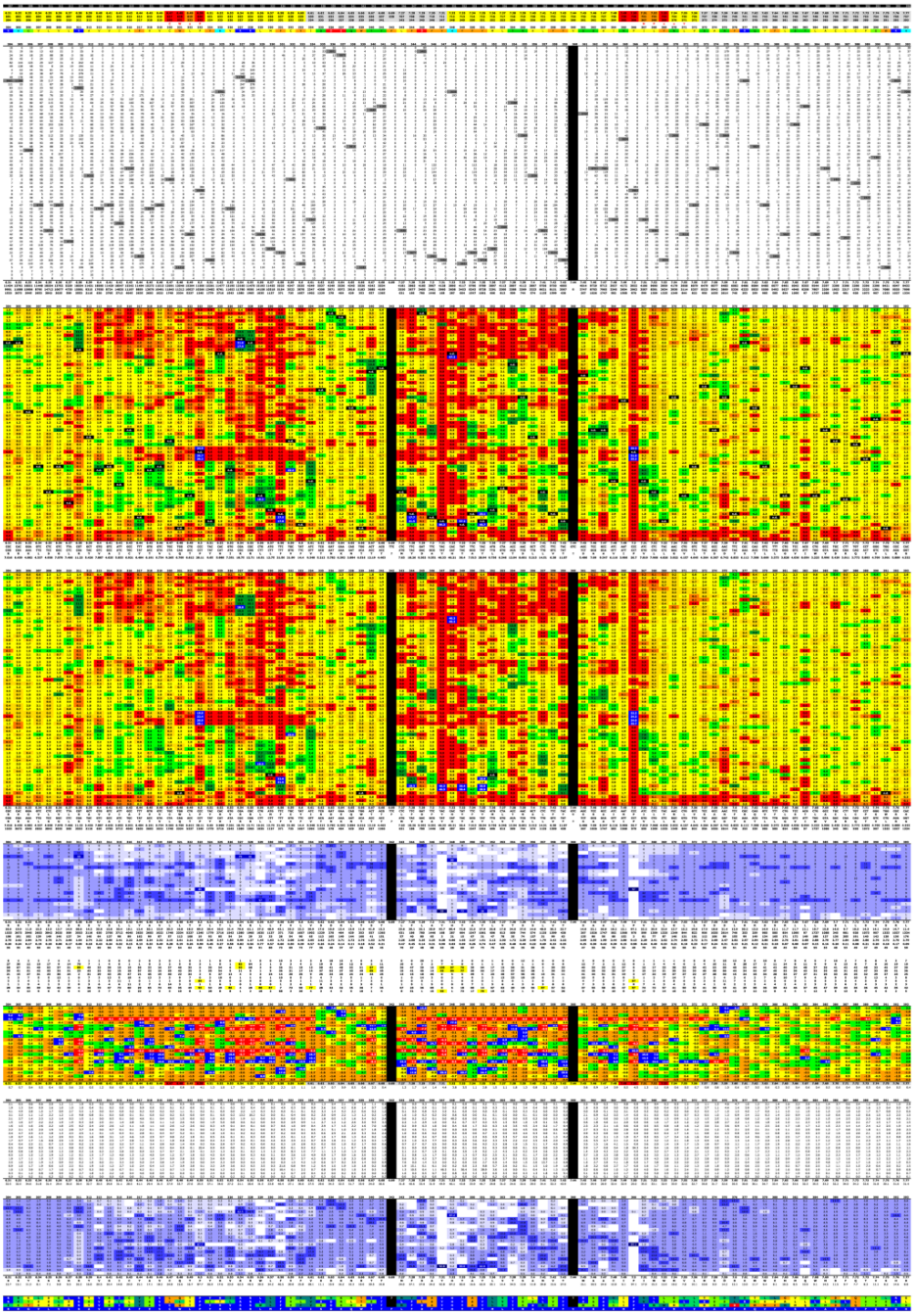

Fig. S7. (Continued)

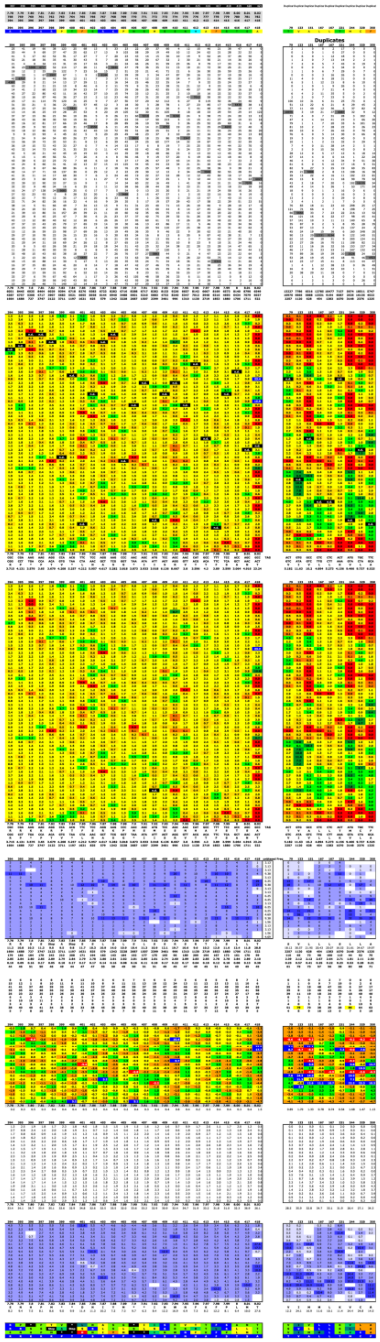

Fig. S7. The 454 sequencing data. (*A*) Raw codon counts enumerate how frequently each codon was encountered in the 454 sequencing results. The high count of the wild-type triplet results from the combination of multiple libraries randomized in different positions in each sequence pool (Fig. S4). (*B*) NNN rel Frequency, no w.t.: the relative frequencies of the different codons, normalized to a sum of 100% and omitting the wild-type codon. (*C*) Freq. Corr, normalized: the frequency of the wild-type codon was estimated as the average of the frequencies of synonymous codons where possible, and the values re-normalized to a sum of 100%; *D*–*I* were derived from these values as described in the legend for Fig. S3.

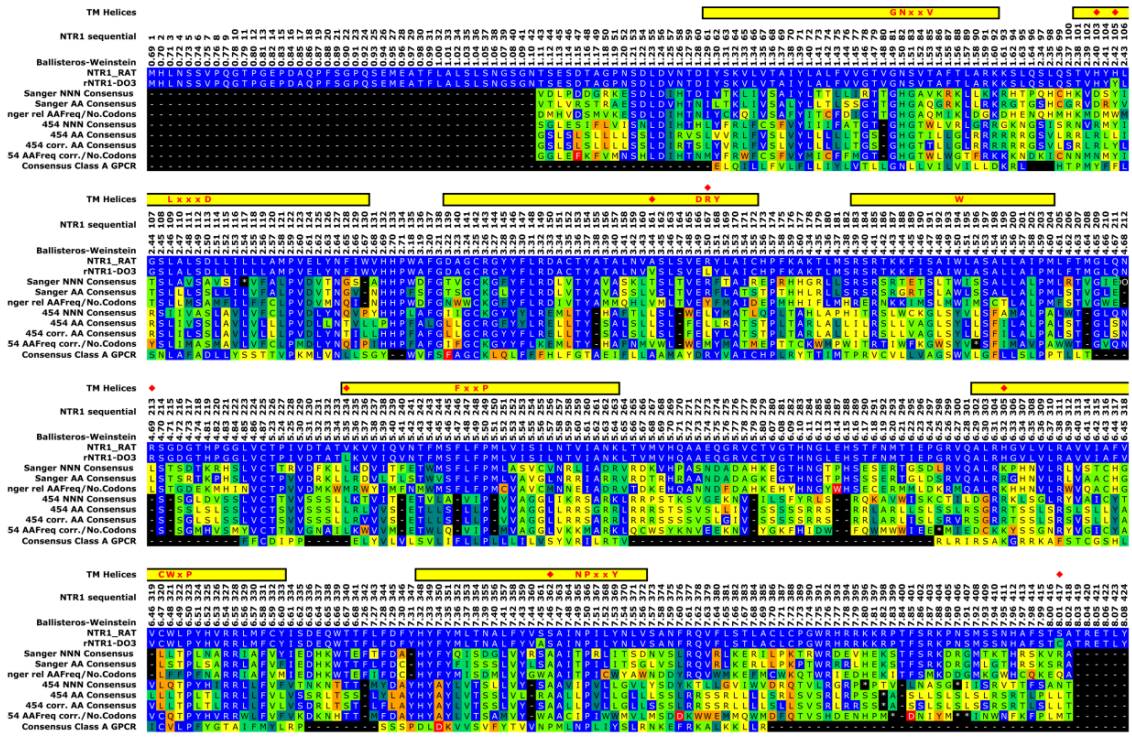

Fig. S8. Alignment of Sanger and 454 consensus sequences with rNTR1, rNTR1-D03, and class A GPCR consensus. Sanger NNN consensus/454 NNN consensus: The NNN consensus shows the amino acid sequence derived from the most frequently observed codon in each position. Sanger AA consensus/454 AA consensus: For the AA consensus, the observed frequencies of synonymous codons were summed up before deriving a consensus. The 454 corr. AA consensus: Because in the 454 experiment the frequency of the wild-type codon cannot be quantitated, its frequency has been deduced as the average of the frequencies of synonymous codons. The 454 AAFreq corr./no. of codons: AA consensus derived from a frequency table that has been corrected for the bias in the initial amino acid library introduced by the degeneracy of the genetic code. Consensus class A GPCR: The classical AA consensus derived from an alignment of all class A GPCR sequences downloaded from the GPCRDB (http://www.gpcr.org/7tm/), omitting the variable loop regions. At this level of sequence divergence, the amino acid frequency distributions show similar influence of codon bias as the 454 results. Figs. S3 and S7 contain the detailed data from which these consensus sequences were derived. In the top line the helices are highlighted, and conserved sequence motifs are indicated. Red diamonds indicate residues predicted to contact the C-terminal helix of Gα, based on transducin peptide contact residues in PDB ID 3DQB.

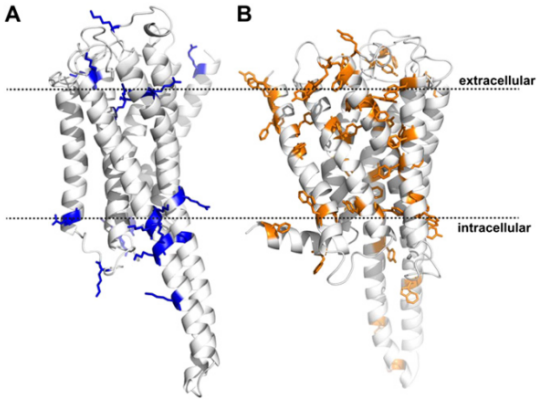

Fig. S9. General amino acid preferences. The figure is based on the consensus sequence shown in Fig. 3. (*A*) Significant selection for positively charged residues (Lys, Arg) is observed at the intracellular surface of the membrane and in the vicinity of the putative ligand binding pocket. (*B*) Membrane-exposed aromatic residues are predominantly located close to the surface of the membrane, whereas toward the center of the membrane, the Leu-Ile-Val-Met pattern predominates, in which these four amino acids predominate in a ratio governed by the codon bias.

Table S1. Diversity of randomized codons

	Codon position			
	1	2	3	Average
A	530	500	526	519
T	567	597	565	576
C	452	523	513	496
G	534	494	526	518
N	88	56	40	61
n = 2,170				

Table S2. Primer sequences

Name	Sequence 5′–3′	Purpose
NTR1longfw	CGCGCAGACTGGATCTAACAACAACAACAATAAC	cPCR
NTR1longre	CAGAACCGCCACCAGAACCGCCACCG	cPCR
p1fw	CTTCCAGTCTCGTCTCGGATCCACCTCGGAATCCGACA CGGCAGGGCCCAACAGCGACC	Library generation/amplification
p2re	AATTCGTAGTGAAGACTCGTCTCCCCGGGTAGCGCAG GTGGAAAAGGCATGGTTGCTGGACATGC	Library generation/amplification
a1fw	CCTGTACTTCCAGTCTGGAT	amplicon 1 PCR (T43–Y104)
a1re	CCTGTACTTCCAGTCTGGAT	Amplicon 1 PCR (T43–Y104)
a2fw	AGCCTGCAGAGCACTGTGG	Amplicon 2 PCR (Y105–L163)
a2re	GAAGGGATGGCAGATGGCC	Amplicon 2 PCR (Y105–L163)
a3fw	GCCACAGCCCTCAATGTAGT	Amplicon 3 PCR (S164–G221)
a3re	GAGTGGCAGTGTCCACAATG	Amplicon 3 PCR (S164–G221)
a4fw	AACCTCAGTGGTGACGGCA	Amplicon 4 PCR (G222–V280)
a4re	AACGTGCTGTGCTCTAAACC	Amplicon 4 PCR (G222–V280)
a5fw	GCCAACAAACTGACAGTCATG	Amplicon 5 PCR (G281–M330)
a5re	CGAAGAGGAACGTAGTCCACT	Amplicon 5 PCR (G281–M330)
a6fw	TGGTCTGCTGGCTGCCCTAC	Amplicon 6 PCR (F331–T383)
a6re	CACCCAGGACAAAGGCAGG	Amplicon 6 PCR (F331–T383)
a7fw	AACCTGGTCTCCGCCAACTT	Amplicon 7 PCR (L384–A418)
a7re	TTCAGAACCGCCACCAGAAC	Amplicon 7 PCR (L384–A418)

Table S3. GPCR Sequence consensus motifs

	Consensus	Position	rNTR1
TM 1	GNxxV	$81^{1.49}$–$85^{1.53}$	GNSVT
TM 2	LxxxD	$109^{2.46}$–$113^{2.50}$	LALSD
TM 3	DRY	$166^{3.49}$–$168^{3.51}$	ERY, D03: ELY
TM 4	W	$194^{4.50}$	W
TM 5	FxxP	$246^{5.47}$–$249^{5.50}$	FLFP
TM 6	CWxP	$320^{6.47}$–$323^{6.50}$	CWLP
TM 7	NPxxY	$365^{7.49}$–$369^{7.53}$	NPILY

3-A.3 Further Experiments

3.2.1 Shift mutants A86L, I253A and F358V: Further characterization of detergent stability

Detergent stability of the single shift mutants in comparison to D03 was assessed in the detergent n-dodecyl-β-D-maltopyranoside (DDM) in the absence of agonist, a condition under which D03 displays a T_m of 30°C (see Chapter 3.1-A, published article and Table 1 therein). The three dominant single shift mutants with strongly increased detergent stability compared to D03 (A86L$^{1.54}$, I253A$^{5.54}$ and F358V$^{7.42}$) were further analyzed in the shorter and harsher detergent n-decyl-β-D-maltopyranoside (DM), a condition under which D03 is barely stable, and additionally in the presence of agonist.

In the absence of agonist, the detergent stability of the shift mutants A86L$^{1.54}$ and I253A$^{5.54}$ in DM is strongly increased compared to D03, which is only marginally stable under these conditions (see Table 3-1).

Table 3-1. Detergent stability in DM in the absence of agonist.

	rmsd 454	T_m (°C)* (n = 2)	T_m, ΔD03 (°C)
S83G	10.2	15.8	0.1
A86L	4.9	23.5	7.8
I253A	5.2	32.0	16.3
I260A	7.1	14.8	-0.9
I260S	7.1	15.7	0.0
F358V	4.8	17.1	1.5
D03 ctrl**		15.7	

* average error 2°C; ** n=3

The shift mutants A86L$^{1.54}$, I253A$^{5.54}$ and F358V$^{7.42}$ do also lead to stabilization of the agonist-bound state, showing that the effect is independent of the receptor state (see Table 3-2).

Table 3-2. Detergent stabilities in the presence of agonist.

		T_m (°C)*			
	rmsd	DDM	DM	NM	OG
A86L	4.9	53	47	39	29
I253A	5.2	55	51	46	35
F358V	4.8	51	47	41	27
D03		47	42	42	16

* n=2; ** n=4

The stabilizing effect of the three shift mutants is most prominent in the harsh short-chain detergent n-octyl-β-D-glucopyranoside (OG), where increases of more than 11°C in T_m are observed (see Table 3-2). It can be concluded that the stabilizing effects are independent of the assay condition, and that positions with crucial role for detergent stability were identified.

Chapter 3-B

Directed evolution of proteins: Analysis of a comprehensive randomization study of a GPCR by deep sequencing.

3-B.1 Article in preparation

3-B.1 Article in preparation

Directed evolution of G proteins: Analysis of comprehensive randomization study of a GPCR by deep sequencing.

Karola M. Schlinkmann[§], Annemarie Honegger[§] and Andreas Plückthun[§*]
[§]Department of Biochemistry, University of Zurich, Winterthurerstrasse 190, 8057 Zürich, Switzerland

*corresponding author: Andreas Plückthun, plueckthun@bioc.uzh.ch, telephone 0041 (0) 44 6355570, fax 0041 (0) 44 6355712

short title: deep sequencing of synthetic libraries

Abstract

Directed evolution techniques provide powerful tools to engineer proteins for an envisaged phenotype, and its applications range from the optimization of industrial enzymes to the generation of new biopharmaceutical drugs.

While generation of genetic diversity and selection procedures are high-throughput compatible, the subsequent analysis of the selection by Sanger sequencing is limited in its sampling capacity since it requires the individual handling of individual, selected variants. The fairly recent development of high-throughput and cost-effective deep sequencing technologies has hence great application potential in directed evolution.

Here, we have used deep sequencing to evaluate the directed evolution of a G protein-coupled receptor (GPCR). GPCRs act as molecular switches in most signal transduction processes, making them key targets in pharmacology. GPCRs have naturally evolved for protein functionality in a membrane environment, requiring low expression levels and fast turnover to sustain efficient signal activation and regulation. However, these poor biophysical properties constitute major roadblocks for *in vitro* characterization and structure determination of GPCRs, as well as for the utilization of purified proteins in high-throughput drug screening. To overcome this problem, directed evolution provides powerful techniques to engineer proteins variants with improved biophysical properties that are able to signal and have ligand binding properties very similar to the wild type. Our recent development of a FACS-based screening and selection technique to efficiently display and isolate GPCRs with high functional expression rendered GPCRs accessible to directed evolution. We have developed technologies to comprehensively randomize a GPCR to understand the critical information content of the GPCR sequence and structure with respect to protein biosynthesis, stability in the lipid bilayer and, after solubilization, in detergent micelles. Every residue of the receptor was separately and fully randomized into all 64 codons, and each library was subsequently selected for high functional expression using the previously established selection method. The combined sequencing of more than 350 independently selected pools required overcoming profound sample preparation challenges and customized data analysis, which will be described in detail in the following chapter. The analysis of the selected pools by deep sequencing revealed the amino acid preference in every position of the receptor. This unique data set allowed us, for the very first time, to compare *in vitro* with natural selection and to identify several positions that restrict functional expression and detergent stability.

1. Introduction

1.1 Application of deep sequencing in directed evolution projects

The recent developments and improvements of deep sequencing approaches have revolutionized many scientific projects that were not accomplishable before by standard sequencing. While *de novo* genome assemblies or SNP detection became feasible and even routine projects by means of the high throughput and oversampling capacities of deep sequencing approaches (reviewed for example in (Pareek *et al.*, 2011)), these technologies do also have a tremendous application potential in mutagenesis and directed evolution projects, where robust analysis of a mutagenic load and correlation or sensitive detection of rare sequence variants and correlation between sequence variants is desired.

Directed evolution projects can be grouped into two types. In the first, a rather diverse collection of sequences is selected, typically for binding affinity. These sequences differ in many positions, as exemplified in the CDRs of antibodies or in the many randomized positions of a synthetic scaffold. *In vitro* directed evolution methods such as ribosome display can easily accommodate libraries with a diversity of 10^{12}, but *in vivo* techniques such as phage display are limited by transformation efficiencies and typically reach diversities of 10^{7}-10^{8}. Iterative rounds of screening and selection lead to enrichment of a subpopulation displaying an envisaged phenotype, e.g. a tight binding to a target molecule. Since in general the binding properties (phenotype) of individual selected clones need to be connected to their sequences, and since toward the end of the selection the number of molecules of interest becomes small, deep sequencing has not found widespread use. Standard Sanger sequencing appears to be more suitable in this situation, since individual clones can be accessed.

In contrast, deep sequencing offers unparalleled powers when it comes to using the directed evolution process for generating statistical information on sequence preferences. Such a scenario would arise, e.g., in affinity maturation where it can be of interest which amino acid types are enriched during this process, and where one might want to combine the amino acids found afterwards. In other words, unlike in the case of a naïve diverse library, these libraries are closely related point mutants of a defined starting molecule, and thus much more tightly connected to each other than, e.g., a synthetic antibody library. By these means, statistically robust sequence information about an enriched subpopulation can be obtained, and it is easily feasible to monitor selection processes over several rounds. In contrast, the number of analyzed clones in standard Sanger sequencing is not only limited by the availability and capacity of high throughput screening (HTS), but also by the significant costs for standard Sanger sequencing of individual clones.

Here, we have employed deep sequencing using the 454 technology to evaluate the directed evolution of a GPCR for high functional expression and detergent stability, using a comprehensive randomization study of a GPCR. This is conceptually closer to the second scenario, but it required new technologies for the selection itself, as well as for sequence analysis, because the length of the protein far exceeds the read length of

available deep sequencing technologies. Finally, no commercial software was available for the required data analysis, again requiring own developments.

1.2 Principles of directed evolution

Different from rational design approaches, directed evolution does not require any prior structural information about the target protein or any prejudice concerning the stabilizing mechanisms, but is based on the generation of genetic variability, coupled to subsequent selection of the desired phenotype from a diverse library. This process mimics natural evolution *in vitro*, with the advantage that the genetic diversity is artificially introduced and can be controlled in its mutational load, i.e. number of changes and mutant spectrum of allowed amino acids and their percentage by adjustment of the reaction conditions. The key requirement for the directed evolution of any target protein of interest is the availability of a suitable selection system to isolate a rare phenotype from a large and highly diverse library.

A relevant target protein class for directed evolution are G protein-coupled receptors (GPCRs): GPCRs play a key role in most eukaryotic signal transduction processes, and are thus indispensable to nearly all physiological processes. Activation of these receptors by an extracellular stimulus induces a conformational change within the protein, resulting in signal transduction across the cell membrane. GPCRs are embedded in a fine-tuned network of receptor activation, signal transduction to and signal amplification by heterotrimeric G proteins, and regulation of signaling by receptor desensitization and degradation (Deupi and Kobilka, 2007). Their pivotal role in cell signaling and survival is reflected in the fact that many non-olfactory receptors are the target of some the most frequently prescribed drugs, such as the treatment of pathophysiological heart conditions by β-blockers acting on β-adrenergic receptors (Frishman, 2008), or the control of pain by targeting opioid receptors (Stein *et al.*, 2003). Currently, it is estimated that 30% of all prescribed drugs target GPCRs (Lagerström and Schiöth, 2008; Overington *et al.*, 2006).

The pharmacological relevance of GPCRs is fundamental to the huge scientific efforts to functionally and structurally characterize GPCRs. However, the biophysical properties of GPCRs have naturally evolved for activity in a cellular context, and their notoriously poor biophysical properties constitute a major bottleneck for *in vitro* characterization studies. Low expression levels, poor solubilization efficiency and low stability in detergent micelles restrict the spectrum of GPCRs that is accessible to *in vitro* characterization studies, let alone *in vitro* drug screening approaches.

Directed evolution provides promising and powerful method to approach the current limitations in GPCR research, and such studies became accomplishable with the recent development of a FACS-based, high-throughput selection method to isolate well-expressed and functional GPCRs from large receptor libraries (Sarkar *et al.*, 2008). This strategy directly targets the intrinsic bottleneck of the given GPCR, i.e. the primary amino acid sequence, and allows to identify receptor variants with binding and signaling properties close to wild type but with improved expression levels and biophysical

behavior, with the great potential to render non-accessible GPCRs amenable to functional *in vitro* studies.

Randomization by mutagenic PCR is a suitable and well-established method to generate highly diverse libraries (Cadwell and Joyce, 1994), starting from the target sequence, and has been successfully applied to evolve several GCPRs for higher expression levels and detergent stability, using iterative rounds of random mutagenesis and selection (Dodevski and Plückthun, 2011; Sarkar *et al.*, 2008).

However, random mutagenesis techniques are limited with respect to coverage of the target sequence (target space), and with respect to the coverage of the mutant space, the latter being a result of the degeneracy of the genetic code in combination with preferred single-base changes in mutagenic GPCRs. Consequently, it is not possible to fully cover the target sequence and mutant space by random mutagenesis approaches. Alanine-scanning approaches specifically target every residue and have also been recently applied to GPCRs to generate variants with improved protein properties (Rosenbaum *et al.*, 2007; Shibata *et al.*, 2009), but fail to identify beneficial mutations other than alanine. In both cases, critical residues for protein function and stability might remain unidentified.

Thus, the most crucial step is to explore the entire mutant space by full randomization of every receptor position with selection for the amino acid variant conveying the desired phenotype.

1.3 Directed evolution of the GPCR rNTR1-D03 using comprehensive randomization

The rNTR-D03 (D03) variant was chosen as a typical GPCR to perform a saturating and exhaustive randomization with subsequent selection for high and functional expression using the previously established FACS-based selection system (Sarkar *et al.*, 2008). Synthetic libraries with an NNN-diversified codon were generated for receptor positions 43 to 418 (Schlinkmann *et al.*, 2012). The full sampling of the degenerate genetic code is highly valuable for two reasons: First, any codon bias introduced prior to translation, e.g. variable tRNA levels, mRNA secondary structure, codon usage preferences can be excluded or identified. Second, the full codon diversity functions as an internal quality control to ensure phenotype selection. While the full NNN-randomization approach allows to verify the absence – or presence – of any codon bias effects, it also adds a technical bias to the selection that requires bioinformatics correction during data evaluation, which will be explained in detail later. Furthermore, a high enough oversampling of sequencing after selection allows discrimination between real positive selection and tolerance of certain amino acid properties. Theoretically, the presence of stop codons could be reduced by using an NNK triplet at the target residue. However, the presence of stop codons in the naïve library is uncritical when selecting for protein functionality, and their absence after selection provides an important measure of quality control.

For the first time, this study provided knowledge about the preferred residue for every position, including positions where the wild-type residue is preserved. Even more importantly, this study allowed to identify positions where a residue other than wild-type is preferred. The comparison of *in vitro* selection with natural evolution of GPCRs further elucidated the different constraints of protein biosynthesis, integration and folding in the lipid bilayer and formation of a functional ligand binding site as observed during *in vitro* evolution (D03 libraries) in *E. coli*, versus maintenance of a finely tuned signaling network in natural GPCR evolution (Schlinkmann *et al.*, 2012). These results provide a unique data set that will greatly help in future GPCR engineering.

2. Experimental Details

2.1 Generation of synthetic libraries

The specific and separate targeting of every target protein residue, here a GPCR, in combination with full randomization into an NNN-library, assures that every possible permutation is generated and available for selection. Throughout library generation and handling, continuous representation of the entire library diversity is most crucial, since subsequent analysis of the selection outcome is based on the assumption of a fully NNN-randomized position following a theoretical distribution. Naïve library members have to be sequenced to guarantee that the naïve library corresponds to its design, namely that it varies in exactly one codon from the starting sequence and that the NNN-randomization represents all codons at equal frequencies.

Apart from sustaining library diversity throughout all steps by an oversampling threshold of at least 30-fold, the generation of a single library is rather straightforward, albeit laborious, considering the number of libraries that have to be produced. Most importantly, any overrepresentation of the wild-type codon in the resulting library has to be avoided. Main sources for wild-type contamination are the amount of wild-type DNA template during the primary PCR step, and usage of an acceptor plasmid containing the wild-type coding sequence. Consequently, the template amount during the PCR step should be kept at an absolute minimum, and the acceptor plasmid should not contain any receptor coding sequence, but a stuffer sequence or negative selection marker.

To construct the 376 libraries used in this study, the codons encoding the D03 residues 43 to 418 were randomized by replacing them, one at a time, with the diversified trinucleotide NNN, where N stands for an equimolar mixture of A, G, C, and T. Depending on the position of the diversified codon relative to the 5’ and 3’ ends of the gene, one of two PCR-based methods was employed: For codons close to one of the gene ends, an oligonucleotide covering both the target codon site and the restriction recognition site was designed with an NNN trinucleotide annealing to the target codon site. The full-length library fragment was then PCR-amplified using a second amplification oligonucleotide hybridizing to the opposite end of the gene, also containing a suitable restriction recognition site. To randomize codons distant from the two ends, a two-step PCR

assembly strategy was employed. Two complementary oligonucleotides were designed to cover the target codon with a diversified NNN sequence, and each of these oligonucleotides was paired with the appropriate amplification oligonucleotide at either end of the gene, so that by PCR amplification, two half-gene fragments overlapping at the target codon site were generated. The PCR products were then combined and extended in a second PCR reaction to obtain the full-length product containing exactly one diversified codon (for details, see (Schlinkmann and Plückthun, 2012)). The final PCR products were purified, the flanking restriction sites were digested and the library PCR fragment was ligated into the acceptor plasmid pRG-del. pRG-del is a derivative of pRGD03 (Sarkar *et al.*, 2008; Schlinkmann *et al.*, 2012), where, for the reasons explained above, the GPCR-coding sequence was replaced by a stuffer sequence containing multiple restriction recognition sites. The ligation product was then purified and transformed into *E. coli* DH5α cells by electroporation.

Sanger sequencing of a representative subset of library variants verified that library diversity conformed to its design. Sequences of a total of 2170 clones from naïve (unselected) libraries were shown to contain an equal distribution of the four bases in all codon positions (Table 4-1), consistent with full randomization. No overrepresentation of any codon, especially the wild-type codon, was detected. Importantly, since Sanger sequencing can cover the full length of the GPCR, it can be ascertained that the genes do not have any spurious mutations in addition to the randomized position. Thus, one can be assured that the phenotype is indeed caused by the randomized amino acid.

2.2 Library expression and FACS selection

Libraries were transformed into and expressed in *E. coli* DH5α cells. A sufficient oversampling of library diversity was ensured by controlling the transformation efficiency, with a threshold of minimally 2500 colonies after transformation, corresponding to a 30-fold overrepresentation of library diversity.

Briefly, cells were grown to early log-phase (OD_{600} = 0.5) and each GPCR library was expressed for 20 hours at 20°C (Schlinkmann *et al.*, 2012). Low expression temperatures are recommended during library selections, to reduce the toxic effects of GPCR overexpression in *E. coli* and minimize growth rate differences between individual library members, at least before enough stabilizing mutations have accumulated and as long as the phenotype is still wild-type like and poor..

An aliquot of cells was washed in TKCl buffer (50 mM Tris pH 7.4, 150 mM KCl), rendering the outer membrane permeable, and fluorescence-labeled by binding of fluorophor-conjugated agonist, BODIPY-neurotensin, essentially as described in (Sarkar *et al.*, 2008). Hence, cells were fluorescence-labeled according to their level of functional GPCR expression. 2500 cells with expression levels corresponding to the top 1% of functional expression were collected for each library. Note that the parental sequence D03, even though itself already the product of a directed evolution, serves here as "wild type", as all mutants are derived from it. Generally, the selection window has to be adjusted in a proof-of-concept experiment to ensure meaningful selection. Here, the

library of position 347, in the wild-type a tyrosine residue known to be involved in ligand binding (Barroso *et al.*, 2000), was used to optimize and validate the method. With one round of selection, tyrosine was exclusively recovered from the selection, with equal representation of the two synonymous codons (Schlinkmann *et al.*, 2012). Selected cells were recovered and stored as glycerol stocks for later analyses.

2.3 Design and setup of the 454 sequencing reaction

In a first analysis step, 5-20 single clones from each selected pool were analyzed by standard Sanger sequencing. This primary data set allowed to deduce trends for every receptor position, and confirmed, also for conserved positions, phenotype selection by representation of the synonymous codons for a given amino acid. Most importantly, Sanger sequencing of the full-length, selected GPCR sequence assured that no spurious undesired mutations at sites other than the randomized codon influenced the selected phenotype.

Nevertheless, a robust statistical analysis of preferred, tolerated and avoided amino acids at each receptor position required a larger dataset. For this purpose, each selected library pool was further analyzed by 454 sequencing. The D03 gene is about 1200 base pairs long, and thus too long to be covered by the read length of deep sequencing by the 454 technology (at least at the time of the experiment). At the time of the experiment, the 454 read length typically reached 250 bases. By design, each library contains only one diversified codon, allowing us to sequence only a small region of the gene, since the Sanger sequencing of the whole gene had already confirmed the absence of other mutations outside of the designed ones. Ideally, one would have kept each library, in which one amino acid was randomized, separate. However, this would have been an overkill, given that with even a few thousand sequences excellent statistics can be obtained, and the achievable million sequences would offer no additional benefit. More importantly, the independent handling of 376 deep sequencing projects for one single gene is way beyond economic feasibility. Conversely, the multiplexing of samples by pooling of all libraries into one big mixture, with particular primer pairs containing multiplex-identifier-sequences (MIDs) to untangle where a mutation came from, would be hard to achieve in practice and would be so expensive in primer pairs that it would again be not feasible. Multiplexing of samples without the use if MIDs is practically accomplishable and cost-effective, but comes with a drawback affecting later data assignment: In such a setup, conserved sequences are identical to the parental reference sequence D03, and hence the information which position was conserved would be completely lost, as explained in more detail below.

The challenge was therefore to devise a strategy which is a compromise between these two extremes. Seven amplicons were thus designed as 250 bp overlapping fragments to fully cover the receptor sequence (Fig. 4-1A, for primer sequences see (Schlinkmann *et al.*, 2012)), with an sample preparation and analysis strategy explained in the following.

The DNA of each selected pool was isolated, and the DNA fragment covering the diversified codon was amplified by choosing the flanking amplicon primer pair. For this study, 376 amplicon PCR products, each representing the corresponding diversified library codon, were generated (Fig. 4-1A and 4-1B). The PCR products were purified, and the DNA amount corresponding to $2 \cdot 10^{11}$ molecules was used as input material for the 454 sequencing reaction (performed at Functional Genomics Center Zurich, FGCZ).

While the generation of 376 individual PCR products is rather a matter of diligence than finesse, the actual experiment required a sophisticated sample setup: In principle, the DNA of several libraries could be mixed in one reaction. By default, every sequence contains only one diversified codon, thus allowing identification of its origin by alignment to the reference sequence D03 (serving as starting sequence, or new "wild type"). This strategy is both cost- as well as work-effective, as it avoids tagging each library by the above mentioned MIDs. The usage of MIDs to identify the sample origin is clearly valuable when a few samples are mixed in one reaction, a reference sequence is not available and accurate sequence assignment is crucial. In this case, the usage of 376 individual, MID-tagged amplicon primer pairs would have not only dramatically increased and complicated the workflow of sample preparation, but the cost of 376 individual primer pairs would have even exceeded the cost of a large scale 454 sequencing run, and was thus considered inappropriate.

However, as mentioned above, our strategy to mix multiple library samples in one 454 sequencing reaction has one drawback: While sequence reads different from the parental reference sequence D03 can be unambiguously assigned, sequences that perfectly match the reference sequence remain unassigned, since it is not clear from which (maintained) position they originate. These sequences were not processed further, and a bioinformatics correction was applied during data evaluation to account for this shortcoming.

We decided to not sequence all randomized positions falling within one amplicon (typically 50) in the same pool, but rather distribute them over 8 individual 454 sequencing reactions, such that each reaction is pooled from only 6-8 randomized positions falling within one amplicon (Fig. 4-1C), for the following reason: In a mixed sample of 50 different PCR products coming from the 50 different randomized positions within one amplicon, about 2% of the obtained sequence reads would be assignable to its library origin as mutations within this codon. However, for each position, the remaining 98% of sequence reads would be wild type in a given position and thus align perfectly to the D03 reference sequence in that specific codon, since their diversified codon is at a different position. This would make the accurate determination of mutant frequencies rather difficult. From a pilot experiment, we learned that the noise of our 454-sequencing reaction was ~ 0.1%, meaning that 0.1% of sequence reads contain one or more mismatches in the non-randomized gene regions. The observed error frequency here is a sum of base pair mismatches introduced during amplicon PCRs as well as sequencing errors during the 454 sequencing reaction. The 454 sequencing reaction accuracy is mostly limited by shortcomings in the identification of homopolymer length by pyro-sequencing (Chan, 2009; Ronaghi *et al.*, 1998), and the noise of 0.1% here is mainly observed in homopolymeric sequence stretches. Here, all sequences showing miscalled bases in addition to the randomized codon were excluded from analysis. In the given example, an

assignment of 2% of sequences per library and 0.1% noise would have resulted in a signal-to-noise ratio of only 20.

In order to obtain a higher ratio of assignment % over noise % (i. e. signal-over-noise), we have prepared the samples as follows (Fig. 4-1C): 376 different libraries were grouped into 8 individual 454 sequencing reactions, run separately on 1/8 of a 454-picotiterplate. Every reaction contains 45-52 individual PCR products in total, of which 6-8 fall within each of the amplicons 1-7. Alignments of 454 sequence reads to the D03 reference sequence (i.e. assignment of 454 sequence reads to a specific library origin) were later run independently for each 454 sequencing reaction *and* amplicon. One alignment of 454 sequence reads to the D03 reference sequence thus contains sequence reads of 6-8 individual amplicon PCR products, meaning that sequences from this pool are randomized in one of these 6-8 positions. Thus, 12.5 – 16% of sequences are assigned per library (i.e. for a given codon that was randomized in this set, this is the percentage of sequences actually carrying an altered codon in this position), resulting in an improved signal-to-noise ratio of at least 125 (12.5% over 0.1%) (Fig. 4-2).

2.4 Computational analysis of 454 sequencing data

The fast expansion of deep sequencing technologies is facilitated by major technical advances during the last years. The outsourcing of the actual sequencing process to a specialized institution and the comparably low prices per sequence makes deep sequencing essentially accessible to most researchers. However, data evaluation is by far not as easy as sending out a DNA sample: The obtained raw data sets are huge, and the evaluation requires both computational power and suitable processing software. While more and more software packages are available for analysis of deep sequencing data, we have found none of these to fit to our needs for data analysis, let alone statistical corrections that are necessary regarding our sample setup.

Basically, our data evaluation is restricted to one codon per sequence read, and is based on trinucleotide analysis, i.e. codon level and amino acid level. Further, the unique setup of our 454 sequencing reactions required separate analysis of individual amplicons, for which the sequences had to be assigned and separated into individual clusters. We have thus developed customized EXCEL-based visual basic macro functions to serve our needs for sequencing data analysis.

Sequences acquisition and assignment

The raw sequences were transferred from the 454 system as large FASTA-format text files, imported into EXCEL and processed using a set of custom Visual Basic macros.

First, the amplicon and the reading frame had to be identified. We searched for the first 12 base exact match between each sequence and the D03 reference sequence (forwards and reverse), representing a unique sequence string, and cut off all nucleotides before the start of the first in-frame codon match.

The sequence was aligned without gaps and cut into in-frame nucleotide triplets. For our experiment, it was crucial to keep the background of sequencing errors as low as possible. Therefore, we stringently eliminated unreliable parts of the sequence. 454 sequences tend to acquire insertions and deletions in runs of the same nucleotide (homopolymers; see (Chan, 2009)), and indeed most sequences eventually went out of frame. Since we did not expect any frameshifts from a selection for functional receptors, we took the occurrence of frame shifts in the sequence as a sign that the sequence quality had deteriorated and truncated the shifted part of the sequence. Mismatched codons were trimmed back from the end of the sequence until a 4 codon (12 bases) exact match was found. The truncated sequences were compared to the D03 reference sequence. Only those sequences that differed by exactly one codon from the D03 reference sequence were used for further analysis. For the pilot experiment, these were 86,734 out of 206,405 sequences (42%), covering 48 randomized positions. For each randomized position, an average of 1,800 sequences differed from the consensus; for non-randomized positions, only 7.6 sequences (noise < 0.5%). In the actual experiment, 476,322 sequences (69.6%) showed exactly one deviation from the D03 reference sequence, covering 331 positions with 1,400 sequences per randomized position, against a background of 4.4 mutations in nonrandomized positions. The process of sequence acquisition and assignment is illustrated in Figure 4-2.

Analysis of codon and amino acid distribution

For each amplicon, comprising 3 to 8 randomized positions, the frequency distribution of the 64 codons was determined for each position in the sequence. As explained above, the frequency of the wild-type codon in the randomized positions could not be determined directly, as it could not be distinguished from the wild-type codon originating from sequences randomized in a different position. For amino acids encoded by several synonymous codons, the frequency of the wild-type codon was estimated as the average of the frequencies of synonymous codons. This correction could not be applied for the two amino acids encoded by a unique codon, Met (ATG) and Trp (TGG). The codon frequency distribution was normalized to give a sum over all 64 codons of 100%.

The amino acid frequency distribution was derived as the sum of the frequencies of synonymous codons. For further analysis, we evaluated the effects of selection on the width of the frequency distribution (sequence variability) and the peak of the distribution (sequence consensus). The amino acid distributions demonstrated a high tolerance of the D03 towards randomization: The average positional variability in the transmembrane regions of the sequences recovered from the top 1% neurotensin-binding *E. coli* clones isolated by FACS was comparable to that derived from the corresponding regions in an alignment of all Class A (rhodopsin-like) GPCR sequences.

NNN randomization at equal and theoretically expected frequencies, combined with the degeneracy of the genetic code, introduces a technical bias in the amino acid distribution. Ser, Arg and Leu, encoded by 6 codons each, are six-fold overrepresented over Trp and Met, encoded by a single codon; other amino acids lie between the two extremes. For most positions, the selection pressure was not strong enough to overcome this technical bias: amongst amino acids with similar properties, the amino acid sequence

consensus frequently went to the one encoded by the highest number of codons, e.g. to Leu in membrane-embedded positions that tolerated Leu, Val, Ile and Met, or to Arg in positions that required a positively charged amino acid. Usual metrics of sequence variability (e.g. Shannon sequence entropy (Shannon, 1963; Strait and Dewey, 1996) or Kabat sequence variability (Kabat *et al.*, 1977)) and of sequence consensus did not perform well in this context, as they assume all amino acids to be equally probable and therefore affects the results in favor of the amino acids over-represented in the original library, due to the degeneracy of the genetic code. The classical amino acid consensus sequence therefore differed significantly from the translation of the codon consensus (Fig. 4-3), and amino acids encoded by a larger number of codons on average appeared more conserved than amino acids encoded by fewer codons.

The root-mean-squares deviation (rmsd) of the observed amino acid distribution from the input amino acid distribution generated by equal NNN codon randomization was chosen as a measure of the selective pressure shaping the amino acid distribution in a given position. The rmsd for a given position is calculated according to formula (1):

$$rmsd = \sqrt[2]{\frac{\sum_{i=1}^{20}(f_{l_i} - f_{s_i})^2}{20}} \qquad (1)$$

where f_{l_i} is the frequency of amino acid i in the library before selection and f_{s_i} is the frequency after selection. The frequency of amino acid i before selection is deduced from the theoretical distribution of a NNN library. Sanger sequencing of the naïve libraries confirmed the codon distribution according to a theoretical distribution before selection (Table 4-1), and the high oversampling of the library diversity throughout all experimental steps kept the statistical noise low.

A low rmsd denotes a permissive position, where the selection process had little or no effect on the observed amino acid frequency distribution, while a high rmsd is a sign of a restrictive position with a clear amino acid preference. Intermediate rmsds frequently denote positions where the general character of the amino acid is preserved (e.g. aliphatic), but not the exact type (e.g. valine).

This distinction between permissive (low rmsd) and restrictive positions (high rmsd) does not depend on whether the wild-type sequence is conserved or not – a position can be restrictive, but shift away from the wild-type sequence to a new focus, or be permissive and still include and partially preserve the wild-type sequence (e.g. by only selecting for the aliphatic character of the amino acid).

2.5 Data interpretation

The assessment of sequence conservation and sequence shifts was based on the comparison of the wild-type sequence to the selected consensus, generated from a normalized table of the observed amino acid frequencies divided by the number of synonymous codons for each amino acid. This normalized consensus better reflects the influence of the applied selection pressure on the amino acid distribution than the classical

amino acid consensus (Fig. 4-3). We will now discuss the reasons for choosing this strategy.

To correctly analyze and interpret the obtained *in vitro* evolution data, it is necessary to consider the differences between natural evolution and *in vitro* evolution of GPCRs. The classical consensus is derived from natural sequences and both well established and suitable for the analysis of natural evolution over short evolutionary distances.

Natural evolution is primarily driven by the random appearance of single nucleotide exchanges, modifying an ancestral sequence and increasing the width of the amino acid sequence distribution. Over relatively short evolutionary distances, the consensus of natural sequence variants (e.g. different naturally occurring peptide-binding GPCRs, including those from different species) is governed by the ancestral sequence. Few mutations occur, neutral or selected, and the mutational tolerance has not yet been fully tested.

As the evolutionary distance covered by a sequence alignment increases, the different probabilities of introducing different mutations affect the observed amino acid distribution. Only over evolutionary distances large enough to equilibrate the sequence pool (meaning, all nucleotides have been tried) the influence of any codon bias would become observable in natural sequences (e.g. in an alignment of all human Class A GPCRs).

In contrast, in our synthetic library approach we start from a known and theoretical codon distribution (meaning that all of the 64 NNN codons is present at the same frequency) that gets narrowed down by successive selection rounds, until it converges to a single sequence. With a single selection round, the observed amino acid distribution is influenced by the technical codon bias (i.e. that a particular amino acid is being introduced more likely simply because it can be encoded by more synonymous codons) and the importance of a particular sequence position to the “fitness” of the entire molecule.

Classical consensus analysis, not accounting for the number of synonymous codons by which different amino acids are represented, is most suitable to the analysis of natural sequences that have not diverged very far from the ancestral sequence, and to *in vitro* evolved sequences that have undergone a sufficient number of selection round to show clear sequence convergence. In contrast, a consensus corrected for technical codon bias (i.e. number of synonymous codons for amino acid types) yields better information with highly diverged natural sequences and for *in vitro* evolved sequences that have undergone relatively mild selection.

We compared the rmsds obtained from the sequences of the selected members of the D03-based libraries to those derived from more than 20,000 aligned class A GPCR sequences obtained from the GPCRDB (http://www.gpcr.org/7tm/). The ratio of the D03 rmsds to the GPCR class A rmsds indicates in which of the two systems a given position is more highly conserved (Figure 4-4). As expected, positions involved in ligand binding were strongly focused in the D03 libraries, but divergent in Class A GPCRs (which bind to diverse ligands), while residues involved in G-protein interaction were strongly focused in Class A GPCRs but divergent in the D03 libraries (which were selected for ligand binding, not for signal transduction). These positions serve as positive controls, showing the sensitivity of the rmsd as a measure of the selective pressure shaping the amino acid

distribution in given residue position. Residues that appear to be highly focused for less obvious reasons are prime candidates for further analysis, especially if the observed amino acid distribution in those positions reveals a shift towards an amino acid different from the original D03 sequence or Class A GPCR consensus.

2.6 Conclusions and Discussion

The comprehensive randomization in combination with deep sequencing resulted in a unique data set providing unprecedented insight into the constraints of GPCR evolution (Figure 4-4), and the analysis by deep sequencing robustly identified the presence of so called shift positions after selection, which are key mutations for engineering of the protein. The library design allowed us to constrain the deep sequencing to the target region covering the randomized position, and to assign the sequence reads by reference alignment. Even though the actual sequence information was contained in one trinucleotide, the read length performance of the 454 sequencing technology of 250 bases facilitated coverage of the full sequence, i. e. all libraries, by only seven amplicons, which would not have been possible by other deep sequencing technologies available at that time (deep sequencing technologies such as illumina® sequencing or ABI SOLiD systems allowed for maximal read length of only 100 bases). In this specific setup, the obtained data set had to be corrected for the loss of wild-type codon information by statistical methods. With the analyzed data at hand, we can conclude that the approach of sample preparation and sequencing setup taken here proved to be appropriate, providing an enormous gain in information while keeping sample preparation work and -costs at a feasible level.

Unlike our position-specific libraries, most directed evolution studies are based on random mutagenesis of the whole protein sequence (for example random mutagenesis of NTR1 (Sarkar *et al.*, 2008)) or the designed randomization of certain positions within the sequence (for example DARPin libraries (Binz *et al.*, 2003)). The recent advances of the 454 technology led to an average read length of 600-800 bases, representing the most promising technology for deep sequencing of libraries of small proteins. However, for libraries such as the randomized NTR1 sequence with a length of ~1200 base pairs, individual mutations can be separated by hundreds of base pairs while coevolving for functional or structural reasons. While deep sequencing can easily generate statistically robust data about mutational load and distribution under these conditions, it fails to allow correlated analysis of individual mutations, since it is not (yet) processive enough to cover one sequence in one read.

Fairly recently, so-called third generation sequencing technologies (single molecule sequencing) have become available (Pareek *et al.*, 2011; Schadt *et al.*, 2010), among which the SMRTTM sequencing technology (Pacific Biosciences) is most advanced regarding the read length, with expected read lengths of 1-10 kilobases. This will greatly simplify the analysis of libraries as those of GPCRs described here and facilitate further analyses.

References

Barroso, S., Richard, F., Nicolas-Ethève, D., Reversat, J.L., Bernassau, J.M., Kitabgi, P., Labbé-Jullié, C. (2000). Identification of residues involved in neurotensin binding and modeling of the agonist binding site in neurotensin receptor 1. *J. Biol. Chem.* **275**, 328-336.

Binz, H.K., Stumpp, M.T., Forrer, P., Amstutz, P., Plückthun, A. (2003). Designing repeat proteins: well-expressed, soluble and stable proteins from combinatorial libraries of consensus ankyrin repeat proteins. *J. Mol. Biol.* **332**, 489-503.

Cadwell, R.C., Joyce, G.F. (1994). Mutagenic PCR. *PCR Methods Appl.* **3**, S136-140.

Chan, E.Y. (2009). Next-generation sequencing methods: impact of sequencing accuracy on SNP discovery. *Methods Mol. Biol.* **578**, 95-111.

Deupi, X., Kobilka, B. (2007). Activation of G protein-coupled receptors. *Adv. Protein Chem.* **74**, 137-166.

Dodevski, I., Plückthun, A. (2011). Evolution of three human GPCRs for higher expression and stability. *J. Mol. Biol.* **408**, 599-615.

Frishman, W.H. (2008). Fifty years of β-adrenergic blockade: a golden era in clinical medicine and molecular pharmacology. *Am. J. Med.* **121**, 933-934.

Kabat, E.A., Wu, T.T., Bilofsky, H. (1977). Unusual distributions of amino acids in complementarity-determining (hypervariable) segments of heavy and light chains of immunoglobulins and their possible roles in specificity of antibody-combining sites. *J. Biol. Chem.* **252**, 6609-6616.

Lagerström, M.C., Schiöth, H.B. (2008). Structural diversity of G protein-coupled receptors and significance for drug discovery. *Nat. Rev. Drug Discov.* **7**, 339-357.

Overington, J.P., Al-Lazikani, B., Hopkins, A.L. (2006). How many drug targets are there? *Nat. Rev. Drug Discov.* **5**, 993-996.

Pareek, C.S., Smoczynski, R., Tretyn, A. (2011). Sequencing technologies and genome sequencing. *J. Appl. Genet.* **52**, 413-435.

Ronaghi, M., Uhlen, M., Nyren, P. (1998). A sequencing method based on real-time pyrophosphate. *Science* **281**, 363, 365.

Rosenbaum, D.M., Cherezov, V., Hanson, M.A., Rasmussen, S.G., Thian, F.S., Kobilka, T.S., Choi, H.J., Yao, X.J., Weis, W.I., Stevens, R.C., Kobilka, B.K. (2007). GPCR engineering yields high-resolution structural insights into β2-adrenergic receptor function. *Science* **318**, 1266-1273.

Sarkar, C.A., Dodevski, I., Kenig, M., Dudli, S., Mohr, A., Hermans, E., Plückthun, A. (2008). Directed evolution of a G protein-coupled receptor for expression, stability, and binding selectivity. *Proc. Natl. Acad. Sci. U. S. A.* **105**, 14808-14813.

Schadt, E.E., Turner, S., Kasarskis, A. (2010). A window into third-generation sequencing. *Hum. Mol. Genet.* **19**, R227-240.

Schlinkmann, K.M., Honegger, A., Türeci, E., Robison, K.E., Lipovšek, D., Plückthun, A. (2012). Critical features for biosynthesis and functionality of a GPCR uncovered by all-versus-all mutations *Proc Natl Acad Sci USA* **109**, 9810-9815.

Schlinkmann, K.M., Plückthun, A. (2012). Directed evolution of G protein-coupled receptors for high functional expression and detergent stability. *Methods Enzymol.* **in press.**

Shannon, C.E. (1963). The mathematical theory of communication. *M.D. computing: computers in medical practice* **14**, 306-317.

Shibata, Y., White, J.F., Serrano-Vega, M.J., Magnani, F., Aloia, A.L., Grisshammer, R., Tate, C.G. (2009). Thermostabilization of the neurotensin receptor NTS1. *J. Mol. Biol.* **390**, 262-277.

Stein, C., Schäfer, M., Machelska, H. (2003). Attacking pain at its source: new perspectives on opioids. *Nat. Med.* **9**, 1003-1008.

Strait, B.J., Dewey, T.G. (1996). The Shannon information entropy of protein sequences. *Biophys. J.* **71**, 148-155.

Figure legends

Figure 4-1. 454 sequencing setup. (A) Seven amplicon PCR products (amplicons) of ~250 bp are designed to cover the GPCR gene. (B) For each selected library pool, an amplicon PCR containing the diversified codon is generated (1a-1d). (C) One 454 sequencing reaction contains 6-8 members of each amplicon. 8 individual 454 sequencing reactions are performed to analyze all 380 amplicon PCR products (2), kept separately on a subdivided picotiter plate.

Figure 4-2. 454 sequencing read assignment. After amplification of the gene region containing the diversified codon (1-3), various amplicon PCR products are analyzed in one 454 sequencing reaction (4). The resulting 454 sequencing reads (5) are assigned by alignment to the starting sequence D03 (6). The diversified codon unambiguously identifies the library origin (6; library positions n, m, x and y). However, 454 sequence reads with perfect alignment to the starting sequence D03 cannot be assigned to a particular randomized codon and statistical correction is applied for compensation.

Figure 4-3. Alignment of Sanger and 454 consensus sequences with rNTR1, rNTR1-D03 and class A GPCR consensus.

Sanger NNN consensus/ 454 NNN consensus: The NNN consensus shows the amino acid sequence derived from the most frequently observed codon in each position.

Sanger AA consensus/ 454 AA consensus: For the AA consensus, the observed frequencies of synonymous codons were summed up before deriving a consensus.

454 corr. AA consensus: Since in the 454 experiment, the frequency of the wild-type codon cannot be quantitated, its frequency has been deduced as the average of the frequencies of synonymous codons.

454 AAFreq corr./No. of codons: AA consensus derived from a frequency table that has been corrected for the technical bias in the initial amino acid library introduced by the degeneracy of the genetic code.

Consensus Class A GPCR: The classical AA consensus derived from an alignment of all Class A GPCR sequences downloaded from the GPCRDB (http://www.gpcr.org/7tm/), omitting the variable loop regions. At this level of sequence divergence, the amino acid frequency distributions show similar influence of codon bias as the 454 results.

Figure 4-4. Correlation between sequence constraints in natural GPCRs and in the rNTR1-D03 454 sequencing experiment. Colors indicate whether the amino acid distribution in a given position is equally constrained in both systems (purple), more constrained in natural class A GPCR sequences (blue) or in the deep sequencing from rNTR1-D03 (red). The size of the circles indicates the constraints imposed by the respective system, where large circles indicate positions with high constraints.

Table 4-1. Diversity of randomized codons.

	codon position			average
	1	**2**	**3**	
A	530	500	526	519
T	567	597	565	576
C	452	523	513	496
G	534	494	526	518
N	88	56	40	61

n = 2170

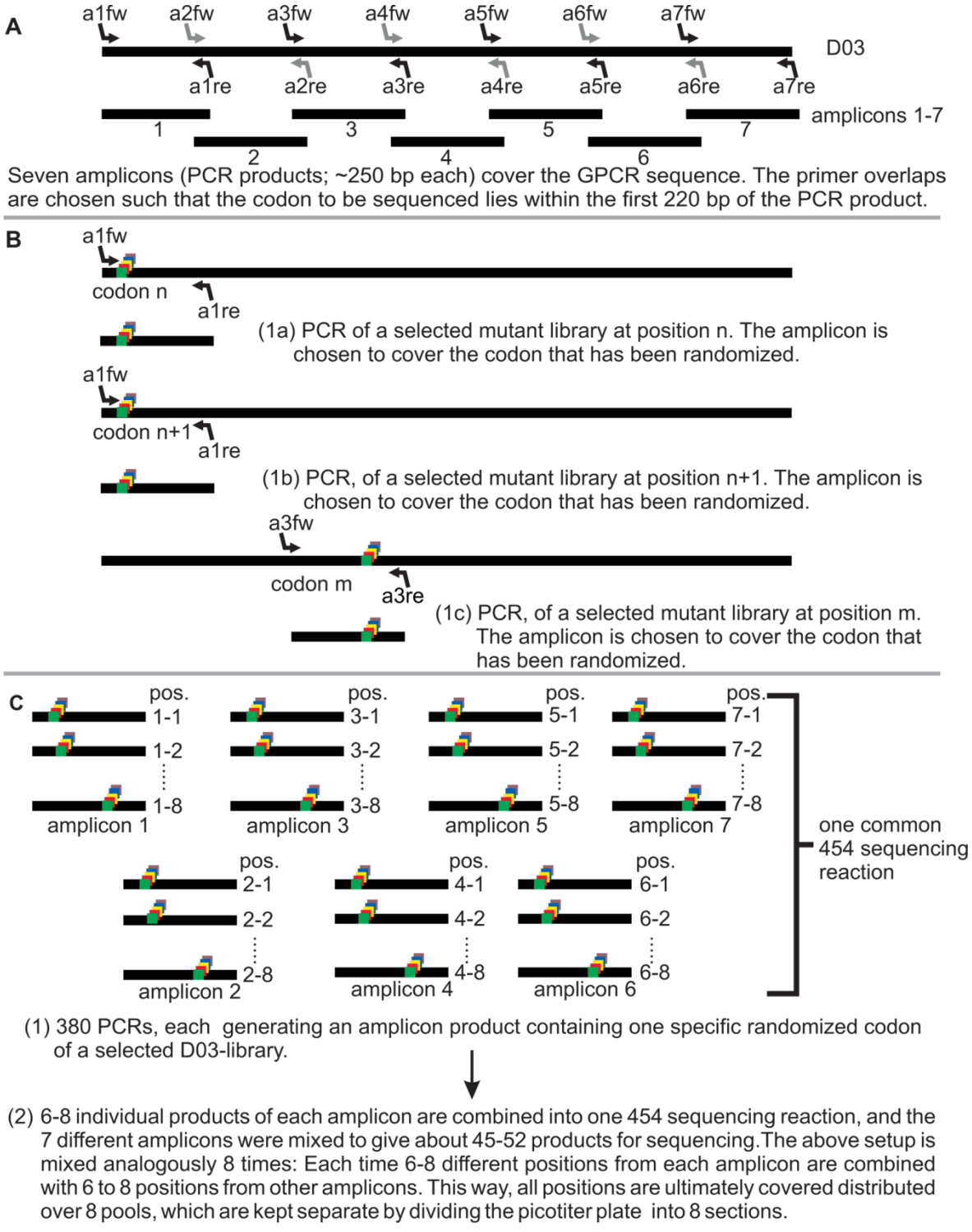
A
a1fw
a2fw
a3fw
a4fw
a5fw
a6fw
a7fw
D03
a1re
a2re
a3re
a4re
a5re
a6re
a7re
amplicons 1-7
1
2
3
4
5
6
7
Seven amplicons (PCR products; ~250 bp each) cover the GPCR sequence. The primer overlaps are chosen such that the codon to be sequenced lies within the first 220 bp of the PCR product.
B
a1fw
codon n
a1re
(1a) PCR of a selected mutant library at position n. The amplicon is chosen to cover the codon that has been randomized.
a1fw
codon n+1
a1re
(1b) PCR, of a selected mutant library at position n+1. The amplicon is chosen to cover the codon that has been randomized.
a3fw
codon m
a3re
(1c) PCR, of a selected mutant library at position m. The amplicon is chosen to cover the codon that has been randomized.
C
pos.
1-1
1-2
1-8
amplicon 1
3-1
3-2
3-8
amplicon 3
5-1
5-2
5-8
amplicon 5
7-1
7-2
7-8
amplicon 7
one common 454 sequencing reaction
2-1
2-2
2-8
amplicon 2
4-1
4-2
4-8
amplicon 4
6-1
6-2
6-8
amplicon 6
(1) 380 PCRs, each generating an amplicon product containing one specific randomized codon of a selected D03-library.
(2) 6-8 individual products of each amplicon are combined into one 454 sequencing reaction, and the 7 different amplicons were mixed to give about 45-52 products for sequencing.The above setup is mixed analogously 8 times: Each time 6-8 different positions from each amplicon are combined with 6 to 8 positions from other amplicons. This way, all positions are ultimately covered distributed over 8 pools, which are kept separate by dividing the picotiter plate into 8 sections.

Figure 1.

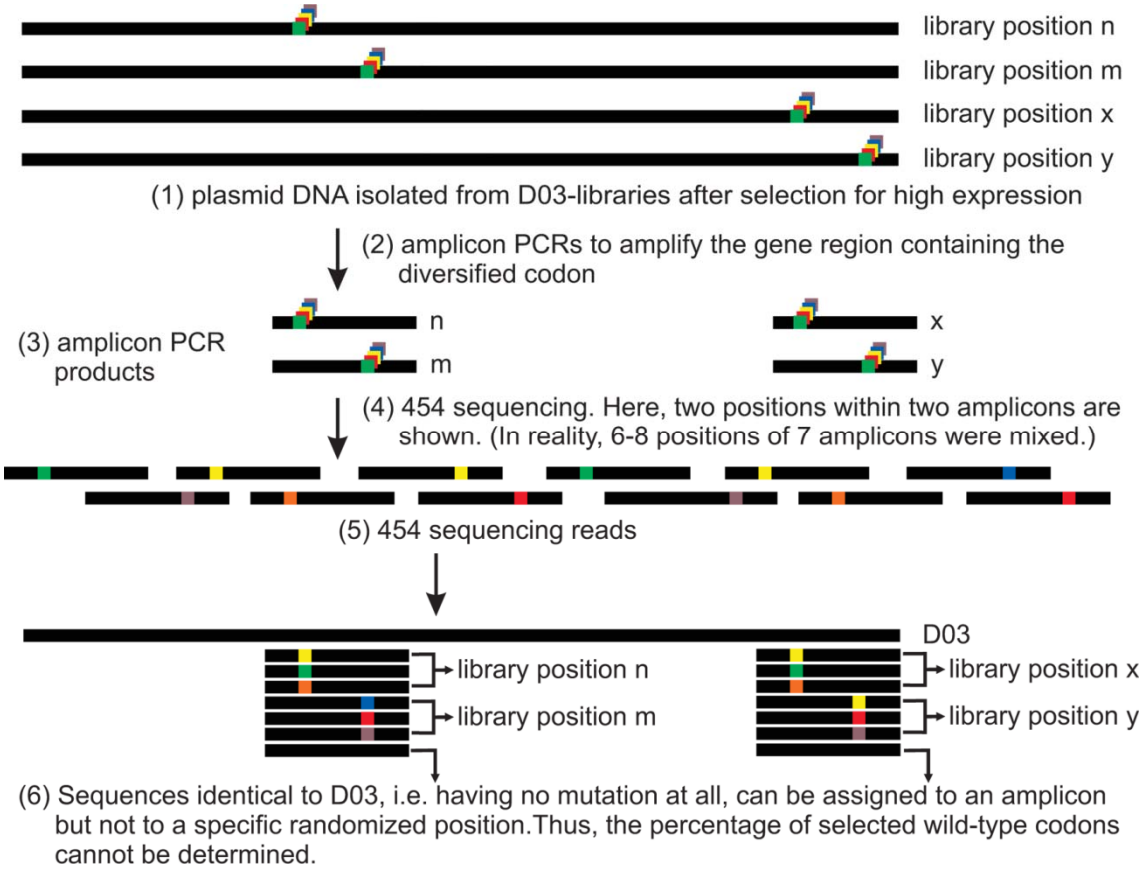
library position n
library position m
library position x
library position y
(1) plasmid DNA isolated from D03-libraries after selection for high expression
(2) amplicon PCRs to amplify the gene region containing the diversified codon
(3) amplicon PCR products
n
m
x
y
(4) 454 sequencing. Here, two positions within two amplicons are shown. (In reality, 6-8 positions of 7 amplicons were mixed.)
(5) 454 sequencing reads
D03
library position n
library position m
library position x
library position y
(6) Sequences identical to D03, i.e. having no mutation at all, can be assigned to an amplicon but not to a specific randomized position.Thus, the percentage of selected wild-type codons cannot be determined.

Figure 2.

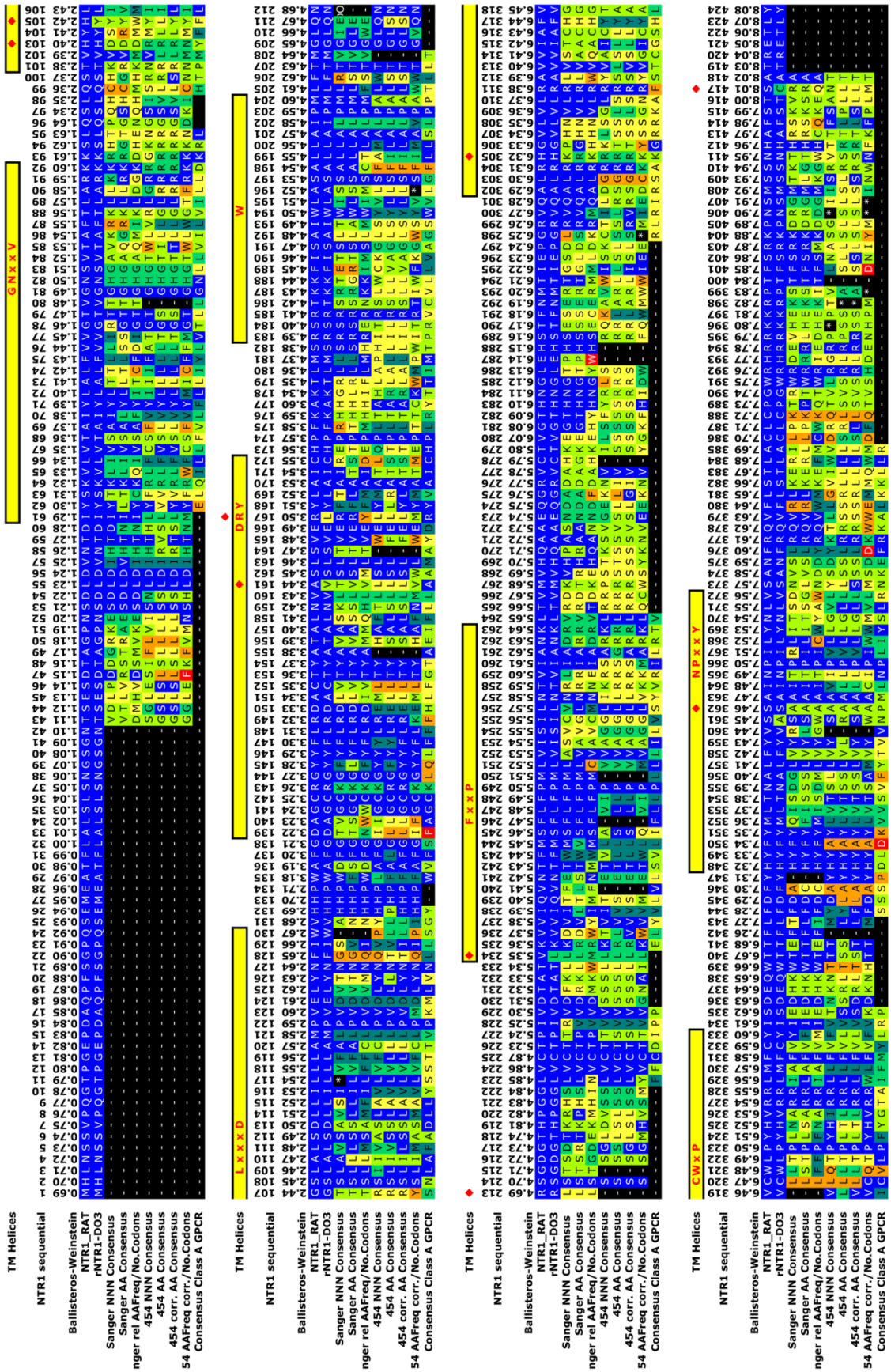

Figure 3.

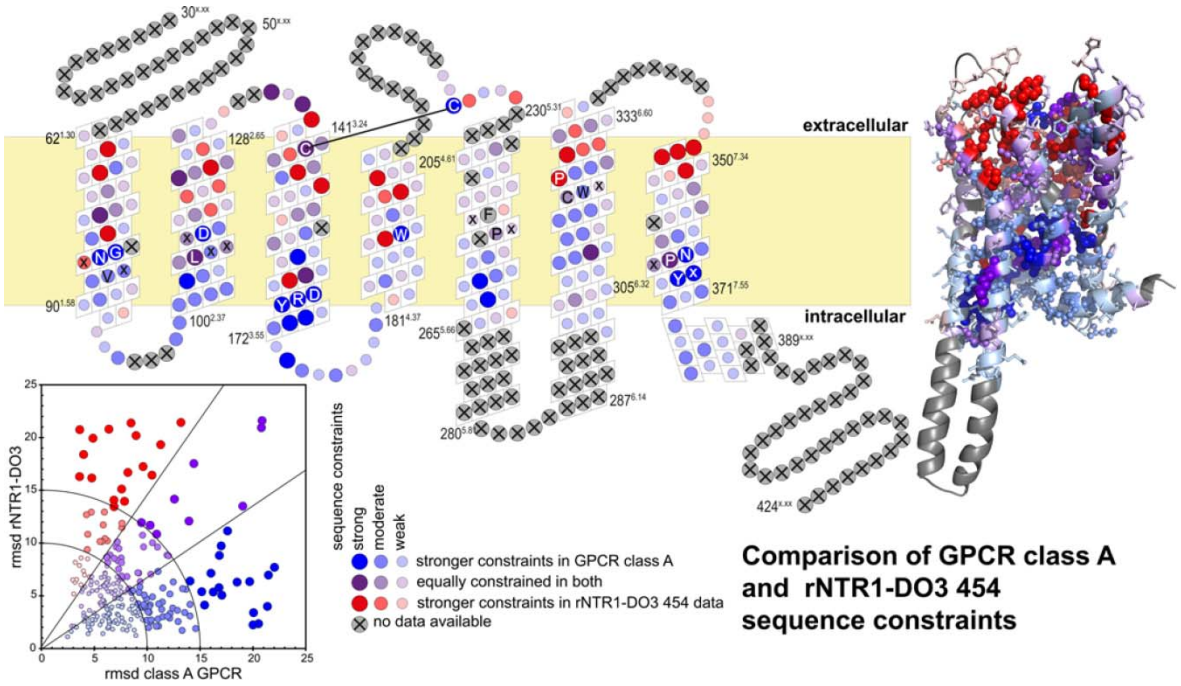
extracellular
intracellular
sequence constraints
strong
moderate
weak
stronger constraints in GPCR class A
equally constrained in both
stronger constraints in rNTR1-DO3 454 data
no data available
rmsd rNTR1-DO3
rmsd class A GPCR
Comparison of GPCR class A and rNTR1-DO3 454 sequence constraints

Figure 4.

Chapter 4

Maximizing detergent stability and functional expression of a GPCR by exhaustive recombination and evolution.

4.1 Published article

doi:10.1016/j.jmb.2012.05.039 J. Mol. Biol. (2012) 422, 414–428

Contents lists available at www.sciencedirect.com

Journal of Molecular Biology

journal homepage: http://ees.elsevier.com.jmb

Maximizing Detergent Stability and Functional Expression of a GPCR by Exhaustive Recombination and Evolution

Karola M. Schlinkmann [1], Matthias Hillenbrand [1], Alexander Rittner [1], Madeleine Künz [1], Ralf Strohner [2] and Andreas Plückthun [1]*

[1] *Department of Biochemistry, University of Zurich, Winterthurerstrasse 190, 8057 Zurich, Switzerland*
[2] *Sloning Group at MorphoSys AG, Lena-Christ-Strasse 48, 82152 Martinsried/Planegg, Germany*

Received 23 March 2012; received in revised form 27 May 2012; accepted 30 May 2012
Available online 6 June 2012

Edited by J. Bowie

Keywords:
in vitro DNA recombination; screening and selection; plasmid copy number; membrane protein expression; coevolution

To identify structural features in a G-protein-coupled receptor (GPCR) crucial for biosynthesis, stability in the membrane and stability in detergent micelles, we developed an evolutionary approach using expression in the inner membrane of *Escherichia coli*. From the analysis of 800,000 sequences of the rat neurotensin receptor 1, in which every amino acid had been varied to all 64 codons, we uncovered several "shift" positions, where the selected population focuses on a residue different from wild type. Here, we employed *in vitro* DNA recombination and a comprehensive synthetic binary library made by the Slonomics® technology, allowing us to uncover additive and synergistic effects in the structure that maximize both detergent stability and functional expression. We identified variants with >25,000 functional molecules per *E. coli* cell, a 50-fold increase over wild type, and observed strong coevolution of detergent stability. We arrived at receptor variants highly stable in short-chain detergents, much more so than those found by alanine scanning on the same receptor. These evolved GPCRs continue to be able to signal through the G-protein. We discuss the structural reasons for these improvements achieved through directed evolution.

Introduction

G-protein-coupled receptors (GPCRs) constitute the largest group of cell-surface receptors found in nature. GPCRs are involved in all kinds of signaling processes, giving this class of proteins enormous pharmacological relevance. Currently, it is estimated that 30% of all marketed drugs target GPCRs.[1,2] However, our understanding of GPCR architecture and mechanism has remained limited, and the design features of agonists and antagonists for the diverse set of receptors have remained mostly enigmatic. Low expression levels, poor biophysical behavior of solubilized GPCRs and their intrinsic conformational flexibility make their structural characterization very challenging. For the same reasons, drug screening remains largely limited to assays in whole cells.

The first crystal structure of a GPCR, bovine rhodopsin, was solved in the year 2000 and remained unchallenged for several years. Recently, GPCR structures of the inactive states of the human adenosine receptor A_{2A},[3] human β2-adrenergic

*Corresponding author. E-mail address: plueckthun@bioc.uzh.ch.

Present address: M. Künz, Institute for Biochemistry and Molecular Biology, Laboratory for Structural Biology of Infection and Inflammation, University of Hamburg, c/o DESY Bldg. 22a, Notkestrasse 85, 22607 Hamburg, Germany.

Abbreviations used: GPCR, G-protein-coupled receptor; StEP, staggered extension process; MFI, mean fluorescence intensity; DDM, *n*-dodecyl-β-D-maltopyranoside; CHS, cholesteryl hemisuccinate; DM, *n*-decyl-β-D-maltopyranoside; NM, *n*-nonyl-β-D-maltopyranoside; OG, *n*-octyl-β-D-glucopyranoside; HTG, *n*-heptyl-β-D-thioglucopyranoside; RLBA, radioligand binding assay; EDTA, ethylenediaminetetraacetic acid.

0022-2836/$ - see front matter © 2012 Elsevier Ltd. All rights reserved.

receptor,[4,5] turkey β1-adrenergic receptor,[6] C-X-C chemokine receptor type 4[7] and human dopamine D3 receptor[8] were determined. In most cases, crystallization was enabled by allowing efficient crystal contact formation by fusion protein strategies (e.g., Ref. 4); however, this strategy hampers functional characterization, as it prevents binding of the G-proteins. In some cases, receptor stability was also improved by mutagenesis.[6,9] First insight into the signaling process itself was provided by the determination of the structure of the complex of the β2-adrenergic receptor with the heterotrimeric G-protein.[10]

In our laboratory, we had previously developed a FACS (*f*luorescence-*a*ctivated *c*ell *s*orting)-based selection system to evolve and engineer further GPCRs for high functional expression and stability in detergents and have successfully applied it to several GPCRs.[11,12] More importantly, we wished to exploit this technology to elucidate and understand the structural features that determine biosynthesis, stability in the bilayer membrane and, after solubilization, stability in detergent micelles. This will help describe the evolutionary forces that have shaped this family.

Because of the incomplete coverage of mutant space by random mutagenesis, we recently performed an exhaustive saturation mutagenesis to determine, for every position of rNTR1-D03, the amino acid residues that are not permitted, are permitted and are preferred.[13] The already improved mutant rNTR1-D03 was used as framework,[11] since rNTR1-wt expression levels were so low that they would not allow these experiments. Here, we have generated both shuffled and exhaustive designed synthetic DNA libraries for selection of the optimal combination of shift mutations with respect to expression levels and stability in detergents. Receptor variants with unanticipated gains in functional expression and stability in detergents were generated, which maintained the ability to signal through G-proteins, allowing us to now formulate detailed structural hypotheses of the architectural basis of such biophysical improvements.

Results

Library design

In a previous comprehensive randomization study, every receptor position had been turned into a separate NNN library representing all 64 codons.[13] Thus, 376 position-specific libraries were created and then selected for high functional expression using our previously developed FACS-based approach.[11] The selected library pools were analyzed by deep sequencing, and the evaluation of 800,000 sequences led to the identification of 30 shift positions (Table 1, see M30), defined as those

Table 1. Sequence of NTR1-related evolved GPCRs at crucial positions

	TM1						TM2							TM3			I2	TM4			E2		TM5			TM6		E3		TM7	
D03 reference	V	N	T	I	F	S	A	T	A	D	L	M	E	L	R	D	C	A	A	I	M	K	V	I	I	N	K	C	Y	C	F	T	F
NTR1 position (aa)	57	58	68	70	75	83	86	101	110	113	119	121	124	125	143	150	172	177	201	202	208	235	240	253	260	262	263	320	324	332	342	354	358
Ballesteros–Weinstein			1.36	1.38	1.43	1.51	1.54	2.38	2.47	2.50	2.56	2.58	2.61	2.62	3.26	3.33	3.55		4.57	4.58	4.64	5.36	5.41	5.54	5.61	5.63	5.64	6.47	6.51	6.59		7.38	7.42
M30	I	R	S	L	L	G		R	L	S	F	L	D	V	K	E	R	H	S	L	V	R	L	A		R	R	L	L	V		S	V
M303	I	R	S	L	L	G	L	R	L	S	F	L	D	V	K	E	R	H	S	L	V	R	L	A	A	R	R	L	L	V	A	S	V
C7E02	I	R	S	L	L	G	L								K	E								A							A	S	V
L5X	I				L			R		S	F	L			K	E		H					L	A				L		V		S	V
TM86V							L																	A									V

positions where selection has focused on a new residue that is different from rNTR-D03 (abbreviated as D03).[13] Each single shift mutation positively affects expression levels, and some of these also significantly increase receptor stability in detergent. Shifts often come in clusters, where shifted residues close in space appear to address the same structural problem independently.[13] Hence, from simply combining the mutations, additivity does not necessarily result, and the optimal combination of shifted residues cannot be deduced directly. We thus explored the combinatorial space of the shift mutations experimentally. Here, we used two independent approaches to create such libraries, and we selected them for variants of highest expression and stability in detergent to bring out the crucial structural features more clearly than would be possible with a single mutation set.

In a first approach, we created a library by *in vitro* DNA shuffling of two genes, (i) D03 (having no shift mutations) with (ii) a synthetic gene carrying all shift mutations at once (termed M30) (Table 1). Methods based on shuffling are straightforward to carry out[14,15] but are not comprehensive in the combinations they generate, since the number of crossovers per gene is limited; thus, the chance of separating two mutations very closely spaced in sequence is finite.

In a second approach, a true "binary" library was synthetically constructed with codons of both D03 and shift amino acids in question at equal frequency at each shift position. This very comprehensive approach requires a demanding synthesis, for which the Slonomics® technology is one of the very few technologies available.[16,17] Both libraries were selected using our established FACS technique,[11] and the selection output was screened for detergent-stable variants.

In a third approach, guided by the statistics of occurrence of particular shift mutations and their biophysical properties when known, we combined several of these mutations to rationally engineer a detergent-stable variant directly.

In vitro DNA shuffling of D03 and M30 by the staggered extension process

We created a diverse DNA library (StEPM30) by *in vitro* DNA shuffling of the D03 with the M30 gene by means of the staggered extension process (StEP)[14,15] (see Supplementary Fig. S1 for illustration). Briefly, an equimolar mixture of D03 and M30 genes was used as input for PCR, in which extremely short elongation cycles (6 s) allow for only short primer extensions. By this staggered extension, the elongated primer fragment can switch templates after the subsequent denaturation step, and 125 cycles are performed to eventually obtain a chimeric full-length PCR product. While carrying out these studies, Shibata *et al.*reported the identification of NTS1-7m,[18] an rNTR1 mutant that is somewhat more stable than rNTR1-wt. NTS1-7m contains four point mutations, A86L$^{1.54}$, I260A$^{5.61}$, F342A (loop E3) and F358A$^{7.42}$. We use the sequential numbering in plain text and the Ballesteros–Weinstein numbering[19] as superscript: here, the first number denotes the helix in sequential order; the second number defines the position within the helix, where the most conserved position of a helix is denoted as x.50, counting downwards toward the N-terminus and upwards to the C-terminus. We had previously identified the strong shift mutation F358V$^{7.42}$ in the D03 background, and thus, we decided to include the mutations A86L$^{1.54}$, I260A$^{5.61}$ and F342A in a further StEP library (termed StEPM303).

The theoretical library diversities of 2^{30} ($\approx 1\times10^{9}$) for the StEPM30 library and 2^{33} ($\approx 8\times10^{9}$) for the StEPM303 library cannot be reached in practice due to limited recombination of mutations close in sequence in the StEP method, even though libraries with this number of colonies can easily be created in our *Escherichia coli*-based system. Here, after optimization of StEP parameters such as $MgSO_4$ and primer concentration as well as extension time, recombination events as short as within a 30-bp distance were obtained.

Selection of the StEP library for high functional expression

The initial libraries were subjected to three rounds of StEP shuffling, each followed by three to six rounds of selection by FACS,[11] before expression reached a stable plateau. StEPM30 and StEPM303 selections were pooled for a final selection round, testing both expression at 20 °C and 30 °C (C6_20 and C6_30; Fig. 1a). The mean fluorescence intensity (MFI) of the selected libraries, a measure of the mean functional expression, reached 2-fold of D03 (Fig. 1a). Single-clone expression levels were increased 2.5- to 3-fold, compared to D03 (Fig. 1b) (a 30-fold increase compared to rNTR1-wt), and the best variants reached 12,000 receptors per cell. Sequencing of 87 selected individual variants verified that both favorable and unfavorable shifts are efficiently selected for and against, respectively (Fig. 1c).

C332V$^{6.59}$ is the most dominant shift after selection for functional expression, occurring in >90% of selected variants. Shifts further accumulate in TM5, with a focus on I253A$^{5.54}$. TM5 is involved in conformational changes of the receptor upon activation, and its conformational flexibility might provide ample opportunity for improvements. Not all shift mutations originally selected as single shift mutations were maintained in the context of other shift mutations, such as C320L$^{6.47}$ and Y324L$^{6.51}$ (<20% frequency), which are close in sequence to the dominant shift C332V$^{6.59}$ (Fig. 1c). Because of the

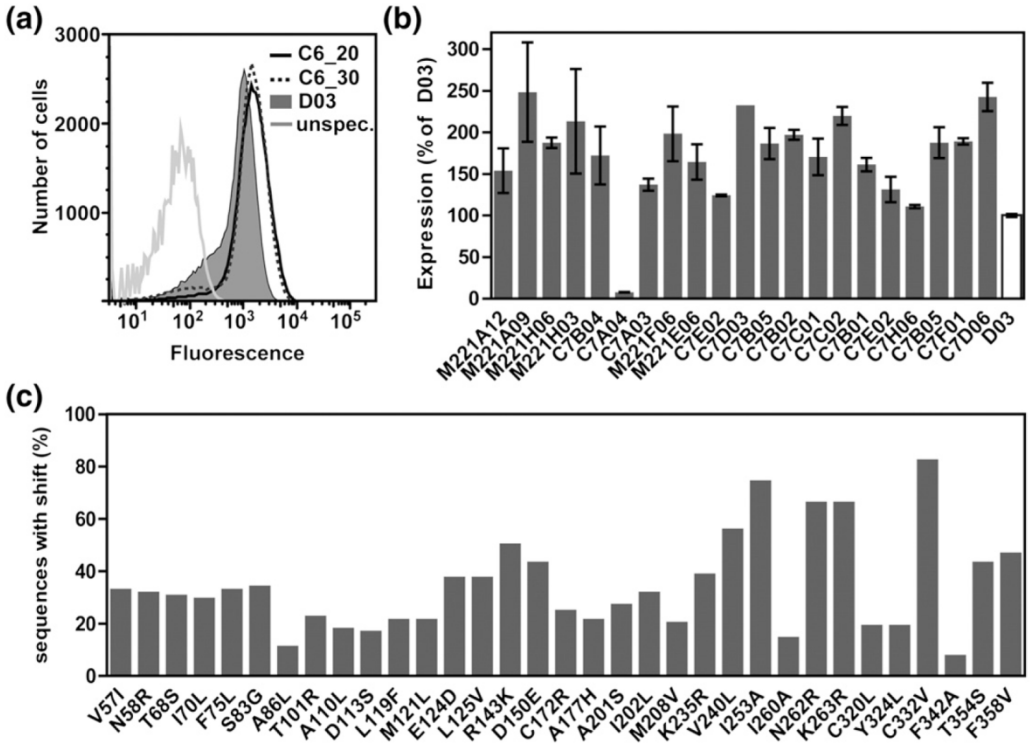

Fig. 1. StEP selections. (a) Expression profiles of final StEP selection pools after 20 h expression at 20 °C (C6_20) and 30 °C (C6_30). Expression is measured as binding of BODIPY-NT(8–13) to receptors and analyzed by flow cytometry. The MFIs of C6_20 and C6_30 are 1660 and 1550, compared to 880 for D03. Nonspecific binding of BP-NT(8–13) is measured in the presence of excess unlabeled neurotensin (10 μM). (b) Expression levels of individual selected StEP variants. Receptors per cell were quantified by RLBA with 15 nM [^{3}H]neurotensin. An average of two independent experiments is given. (c) Frequency of sequences carrying the shift mutation in the final StEP selection pools (C6_20 and C6_30). We sequenced and analyzed 87 individual variants.

incomplete crossover, some shifts might be selected together, displaying a neutral phenotype in the context of other functionally relevant shifts. Interestingly, the shift mutations A86L$^{1.56}$, I260A$^{5.61}$ and F342A (E3 loop), originating from the StEPM303 library and introduced from NTS1-7m, are underrepresented after selection and, thus, must be disfavored in the context of the other selected shift mutations. Thus, it appears that an alternative, more robust solution has been found by our combinatorial approach (see below).

Detergent stability of receptor variants evolved by StEP

Next, we analyzed the stability of selected variants in different detergents, essentially as described previously.[12] About 90% of the selected variants are more stable than D03 in a mild detergent mixture of *n*-dodecyl-β-D-maltopyranoside (DDM), 3-[(3-cholamidopropyl)dimethylammonio]-1-propanesulfonate (Chaps) and cholesteryl hemisuccinate (CHS), supplemented with 30% glycerol, and the most stable variants retain full activity after 20 min at 45 °C (Fig. 2a). The apparent T_m of the variants M221H03 and M221A09 is 65 °C, an increase of 25° compared to D03 (Fig. 2b). The heat-induced inactivation of the receptors is irreversible, and T_m thus reflects the transition point of heat-induced deactivation after a defined incubation. The dramatic increase in detergent stability was intriguing, considering that this particular property was never under direct selection pressure, hence suggesting a strong correlation between functional expression and detergent stability.

Since glycerol is unfavorable for crystallization, we attempted to identify variants that are stable in its absence. In the absence of glycerol, CHS and Chaps, i.e., with DDM as the sole detergent (buffer SABoDDM), we observed a stronger separation of stable from unstable clones, with the most stable variant being C7E02 (Fig. 3a, C7E02 highlighted in black). The apparent T_m of C7E02 under these conditions is 52 °C, a 20° increase compared to D03 (31 °C; Table 2 and Supplementary Fig. S2a). Moreover, C7E02 retains about 75% activity after 24 h at 4 °C, while D03 looses activity during that time (Supplementary Fig. S2b).

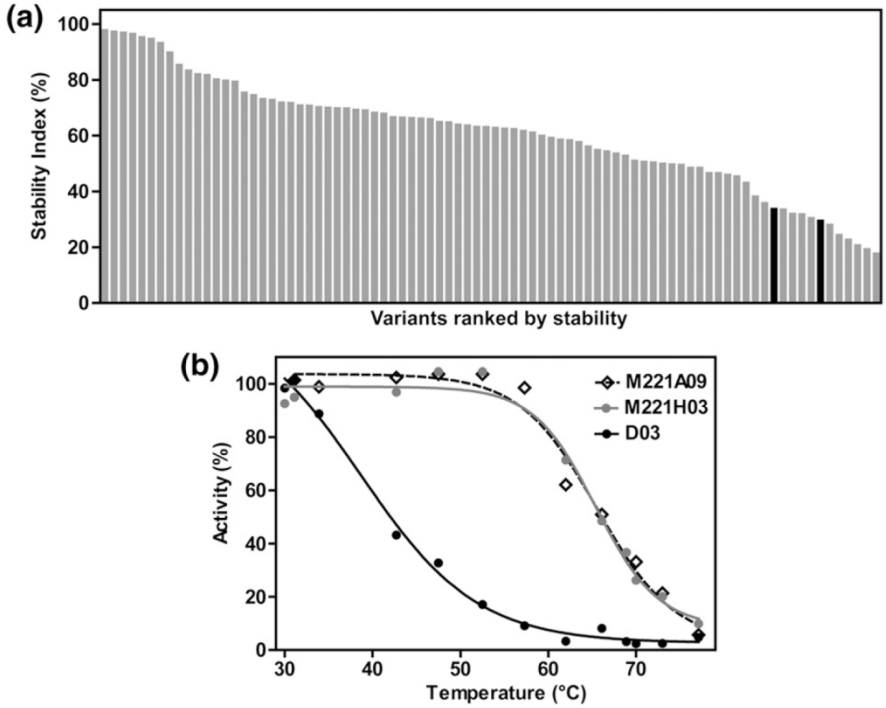

Fig. 2. Stability screening of evolved StEP variants in buffer SAB, ranked by stability. (a) Stability screening in buffer SAB (0.1% DDM, 0.5% Chaps, 0.1% CHS and 30% glycerol). The stability index is the ratio of remaining ligand binding activity after 20 min of incubation at 45 °C compared to incubation at 4 °C. Screening was performed in the ligand-free state. Black bars represent two independent measurements for D03. (b) Thermal denaturation profiles of the most stable evolved StEP variants in buffer SAB. Thermal denaturation was measured in the ligand-free state after 20 min at the indicated temperature. D03 displays an apparent T_m of 39 °C, compared to 65 °C for M221H03 and M221A09. Data from a representative measurement are shown.

In the larger micelles that are formed by longer-chain detergents, the protein part is prevented from making crystal contacts, making the mild detergent DDM unfavorable for membrane proteins devoid of large extracellular regions.[20] We have thus rescreened our best variants in shorter and harsher detergents (Fig. 3b, C7E02 highlighted in black). D03 is essentially unstable in *n*-decyl-β-D-maltopyranoside (DM; buffer SABoDM) with an apparent T_m of approximately 18 °C, while C7E02 quantitatively retains protein activity with an apparent T_m of 41 °C (Table 2 and Supplementary Fig. S2c). All other variants were completely inactivated upon buffer exchange to DM, and detergents shorter than DM

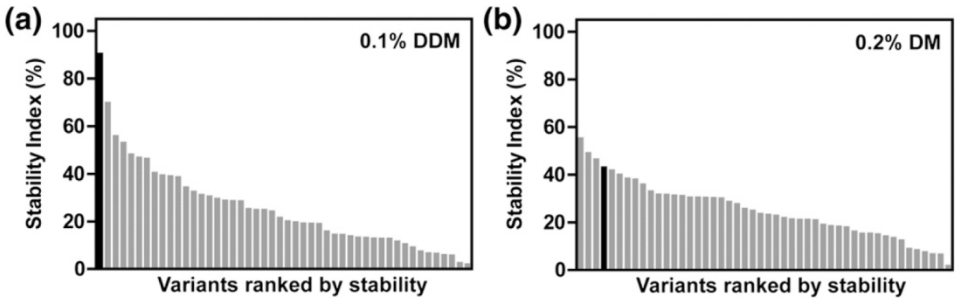

Fig. 3. Stability screening of evolved StEP variants in buffers SABoDDM and SABoDM, ranked by stability. (a) Stability screening in buffer SABoDDM (0.1% DDM as the sole detergent) and (b) buffer SABoDM (0.2% DM as the sole detergent). C7E02 is highlighted in black bars; D03 is inactive in (a) and (b). The stability index is the ratio of remaining ligand binding activity after 20 min of incubation at 45 °C compared to incubation at 4 °C. Screening was performed in the ligand-free state.

Table 2. Melting temperatures (°C) of evolved GPCRs in detergents

	DDM		DM		NM	OG
	+NT	−NT	+NT	−NT	+NT	+NT
rNTR1-wt	40	29	34	(17)	36	(15)
D03	47	31	42	(18)	35	(14)
C7E02	56	52	51	41	45	30
TM86V	59	46	53	37	48	38
L5X	58	42	53	33	50	40
NTS1-7m[a]	50	37	45	27	39	27
wt-TTM	48	41	43	27	38	26

n = 2–9; average error ± 2 °C.
Numbers in parentheses are approximate values, since the protein is too unstable.
[a] Reconstructed according to Ref. 18.

also lead to complete inactivation of C7E02. Reaching stability in such detergents thus required further engineering (see below).

Conformational stabilization of GPCRs by agonist or antagonist binding proved to be a prerequisite for all GPCR structures solved so far (except opsin[21]). Here, we assessed the influence of agonist binding on detergent stability. Agonist stabilization of C7E02 allowed detergent exchange to *n*-nonyl-β-D-maltopyranoside (NM) and *n*-octyl-β-D-glucopyranoside (OG) (Table 2 and Supplementary Fig. S3). The apparent T_m of C7E02 in OG is 30 °C (Table 2 and Supplementary Fig. S3d), a condition under which D03 and rNTR1-wt are essentially unstable (estimated T_m of 14–15 °C; Table 2 and Supplementary Fig. S3d).

C7E02 combines 14 mutations in addition to those present in D03 (Table 1), 13 of which are shift mutations, plus an unrelated mutation R183L$^{4.39}$ located at the cytoplasmic end of TM4, which was most likely introduced during the numerous StEP-PCR cycles (Supplementary Fig. S1). As a single shift, R183L$^{4.39}$ did not significantly influence detergent stability (data not shown). Interestingly, C7E02 does not contain the dominant shift C332V$^{6.59}$. In summary, the evolutionary approach has yielded a clone that is stable in the short-chain detergent OG in the presence of agonist, which is a dramatic improvement, as our previously evolved molecule D03 is essentially unstable in OG.

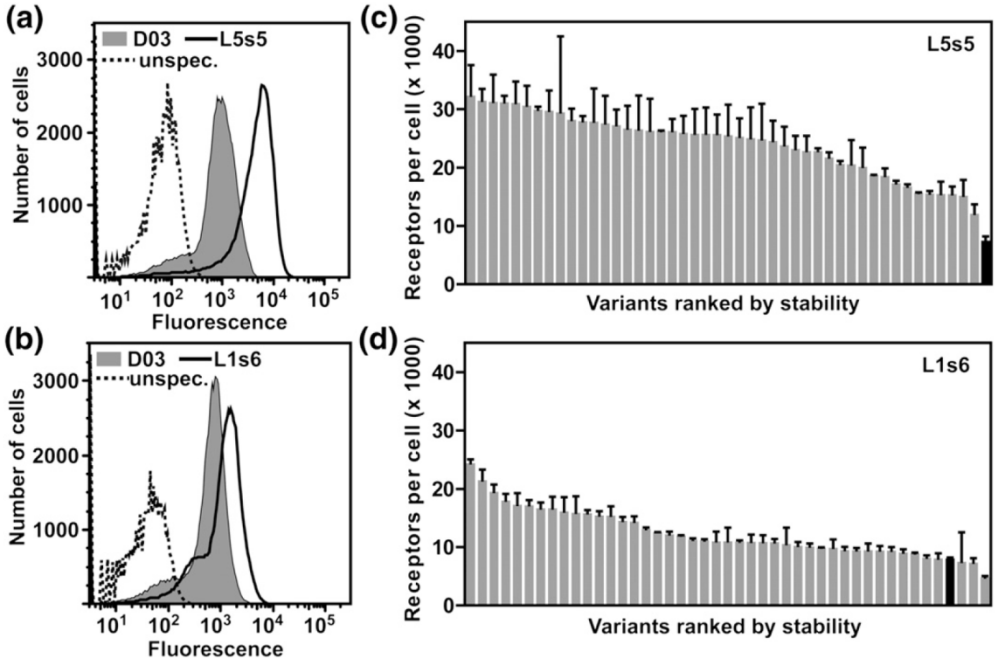

Fig. 4. Slonomics® library selections. (a and b) Expression profiles of final L5 (a) and L1 (b) selections compared to D03. Results for expression at 30 °C are shown. Expression is measured as binding of BODIPY-NT(8–13) to receptors and analyzed by flow cytometry. Nonspecific binding of BOPIPY-NT(8–13) is measured in the presence of excess unlabeled neurotensin (10 μM). (a) After five rounds of selection for high functional expression by FACS, the final evolved L5s5 pool (MFI, 5200) shows a 5-fold increase in MFI compared to D03 (MFI, 970). (b) The final evolved L1s6 pool shows a MFI of 1300 after six selection rounds, a 2-fold increase in MFI compared to D03 with MFI of 670. (c and d) Expression levels of individual selected L5s5 (c) and L1s6 (d) variants (30 °C, 20 h). Receptors were quantified by RLBA with 15 nM [^{3}H] neurotensin. Duplicates of a representative experiment are given. Black bars give the expression level of the respective D03 control.

Comprehensive binary combinatorial library made by Slonomics® technology

Given the success of the StEP libraries but the limitation of having an incomplete separation of mutations closely spaced in sequence, we aimed to generate a comprehensive "binary" library, covering all theoretically possible residue combinations of D03 or M303. The library was synthesized *de novo* using the modified Slonomics® technology for DNA library synthesis.[16,17] Most importantly, to exclude any effects of the nucleotide sequence on the outcome due to codon usage, tRNA levels or mRNA secondary structure formation, we used all degenerate codons for both the randomized positions and the neighboring residues (Supplementary Fig. S4).

Expression levels of highly evolved clones only is limited by plasmid copy number

We had previously observed that a mutation in the origin of replication, resulting in a 2-fold increase in copy number, further enhanced expression levels of D03, a protein improved by evolution, whereas expression levels of the poorly folding rNTR1-wt remained unaffected.[11,22] Furthermore, both StEP library selections arrived at a plateau of expression levels at ~12,000 receptors per cell. We considered the possibility that the plasmid copy number was now limiting expression of the further evolved receptor mutants, which no longer have a limitation through folding and stability in the membrane. We therefore expressed the Slonomics® library in a vector with higher plasmid copy number (eLIC47; containing an engineered ColE1-derived origin,[23] abbreviated as L5). Expression levels were clearly further improved after five to six subsequent rounds of selection, with the MFI of L5 now reaching 6-fold that of D03 (Fig. 4a). In a parallel control experiment with the original plasmid pRGD03[11] (L1), the maximal MFI was only 3-fold that of D03, similar to the StEP libraries (Fig. 4b). This indeed suggests that, for the well-folding receptor mutant, the original copy number becomes limiting. The expression levels of individual variants reached more than 25,000 receptors per cell, a 50- to 60-fold increase compared to rNTR1-wt and even a 5-fold increase compared to D03 (Fig. 4c and d), the product of our first rNTR1 evolution.[11] High plasmid copy numbers thus only become useful with stable and well-folding GPCR variants, as the expression levels of D03 (with intermediate properties) is similar in pRGD03 and eLIC47, while expression of L5X is artificially limited by the lower copy number of pRGD03 (Fig. 5a).

We found that C7E02 is further stabilized by agonist binding, but the observed additional gain in stability is smaller than for unstable receptors such as D03 and rNTR1-wt (Table 2). Hence, we wished to screen for the most stable mutants in the presence of ligand directly. Evolved variants obtained from library L5, the Slonomics® library showing the highest functional expression after selection, were thus analyzed for their stability index in OG and *n*-heptyl-β-D-thioglucopyranoside (HTG), respectively, in the agonist-bound state (Fig. 6a). For that purpose, receptors were solubilized from the membrane and saturated with [^{3}H] neurotensin before incubation at elevated temperatures. The stability index, the ratio of remaining ligand binding activity after 20 min of incubation at the elevated temperature compared to incubation at 4 °C, thus represents the capacity of receptor to

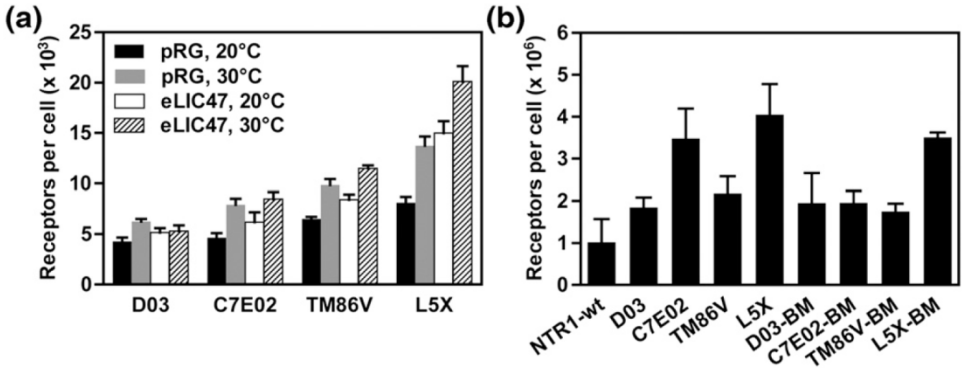

Fig. 5. Expression levels of evolved receptor variants (a) in comparison to D03 as a function of temperature and plasmid copy number in *E. coli* and (b) in *Sf9* cells. (a) D03 displays similar expression levels under all conditions, whereas C7E02, TM86V and L5X express better at 30 °C in both vectors. L5X expression is strongly increased in the high-copy-number eLIC47 vector that was used throughout the selection rounds. C7E02 and TM86V respond less to increased plasmid copy number of eLIC47. The average of three independent expression cultures, each measured in duplicate, is shown. (b) *Sf9* cells were infected at an MOI of 5 and harvested 62 h p.i. All evolved receptor variants are expressed at higher level compared to rNTR1-wt in *Sf9* cells [BM (=back-mutant) refers to restored DRY-motif (L167R$^{3.50}$)]. The average of three independent expressions, each measured in duplicate, is shown.

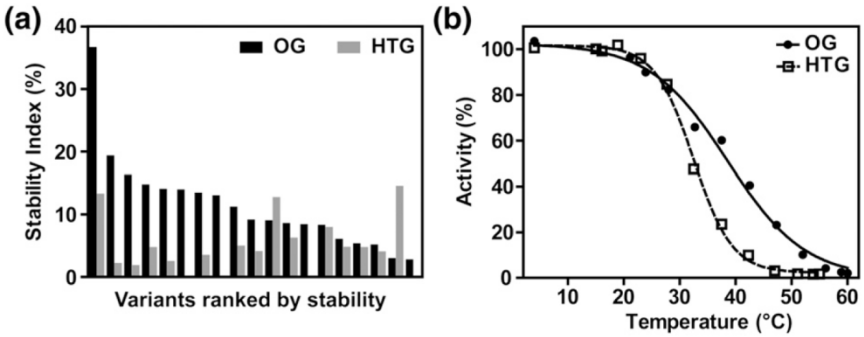

Fig. 6. Stability screening of Slonomics® library selections. (a) Stability screening in buffer SABoOG (0.8% OG as the sole detergent; black bars) and SABoHTG (1.5% HTG as the sole detergent; gray bars). Screening was performed in the agonist-bound state, for which the mutants were saturated with [^{3}H]neurotensin before incubation at elevated temperatures. The stability index is the ratio of remaining activity after 20 min of incubation at 45 °C compared to 4 °C. Only screened variants that retain ligand binding activity are shown. (b) Thermal denaturation profile of L5X, the most stable variant, in SABoOG (OG, filled circles) and SABoHTG (HTG, open squares) in the agonist-bound state. The apparent T_m is 38 °C in OG and 32 °C in HTG.

sustain ligand binding. About 40% of clones showed activity in OG and 30% even in HTG, and the most stable clone, L5X, behaved similarly in both detergents (Fig. 6b).

The apparent T_m of L5X in OG is 40 °C, another 10 °C gain compared to C7E02 and 33 °C in HTG (Fig. 6b and Supplementary Fig. S3d). In OG, L5X retains more than 75% activity after 72 h at 4 °C (Supplementary Fig. S5d), whereas HTG inactivates the receptor over time and is hence not suitable for further studies. L5X comprises 15 mutations, which only partially overlap with the C7E02 subset (Table 1). Agonist-bound L5X also shows high stability in milder detergents (Table 2 and Supplementary Fig. S3 and S5). In the ligand-free state, however, L5X is less stable than C7E02 in both DDM and DM, with a difference of 10° (Table 2 and Supplementary Fig. S2). These data reflect the screening and selection conditions that led to the identification of C7E02 or L5X, respectively, and suggest that L5X is preferentially stabilized in the agonist-bound state and that C7E02 is preferentially stabilized in the ligand-free state.

Structure-guided combination of mutations identified by evolution

We observed a strong correlation between higher functional expression levels and stability in detergents for the StEP and Slonomics® library selections. The effects from single shifts are small and not always significant,[13] and there may be a cooperative or synergistic effect of shifts selected together, making the effect much greater in the present libraries than with single randomized positions. We used the stability data in detergents for the single shifts[13] and for C7E02 (Table 1) to further investigate the contribution of the mutations to the stability increase in detergents and to generate a minimal C7E02-like variant. Here, we analyzed the combinatorial effects of the shifts A86L$^{1.54}$, I253A$^{5.54}$ and F358V$^{7.42}$ that are present in C7E02 and show the strongest effect on detergent stability when analyzed separately. The respective triple mutant, TM86V, was assembled and assayed for its detergent stability. In the ligand-free state, TM86V and C7E02 behave similarly, with C7E02 being slightly more stable in both DDM and DM (Table 2 and Supplementary Fig. S2). In the agonist-bound state, TM86V is superior to C7E02 in all detergents (Table 2 and Supplementary Fig. S3), and the effect is most pronounced in OG. Most important for practical applications such as functional assays and structure determination is that TM86V retains higher activity over time than C7E02 in all detergents in the agonist-bound state (Supplementary Fig. S5). It is thus similar to L5X in this respect (see above). TM86V is also expressed at a higher level than D03, but less than L5X (Fig. 5a).

Influence of the D03 mutation background

TM86V is a highly stable variant of D03, adding the three shift mutations A86L$^{1.54}$, I253A$^{5.54}$ and F358V$^{7.42}$ to D03. The three mutations partially overlap with NTS1-7m, an rNTR1-wt mutant identified by means of alanine-scanning mutagenesis.[18] We remade the NTS1-7m molecule in our laboratory and, in another molecule, introduced the three shifts A86L$^{1.54}$, I253A$^{5.54}$ and F358V$^{7.42}$ into rNTR1-wt (mutant wt-TTM) to test them under the same conditions. Both NTS1-7m and wt-TTM display detergent stability similar to each other in all detergents (Table 2), and both perform better than the unstable rNTR1-wt (Supplementary Fig. S2, S3 and S5). However, functional expression for both

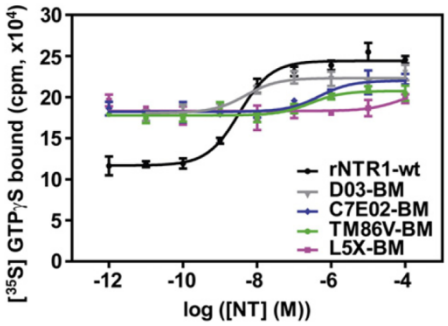

Fig. 7. Signaling activity of evolved receptor mutants. Agonist-stimulated nucleotide exchange at $G\alpha_{i1}$ of C7E02-BM, TM86V-BM and L5X-BM in comparison to rNTR1-wt and D03-BM [BM (=back-mutant) refers to restored DRY-motif ($L167R^{3.50}$)]. Triplicates of a representative experiment are shown (error bars represent standard deviation).

variants is only about 1.5-fold better than the low level of rNTR1-wt (Fig. S6). In contrast, with the evolved mutants C7E02, TM86V and L5X, which are all based on the D03 background, we reach detergent stabilities and expression levels that are greatly superior to NTS1-7m (Table 2 and Fig. 5a).

GPCR activation and signaling

The well-expressed and stable variants C7E02, L5X and TM86V were assayed for their signaling activity. D03 displays only low signaling activity in comparison to rNTR1-wt due to a mutation within the strongly conserved DRY-motif ($R167L^{3.50}$) that is crucial for activation of GPCRs.[24] A version of D03 with restored DRY-motif [D03-$L167R^{3.50}$, denoted in short as D03-BM (BM, *b*ack-*m*utant)] regains signaling activity,[11] and we have thus assayed C7E02, L5X and TM86V after reconstitution of the DRY-motif. For this purpose, we have used the *Spodoptera frugiperda* (*Sf*9) baculovirus system to coexpress our receptor variants with the G-protein $G\alpha_{i1}\beta_1\gamma_{10}$ and have used a nucleotide binding assay using [^{35}S]GTPγS to assess the stimulation of nucleotide exchange at $G\alpha_{i1}$ as a function of agonist binding to our receptor variants and suitable controls. Similar to expression in *E. coli*, C7E02, TM86V and L5X are expressed at a level similar to or higher than that of D03 in *Sf*9 cells (Fig. 5b). Again, this underlines that functional expression is limited by physical features of the protein, and these features appear to be universal for prokaryotes and eukaryotes.

C7E02-$L167R^{3.50}$ (termed C7E02-BM) and TM86V-$L167R^{3.50}$ (termed TM86V-BM), both restored in their DRY-motif, induce exchange of GDP for GTPγS (Fig. 7). All mutants show about the same level of exchange as rNTR1-wt at high agonist concentrations but differ in their behavior at low agonist concentrations. Both C7E02-BM and TM86V-BM are characterized by a higher basal level than rNTR1-wt but still respond to agonist stimulation. The agonist affinities of the evolved receptor variants are very similar to that of D03 (Fig. 8a), excluding any possible influence of changes in agonist binding. The third very stable mutant, L5X-$L167R^{3.50}$ (L5X-BM), seems to be constitutively active, as it shows the same high nucleotide exchange activity independent of agonist concentration. Thus, all mutants are active in GDP/GTP exchange but differ in the degree by which the active state has been stabilized through selection even in the absence of bound agonist.

Discussion

To our knowledge, this is the first study reporting an increase of functional GPCR expression level in *E. coli* to more than 25,000 receptors per cell, starting from only 500 receptors per cell for rNTR1-wt, along

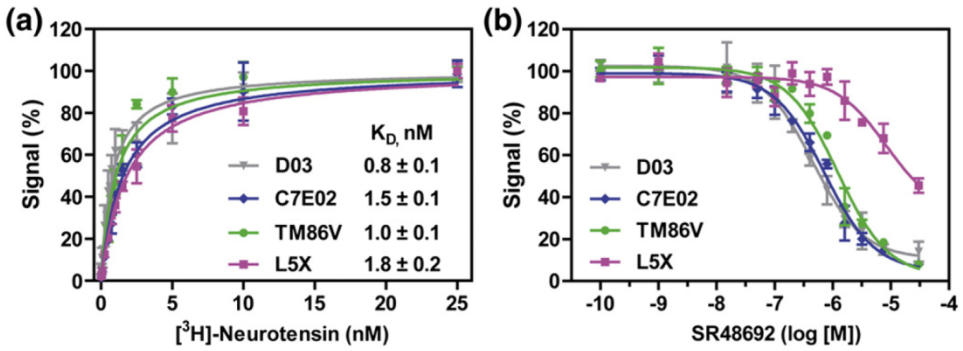

Fig. 8. Ligand binding affinities of the evolved receptor variants. (a) Agonist affinities of C7E02, TM86V and L5X in comparison to D03 was determined by equilibrium titration with [^{3}H]neurotensin using solubilized receptor immobilized via its C-terminus on magnetic beads. (b) Binding of antagonist SR 48692 to the receptor variants was measured by competition with 15 nM [^{3}H]neurotensin. (a and b) The average of two independent duplicate experiments is shown.

with unprecedented gains in detergent stability, such that receptors stable in OG were now obtained. We have also elucidated the structural reasons for this stability gain.

Previously observed apparent limits of functional GPCR expression after directed evolution must be attributed to limitations in exploring sequence space by random mutagenesis, as it does not allow all codon substitutions.[11,12] Our previous comprehensive position-specific mutational analysis of D03 showed that, indeed, only by fully exploring the sequence space, crucial substitutions for further optimization of functional expression and detergent stability could be identified.[13]

Maximization of both expression and stability required combination of some selected shift mutations with wild type in other positions, since some groups of selected shifts address the same problem, and only one of the shifts (but not all) should then be chosen. A binary library is the only way to find the optimal solution. Both approaches, the StEP recombination libraries and the binary (truly comprehensive) Slonomics® library, were successful in the identification of improved receptor variants. Moreover, the potential of the library could only be fully explored by removing measures originally taken to decrease toxicity of GPCR expression in *E. coli*, such as low expression temperatures and low plasmid copy number, as these measures were putting an artificial limit on functional expression (L5 *versus* L1).

During selection, pressure is applied on functional receptor expression, which is a result of the efficiency of correct protein folding, insertion into the lipid bilayer and stability within the lipid bilayer.[25] While host engineering has been successfully used to increase expression of some GPCRs in *E. coli*,[26] it does not address the intrinsic protein properties that limit downstream processes such as protein purification and functional assays in detergent solution. The high expression levels of our evolved receptor variants C7E02, TM86V and L5X are truly a result of the improved biophysical properties: C7E02, TM86V and L5X are also expressed at higher levels than D03 in different *E. coli* strains [e.g., BL21(DE3); data not shown] and *Sf9* insect cells (Fig. 5b). Previously, the higher expression of D03, compared to rNTR1-wt, was shown in *E. coli*, *Pichia pastoris* and human embryonic kidney 293 cells.[11] These results of the same mutants excelling in all expression systems emphasize that the effects are governed by the biophysical properties of the receptor.

In all library selections, functional receptor expression and detergent stability coevolved (Fig. 9), an effect that agrees well with our previous studies on different receptors, underlining the generality of the phenomenon.[11,12] Different from our selection technique, *in vitro* alanine scanning solely for detergent stability leads to uncoupling of receptor expression and stability, and coevolution is thus unlikely to be detected.[6,9] While in our approach, functional receptor expression and detergent stability are coupled, there are, besides mutations with overlapping effects, also individual mutations affecting functional expression only, which is mostly a measure of stability within the lipid bilayer, while others also influence stability in detergent micelles. The shift C332V$^{6.59}$, for example, is dominant after selection for functional expression but less relevant for detergent stability, as it even slightly reduces detergent stability of D03[13] and is found only in one of the three stable variants presented here. C332V$^{6.59}$ is located at the extracellular end of TM6, and it is the only free cysteine pointing toward the oxidizing milieu of the periplasmic space in *E. coli*. rNTR1 contains a disulfide bridge between C225 in extracellular loop 2 and C142$^{3.25}$ in TM3, and this particular shift mutation may mostly affect biosynthesis by preventing incorrect disulfide formation (see above) but not influence detergent stability per se. This hypothesis is supported by the 454 sequencing results obtained for positions C142$^{3.25}$ and C225 (for details, see Ref. 13).

However, not all shift mutations selected for high functional expression did significantly influence detergent stability, when studied individually.[13] Combined in M303, on the other hand, carrying all 33 shift mutations, this GPCR displays higher detergent stability than D03 (Supplementary Fig. S7b) yet is functionally expressed at a level similar to that of D03 (Supplementary Fig. S7a). Thus, individual mutations may also counteract the beneficial effect of others when combined. The selection from a combinatorial library, such as the StEP and Slonomics® libraries described here, can solve this problem. We observed cooperative effects of a subset of shift mutations with respect to detergent stability, and those positive effects seem to be dominant over any stability-decreasing effect of single mutations. Since the selection is for stability in the bilayer by means of functional expression level, both this property and stability in detergents coevolve.

TM86V is a minimal mutant of the selected C7E02, which still confers the desired phenotype. It combines the three shift mutations A86L$^{1.54}$, I253A$^{5.54}$ and F358V$^{7.42}$ with the most significant contribution to functional expression and detergent stability. For TM86V, the gain in detergent stability is additive, consistent with the fact that, according to an rNTR1 homology model, these shift mutations are not in a distance where they could interact with each other (Fig. 10). Moreover, these three shift mutations have a positive effect on detergent stability on both the rNTR1-wt background (wt-TTM) and the already evolved D03 background (TM86V; Table 2 and Supplementary Fig. S2, S3 and S5), emphasizing that positions with crucial relevance for improving the biophysical properties of rNTR1 were found,

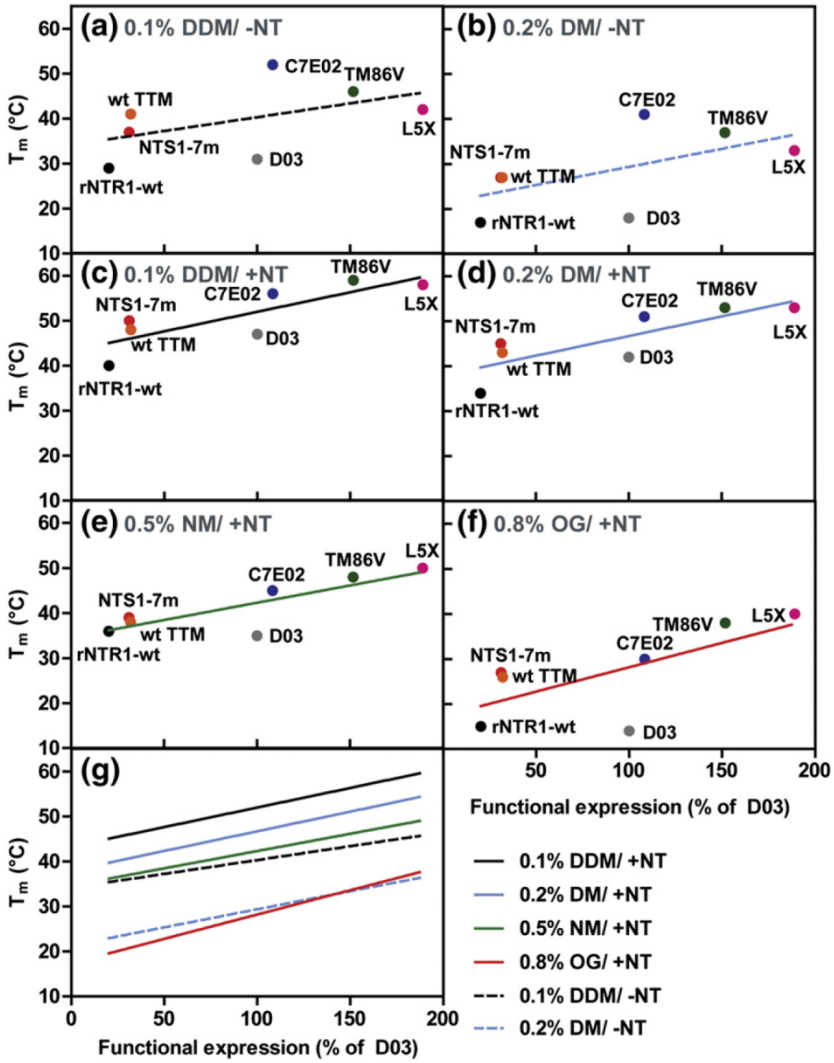

Fig. 9. Correlation between functional expression and detergent stability. The functional expression levels relative to D03 (expression in vector pRGD03, 20 h at 20 °C) are plotted against detergent stability.(a) Ligand-free state in DDM, (b) ligand-free state in DM, (c) agonist-bound state in DDM, (d) agonist-bound state in DM, (e) agonist-bound state in NM, and (f) agonist-bound state in OG. The linear regressions [black broken lines in (a)–(f) are replotted in (g)]. The correlation between high functional expression and detergent stability is highest for harsher detergent conditions, that is, DM in the absence of agonist (b) and OG in the presence of agonist (f).

independent of the receptor variant (rNTR1-wt or D03). It should be noted, however, that the maximal stabilizing effects and the maximal expression levels can only be obtained in the D03 background, which is already a product of directed evolution (Table 2, Fig. 5 and Supplementary Fig. S6).

As discussed in Schlinkmann *et al.*,[13] I253A$^{5.54}$, pointing toward the helical core, might restrict conformational flexibility of the receptor and increase compactness of the helical core, thus leading to increased detergent stability, while A86L$^{1.54}$ and F358V$^{7.42}$ might optimize helix packing, thus decreasing the sensitivity to detergent denaturation.

The selected variants TM86V and C7E02 retain agonist-stimulated signaling activity, that is, activation of heterotrimeric G-proteins, which is intriguing considering that this particular characteristic was never under direct selection pressure. The determination of the transition point for rNTR1-wt is very robust (log [EC_{50}] = −8.5 ± 0.1) but more uncertain for D03 and the evolved receptor variants as a result of the small changes in total signal. The increased level of basal activation can most probably be attributed to partial stabilization of the receptor variant in the activated state as a consequence of the applied selection pressure in the presence of agonist. While all evolved variants are characterized by high

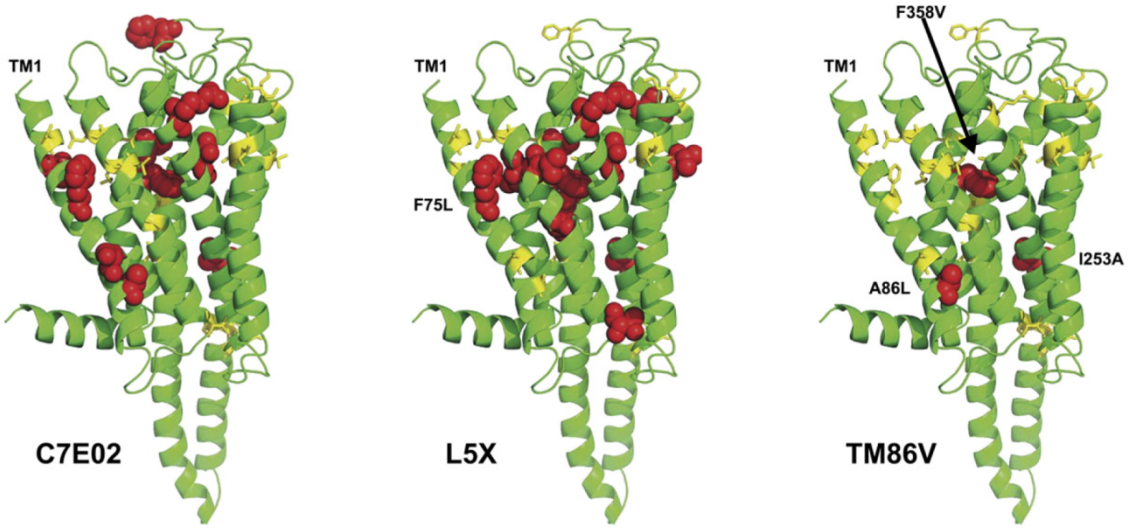

Fig. 10. Homology model of C7E02, L5X and TM86V. The 33 StEP-shuffled positions are highlighted in yellow. The positions of mutations in C7E02, L5X and TM86V in comparison to D03 are highlighted in red spheres (the D03 amino acid is given). For C7E02 and L5X, some mutations are in a distance where they could possibly interact. Generation of the homology model is described in detail in Ref. 13.

basal activity, stabilization of the agonist-bound state is strongest for L5X, which does not respond to agonist stimulation. This hypothesis of selected stabilization of the agonist-bound state is strongly supported by the high detergent stability of L5X in the agonist-bound state and, particularly, by the strongly decreased affinity of L5X to bind the small-molecule antagonist SR 48692[27] in comparison to D03 as well as to TM86V and C7E02 (Fig. 8b).

Nevertheless, the high basal activity of the receptor variants observed could in principle also result from higher functional expression of the above variants compared to rNTR1-wt. However, higher basal activity is only observed after reconstitution of the DRY-motif (L167R$^{3.50}$ back-mutation), suggesting that this phenomenon is signaling dependent and a true property of the evolved receptors. Additionally, although the G-protein coexpression levels between different receptor variants were carefully adjusted using quantitative Western blots, the quantitative comparison of receptor variants in this assay remains difficult and is of limited accuracy (cf. Ref. 28, chapter 12). Here, we have shown that the evolved receptor mutants are signaling-active, but the detailed characterization of G-protein binding and activation will be the focus of a separate study.

All three variants (TM86V, C7E02 and L5X) contain F358V$^{7.42}$, a position in TM7 that, when mutated to alanine, is known to confer constitutive activity.[29] The valine substitution in our variants retains agonist-dependent stimulation of signaling in C7E02 and TM86V, albeit with an increased basal activity, and may thus be an intermediate conformation. The fact that L5X is indeed constitutively active must then be due to further effects, such as a strong rigidification as a result of small additive effects of its 15 shift mutations.

With C7E02, TM86V and L5X, we have a unique set of evolved receptor variants with improved expression levels and stability in detergents. Despite their mutational load, all three variants are still highly identical with rNTR1-wt (TM86V is 97% identical; C702, 95%; L5X, 94%). Their improved biophysical properties will facilitate structural studies, and their differences in signaling activity will help in functional investigation of rNTR1.

In summary, we show that, by fully exploring the enormous sequence space of a GPCR by a directed evolution approach, we can arrive at molecules that are functional in agonist binding and signaling and are stable in short-chain detergents, and we can reach the expression level of abundant bacterial membrane proteins. In this proof-of-principle experiment, we proceeded in three steps. After initial random mutagenesis, an improved variant was evolved (D03),[11] with which a comprehensive evaluation of every codon at every position became possible.[13] By now screening a comprehensive *binary* library of all "shifted" amino acids with their D03 counterparts, we obtained variants with 50-fold improved expression levels and with stability in detergents as short as octylglucoside. The insight into the parts of the GPCR critical for stability both in the bilayer membrane and in detergents that has been reached in the present study may allow to greatly shortcut this approach for other GPCRs by already introducing a number of these changes identified here.

Materials and Methods

StEP library design and generation

The D03 gene and either the synthetic M30 or the M303 gene were used as input for *in vitro* DNA shuffling using the StEP (see Supplementary Fig. S1 for illustration) using the amplification primers NTR1longfw (CGCGCAGACTGGATCTAACAACAACAACAATAAC) and NTR1longrev (CAGAACCGCCACCAGAACCGCCACCG). We mixed 10 ng of each template DNA per 50 µl PCR reaction using Vent$_R$® DNA Polymerase (NEB) and 30 pmol of each flanking primer, introducing a restriction site. Shuffling was performed for 125 cycles on a Biometra T3 cycler with 30 s of denaturation (94 °C) and 6 s of annealing/elongation at 50 °C and 2 min of initial denaturation. Twelve reactions were run in parallel. The PCR product was treated with DpnI (Fermentas) for digestion of the input DNA that was obtained from propagation of the template plasmid in *E. coli*. The StEP product was then purified from a preparative 1.5% agarose gel. The purified DNA was digested with BamHI (NEB) and Cfr9I (Fermentas), and 3 µg of purified DNA was ligated into 5 µg of vector pRGD03[11] (insert in 3-fold molar excess) overnight at 16 °C. Ligation products were purified using Qiagen MinElute PCR purification columns, eluted in a total volume of 20 µl of 2 mM Tris–Cl (pH 8.5) and used for electroporation of 500-µl electrocompetent *E. coli* DH5α cells. Cells were recovered in 5 ml SOC medium for 1 h at 37 °C and further cultivated in 500 ml 2YT medium supplemented with 1% glucose and 100 µg/ml ampicillin for 12–16 h at 28 °C. Dilution series were plated on 2YT–agar plates (1.5% agar, 1% glucose and 100 µg/ml ampicillin) to determine the library size. Typically, the library size was between 5×10^7 and 3×10^8. Aliquots of $>10^9$ cells were supplemented with 20% glycerol, snap-frozen in liquid N_2 and stored at −80 °C until further use.

Slonomics® library design and generation

The design of the library is schematically shown in Supplementary Fig. S4. The 33 randomized positions contain all codons specifying both the D03-specific residue and the respective shift residue. All degenerate codons were equally represented in order to exclude any bias due to codon usage, tRNA levels or mRNA secondary structure formation. For the same reason, the positions flanking the randomized positions were also represented equally with all codons for the respective amino acid except at three positions (L74, L343 and L357) where a single leucine codon (CTC) was omitted to avoid the generation of specific restriction enzyme motifs. Thus, on the amino acid level, the library is binary and equimolar, and on the nucleotide level, it is agnostic. On the amino acid level, the library diversity is $2^{33}=8.5\times10^9$. The library was generated by the Slonomics® technology[16,17] and shipped as a linear DNA fragment. The library DNA was then amplified using the amplification primers SLK_fw2 (CCAGTCTGGATCCACCTCGGAATCCGACACGGCAGGGCCC) and SLK_rev1 (GAAGTACAGGTTCTCCCGGGTAGCGCAGGTGGAAAAGGCA). Cloning and transformation was performed as for the StEP libraries. Transformation efficiencies and thus library diversity were 3×10^8 for L1 and 1.3×10^8 for L5.

Library expression and selection

Libraries were expressed in 60 ml 2YT medium with 0.2% glucose and 100 µg/ml ampicillin. Cultures were inoculated to $OD_{600}=0.05$ and grown at 37 °C to $OD_{600}=0.5$, at which time protein expression was induced with 250 µM IPTG and continued for 20 h at 20 °C or 30 °C, respectively. For all libraries, the first two rounds of selection were performed with an expression temperature of 20 °C, after which the expression temperature was increased to 30 °C. An aliquot of cells was washed in ice-cold TKCl buffer [50 mM Tris–HCl (pH 7.4) and 150 mM KCl] and saturated with 20 nM BODIPY-neurotensin (8–13) for 1–2 h at 4 °C. Nonspecific binding was determined in the presence of 10 µM neurotensin (8–13). Cells were washed twice in TKCl buffer and resuspended in 1 ml TKCl buffer. Selections were performed on a BD FACS Aria I (Flow Cytometry Laboratory, UZH/ETHZ), and 100,000 cells of the top 1% expressing cells were isolated in the yield mode (selection of naïve libraries) or purity mode (all further selections). Selected cells were directly sorted into 2 ml 2YT medium (1% glucose and 100 µg/ml ampicillin), recovered for 1–2 h at 37 °C, diluted into 30 ml 2YT (1% glucose and 100 µg/ml ampicillin) and grown for 12–16 h at 28 °C. Aliquots of $>10^8$ cells were supplemented with 20% glycerol, snap-frozen in liquid N_2 and stored at −80 °C until further use.

Whole-cell radioligand binding assays

Radioligand binding assays (RLBAs) were used to quantify receptor expression levels. Expression in *E. coli* was performed essentially as described for library expression (see above), whereas in *S. frugiperda* (*Sf9*) 10^7 cells were seeded as monolayer in 10-cm cell culture dishes, infected at an MOI (*m*ultiplicity *o*f *i*nfection) of 5 with the respective virus and harvested 62 h p.i. (*p*ost-*i*nfection). To allow for agonist binding, we resuspended 10^7 *E. coli* cells or 10^5 *Sf9* cells in 200 µl TEBB buffer [50 mM Tris–HCl (pH 7.4), 1 mM ethylenediaminetetraacetic acid (EDTA), 0.1% (w/v) BSA (*b*ovine *s*erum *a*lbumin) and 40 µg/ml bacitracin] containing 15 nM [^{3}H]neurotensin (PerkinElmer) and incubated for 2 h at 4 °C. Nonspecific binding was determined in the presence of 5 µM unlabeled agonist. Cells were applied to glass fiber filters (Millipore), separated from free ligand using a 96-well vacuum manifold (Millipore) and washed four times with 200 µl TEBB buffer. Filters were dried for 1 h at 60 °C and allowed to dissolve in 200 µl OptiPhase SuperMix (PerkinElmer) for 6–14 h. Filter-bound radioactivity was measured by liquid scintillation counting (Microbeta 1450 Plus liquid scintillation counter; Wallac).

Analysis of detergent stability

Stability measurements of evolved receptor variants in the ligand-free state were essentially performed as described previously.[12] All stability assay buffers contained 50 mM Hepes (pH 7.4), 100 mM NaCl, 1 mM EDTA and Complete Protease Inhibitor (Roche). Buffer

SAB additionally contained 30% glycerol and 0.1% (w/v) DDM (Anatrace), 0.5% (w/v) Chaps (Anatrace) and 0.1% (w/v) CHS (Sigma-Aldrich); buffer SABoDDM contained 0.1% (w/v) DDM; buffer SABoDM contained 0.2% (w/v) DM (Anatrace); buffer SABoNM contained 0.5% (w/v) NM (Anatrace); buffer SABoOG contained 0.8% (w/v) OG (Anatrace) and buffer SABoHTG contained 1.5% HTG (Anatrace). Detergent and glycerol concentrations for ligand binding buffers were changed accordingly. For all measurements, receptors were solubilized in DM, and detergent was exchanged after immobilization (Dynabeads® MyOne™ Streptavidin T1; Invitrogen). For detergent exchange, beads were captured using a magnetic tube holder, and beads were washed two times with 150 µl of desired assay buffer for 5 min each and resuspended in a final volume of 150 µl assay buffer. For stability measurements in the agonist-bound state, receptors were solubilized in DM and saturated with 120 nM [^{3}H]neurotensin (PerkinElmer) in a volume of 150 µl for 90 min, before detergent exchange. Data were analyzed by nonlinear regression using GraphPad Prism 5.

Affinity measurements

Receptors were solubilized and immobilized in DM as described in Ref. 12. Aliquots of the receptors immobilized on magnetic beads were incubated with increasing concentrations of the agonist [^{3}H]neurotensin in a volume of 200 µl for 2 h at 4 °C in assay buffer LBB-DM [50 mM Tris–HCl (pH 7.4), 0.2% DM, 1 mM EDTA, 0.1% (w/v) BSA and protease inhibitor (Complete Protease Inhibitor Cocktail; Roche)]. Unbound agonist was removed by capturing the beads using a magnetic tube holder and washing of the beads with 200 µl of buffer LBB-DM. Receptor-bound agonist was quantitated by liquid scintillation counting. Data were analyzed by nonlinear regression using GraphPad Prism 5. Binding of the antagonist SR 48692 was determined accordingly by titration of SR 48692 in the presence of 15 nM [^{3}H]neurotensin.

[^{35}S]GTPγS binding assay

Receptors and the G-protein ($\alpha_{i1}\beta_1\gamma_{10}$) were expressed in *S. frugiperda* (*Sf9*) cells by co-infection with two baculoviruses, one encoding the receptor and the other encoding the whole G-protein complex. Baculoviruses were generated essentially as described for the MultiBac system.[30,31] Receptors were preceded by an N-terminal melittin signal sequence, a FLAG tag, a His_{10} tag and a TEV cleavage site, whereas the C-terminus was unmodified. The $G\alpha_{i1}$ subunit was internally His_6 tagged at position 121,[32] γ_{10} was N-terminally HA tagged and β_1 was untagged.

Sf9 cells at a density of 1×10^6 cells/ml were co-infected with receptor virus and G-protein virus at a MOI of 2 and 1, respectively. At 72 h p.i., cells were harvested by centrifugation (10 min, 500*g*, 4 °C) and washed with phosphate-buffered saline twice. Cells were resuspended in lysis buffer [50 mM Tris–HCl (pH 8.0), 1 mM EDTA and protease inhibitor (Complete Protease Inhibitor Cocktail; Roche)] and were lysed by sonication. The lysate was centrifuged (10 min, 500*g*, 4 °C), and the resulting supernatant was centrifuged again (30 min, 20,000*g*, 4 °C). The membrane pellet was washed once with lysis buffer, and the membranes were finally resuspended in lysis buffer containing 20% sucrose and flash-frozen. Protein concentration was determined by the Quant-iT™ Protein Assay Kit (Life Technologies), and expression was controlled by quantitative IR Western blot analysis using the Odyssey® system (LI-COR).

Stimulation of [^{35}S]GTPγS (1250 Ci/mmol; PerkinElmer) binding was performed with 20 µg membrane protein in 100 µl binding buffer [50 mM Tris–HCl (pH 7.4), 5 mM $MgCl_2$, 50 mM NaCl, 1 mM EDTA, 0.1% (w/v) BSA, 0.1 mM DTT, 1 µM 1,10-phenanthroline and 1 µM GDP] containing various neurotensin concentrations (2 pM–200 µM). After preincubation (15 min at room temperature), 100 µl binding buffer with 2 nM [^{35}S]GTPγS (final concentration, 1 nM) was added, and the mixture was further incubated (45 min at room temperature). The reaction was stopped by filtration through 96-well MultiScreen glass fiber filter plates (Millipore) and washed five times with 200 µl washing buffer [50 mM Tris–HCl (pH 7.4), 5 mM $MgCl_2$, 50 mM NaCl and 1 mM EDTA]. Filter-bound radioactivity was determined by liquid scintillation counting.

Acknowledgements

We would like to thank Stefan Heiderich for excellent technical assistance during Slonomics® library synthesis and Annemarie Honegger for preparation of the rNTR1 homology model (Fig. 10). We are thankful to Anette Schütz and Malgorzata Kisielow (Flow Cytometry Laboratory, ETHZ/UZH) for expert technical support during FACS selections. This work was supported by a grant from the NCCR Structural Biology (Swiss National Science Foundation) to A.P.

Author Contributions. K.M.S. designed and generated the StEP libraries. R.S. planned and supervised the Slonomics® library synthesis project. K.M.S. performed FACS selections and analysis of the StEP libraries and Slonomics® libraries. K.M.S. performed expression analysis in *E. coli*, detergent stability and affinity measurements. M.H. and A.R. designed and performed signaling and expression analysis experiments in *Sf9* cells. M.K. helped in the optimization of signaling assay conditions. A.P. planned and supervised the project. K.M.S. and A.P. wrote the manuscript.

Supplementary Data

Supplementary data to this article can be found online at http://dx.doi.org/10.1016/j.jmb.2012.05.039

References

1. Lagerström, M. C. & Schiöth, H. B. (2008). Structural diversity of G protein-coupled receptors and significance for drug discovery. *Nat. Rev., Drug Discov.* **7**, 339–357.
2. Overington, J. P., Al-Lazikani, B. & Hopkins, A. L. (2006). How many drug targets are there? *Nat. Rev., Drug Discov.* **5**, 993–996.
3. Jaakola, V. P., Griffith, M. T., Hanson, M. A., Cherezov, V., Chien, E. Y., Lane, J. R. *et al.* (2008). The 2.6 Ångström crystal structure of a human A_{2A} adenosine receptor bound to an antagonist. *Science*, **322**, 1211–1217.
4. Cherezov, V., Rosenbaum, D. M., Hanson, M. A., Rasmussen, S. G., Thian, F. S., Kobilka, T. S. *et al.* (2007). High-resolution crystal structure of an engineered human β_2-adrenergic G protein-coupled receptor. *Science*, **318**, 1258–1265.
5. Rosenbaum, D. M., Cherezov, V., Hanson, M. A., Rasmussen, S. G., Thian, F. S., Kobilka, T. S. *et al.* (2007). GPCR engineering yields high-resolution structural insights into β_2-adrenergic receptor function. *Science*, **318**, 1266–1273.
6. Warne, T., Serrano-Vega, M. J., Baker, J. G., Moukhametzianov, R., Edwards, P. C., Henderson, R. *et al.* (2008). Structure of a β_1-adrenergic G-protein-coupled receptor. *Nature*, **454**, 486–491.
7. Wu, B., Chien, E. Y., Mol, C. D., Fenalti, G., Liu, W., Katritch, V. *et al.* (2010). Structures of the CXCR4 chemokine GPCR with small-molecule and cyclic peptide antagonists. *Science*, **330**, 1066–1071.
8. Chien, E. Y., Liu, W., Zhao, Q., Katritch, V., Han, G. W., Hanson, M. A. *et al.* (2010). Structure of the human dopamine D3 receptor in complex with a D2/D3 selective antagonist. *Science*, **330**, 1091–1095.
9. Serrano-Vega, M. J., Magnani, F., Shibata, Y. & Tate, C. G. (2008). Conformational thermostabilization of the β_1-adrenergic receptor in a detergent-resistant form. *Proc. Natl Acad. Sci. USA*, **105**, 877–882.
10. Rasmussen, S. G., DeVree, B. T., Zou, Y., Kruse, A. C., Chung, K. Y., Kobilka, T. S. *et al.* (2011). Crystal structure of the β_2 adrenergic receptor–Gs protein complex. *Nature*, **477**, 549–555.
11. Sarkar, C. A., Dodevski, I., Kenig, M., Dudli, S., Mohr, A., Hermans, E. & Plückthun, A. (2008). Directed evolution of a G protein-coupled receptor for expression, stability, and binding selectivity. *Proc. Natl Acad. Sci. USA*, **105**, 14808–14813.
12. Dodevski, I. & Plückthun, A. (2011). Evolution of three human GPCRs for higher expression and stability. *J. Mol. Biol.* **408**, 599–615.
13. Schlinkmann, K. M., Honegger, A., Tureci, E., Robison, K. E., Lipovsek, D. & Plückthun, A. (2012). Critical features for biosynthesis, stability and functionality of a G protein-coupled receptor uncovered by all-*versus*-all mutations. *Proc. Natl Acad. Sci. USA*, **109**, 9810–9815.
14. Zhao, H. & Zha, W. (2006). *In vitro* "sexual" evolution through the PCR-based staggered extension process (StEP). *Nat. Protoc.* **1**, 1865–1871.
15. Aguinaldo, A. M. & Arnold, F. (2002). Staggered extension process (StEP) *in vitro* recombination. *Methods Mol. Biol.* **192**, 235–239.
16. Van den Brulle, J., Fischer, M., Langmann, T., Horn, G., Waldmann, T., Arnold, S. *et al.* (2008). A novel solid phase technology for high-throughput gene synthesis. *BioTechniques*, **45**, 340–343.
17. Zhai, W., Glanville, J., Fuhrmann, M., Mei, L., Ni, I., Sundar, P. D. *et al.* (2011). Synthetic antibodies designed on natural sequence landscapes. *J. Mol. Biol.* **412**, 55–71.
18. Shibata, Y., White, J. F., Serrano-Vega, M. J., Magnani, F., Aloia, A. L., Grisshammer, R. & Tate, C. G. (2009). Thermostabilization of the neurotensin receptor NTS1. *J. Mol. Biol.* **390**, 262–277.
19. Ballesteros, J. A. & Weinstein, H. (1992). Analysis and refinement of criteria for predicting the structure and relative orientations of transmembranal helical domains. *Biophys. J.* **62**, 107–109.
20. Ostermeier, C. & Michel, H. (1997). Crystallization of membrane proteins. *Curr. Opin. Struct. Biol.* **7**, 697–701.
21. Park, J. H., Scheerer, P., Hofmann, K. P., Choe, H. W. & Ernst, O. P. (2008). Crystal structure of the ligand-free G-protein-coupled receptor opsin. *Nature*, **454**, 183–187.
22. Tucker, J. & Grisshammer, R. (1996). Purification of a rat neurotensin receptor expressed in *Escherichia coli*. *Biochem. J.* **317**, 891–899.
23. Bayer, K., Grabherr, R., Nilsson, E. & Striedner, G. (2007). Expression vectors with modified ColE1 origin of replication for control of plasmid copy number European Patent EP 1 326 989 B1.
24. Rovati, G. E., Capra, V. & Neubig, R. R. (2007). The highly conserved DRY motif of class A G protein-coupled receptors: beyond the ground state. *Mol. Pharmacol.* **71**, 959–964.
25. Jungnickel, B., Rapoport, T. A. & Hartmann, E. (1994). Protein translocation: common themes from bacteria to man. *FEBS Lett.* **346**, 73–77.
26. Skretas, G. & Georgiou, G. (2010). Simple genetic selection protocol for isolation of overexpressed genes that enhance accumulation of membrane-integrated human G protein-coupled receptors in *Escherichia coli*. *Appl. Environ. Microbiol.* **76**, 5852–5859.
27. Labbe-Jullie, C., Botto, J. M., Mas, M. V., Chabry, J., Mazella, J., Vincent, J. P. *et al.* (1995). [^{3}H]SR 48692, the first nonpeptide neurotensin antagonist radioligand: characterization of binding properties and evidence for distinct agonist and antagonist binding domains on the rat neurotensin receptor. *Mol. Pharmacol.* **47**, 1050–1056.
28. Manning, D. R. (1999). *G proteins: techniques of analysis*. CRC Press.
29. Barroso, S., Richard, F., Nicolas-Etheve, D., Kitabgi, P. & Labbe-Jullie, C. (2002). Constitutive activation of the neurotensin receptor 1 by mutation of Phe(358) in helix seven. *Br. J. Pharmacol.* **135**, 997–1002.
30. Fitzgerald, D. J., Berger, P., Schaffitzel, C., Yamada, K., Richmond, T. J. & Berger, I. (2006). Protein complex expression by using multigene baculoviral vectors. *Nat. Methods*, **3**, 1021–1032.
31. Bieniossek, C., Imasaki, T., Takagi, Y. & Berger, I. (2012). MultiBac: expanding the research toolbox for multiprotein complexes. *Trends Biochem. Sci.* **37**, 49–57.
32. Kozasa, T. (2004). Purification of G protein subunits from Sf9 insect cells using hexahistidine-tagged a and bg subunits. *Methods Mol. Biol.* **237**, 21–38.

4.2 Supplementary Online Information

Supplementary Online Information for

Maximizing detergent stability and functional expression of a GPCR by exhaustive recombination and evolution.

*Karola M. Schlinkmann[1], Matthias Hillenbrand[1], Alexander Rittner[1], Madeleine Künz[1,3], Ralf Strohner[2], and Andreas Plückthun[1]**

[1] Department of Biochemistry, University of Zurich, Winterthurerstrasse 190, 8057 Zurich, Switzerland

[2] Sloning group at MorphoSys AG, Lena-Christ-Strasse 48, 82152 Martinsried/Planegg, Germany

** Corresponding author*

[3] Present address: Institute for Biochemistry and Molecular Biology, Laboratory for Structural Biology of Infection and Inflammation, University of Hamburg, c/o DESY Bldg. 22a, Notkestrasse 85, 22607 Hamburg, Germany

Figure S1. The StEP process [1; 2] for *in vitro* shuffling of D03 and M30/ M303. Two different GPCR templates are used for *in vitro* DNA shuffling, either D03 (containing no additional mutation) and M30 (containing 30 additional mutations) or D03 and M303 (containing 33 additional mutations). The procedure is illustrated for M30 (1). By using high numbers of very short StEP-PCR cycles (125 cycles; 6 seconds each), the flanking primers are only extended by a few nucleotides (3a - 3c) until eventually a full-length and chimeric GPCR sequence is generated (3d). By template switching within the StEP-PCR cycles, mutations from the two templates are combined into one StEP-PCR product (3d). The StEP-PCR product is then purified from an agarose gel (4) and the flanking restriction sites are digested (5) for ligation into the expression vector (6).

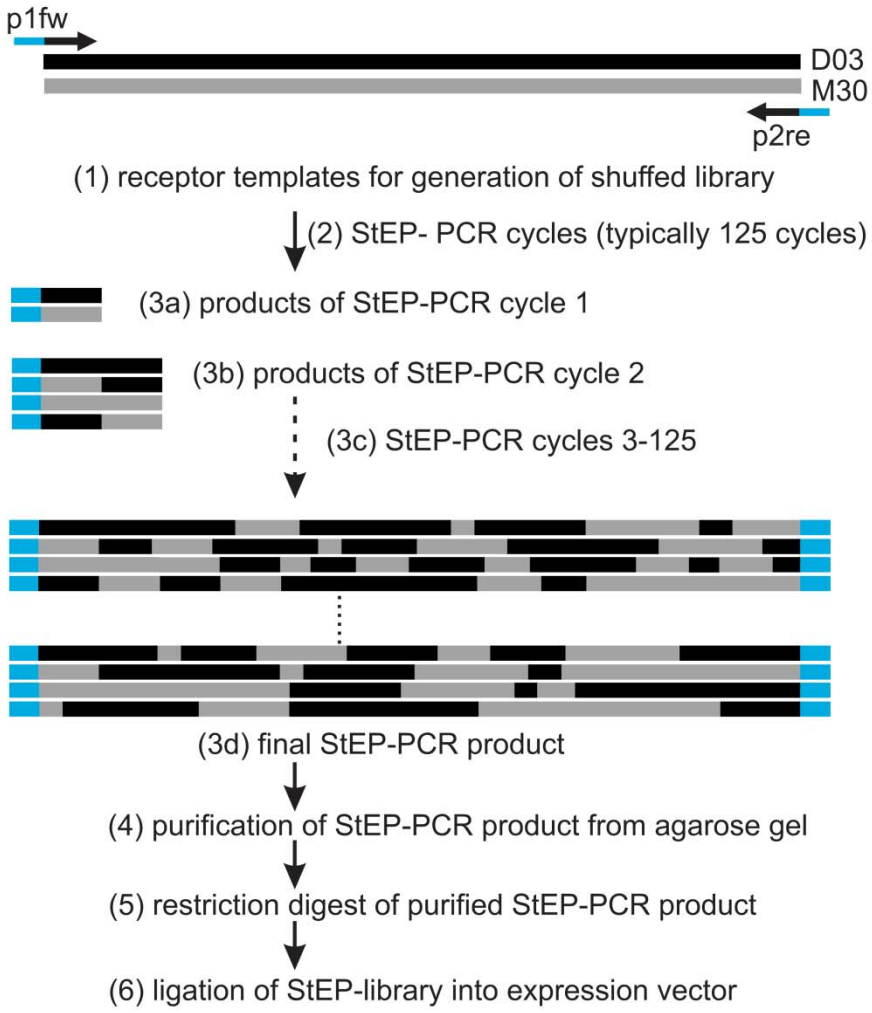
p1fw
D03
M30
p2re
(1) receptor templates for generation of shuffled library
(2) StEP- PCR cycles (typically 125 cycles)
(3a) products of StEP-PCR cycle 1
(3b) products of StEP-PCR cycle 2
(3c) StEP-PCR cycles 3-125
(3d) final StEP-PCR product
(4) purification of StEP-PCR product from agarose gel
(5) restriction digest of purified StEP-PCR product
(6) ligation of StEP-library into expression vector

Figure S1.

Figure S2. **Detergent-stability in DDM (a) and DM (b) in the ligand-free state.** Receptors were solubilized in DM, and then detergent-exchanged before incubation at elevated temperatures. Remaining agonist-binding activity was determined after incubation with 15 nM [^{3}H]-NT. Time-dependent detergent-stability is measured at 4°C in DDM (c) and DM (d). NTS1-7m was constructed according to [3].

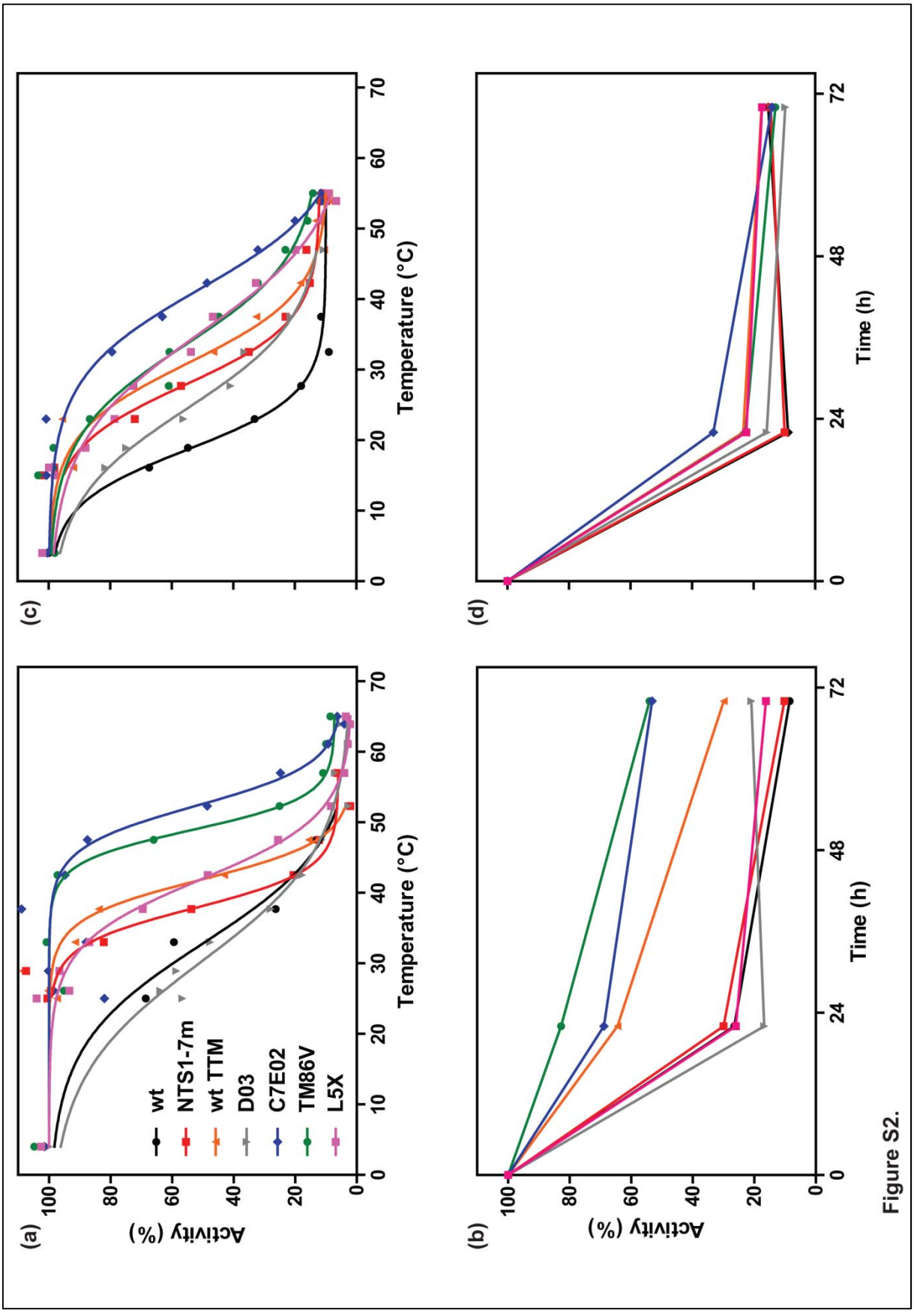
(a)
(b)
(c)
(d)
Activity (%)
Temperature (°C)
Time (h)
wt
NTS1-7m
wt TTM
D03
C7E02
TM86V
L5X

Figure S2.

Figure S3. Agonist-bound detergent stability of different mutants in DDM (a), DM (b), NM (c) and OG (d). Receptors were solubilized in DM, saturated with agonist [^{3}H]-neurotensin and then detergent-exchanged. Samples were incubated at elevated temperatures and the remaining agonist-binding activity was determined. NTS1-7m was constructed according to ref [3].

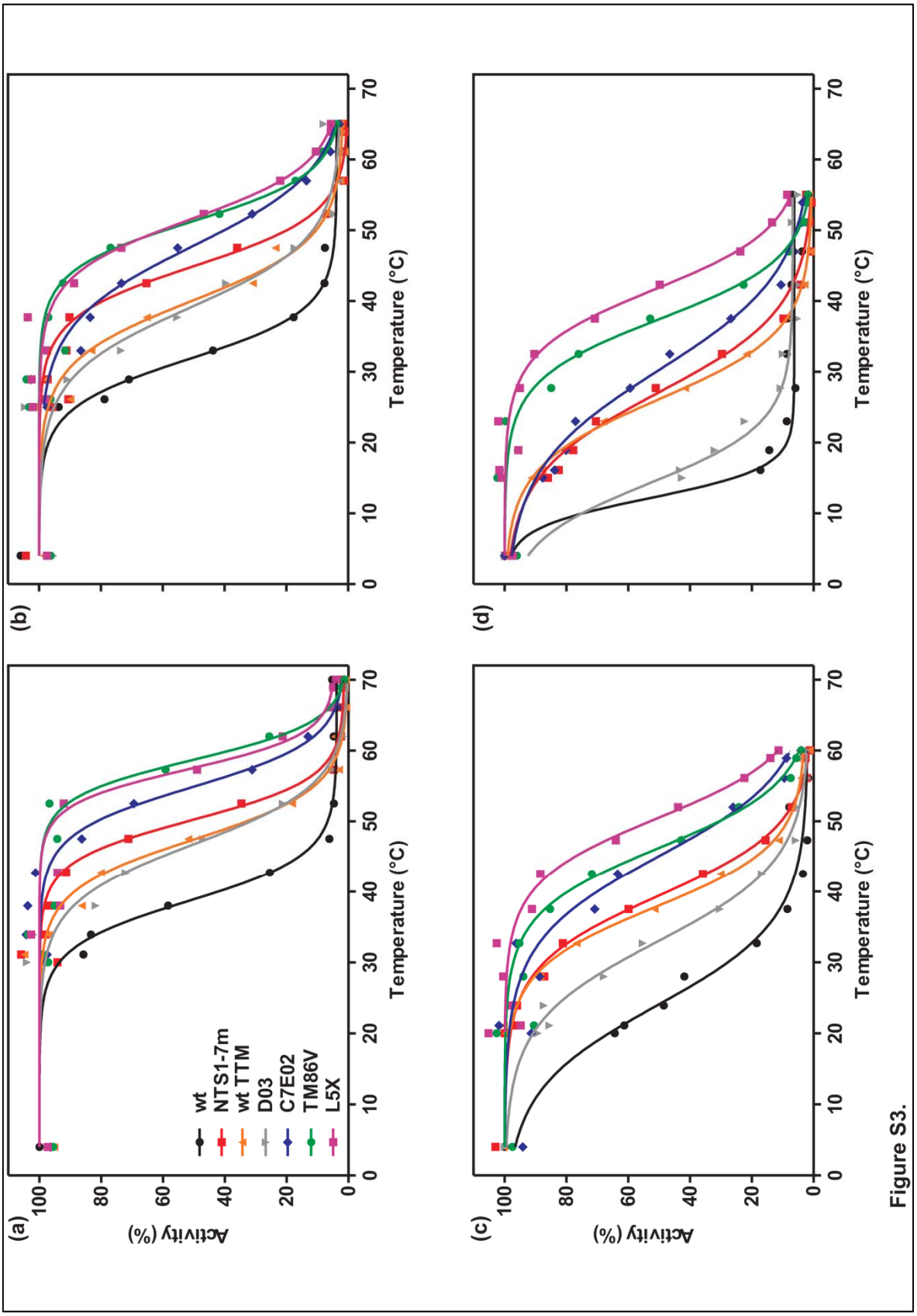
(a)
(b)
(c)
(d)
Activity (%)
Temperature (°C)
wt
NTS1-7m
wt TTM
D03
C7E02
TM86V
L5X

Figure S3.

Figure S4. **Slonomics® library design**. 33 positions of D03 are randomized and both the D03 and the shift amino acid are represented equally by their degenerate codons (yellow). All positions adjacent to a randomized position were also represented by all degenerate codons (brown). For illustration, the codons used for positions 353 to 359 are shown in detail.

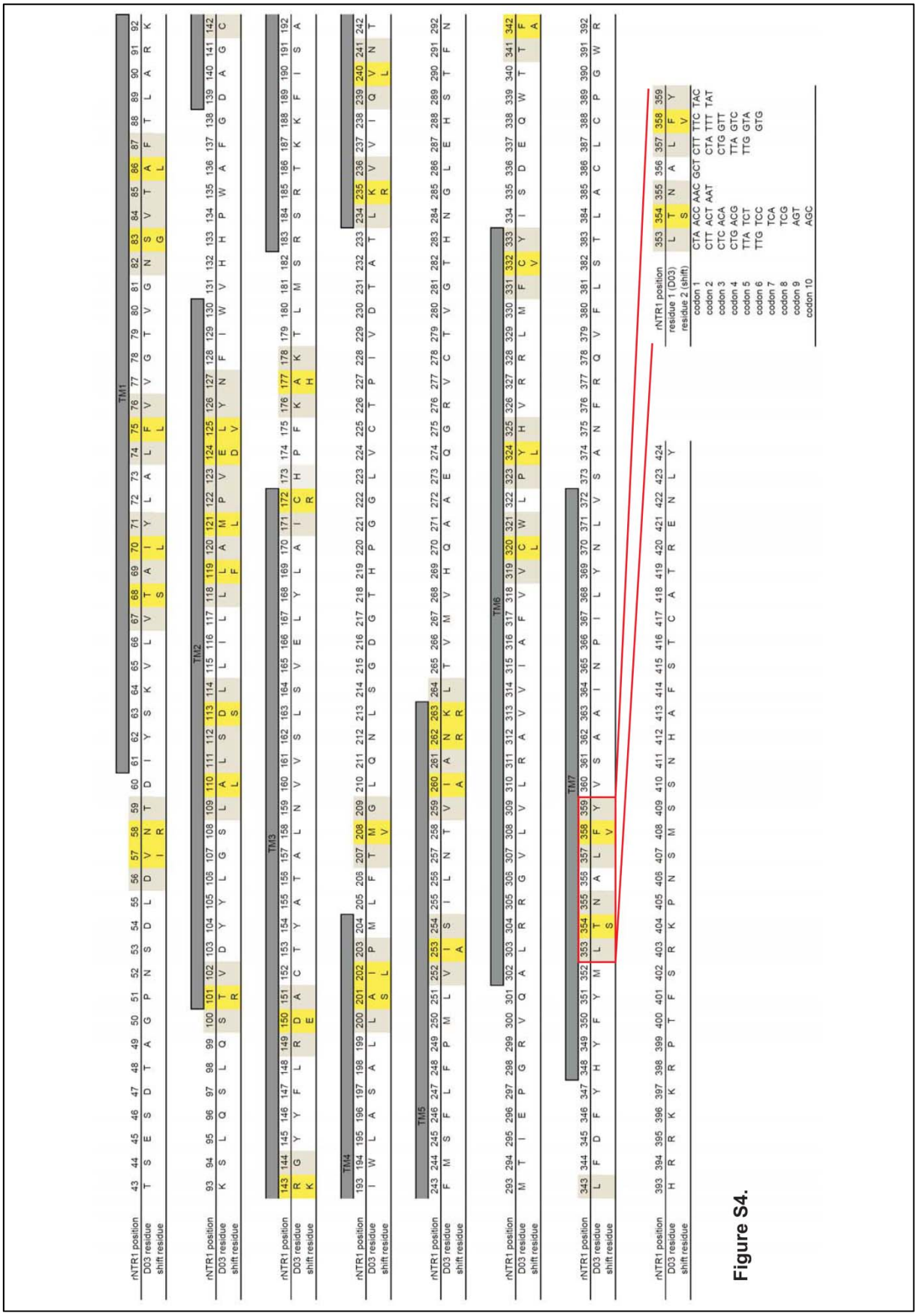
TM1
TM2
TM3
TM4
TM5
TM6
TM7
rNTR1 position
D03 residue
shift residue
rNTR1 position
residue 1 (D03)
residue 2 (shift)
codon 1
codon 2
codon 3
codon 4
codon 5
codon 6
codon 7
codon 8
codon 9
codon 10
CTA ACC AAC GCT CTT TTC TAC
CTT ACT AAT CTA TTT TAT
CTC ACA CTG GTT
CTG ACG TTA GTC
TTA TCT TTG GTA
TTG TCC GTG
TCA
TCG
AGT
AGC

Figure S4.

Figure S5. Time-dependence of detergent stability of different mutants with bound agonist in DDM (a), DM (b), NM (c) and OG (d). After detergent exchange, samples were incubated at 4°C for the indicated time and the remaining agonist-binding activity was determined. NTS1-7m was constructed according to ref [3].

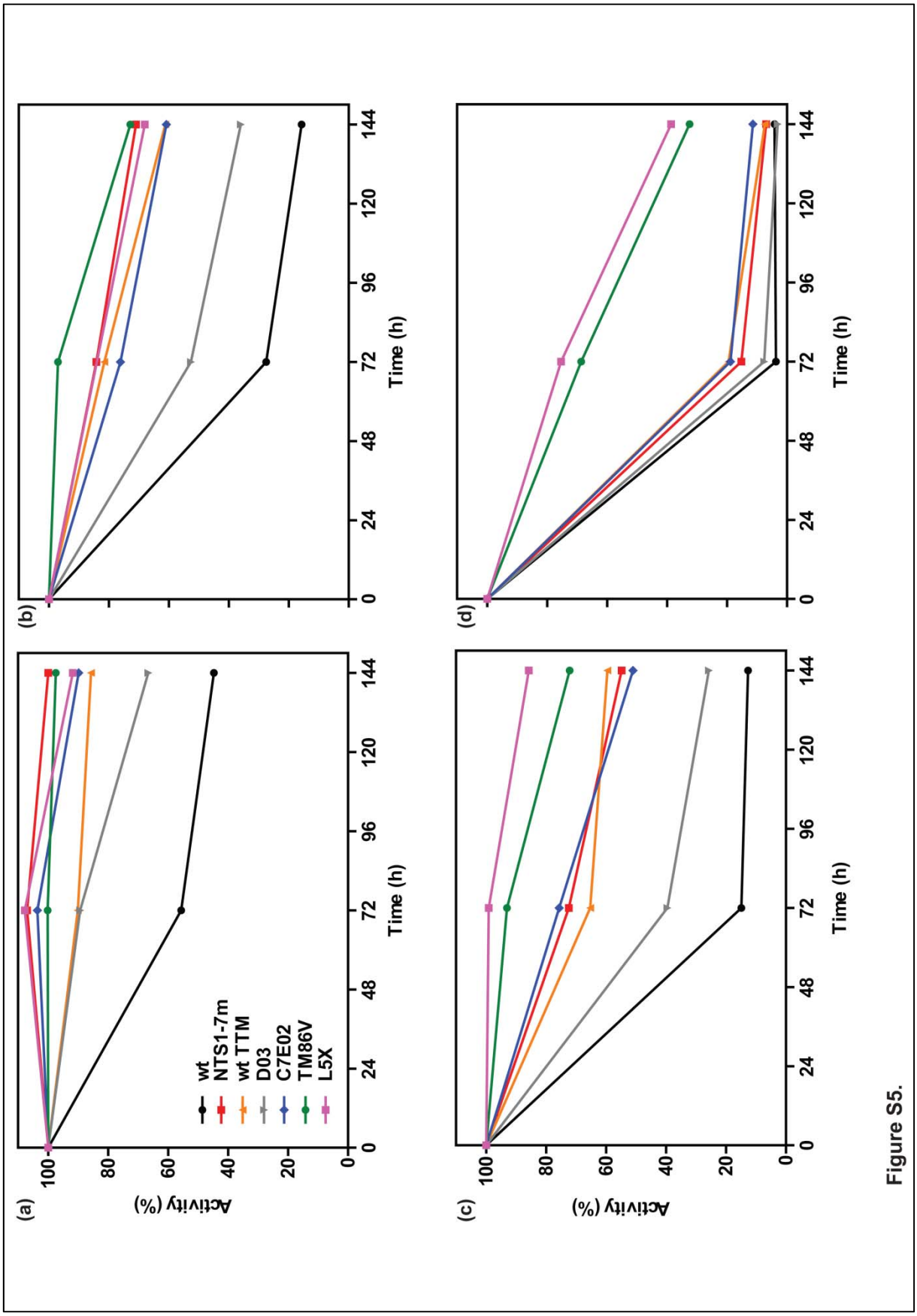
(a)
(b)
(c)
(d)
Activity (%)
Time (h)
0
24
48
72
96
120
144
20
40
60
80
100
wt
NTS1-7m
wt TTM
D03
C7E02
TM86V
L5X

Figure S5.

Figure S6. Functional expression levels of rNTR1-wt, wt-TTM and NTS1-7m in *E. coli*. An average of three independent expressions (20 h at 20°C) is shown.

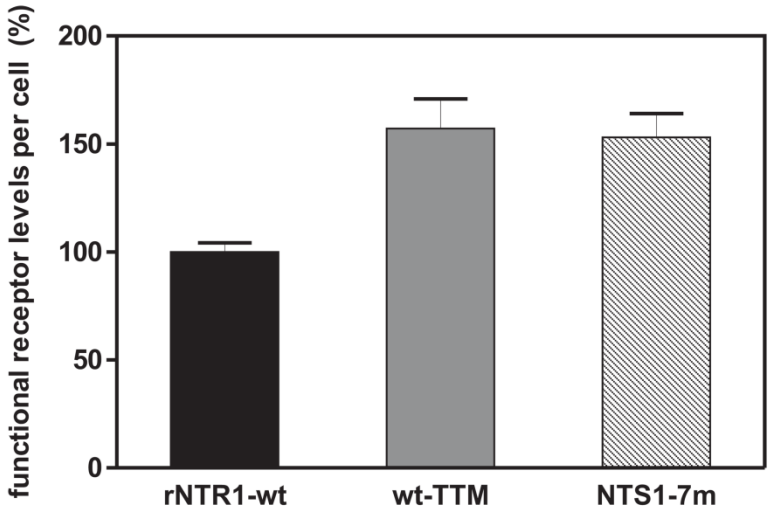
functional receptor levels per cell (%)
200
150
100
50
0
rNTR1-wt
wt-TTM
NTS1-7m

Figure S6.

Figure S7. Expression (A) and detergent stability (B) of mutant M303 in comparison to D03. (a) Expression levels of D03 and M303 were analyzed by flow cytometry. The MFI of D03 and M303 are comparable. Nonspecific binding of BODIPY-NT to cells was measured in the presence of 10 µM unlabeled neurotensin. (b) Detergent stability of D03 (solid circles), M303 (open squares), and a randomly chosen StEP-variant MutR (open triangles) is compared in a buffer containing DDM, CHAPS and CHS (buffer SAB).

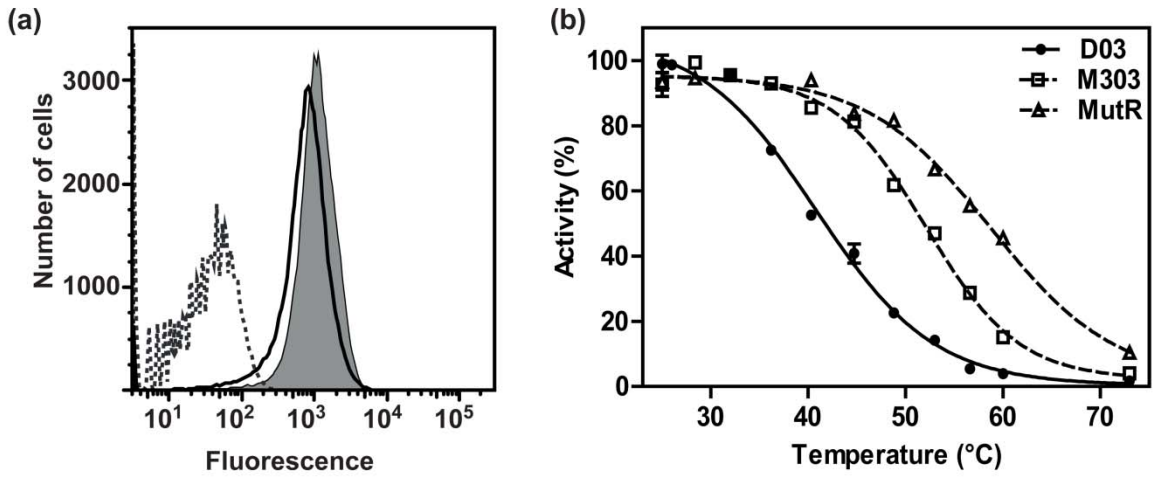
(a)
Number of cells
3000
2000
1000
10^1 10^2 10^3 10^4 10^5
Fluorescence
(b)
Activity (%)
100
80
60
40
20
0
30 40 50 60 70
Temperature (°C)
D03
M303
MutR

Figure S7.

References

1. Aguinaldo, A. M. & Arnold, F. (2002). Staggered extension process (StEP) *in vitro* recombination. *Methods Mol. Biol.* **192**, 235-239.
2. Zhao, H. & Zha, W. (2006). *In vitro* 'sexual' evolution through the PCR-based staggered extension process (StEP). *Nat. Protoc.* **1**, 1865-1871.
3. Shibata, Y., White, J. F., Serrano-Vega, M. J., Magnani, F., Aloia, A. L., Grisshammer, R. & Tate, C. G. (2009). Thermostabilization of the neurotensin receptor NTS1. *J Mol Biol* **390**, 262-277.

4.3 Further Experiments

4.3.1 Generation and selection of the StEP30x library

With optimal reaction conditions, we could successfully shuffle mutations within a 30 bp-distance by means of the staggered extension process (StEP). Such recombination frequencies were achievable by shuffling of the D03 sequence with the synthetic M30 or M303 sequence, respectively. M30 and M303 combine 30 or 33 shift mutations in one synthetic DNA sequence, providing an equimolar representation of all wild-type and shift residues in the StEP reaction. Iterative shuffling and selection of D03 with M30 and M303 lead to the identification of C7E02, a well-expressed and detergent-stable variant of D03 (see published article, pages 102 ff).

To begin with, we had first of all shuffled the thirty individual shift mutants with each other. Under these conditions, the frequency of each shift mutant codon in the template mix is only 3.4%, while 96.6% are wild type (originating from the other shift mutants that have a wild-type codon in the respective codon position; see Figure 4-1 for illustration). In other words, the mixing of 30 individual shift mutants results in a dilution effect that reduces the apparent shuffling efficiency, since most recombination events shuffle a wild-type codon against a wild-type codon and are hence ineffective.

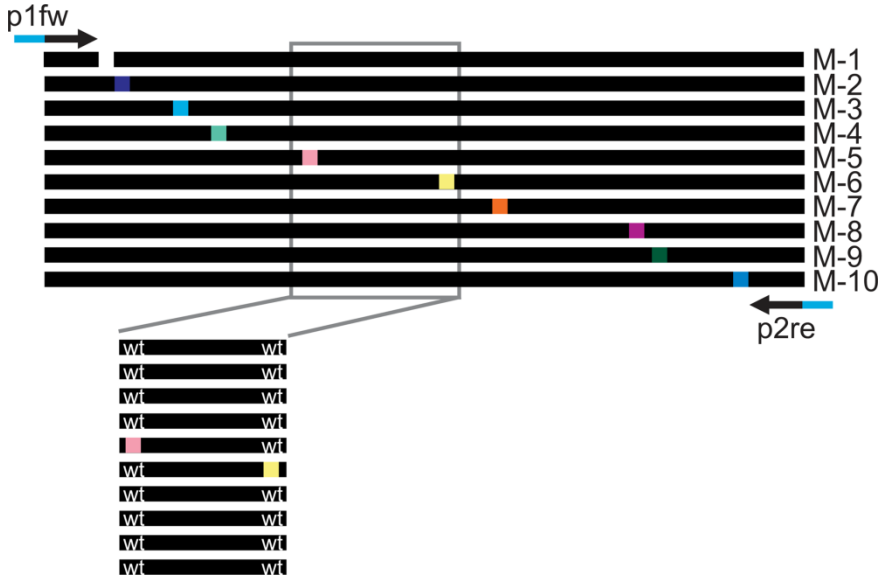

Figure 4-1. Illustration of the dilution effect in StEP shuffling of individual shift mutants. In this illustration, the DNA of ten shift mutants is mixed. For every shift mutant that is added to the reaction, the remaining nine template sequences carry a wild-type codon in the respective position. Hence, the apparent shuffling efficiency is low, since many recombination events shuffle wild type versus wild type.

The resulting library, termed StEP30x, was subjected to three rounds of StEP shuffling (termed A to C), each followed by three rounds of FACS-based selection for high functional expression (in pRGD03 (ID 3428), selections as described in the published

article, page 114). Figure 4-2 shows the increase in expression levels after round A (StEP30x_A111) and B (StEP30x_B111), respectively. Both pools show a step-wise shift towards higher expression levels, which is however much smaller than the shifts observed for the StEPM30 and StEPM303 libraries (published article, page 105), and far below the expression levels of the Sloning libraries (published article, page 104).

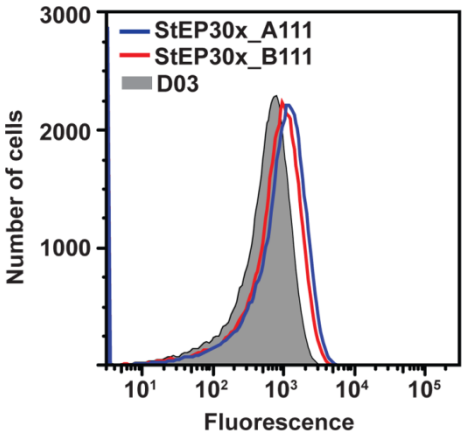

Figure 4-2. Expression levels of the evolved StEP30x pools. The final selected pools of StEP-shuffling round A (StEP30x_A111, blue line) and round B (StEP30x_B111, red line) were analyzed by flow cytometry, showing a successive increase in expression levels compared to D03 (grey).

The shuffling and selection was continued for a third round (round C), and was subsequently analyzed by sequencing of 24 individual clones from selection rounds A, B and C. By shuffling of 30 individual gene sequences, a maximum of three shift mutations was combined into a new chimeric sequence (Table 4-1, C332V$^{6.59}$ highlighted by a red box). C332V$^{6.59}$ is enriched during iterative shuffling and selection rounds, and strongly dominates the final evolved pool. Only a few sequences carry further mutations, of which I253A$^{5.54}$ shows the highest frequency. The selection result of the StEP30x library emphasizes the relevance of the C332V$^{6.59}$ for high functional expression of the evolved variants.

Table 4-1. Sequences of the evolved StEP30x pools after round A (A), B (B) and C (C).

(A) 24 random sequences from StEP30xA111 pool — low sequence quality

	TM1								TM2							TM3			I2	TM4			E2	TM5					TM6		E3		TM7	
D03 residue	V	N	T	I	F	S	A	T	A	D	L	M	E	L	R	D	C	A	A	I	M	K	V	I	I	N	K	C	Y	C	F	T	F
NTR1 position (aa)	57	58	68	70	75	83	86	101	110	113	119	121	124	125	143	150	172	177	201	202	208	235	240	253	260	262	263	320	324	332	342	354	358
Ballesteros-Weinstein			1.36	1.38	1.43	1.51	1.54	2.38	2.47	2.50	2.56	2.58	2.61	2.62	3.26	3.33	3.55		4.57	4.58	4.64	5.36	5.41	5.54	5.61	5.63	5.64	6.47	6.51	6.59		7.38	7.42
shift residue	I	R	S	L	L	G		R	L	S	F	L	D	V	K	E	R	H	S	L	V	R	L	A		R	R	L	L	V		S	V
clone 1																																V	
clone 2												L											L										
clone 3						G										E														V			
clone 4																																	
clone 5																						R											
clone 6																														V			
clone 7																														V			
clone 8																																V	
clone 9										S																		L					
clone 10																																	
clone 11								R		S																							
clone 12																E																	
clone 13																																S	
clone 14	I																																
clone 15										S																							
clone 16																								A									
clone 17																														V			
clone 18																														V			
clone 19																								A									
clone 20						G		R																									
clone 21																														V			
clone 22											F													A									
clone 23																														V			
clone 24																					V												

(B) 24 random sequences from StEP30xB111 pool — low sequence quality

	TM1								TM2							TM3			I2	TM4			E2	TM5					TM6		E3		TM7	
D03 residue	V	N	T	I	F	S	A	T	A	D	L	M	E	L	R	D	C	A	A	I	M	K	V	I	I	N	K	C	Y	C	F	T	F
NTR1 position (aa)	57	58	68	70	75	83	86	101	110	113	119	121	124	125	143	150	172	177	201	202	208	235	240	253	260	262	263	320	324	332	342	354	358
Ballesteros-Weinstein			1.36	1.38	1.43	1.51	1.54	2.38	2.47	2.50	2.56	2.58	2.61	2.62	3.26	3.33	3.55		4.57	4.58	4.64	5.36	5.41	5.54	5.61	5.63	5.64	6.47	6.51	6.59		7.38	7.42
shift residue	I	R	S	L	L	G		R	L	S	F	L	D	V	K	E	R	H	S	L	V	R	L	A		R	R	L	L	V		S	V
clone 1																				L										V			
clone 2																														V			V
clone 3																														V			
clone 4																														V			
clone 5																														V			
clone 6						G																								V			
clone 7																														V			
clone 8						G																		A						V			
clone 9								R																						V			
clone 10																														V			
clone 11				L																										T			
clone 12																																	V
clone 13																										R							V
clone 14																														V			
clone 15																								A									
clone 16																														V			
clone 17																														V			V
clone 18										S																							
clone 19										S																							
clone 20																														V			
clone 21																								A		R							
clone 22																																	
clone 23						G		R												L													
clone 24																										R				V			

bad sequence quality

(C) 24 random sequences from StEP30xC111 pool — low sequence quality

	TM1								TM2							TM3			I2	TM4			E2	TM5					TM6		E3		TM7	
D03 residue	V	N	T	I	F	S	A	T	A	D	L	M	E	L	R	D	C	A	A	I	M	K	V	I	I	N	K	C	Y	C	F	T	F
NTR1 position (aa)	57	58	68	70	75	83	86	101	110	113	119	121	124	125	143	150	172	177	201	202	208	235	240	253	260	262	263	320	324	332	342	354	358
Ballesteros-Weinstein			1.36	1.38	1.43	1.51	1.54	2.38	2.47	2.50	2.56	2.58	2.61	2.62	3.26	3.33	3.55		4.57	4.58	4.64	5.36	5.41	5.54	5.61	5.63	5.64	6.47	6.51	6.59		7.38	7.42
shift residue	I	R	S	L	L	G		R	L	S	F	L	D	V	K	E	R	H	S	L	V	R	L	A		R	R	L	L	V		S	V
clone 1																														V			
clone 2																								A						V			
clone 3																														V			
clone 4															K															V			
clone 5																														V			
clone 6	I																													V			
clone 7																								A						V			
clone 8																														V			
clone 9																								A						V			
clone 10																														V			
clone 11																				L										V			
clone 12																														V			
clone 13																														V			
clone 14						?																								V			
clone 15	I																													V			
clone 16																														V			
clone 17																																	
clone 18																														V			
clone 19																														V			
clone 20																								?						V			
clone 21																														V			
clone 22																														V			
clone 23																														V			
clone 24																														V			

bad sequence quality

4.3.2 Design and analysis of a minimal C7E02-like receptor variant

As explained in the published article (Sections 4.1 and 4.2), TM86V was rationally designed for detergent stability. More precisely, TM86V was originally identified as the strongest mutant from a screening and comparison of individual and rational combinations of shift mutations. In detail, four individual triple mutant combinations were generated: TM86V (A86L$^{1.54}$, I253A$^{5.54}$ and F358V$^{7.42}$), TM86A (A86L$^{1.54}$, I253A$^{5.54}$ and F358A$^{7.42}$), TM83V (S83G$^{1.51}$, I253A$^{5.54}$ and F358V$^{7.42}$) and TM83A (S83G$^{1.51}$, I253A$^{5.54}$ and F358A$^{7.42}$). TM86V combines the three shift mutations showing the highest increase in detergent stability when studied individually. Mutant TM86A, in comparison to TM86V, allows to judge whether the observed effect is specific for the F358V$^{7.42}$ mutation, which we had identified previously after full randomization of the receptor position (see Chapter 3). F358A$^{7.42}$, on the other hand, was reported to affect detergent stability of the wild-type receptor according to alanine-scanning mutagenesis (Shibata *et al.*, 2009). The effect of A86L$^{1.54}$ and S83G$^{1.51}$ was compared side-by-side with the mutants TM83V and TM86V. From the homology model we assume that A86L$^{1.54}$ leads to improved helix packing and compact folding, which reduces detergent-accessibility (homology modeling described in Schlinkmann *et al.*, 2012, Chapter 3-A, page 59). S83G$^{1.51}$ might achieve a similar effect by introduction of a glycine residue. While glycines display unfavorable helix propensities in soluble proteins and are grouped as “helix breakers” together with proline, they are found rather frequently in transmembrane helices, where they exhibit a structural role and are often found in helix-helix interaction motifs (Javadpour *et al.*, 1999). In this context, S83G$^{1.51}$ could independently address the same helix packing issue as A86L$^{1.54}$ by allowing helix bending. All four triple mutants were assessed for their detergent stability in DDM and DM in the absence of agonist (Figure 4-3).

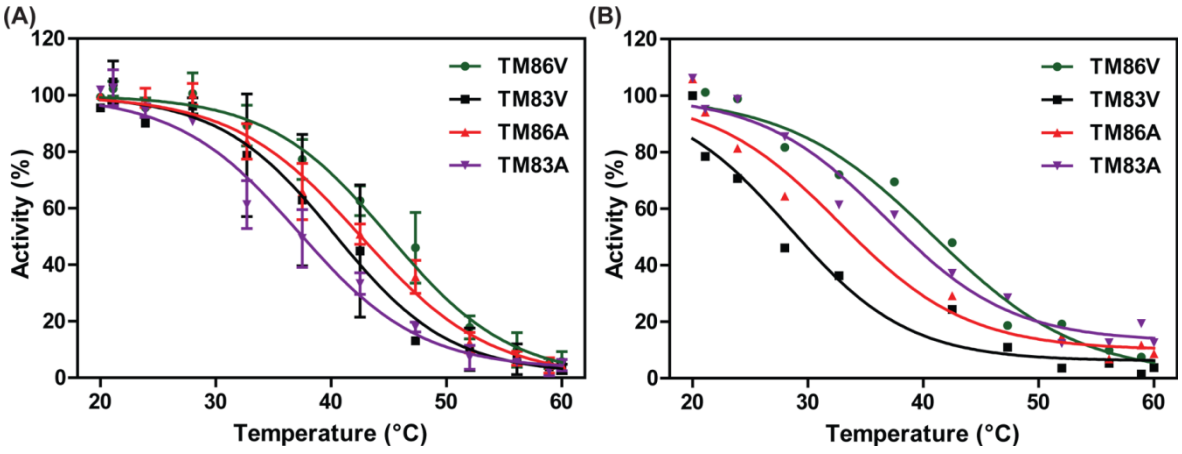

Figure 4-3. Detergent stability of the triple mutants TM86V, TM86A, TM83V and TM83A in DDM (A) and DM (B) in the absence of ligand. Experiments were performed as described before (published article, Sections 4.1 and 4.2).

Measurements of detergent stability in the absence of agonist were chosen since C7E02 is most stable under these conditions, and the core motif of C7E02 was under

investigation here. TM86V displayed highest detergent stability in both detergents, while the ranking of the remaining triple mutants is different between the two detergents (Figure 4-3). In the harsher detergent DM, we see that the presence of A86L$^{1.54}$ is of key importance to achieve high detergent stability, since the mutant TM83V is far less stable (Figure 4-3B). Further experiments revealed that TM86V is a true core mutant of C7E02 and ranked among the top three receptor variants regarding detergent stability (see published article, Sections 4.1 and 4.2).

4.3.3 Combination and analysis of the most-detergent stable shift mutations to double mutants

TM86V shows similar expression levels and even higher detergent stability than C7E02 (see published article, Sections 4.1 and 4.2). The detergent stability of TM86V in the presence of agonist is similar to L5X, the most stable variant identified (see published article, page 85). To further elucidate the contribution of the three shift mutations, all three possible double mutants of the three shifts A86L$^{1.54}$ (Figure 4-4), I253A$^{5.54}$ and F358V$^{7.42}$ were generated. The detergent stability of the double mutants DM-A (A86L$^{5.54}$ and I253A$^{5.54}$), DM-B (I253A$^{5.54}$ and F358V$^{7.42}$) and DM-C (A86L$^{1.54}$ and F358V$^{7.42}$) was assayed in the presence of agonist and compared to TM86V (Figure 4-5). Experiments were performed in the presence of agonist, since the single shift mutants are not very stable in the absence of ligand.

Mutant DM-A, combining the two shift mutations A86L$^{1.54}$ and I253A$^{5.54}$, is the strongest double mutant with respect to detergent stability. DM-A is very similar to TM86V in all detergents tested. As discussed in the published article (Sections 4.1 and 4.2), A86L$^{1.54}$ potentially optimizes helix packing (Figure 4-4), while I253A$^{5.54}$ restricts conformational flexibility.

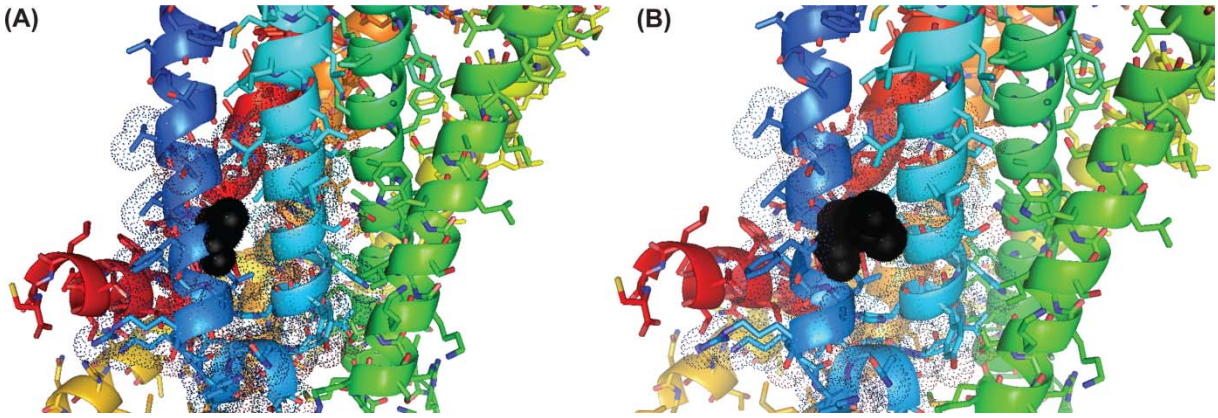

Figure 4-4. Homology model of rNTR1 with position A86$^{1.54}$ highlighted in black. Surrounding side chains are highlighted with dots. (A) A86$^{1.54}$ and (B) mutation A86L$^{1.54}$.

The combination of these two mutations might thus lead to increased detergent stability. The comparably low detergent stability of DM-B (I253A$^{5.54}$ and F358V$^{7.42}$) further

emphasizes the important role of A86L$^{1.54}$ for detergent stabilization (Figure 4-5). Additionally, it marks the difference between TM86V and C7E02 compared to L5X, which does not contain A86L$^{1.54}$.

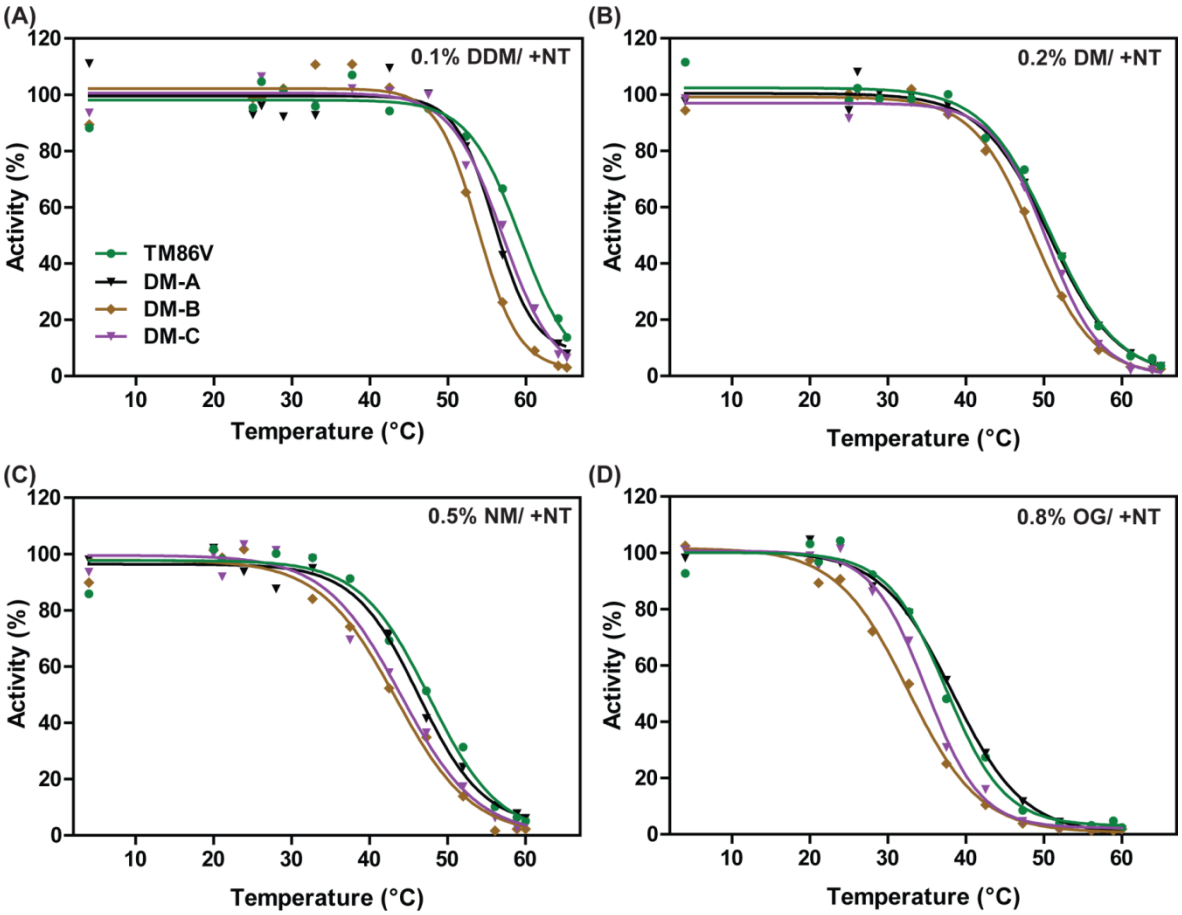

Figure 4-5. Agonist-bound detergent stability of the double mutants DM-A, DM-B and DM-C compared to TM86V. Measurements were performed as described in the published article, page 114.

4.3.4 Expression and detergent stability of the chimeric TM86V: L5X constructs MT1-3 and ML1-5

L5X combines 15 shift mutations that result in maximal functional expression per cell and highest detergent stability. Despite the fact that L5X originates from the fully binary Sloning Library (published article, Sections 4.1 and 4.2), not every of the 15 shift mutations is necessarily essential for the L5X phenotype: A subset of shift mutations might exhibit a neutral phenotype, and might thus have been co-selected in the presence of other, beneficial mutations while being dispensable for the observed phenotype. Furthermore, certain shift mutations might be essential to achieve high detergent stability, and others might be required for increased expression level or for both. In this context, it is interesting to note that TM86V behaves similar to L5X with respect to detergent stability,

but displays much lower expression levels under all conditions tested (published article, Sections 4.1 and 4.2).

To elucidate better the contribution of certain shift mutations to the phenotype of L5X, two sets of mutants were generated: First, certain shift mutations that are present in L5X were added onto TM86V (mutants of TM86V, termed MT), and second, the same shift mutations were removed from L5X (mutants of L5X, termed ML). Subsequently, the mutants MT1-MT3 and ML1-ML5 (Table 4-2 for sequences) were studied for their expression levels in both pRGD03 (plasmid ID 2438) and eLIC47D03 (plasmid ID 3254) and for their detergent stability.

Table 4-2. Sequences of the mutants MT1-MT3 and ML1-ML5 compared to their parental sequences TM86V and L5X.

	TM1							TM2							TM3			I2	TM4			E2	TM5					TM6		E3	TM7		
D03 reference	V	N	T	I	F	S	A	T	A	D	L	M	E	L	R	D	C	A	A	I	M	K	V	I	I	N	K	C	Y	C	F	T	F
NTR1 position (aa)	67	58	68	70	75	83	86	101	110	113	119	121	124	125	143	160	172	177	201	202	208	235	240	253	260	262	263	320	324	332	342	354	358
Ballesteros-Weinstein			1.36	1.38	1.43	1.51	1.54	2.38	2.47	2.50	2.56	2.58	2.61	2.62	3.26	3.33	3.55		4.57	4.58	4.64	5.36	5.41	5.54	5.61	5.63	5.64	6.47	6.51	6.59		7.38	7.42
TM86V							L																	A									V
TM86A							L																	A									A
TM83V						G																		A									V
TM83A						G																		A									A
DM-A							L																	A									
DM-B																								A									V
DM-C							L																										V
MT1							L			S														A						V			V
MT2					L		L																	A									V
MT3							L	R										H						A									V
L5X	I				L			R		S	F	L			K	E		H					L	A				L		V		S	V
ML1	I				L			R			F	L			K	E		H					L	A				L				S	V
ML2	I							R		S	F	L			K	E		H					L	A				L		V		S	V
ML3	I				L					S	F	L			K	E							L	A				L		V		S	V
ML4	I				L		L	R		S	F	L			K	E		H					L	A				L		V		S	V
ML5	I				L			R		S	F	L			K	E		H					L	A				L		V		S	

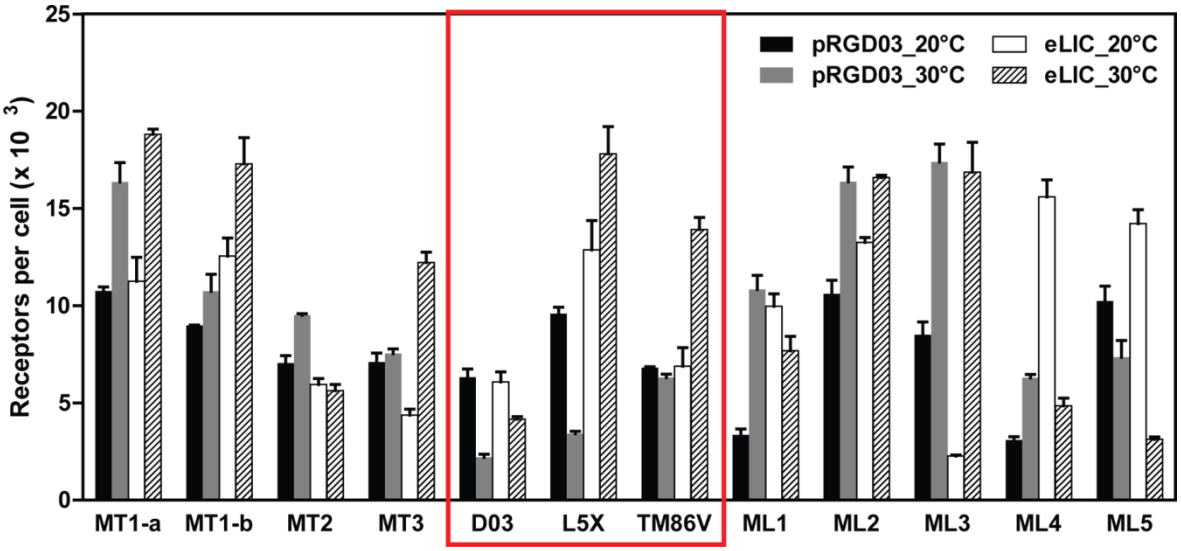

Figure 4-6. Expression levels of the mutants MT1-3 and ML1-5. Expression levels were analyzed after 20 h expression at 20°C or 30°C in the plasmids pRGD03 (ID 2438) and eLIC47D03 (ID 3254). D03, L5X and TM86V (red box) are simultaneously expressed for comparison. Expression of MT1 is performed in duplicates (MT1-a and MT1-b).

The expression levels of mutant MT1, adding D113S$^{2.50}$ and C332V$^{6.59}$ onto TM86V, are increased compared to TM86V and show a L5X-like phenotype in the high

copy plasmid eLIC47D03 (Figure 4-6), pointing towards a key role for D113S$^{2.50}$ and C332V$^{6.59}$ for high functional expression.

The role of D113S$^{2.50}$ and C332V$^{6.59}$ in high functional expression is further emphasized by the phenotype of mutant ML1: ML1 is derived from L5X, with D113S$^{2.50}$ and C332V$^{6.59}$ reverted to aspartate and cysteine, respectively. Restoration of the D03 phenotype in these positions significantly decreases expression to a level similar to TM86V (Figure 4-6).

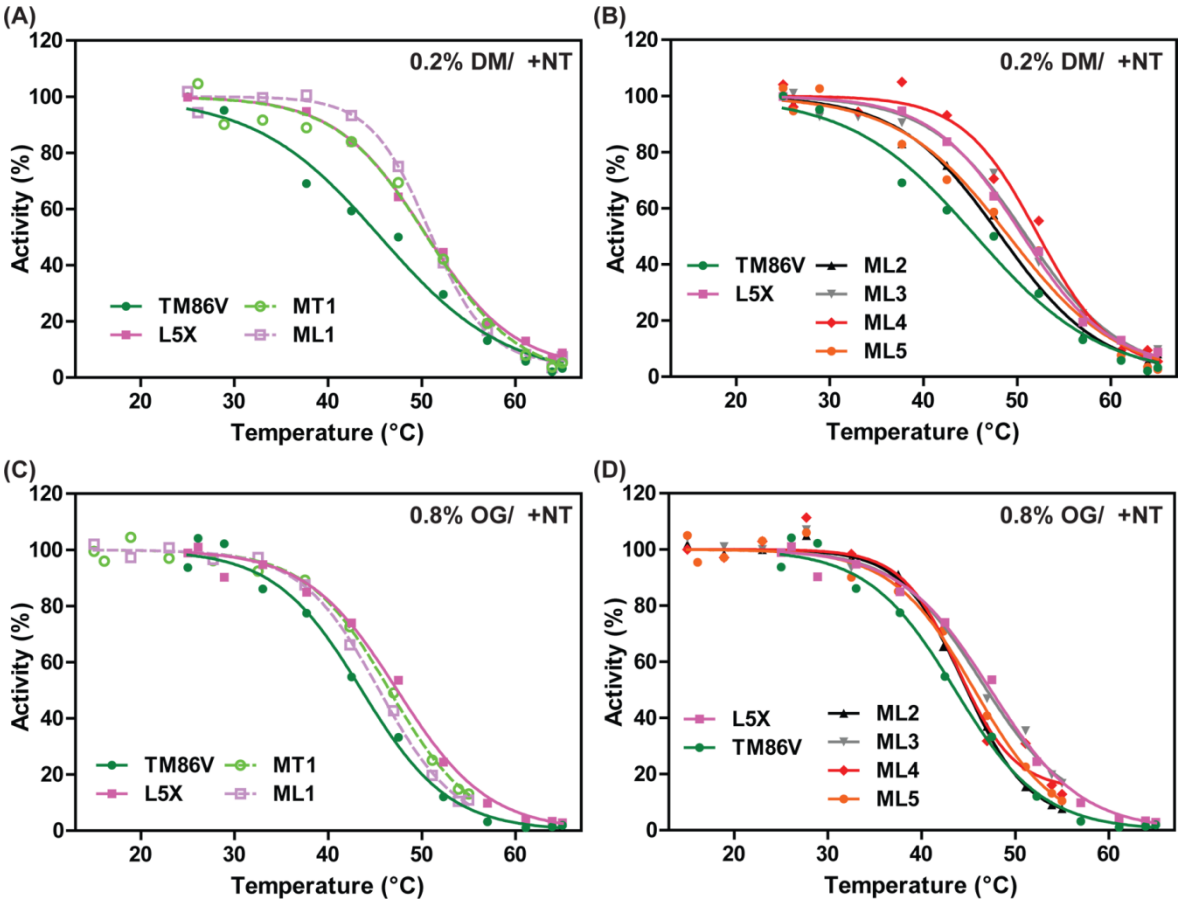

Figure 4-7. Detergent stability of MT1-3 and ML1-5 in the presence of agonist in the detergent DM (A, B) and OG (C, D). Comparison of MT1 and ML1 with TM86V and L5X is separately illustrated in (A) and (C).

The detergent stability of TM86V and L5X is rather similar, and the intermediate variant MT1 is slightly increased compared to TM86V and identical to L5X in both DM (Figure 4-7A) and OG (Figure 4-7C). ML1, on the other side, also retains detergent stability. It thus looks that D113S$^{2.50}$ and C332V$^{6.59}$ do only minimally affect detergent stability. The mutants ML2, ML3, ML4 and ML5 do have no dramatic effect on detergent stability of L5X (Figure 4-7B and D).

It can be summarized that MT1 is a minimal mutant of L5X that exhibits high expression, and the phenotype of high expression can be directly attributed to the shift mutations D113S$^{2.50}$ and C332V$^{6.59}$. Different from that, high detergent stability can

apparently be achieved by individual solutions: TM86V carries only the three most stabilizing shift mutations A86L$^{1.54}$, I253A$^{5.54}$ and F358V$^{7.42}$, while L5X carries only I253A$^{5.54}$ and F358V$^{7.42}$ among its 15 shift mutations. Detergent stability of L5X is hence conveyed by a more complex mechanism and synergistic effects between individual shift mutations.

4.3.5 Design and selection of additional Sloning library constructs for high functional expression and detergent stability

The fully binary Sloning library provided an excellent system to assess the influence of various expression conditions on the directed evolution of this library. The improved expression levels of the previously identified receptor variants, among them C7E02, indicated a reduced toxicity of overexpression. To exclude that expression is artificially limited by external parameters, the Sloning library was expressed in the standard plasmid pRGD03 (Sloning library L1, ID 3493) and furthermore in the high copy plasmid eLIC47D03 (Sloning library L5, ID 3501). It turned out that, indeed, high expression of evolved variant L5X was dependent on expression from the high-copy plasmid eLIC47D03 (published article, Sections 4.1 and 4.2).

Table 4-3. Overview of Sloning library constructs.

Library	vector origin	copy number	fusion protein construct						
D03 reference	pRGD03	low	MBP	TEV site	Full length D03 sequence (T43-Y424)	TEV site	trx	His_{10}	**
L1	pRGD03	low	MBP	TEV site	Full length GPCR library (T43-Y424)	TEV site	trx	His_{10}	**
L2	pRGD03	low	MBP	TEV site	truncated GPCR library including H8 (T43-C389)	TEV site	trx	His_{10}	**
L3	pRGD03	low	MBP	TEV site	truncated GPCR library including H8 (T43-C389)	**			
L4	pRGD03	low	MBP	TEV site	truncated GPCR library including H8 (T43-C389)	His_{10}	**		
L5	eLIC47D03	medium	MBP	TEV site	Full length GPCR library (T43-Y424)	TEV site	trx	His_{10}	**
L6	eLIC47patD03	high	MBP	TEV site	Full length GPCR library (T43-Y424)	TEV site	trx	His_{10}	**

MBP, maltose binding protein; TEV site, cleavage recognition site for TEV protease; trx, thioredoxin; His_{10}, 10-fold histidine tag; **, 2 stop codons

Additional to the successfully evolved libraries L1 and L5, we have tried to evolve the Sloning library under further conditions (Table 4-3 and Appendix 1.3 for construct design): Library L6 was expressed from the plasmid eLIC47patD03, a derivative of eLIC47D03 carrying additional mutations in the origin of replication that increase plasmid copy number (termed “patent mutations”, mutant 9 from Bayer *et al.*, 2007). Libraries L2 to L4 were expressed from the plasmid pRGD03, and are characterized by truncation of the GPCR sequence after helix 8 (truncation after amino acid C389). In library L2 (ID 3495), C389 was followed by the asparagine linker, TEV cleavage site and thioredoxin, similar to the standard fusion construct. In libraries L3 (ID 3497) and L4 (ID 3499), the Sloning library was expressed without a C-terminal fusion protein but terminated directly after C389 with two stop codons (L3) or a His_{10}-tag followed by two stop codons (L4). The rational behind these constructs is that in previous selections, enrichment of stop codons in the flexible receptor C-terminus was observed, indicating that expression without a C-terminal fusion protein (trx) might be advantageous. Also the ultra-deep sequencing data of the C-terminal positions show a higher tolerance towards stop codons, which is in agreement with the previous data (published article, Chapter 3).

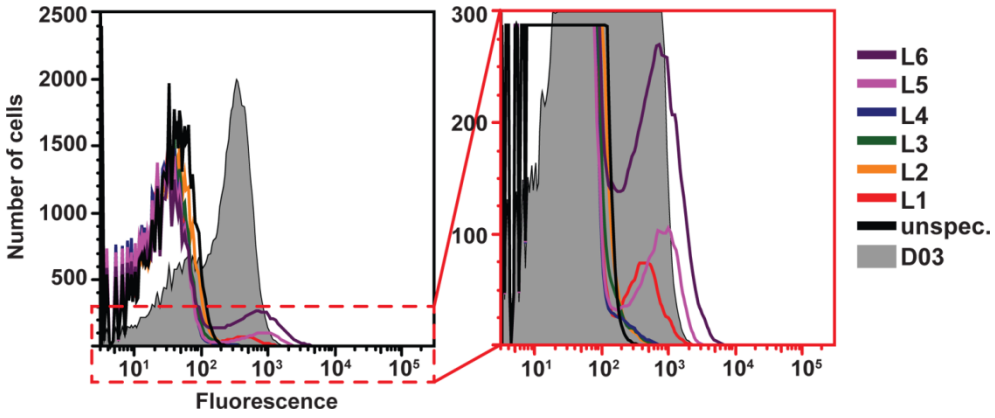

Figure 4-8. Expression of the naïve libraries L1-L6 measured by flow cytometry. Libraries were expressed for 20 h at 20°C, and specific ligand binding was measured in the presence of 20 nM BODIPY-neurotensin.

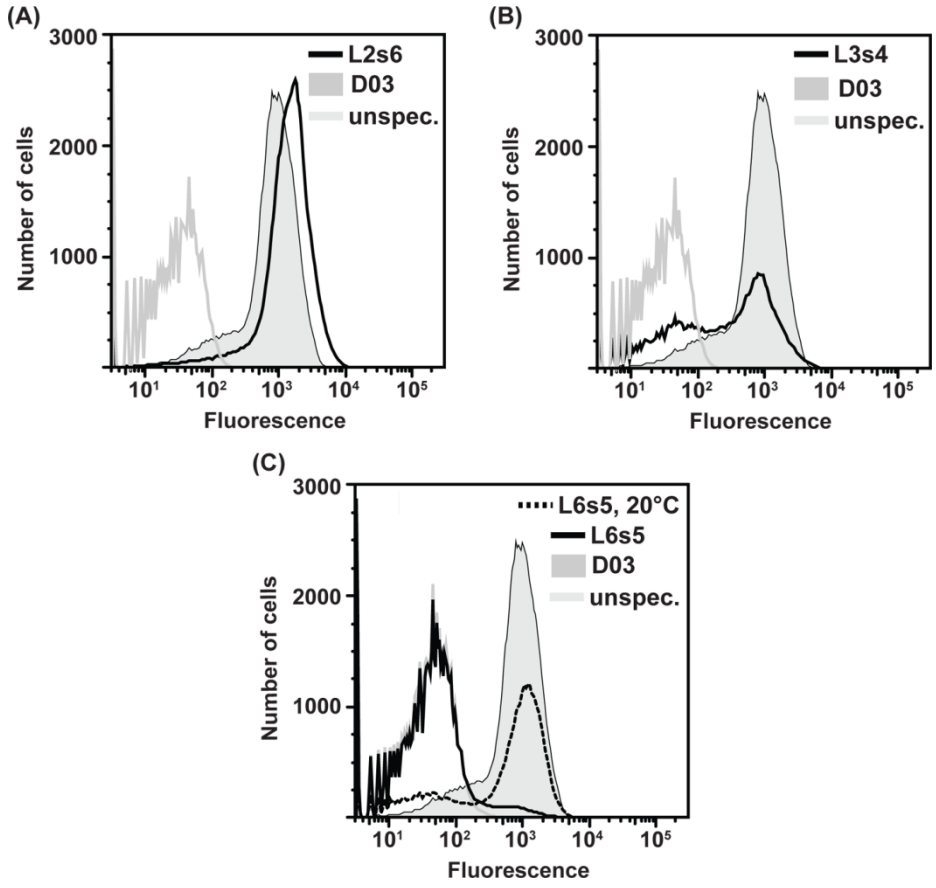

Figure 4-9. Expression levels of the evolved libraries L2s6 (A), L3s4 (B) and L6s5 (C) analyzed by flow cytometry. (A) and (B) Final selection after expression at 30°C, (C) final selection after expression at 20°C. L6s5 expressed poorly at 30°C. Expression and fluorescence-labeling were performed as described in the published article, page 114. Expression levels of the evolved pools L1s6 and L5s5 are described in the published article, page 107.

Expression of the naïve libraries L1 to L6 was characterized two subpopulations, a dominant population of ca. 85-95% that did not bind the agonist (fluorescence-labeled neurotensin), and a small population that expressed functional receptor variants and specifically bound the agonist, hence showing a shift towards high fluorescence (Figure 4-8). Expression of L2, L3 and L4 was hardly detectable, while L1, L5 and L6 showed small, but clear expression peaks (Figure 4-8, see zoom-in on right side). L1, L5 and L6 express the Sloning library in the identical fusion protein construct (MBP - Sloning library - thioredoxin) from plasmids with different copy numbers (Table 4-3), and these differences apparently affect expression levels of the naïve libraries, and the degree of expression positively correlates with plasmid copy number.

Interestingly, L5 could be successfully evolved and was highly superior to L1 with respect to expression levels (published article, page 107). L6 however could not be evolved further, but showed a plateau at much lower expression levels (Figure 4-9C). This observation is intriguing with respect to the fact that the high copy library L6 showed the highest degree of expression for the naïve library (Figure 4-8). It thus looks that the NTR1-variants represented within the Sloning library are still too toxic to be expressed from high copy plasmids in *E. coli*. L2 could be successfully evolved (Figure 4-9A), but the final expression niveau was only slightly higher compared to D03. Selection of L3 could not be evolved to even reach expression of D03, and L4 could not be enriched for high expression.

Hence, from these results, it can be deduced that for maximal expression, the C-terminally fused thioredoxin is required.

4.3.6 Expression levels and detergent stability of the cysteine-free variants of rNTR1-wt, D03 and C7E02

C332V$^{6.59}$ is a shift mutation with highest relevance for expression. C332V$^{6.59}$ was retrieved as the dominant mutation from the StEP-recombination of the 30 individual shift mutations (StEP30x), and it is essential for the high-expression phenotype of L5X and MT1. We assume that expression is positively affected by the absence of a free cysteine in the periplasmic space, since this could facilitate fast and correct disulfide formation between C142$^{3.25}$ and C225 (EL2). We might observe this as a result of expression in *E. coli*, for which oxidizing conditions and disulfide formation and shuffling are different from mammalian cells. Furthermore, long-term experiments under oxidizing buffer conditions might result in uncontrolled and undesired oxidation, which could hamper for example crystallization. We have thus designed synthetic sequences of rNTR1-wt, D03 and C7E02 in which all non-essential cysteines, apart from those involved in disulfide formation, are replaced by the most tolerated amino acid according to the 454 results from the saturating mutagenesis study (Table 4-4 and published article, Chapter 3). The resulting variants wt-cf (cysteine-free), D03-cf and C7E02-cf were studied for their expression and detergent stability in comparison to their parental sequence.

Table 4-4. Cysteine substitutions of the cysteine-free mutants D03-cf, C7E02-cf and wt-cf.

	amino acid position									
variant	142	152	172	226	278	320	332	386	388	417
D03_cf	C	L	R	C	S	L	V	S	S	S
D03	C	C	C	C	C	C	C	C	C	C

yellow – hydrophobic aa, green – polar aa, blue – charged aa

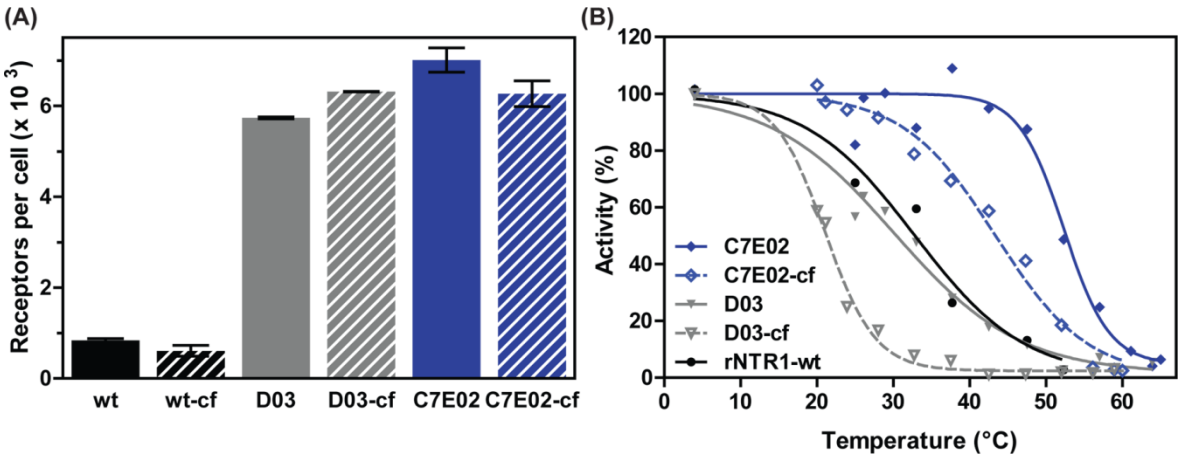

Figure 4-10. Analysis of expression levels (A) and detergent stability (B) of the cysteine-free variants of rNTR1-wt (wt), D03 and C7E02. (A) All variants were expressed from the plasmid pRGD03 for 20 h at 20°C. (B) Detergent stability was assessed in the absence of agonist in the detergent DDM (as described in the published article, page 114).

Replacement of all non-essential cysteines did not significantly affect expression levels (Figure 4-10A), but lead to decreased detergent stability (Figure 4-10B) for all the receptor variants. rNTR1-cf could not be analyzed due to the decrease in detergent stability.

In agreement with previous results, it appears that certain substitutions have different effects on expression and detergent stability. We have observed for the thirty individual shift mutations that while all do individually increase expression levels, only a subset of these shift mutants show also increased detergent stability. While any cysteine was replaced by the most suitable amino acid according the selection and sequencing results, it might well be that the combination of these mutations is not compatible with respect to detergent stability.

4.3.7 Detergent stability of the signaling-active evolved variants C7E02-BM, TM86V-BM and L5X-BM

D03, the basis of all shift mutants and evolved variants with multiple shift mutations, carries nine mutations compared to rNTR1-wt. Among these, we find R167L$^{3.50}$, a mutation that is located in the highly conserved E/DRY motif of TM3. The

E/DRY motif is involved in the formation of the so-called ionic lock that keeps the receptor in the inactive state (Deupi and Kobilka, 2007), and is released during receptor activation to facilitate downstream signaling. Mutation of the E/DRY motif leads to decreased signaling competence, as observed for D03 in comparison to rNTR1-wt (Sarkar *et al.*, 2008). Reconstitution of the E/DRY motif for D03 (D03-L167R$^{3.50}$) recovers signaling competence (Sarkar *et al.*, 2008).

Consequently, we also recovered the E/DRY motif for the evolved variants C7E02, TM86V and L5X to assess their signaling competence (published article, page 110). To confirm that the "backmutation" L167R$^{3.50}$ ("BM") did not affect detergent stability, the respective variants C7E02-BM, TM86V-BM and L5X-BM were studied for their agonist-bound detergent stability.

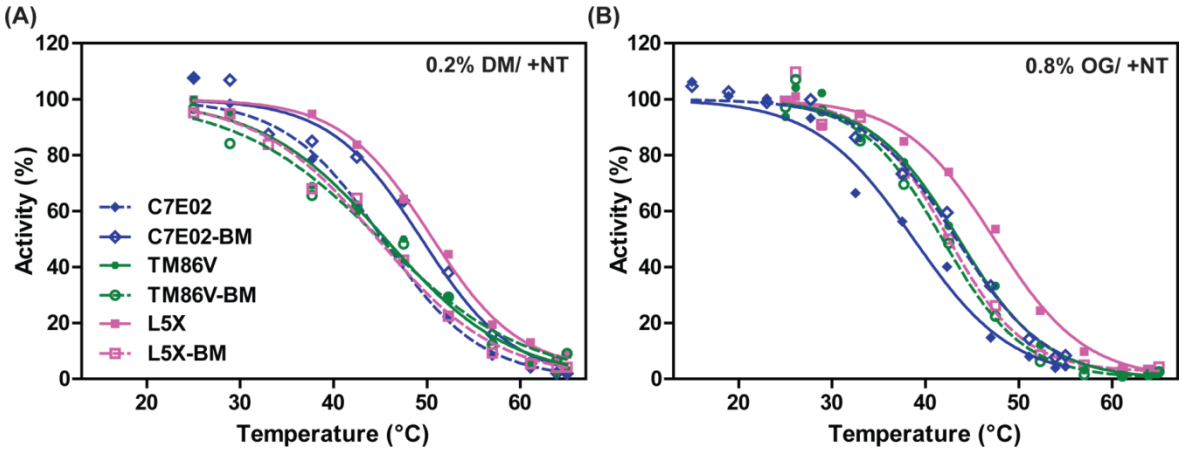

Figure 4-11. Detergent stability of the evolved variants C7E02, TM86V, L5X and their backmutants (BM) with reconstituted E/DRY motif in DM (A) and OG (B).

Restauration of the E/DRY-motif leads only to small and negligible changes in the detergent stability of the respective variant. Studies aiming at the cocrystallization of GPCR and heterotrimeric G protein complex might thus rely on the BM-receptor versions with restored E/DRY-motif, while the original variant might be preferred for crystallization of the receptor alone.

4.4 Summary and Discussion

For the shuffled StEP- and Sloning libraries, coevolution of expression and detergent stability was observed (see published article, page 102 ff.). This coevolution is loose, meaning that the while both expression and detergent stability are increased for any selected receptor variant compared to the parental D03, they are affected to a different degree for individual receptor variants. Obviously, expression- and stability-increasing shift mutations are efficiently selected for, and shift mutations that, when combined, are incompatible which each other, are efficiently selected against. Besides the required shift mutations that define the phenotype of an evolved receptor variant, these receptor variants may contain additional shift mutations with a neutral phenotype. Such

shift mutations are, other than beneficial or detrimental shift mutations, not detected by the selection system, and thus co-selected with beneficial shift mutations.

The fully binary library proved to be superior the StEP-shuffled libraries, and this is likely a consequence of the fact that only a fully binary library allows efficient separation of required from incompatible shift mutations that are close in sequence and not separated by StEP shuffling. The efficient but incomplete shuffling by StEP is reflected by the mutant C7E02 and its core mutant TM86V, which displays even higher detergent stability than the parental C7E02.

L5X is derived from the fully binary Sloning library, but nevertheless includes also shift mutations with a neutral phenotype with respect to expression and detergent stability. The additional experiments presented here provide further insight into the combinatorial effects of the evolved receptor variants, and identify the required and neutral shift mutations of L5X with respect to functional expression. In particular, the chimeric constructs MT1 (Figure 4-12) and ML1 allowed us to identify the shifts D113S$^{2.50}$ and C332V$^{6.59}$ to be crucial for the high-expression phenotype of L5X.

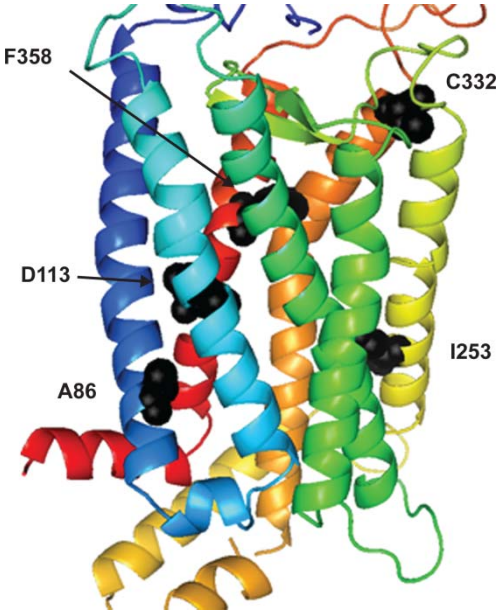

Figure 4-12. Location of the MT1-defining shift mutations in the homology model of rNTR1 (homology model by A. Honegger). Positions of MT1-mutations are highlighted in black. The highlighted positions illustrate the rNTR1-side chain.

According to the homology model (Figure 4-12), the 5 shift mutations of MT1 are not in a distance where they could interact, which is different for L5X. MT1 retains L5X-like detergent-stability, indicating that this phenotype is rather the sum of individual effects, than of synergistic effects.

C332V$^{6.59}$ likely affects expression by avoiding alternative oxidation pathways during formation of the crucial disulfide bridge between C142$^{3.25}$ and C225 (EL2), since removal of C332$^{6.59}$ leaves only these two cysteines accessible to disulfide formation in the periplasmatic space. D113$^{2.50}$ confers sodium sensitivity to the receptor (Martin *et al.*,

1999), and is thus functionally relevant *in vivo*. From the homology model of rNTR1, we assume that D113$^{2.50}$ is close to N82$^{1.50}$, which itself is also identified as a shift position. Potential sterical constraints could affect protein folding, which might be relieved by either of the two shifts D113S$^{2.50}$ or N82H$^{1.50}$.

On the other hand, these shift mutations are not essential for detergent stability, indicating the different forces that drive high expression compared to high detergent stability.

While the phenotype of MT1 and ML1 clearly identify the determinants of high functional expression, we did not identify a “killer mutation” or a “winner mutation” for the high detergent stability of L5X. L5X does not contain the highly stabilizing shift mutation A86L$^{1.54}$, and its high detergent stability is thus rather the sum of many small effects, using an alternative route to detergent-stability compared to TM86V and C7E02, that makes only partial use of the “stability motif” A86L$^{1.54}$, I253A$^{5.54}$ and F358V$^{7.42}$. Further experiments, especially structure determination, could elucidate the underlying principles of improved detergent stability.

References

Bayer, K., Grabherr, R., Nilsson, E., Striedner, G. (2007). Expression vectors with modified ColE1 origin of replication for control of plasmid copy number. **EP 1 326 989 B1**.

Deupi, X., Kobilka, B. (2007). Activation of G protein-coupled receptors. *Adv. Protein Chem.* **74**, 137-166.

Javadpour, M.M., Eilers, M., Groesbeek, M., Smith, S.O. (1999). Helix packing in polytopic membrane proteins: role of glycine in transmembrane helix association. *Biophys. J.* **77**, 1609-1618.

Martin, S., Botto, J.M., Vincent, J.P., Mazella, J. (1999). Pivotal role of an aspartate residue in sodium sensitivity and coupling to G proteins of neurotensin receptors. *Mol. Pharmacol.* **55**, 210-215.

Sarkar, C.A., Dodevski, I., Kenig, M., Dudli, S., Mohr, A., Hermans, E., Plückthun, A. (2008). Directed evolution of a G protein-coupled receptor for expression, stability, and binding selectivity. *Proc. Natl. Acad. Sci. USA* **105**, 14808-14813.

Schlinkmann, K.M., Honegger, A., Türeci, E., Robison, K.E., Lipovsek, D., Plückthun, A. (2012). Critical features for biosynthesis, stability, and functionality of a G protein-coupled receptor uncovered by all-versus-all mutations. *Proc. Natl. Acad. Sci. USA* **109**, 9810-9815.

Shibata, Y., White, J.F., Serrano-Vega, M.J., Magnani, F., Aloia, A.L., Grisshammer, R., Tate, C.G. (2009). Thermostabilization of the neurotensin receptor NTS1. *J. Mol. Biol.* **390**, 262-277.

Chapter 5

Selection of DARPin binders to TM86V and L5X by ribosome display

5.1 Introduction

D03 was successfully evolved for high functional expression and detergent stability, leading to the identification of C7E02, TM86V and L5X. These three receptor variants were identified under different selection and screening conditions (Schlinkmann *et al.*, 2012 , Chapter 4 of this work). C7E02, selected from the StEP303 library, displays the highest detergent stability in the absence of ligand. Thirteen individual shift mutations are the basis for the C7E02 phenotype. Selection of the fully binary Sloning library resulted in the highly evolved variant L5X, with the highest obtained expression level of up to 25,000 receptors per *E. coli* cell. Interestingly, the high expression level of L5X is dependent on expression from a high copy plasmid (eLIC47D03, (Schlinkmann *et al.*, 2012 , Chapter 4 of this work), meaning that the toxicity of overexpression is strongly reduced for L5X such that the high copy number is tolerated and leads to more functional protein. L5X is strongly stabilized in the agonist-bound state as a direct consequence of screening for detergent-stability in the presence of agonist. In contrast to C7E02, signaling competence and antagonist binding of L5X is decreased. In a parallel rational design approach, TM86V was generated by combination of the three most stabilizing shift mutations. TM86V is a minimal core mutant, characterized by an intermediate expression level compared to L5X and C7E02, high detergent-stability in both the ligand-free as well as the agonist-bound state, and a signaling competence similar to C7E02.

The similar high detergent-stability of TM86V and L5X is achieved by independent solutions: While TM86V combines solely the three most stabilizing shift mutations when analyzed individually, L5X carries 15 shift mutations, but contains only two of these most stabilizing shift mutations. The differences in signaling competences allow us to conclude that TM86V and L5X likely prefer different receptor conformations.

Crystallization of membrane proteins in general requires approaches that are especially adapted to the characteristics of membrane proteins. Even though the evolved receptor variants allow us to produce high amounts of pure, homogeneous and detergent-stable receptor preparations that are optimal for crystallization purposes, we could not yet successfully crystallize all of these receptor variants. A likely explanation is the high flexibility of the helix-connecting loops, which are solvent-accessible and present the main available surface for crystal contact formation. Recent progress in crystallization of GPCRs was in most cases facilitated by replacement of the intracellular loop 3 (IL3) by the rigid protein T4-lysozyme (Rosenbaum *et al.*, 2007), providing a large hydrophilic surface for crystal contact formation. Despite its advantages, the excision and replacement of functional receptor parts, in this case the interaction surface with downstream effector proteins, is a main drawback of this strategy.

An optimal solution to this issue would be a binding protein that specifically recognizes the receptor surface, constraining the flexibility of the loop regions and adding a rigid hydrophilic surface for crystal contact formation.

The aim here is to employ the DARPins as binding proteins to the evolved receptor variants to facilitate crystallization. L5X and TM86V were chosen as targets for the selection of DARPin binders, since these variants display highest detergent-stability and most likely prefer different receptor conformations.

5.1.1 DARPin as binding molecules

Designed ankyrin repeat proteins (DARPins) are versatile binding proteins. DARPins are small, highly expressed and soluble proteins with extremely high stability (Binz *et al.*, 2003; Kohl *et al.*, 2003). DARPins are derived from naturally occurring ankyrin repeat proteins (Forrer *et al.*, 2003). The scope and diversity of repeat proteins is illustrated by the fact that the immune system of jawless vertebrates is based on the diverse repertoire of leucine-rich repeat proteins (Alder *et al.*, 2005). The scaffold of DARPins is based on a consensus design, and characterized by an α-helical fold (Forrer *et al.*, 2004). A single ankyrin repeat is composed of a β-turn followed by two antiparallel helices, connected to the next repeat by a flexible loop. The α-helical scaffold results in a slight curvature, giving the DARPin a paraglider-like appearance (Binz *et al.*, 2004). The flexible loops and the more concave side make up the binding interface with the target protein. The DARPin library carries randomized positions in the flexible loops and in one of the helices, providing an enormous theoretical diversity for possible binding to a given target (Figure 5-1).

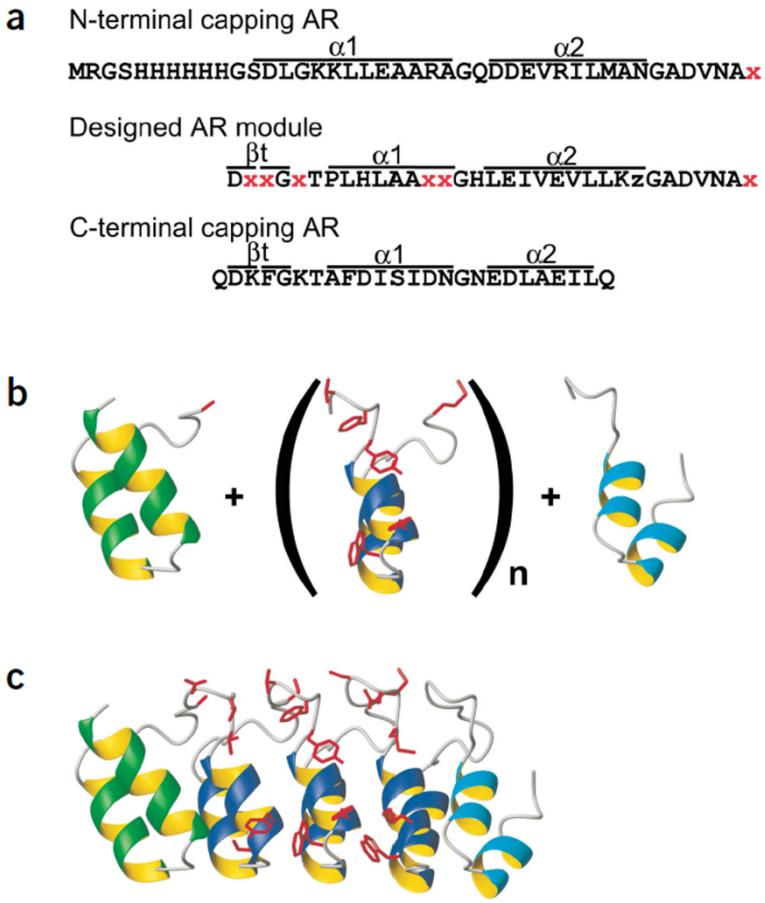

Figure 5-1. DARPin design and structure. (A) Consensus sequences of the N-cap, internal and C-cap modules. Randomized positions are highlighted in red letters (x, any aa except C, G or P; z, N, H or Y). (B) Schematic assembly of a DARPin from the individual modules. (C) Structure of off7, an MBP-binding DARPin. Figure taken from Binz *et al*., 2004.

5.1.2 DARPin libraries

DARPins are composed of randomized repeat modules, with a C-terminal and N-terminal capping repeat. The conventional DARPin libraries contain two and three internal repeats, called the N2C and N3C libraries. These libraries have been successfully used to select DARPin binders against a range of soluble proteins, for example MBP (Binz *et al.*, 2004). Conventional DARPin libraries are well-suitable for the binding of rather flat surfaces, but cannot protrude into target protein cavities. Recently, a DARPin library was engineered that carries a new internal repeat in which the β-turn was extended into a flexible loop by the introduction of 13 additional amino acids (J. Schilling, unpublished). The randomized positions in this extended loop allow binding of groves in the target protein surfaces, thus extending and broadening the application potential of DARPins (N3Cloop library). The loop library might be ideal for the binding of a GPCR surface, which display flexible loops and cavities within the GPCR helix bundle. Further engineering was applied to the capping N-terminal and C-terminal repeats (N-cap and C-cap), which display a hydrophilic surface to the solvent. Extensive optimization of the C-cap sequence resulted in improvement of protein stability (Interlandi *et al.*, 2008), by better packing of the capping repeat to the internal repeats (library N3Cnew). Furthermore, crystal structure analysis of DARPin-target complexes revealed that the N- and C-cap could potentially make contacts to the target. Selection of DARPin-binders to a given target might thus be artificially limited by the consensus design of the N- and C-cap, which excludes binders for which the consensus design of the N- and C-cap is not compatible with the target surface. In an improved DARPin library, certain positions in the N- and C-cap were randomized, adding a further degree of diversity to the DARPin libraries (design and synthesis: J. Schilling). The resulting libraries N3Cloopran and N3Cran were also used for selection. All individual libraries were used for panning against the target receptors, thus fully exploring the available DARPin library space for selection of DARPin binders. Table 5-1 gives an overview of the libraries used.

Table 5-1. DARPin libraries used in selections.

DARPin library	description
N2C	two randomized repeat modules, N- and C-cap module
N3C	three randomized repeat modules, N- and C-cap module
N3Cloop	as N3C; loop extension in middle repeat module
N3CloopRan	as N3Cloop; randomized N- and C-cap
N3Cnew	as N3C; new C-cap
N3Cran	as N3C; randomized N- and C-cap

5.1.3 Ribosome display – an *in vitro* selection system

Ribosome display (RD) is an *in vitro* selection system (Hanes and Plückthun, 1997) for the screening and selection of large and diverse libraries, and commonly used in directed evolution of proteins. The main advantage of RD is the absence of any *in vivo* step: *In vivo* selection methods such as phage display and *E. coli*-based selection systems require a transformation step, which constitutes the bottleneck of any *in vivo* approach and thus limits the library diversity to approximately 10^7-10^8 library members. In RD, diversity of the displayed library is instead limited by the number of ribosomes in the reaction and PCR amplification of the displayed library. In a typical RD selection, about 10^{14} active ribosomes are present (Plückthun, 2012).

The DARPin libraries are transcribed *in vitro* from a PCR product carrying a ribosome binding site (RBS) and a T7 promotor sequence (Figure 5-2 for illustration). The absence of a stop codon leads to the formation of ribosome-nascent-chain complexes (RNCs), in which the translated and folded DARPin stays linked to its genetic template in the form of mRNA that is stalled within the ribosome decoding center. An unfolded peptide sequence originating from the TolA protein acts as a spacer to allow the DARPin to extend out of the ribosome exit tunnel and to fold properly. The *in vitro* translated DARPins are then bound to the immobilized target protein, and unspecific binding is reduced by several washing steps. At this stage, the washing steps can be extended in subsequent selection rounds to increase specificity and affinity. The mRNA of specific binders is subsequently eluted by destabilization of the RNCs by high amounts of EDTA and excess of unspecific RNA (*Saccharomyces cerevisae* RNA, short scRNA) and reverse-transcribed into cDNA. The resulting DNA is ligated into pRDVLDnew (a derivative of pRDV, designed by J. Schilling, plasmid ID 2228). This ligation step is necessary to reappend an RBS and a promotor sequence to the ligated cDNA by PCR-amplification with primers binding outside of the ligated cDNA and within in the pRDVLDnew sequence. This step is necessary since the cDNA and the subsequent PCR amplification (PCRonRT) are generated with internal primers, in order to exclude biased reverse transcription and amplification due to partial terminal degradation of the mRNA. Hence, only the more central DARPin coding sequence is reverse transcribed. The PCR pool amplified from ligation into pRDVLDNew (PCR on ligation) can be directly used for subsequent selection rounds (Dreier and Plückthun, 2011; Hanes and Plückthun, 1997; Plückthun, 2012).

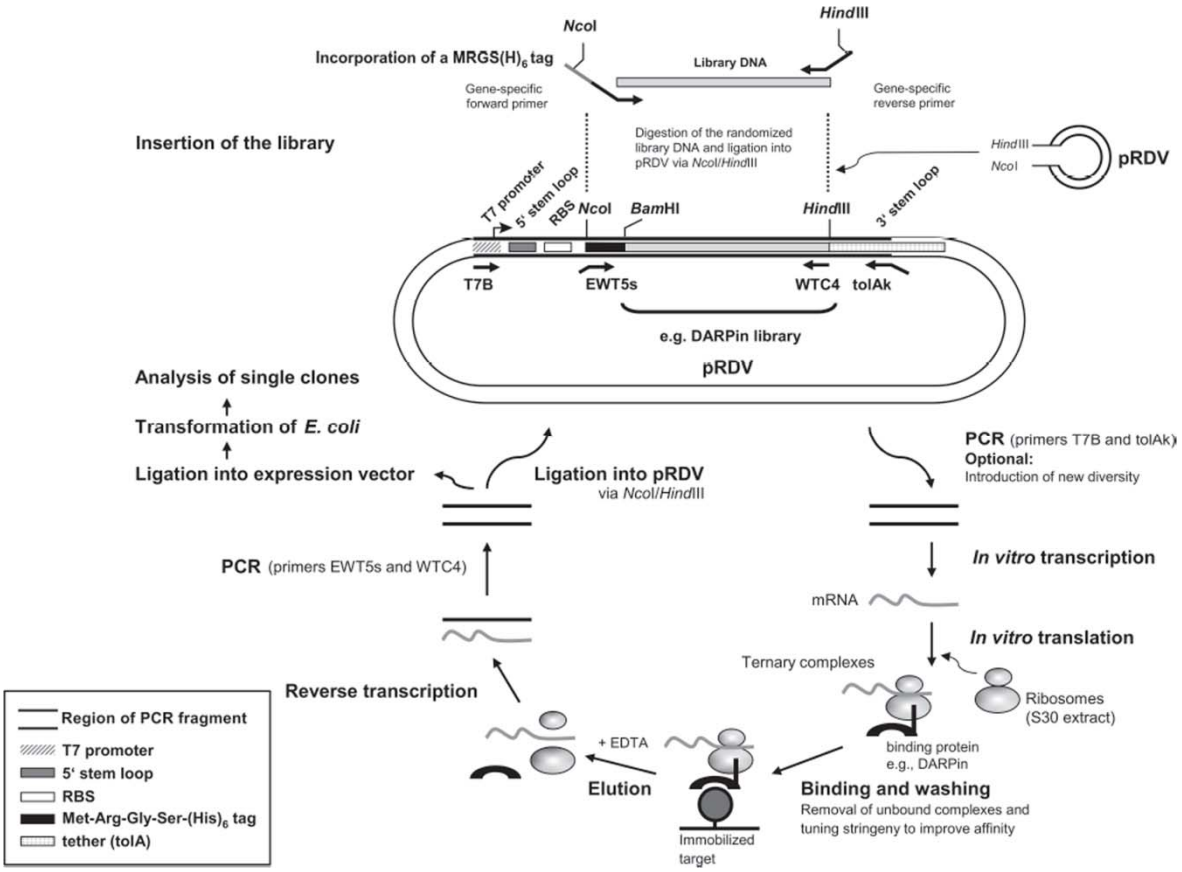

Figure 5-2. Scematic overview of the ribosome display process (taken from (Dreier and Plückthun, 2011)). All selection steps are performed *in vitro*. A selection round starts from the PCR product of a library (top) that is *in vitro* transcribed into mRNA and subsequently translated into protein. The nascent DARPin-polypeptide chain folds into its tertiary structure upon exit from the ribosomal exit tunnel, facilitated by an unstructured spacer that allows the DARPin to fully exit the ribosome. The DARPin remains covalently linked to its mRNA and translating ribosome due to the absence of any stop codon. The mRNA of DARPins that have bound to a target molecule is eluted by addition of EDTA and excess of unspecific scRNA. The eluted mRNA is reverse-transcribed into cDNA, and amplified by PCR. The enriched PCR pool is ligated into the vector pRDVLDnew. PCR-amplification of the library with outer primers annealing on pRDVLDnew allows to include again the ribosome binding site and the spacer sequence necessary for subsequent selection rounds.

5.1.4 GPCR target constructs

TM86V and L5X were chosen as targets for selection of DARPin binders. Immobilization of the targets during selection is preferably achieved via biotin-streptavidin or biotin-neutravidin, respectively. For this purpose, TM86V and L5X were fused with the AviTag (AviTag, (Cull and Schatz, 2000)). The AviTag is a 15 amino acid peptide (GLNDIFEAQKIEWHE), in which the central lysine is recognized and biotinylated by the *E. coli* BirA ligase (Chapman-Smith and Cronan, 1999; Schatz, 1993). *In vivo* biotinylation is highly advantageous over chemical *in vitro* biotinylation, since it is stoichiometric and directed.

The GPCR is expressed as a fusion protein with an N-terminal MBP and a C-terminal thioredoxin, separated in the standard expression construct by recognition sites for the tobacco etch virus protease (TEV) (Figure 5-3A).

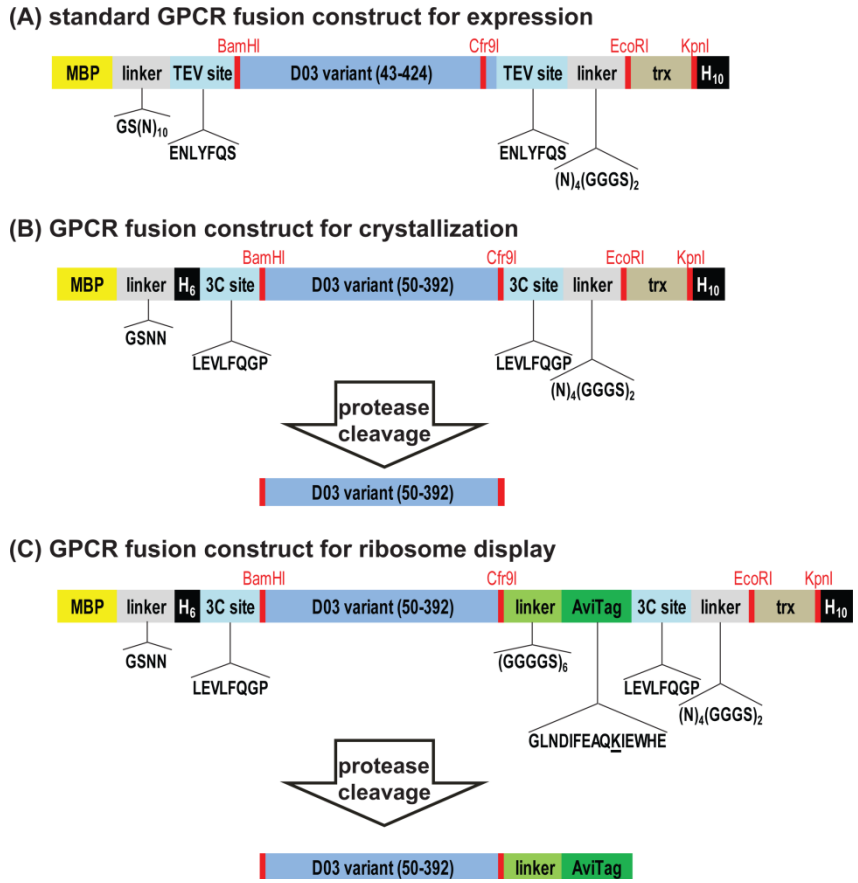

Figure 5-3. Overview of the GPCR constructs used in this study. (A) Standard fusion protein construct for expression with FACS-based selection. (B) Adapted construct for crystallization purposes. The flexible N-termini are shortened, and the 3C-cleavage sites allow optimal cleavage under purification conditions (pRG-TM86V-P51-dW392_3C, obtained from P. Egloff; termed pRG-xD_TM86V in this study). (C) Fusion protein construct for target immobilization in RD selections. An AviTag is C-terminally attached to the GPCR via an $(G_4S)_6$-linker. H_6/H_{10}, Histidine tag with 6/10 histidines.

To allow efficient cleavage under the applied purification conditions, the TEV-cleavage sites between the fusion tags and the GPCR were replaced by recognition sites for the 3C-protease (human rhinovirus 3C protease; LEVLFQGP), and the flexible termini of the receptors were shortened to allow efficient crystallization (termini optimized by P. Egloff, see Figure 5-3).

5.2 Results

5.2.1 Expression and purification of target proteins

Biotinylated TM86V (abbreviated b-TM86V, plasmid pRG-RD_TM86V, ID 3370, Appendix page 191) and b-L5X (plasmid pRG-RD_L5X, ID 3369, Appendix page 191) were expressed in *E. coli* BL21(DE3) in a 50 L-fermenter (Bioengineering) for 18 h at 28°C (see Section 5.4, Materials and Methods). 100 g wet cell pellet was used for one purification process. Briefly, cells were opened by sonification, receptor molecules were detergent-solubilized and captured by binding to the agonist neurotensin immobilized on Sepharose resin ("NT-column") as a fusion with protein D (pD, the bacteriophage λ head protein (Forrer and Jaussi, 1998)). The neurotensin peptide was connected to its fusion partner pD by a 3C-protease recognition site, allowing cleavage of the agonist-bound receptor from the resin together with the fusion protein tags MBP and thioredoxin (Figure 5-3). The agonist-bound receptor was separated from MBP by ion exchange chromatography (IEX), and subsequently purified via size exclusion chromatography (SEC) for separation of the remaining protein tags (Figure 5-4).

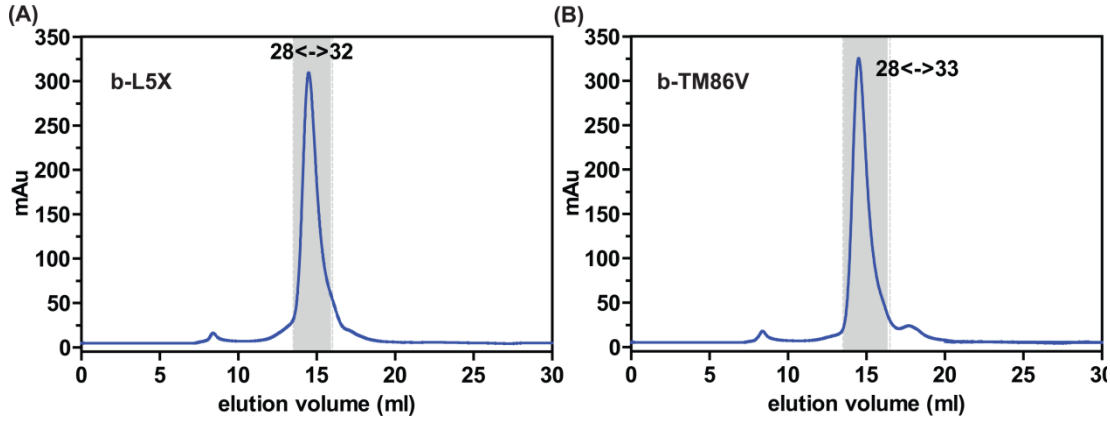

Figure 5-4. SEC-profiles of purified b-L5X (A) and b-TM86V (B). For the final purification step, the receptor preparation was loaded onto a preparative S200 (20 ml CV). Grey areas highlight the fractions that are pooled and used for ribosome display selections.

The individual purification steps of the receptor preparations were subsequently analyzed by SDS-PAGE (Figure 5-5). Both receptor variants were successfully separated from their fusion partners and the 3C protease. The two additional bands at low molecular weight resulted from cleavage of an intrinsic and unspecific 3C-recognition site in IL3 (P. Egloff, personal communication). The monodisperse behavior of the receptor preparation in SEC analysis suggests that the helix-helix interactions keep the receptor fragments connected and intact within a detergent micelle, while they fall apart under the denaturating conditions of an SDS-PAGE (Figure 5-5). For both receptor variants, 1 mg of purified receptor was obtained. Unbiotinylated receptor for competition ELISA experiments was expressed in the absence of BirA and was purified accordingly (plasmids pRG-xD_TM86V and pRG-xD_L5X, Appendix page 191).

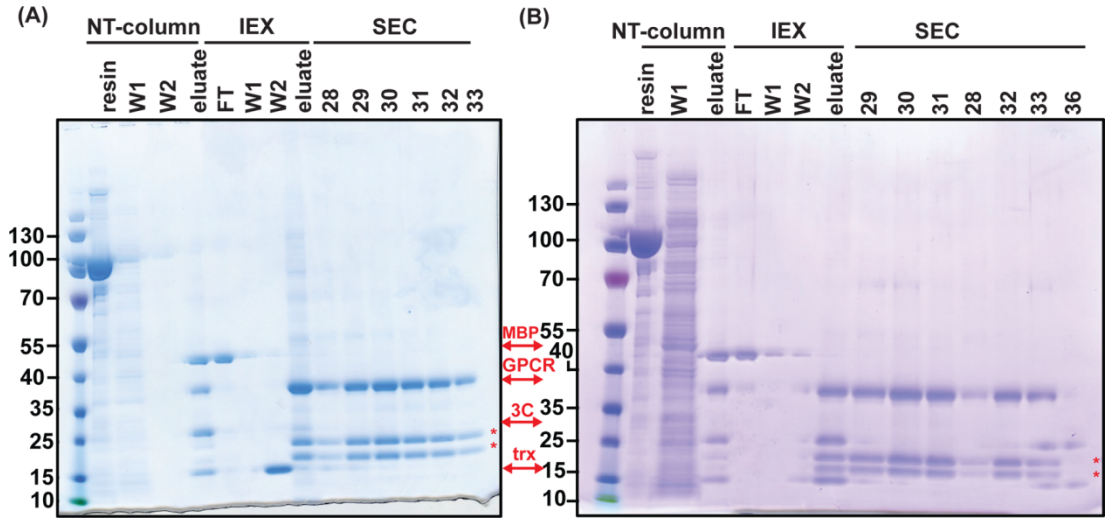

Figure 5-5. Analysis of the purification process of b-L5X (A) and b-TM86V (B) by SDS-PAGE. Resin: column material after sample loading; W1, W2: wash fractions; FT: flow-through fraction; 28-33: SEC fraction number. 20 µl (Resin, W1, W2, FT, eluate) or 5 µl (SEC fractions) were loaded on a gradient SDS-PAGE 4-15% (NuPAGE). Red arrows indicate the size of MBP, the GPCR, 3C protease (3C) and thioredoxin (trx).

For quantitative *in vivo* biotinylation, b-L5X was co-expressed with the *E. coli* biotin-ligase BirA (plasmid pBirAcm, plasmid ID 212). The expression product of b-L5X could be processed without difficulty, yielding purified and biotinylated receptor cleaved from its fusion protein tags. Notably, processing of b-TM86V from cells co-expressing b-TM86V and BirA failed during the 3C-protease cleavage step, because the fusion protein tags MBP and thioredoxin were not efficiently cleaved. When expressed in the absence of BirA, b-TM86V could be successfully cleaved and purified. The reasons for this observation are not clear, since TM86V and L5X differ only in a few shift mutations located within the transmembrane helices. Importantly, biotinylation efficiency was similar in both expression constructs at approximately 95% (Figure 5-6), showing that with the moderate expression level of GPCRs, compared to soluble and highly-expressed proteins such as DARPins, the intrinsic *E. coli* BirA ligase is sufficient for quantitative biotinylation. Biotinylation efficiency was quantified according to the approach from Petris and coworkers (Petris *et al.*, 2011), exploiting the fact that the biotin-streptavidin binding does not fall apart in SDS-PAGE. This method is most suitable for our needs, since it allows accurate quantification of low protein amounts, which is not the case for any commercially available biotin-quantification kit.

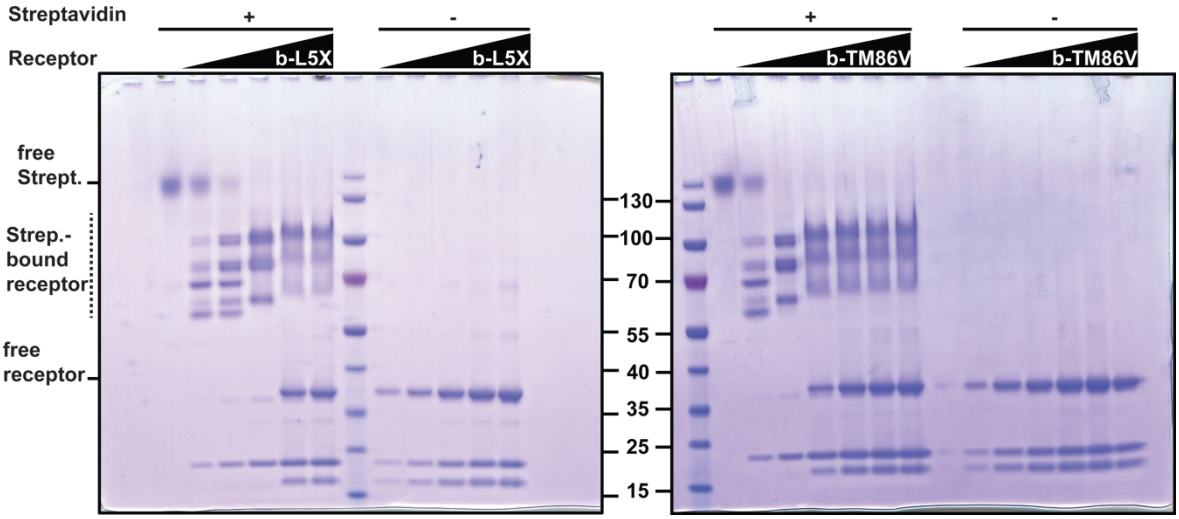

Figure 5-6. Quantification of biotinylation efficiency of b-L5X and b-TM86V. Increasing amounts of receptor were incubated with 1 µg Streptavidin in 1x SDS-loading buffer for 30 min at RT and resolved on a 4-15% NuPAGE (Invitrogen) SDS-PAGE. Free receptor is quantified with ImageJ software (http://rsbweb.nih.gov/ij/). Receptor is in excess over streptavidin at the higher titration points. The ratio of free receptor in the presence of Streptavidin and the total amount of receptor gives the fraction of biotinylated receptor (see section 5.4, Materials and Methods).

5.2.2 DARPin selections by ribosome display

As explained above, the purified receptor variants are embedded in a detergent micelle, with only the helix-connecting loops on the top (extracellular) and bottom (intracellular side) facing the solvent. The available surface for binding of DARPins is thus rather small, compared to soluble proteins. To explore all possibly binders, different DARPin libraries were used for selection experiments.

Conventional RD makes use of the detergent Tween-20 during the washing steps, in order to remove unspecifically bound DARPin binders. However, such harsh detergents are detrimental to membrane proteins, and the RD protocol thus had to be adapted for the work with GPCRs. First of all, we have tested two detergents that are commonly used with GPCRs, namely DM and OG, for their compatibility with ribosome display components. OG would be advantageous due to its small micellar size, which would present a larger solvent-accessible surface compared to DM. However, it is known that short-chain and harsh detergents such as OG can disturb *in vitro* selection systems (Spirin and Swartz, 2007). These detergents were thus tested with the established test system of MBP as target protein and off7 as the binding DARPin (Binz *et al.*, 2004). Under both detergent conditions, we could efficiently enrich the off7-specific mRNA in a selection performed in solution (Figure 5-7).

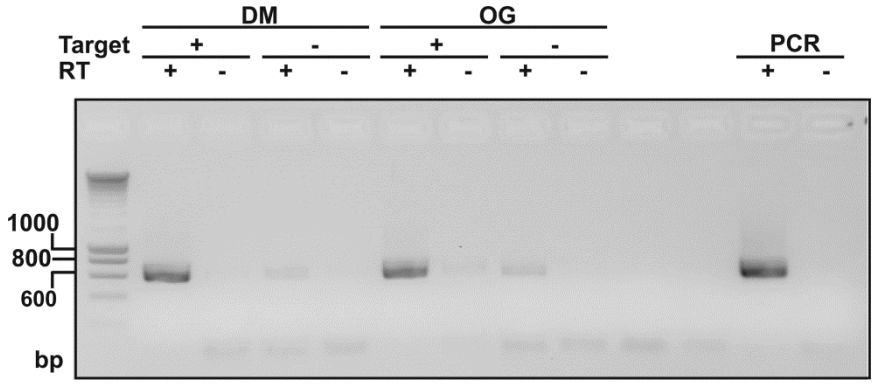

Figure 5-7. Analysis of detergent compatibility with ribosome display selections. MBP and its DARPin binder off7 were used to compare the enrichment of off7-mRNA in the presence of DM or OG. The output after PCR on RT (3 µl volume) is analyzed on a 1.5% agarose gel. RT +/-, reverse transcription in presence/absence of reverse transcriptase

Selection in solution was chosen for this test round, since subsequent selections were performed using the KingFisher Flex (KFF), an automated platform for the parallel in-solution selection of high sample numbers. DM was chosen as the standard detergent for our target selections, since the evolved receptor variants show very high stability in this detergent over a long time period (see published article, sections 4.1 and 4.2).

Six different DARPin libraries (Table 5-1) were used for selection of DARPin binders against the two target receptors by means of ribosome display. During subsequent selection rounds, the stringency of the washing steps was increased stepwise to favor selection of specific binders with high affinity. The washing conditions turned out to be highly crucial for efficient enrichment and recovery of binders when selecting against membrane protein targets, and the washing stringency was lower than for soluble proteins. In the fourth and final selection round, a total washing time of 68 minutes was used (Table 5-2).

Table 5-2. Washing stringency during individual RD selection rounds.

		RD selection round			
		1	2	3	4
wash step (min)	1	-	1	2	2
	2	-	5	5	5
	3	-	5	8	10
	4	-	5	8	10
	5	-	1	5	15
Σ wash time		20	38	48	62

* the total wash time is the sum of the actual duration plus the transfer times between individual steps.

The conventional libraries N2C and N3C showed no enrichment after two iterative selection rounds and were thus excluded from further experiments. Libraries N3Cloop and N3Cloopran were evolved for four rounds, and libraries N3Cnew and N3Cloop for three rounds. After the first selection round, the band intensity was similar for the target and no-target selection (Figure 5-8). During later selection rounds, a continuous enrichment of a

specific DARPin band was observed for the target-selections (Figure 5-9). The theoretical and expected band sizes are given in Table 5-3 (primer pair T7B and TolAk for PCR on ligation; primer pair JSCRDif4 and JSCRDir2 for PCR on RT).

Table 5-3. PCR product sizes for the different DARPin libraries.

DARPin library	primer pair	
	T7B / TolAk	JSCDif4 / JSCDir2
N2C	839	517
N3C	938	616
N3Cloop	980	654
N3CloopRan	980	654
N3Cnew	938	616
N3Cran	938	616

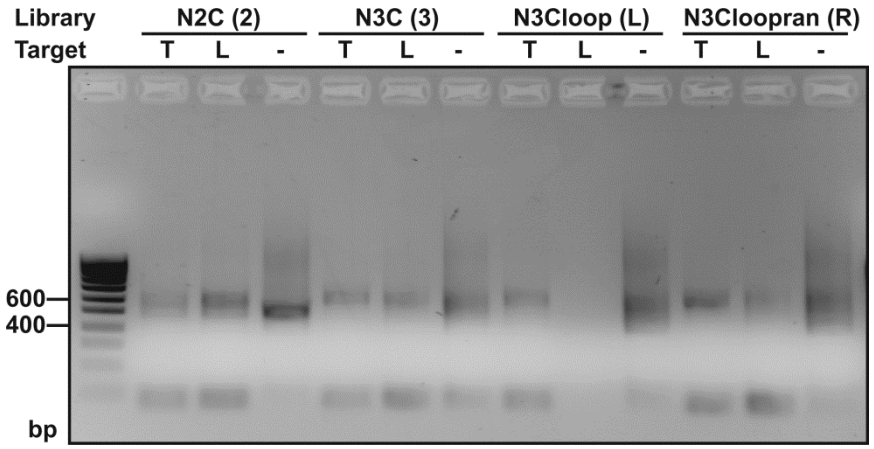

Figure 5-8. Analysis of RD selection round 1. Enrichment of DARPin binders analyzed after PCR on RT (3 µl PCR, 1.5% agarose gel). Specific band sizes are given in Table 5-3. Target T, TM86V; target L, L5X.

However, in the final selection round, a PCR product corresponding to the size of an N2C library was strongly enriched (Figure 5-9C), and this result was confirmed in an independent duplicate. The size of the input library is that of an N3C library, showing that the observed enrichment is truly the result of the final selection round (Figure 5-10).

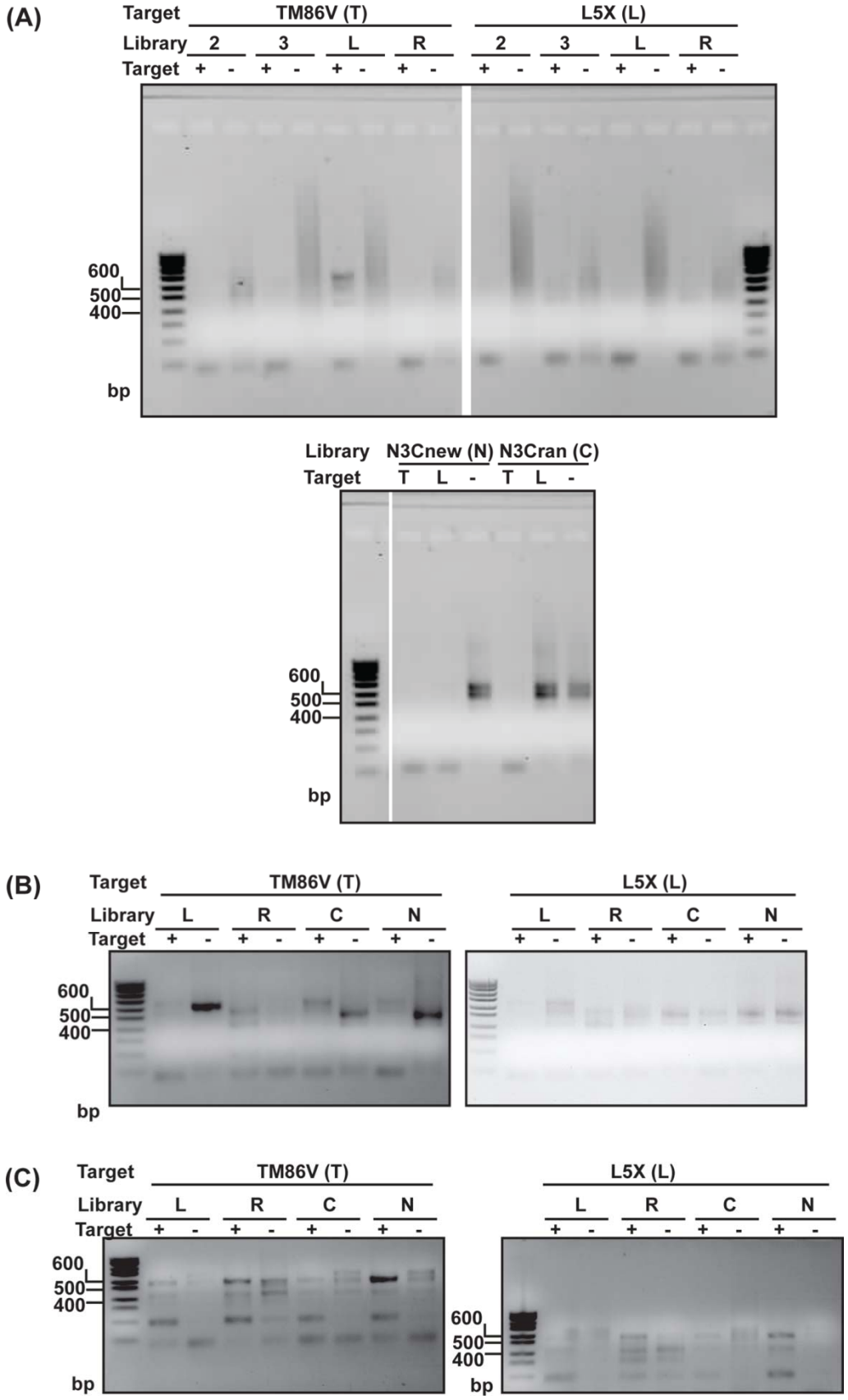

Figure 5-9. Analysis of RD selection rounds 2 (A), 3 (B) and 4 (C). Enrichment of DARPin binders analyzed after PCR on RT (3 µl PCR, 1.5% agarose gel). Specific band sizes are given in Table 5-3. Target +/-, selection in presence/absence of target; 2, N2C library; 3, N3C library; L, N3Cloop library; R, N3CloopRan library; N, N3Cnew library; C, N3Cran library.

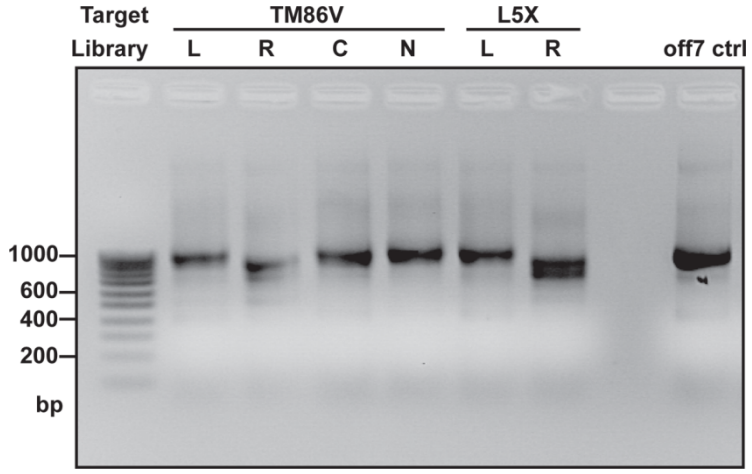

Figure 5-10. Quality analysis of the input DARPin library before RD selection round 4. The PCR products used for *in vitro* transcription are about 1000 bp, in agreement with the correct fragment sizes of 980 bp (N3Cloop libraries; compare the PCR product of off7, an N3C) and 938 bp (conventional N3C libraries), respectively. Only the selections with N3CloopRan library (R) shows a shift towards smaller fragments. L, N3Cloop library; R, N3CloopRan library; N, N3Cnew library; C, N3Cran library.

Additives (5% DMSO or 240 mM urea) to the PCR on RT did not improve amplification of the specific library fragment, but substantially decreased the PCR output below a detectable limit (Figure 5-11).

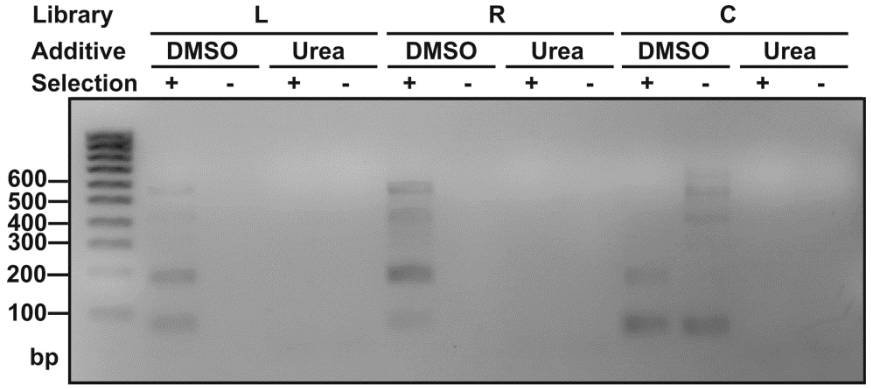

Figure 5-11. Influence of additives on the PCRonRT reaction after RD selection round 4. Addition of 240 mM urea (3% of 8 M stock solution) was tested in comparison to 5% DMSO (standard reaction condition) with respect to specific amplification of the DARPin library. In the presence of urea, the PCR reaction did not give specific product.

It thus appears that under the current conditions, no further improvement of the selection is possible. The output of the last selection round was nevertheless subcloned into the expression vector pDST67 for screening of DARPin binders by ELISA.

5.2.3 Screening of the final evolved pools for DARPin binders

The final selected pools were subcloned into the expression plasmid pDST67 (plasmid ID 827), and individual DARPin clones were expressed in the *E. coli* XL1blue strain fur subsequent screening by crude-extract ELISA (ceELISA). Depending on the enrichment of the selected pool, between 50 and 200 individual clones were screened for each library selection, with a total of 900 screened clones. MBP and its DARPin binder off7 were used as control.

From the 900 screened DARPin clones, 48 DARPins showed a signal-to-noise ratio in crude-extract ELISA above 6, while the signal-to-noise ratio of off7-MBP was above 6 (Figure 5-12). The remaining >90% of clones were characterized by high unspecific binding in the absence of target. These DARPins likely bind to empty detergent micelles, thus explaining the high crude-extract ELISA signal both in the presence and absence of receptor.

The 48 DARPins with the highest signal-to-noise ratio were further characterized by SDS-PAGE and sequence analysis, showing that many of these clones are truncated DARPins, with an early frameshift or stop codon within the N-cap or first internal repeat module. The fact that such truncated DARPin sequences give some of the strongest signals observed in this screening is very unusual and indicative of highly unspecific binding. Since the His_6-tag used for ELISA detection is N-terminal to the DARPin sequence, it is correctly translated and an ELISA signal can be detected if these clones bind unspecifically to detergent micelles.

As explained within the next paragraph, the remaining 12 clones represent only 5 unique sequences, and are furthermore characterized by deletion of one internal repeat. These binders, indicated by name in Figure 5-12C, are not the clones giving the highest ELISA signal, but are the only intact DARPin sequences that are of correct size in SDS-PAGE analysis (see Section 5.2.5).

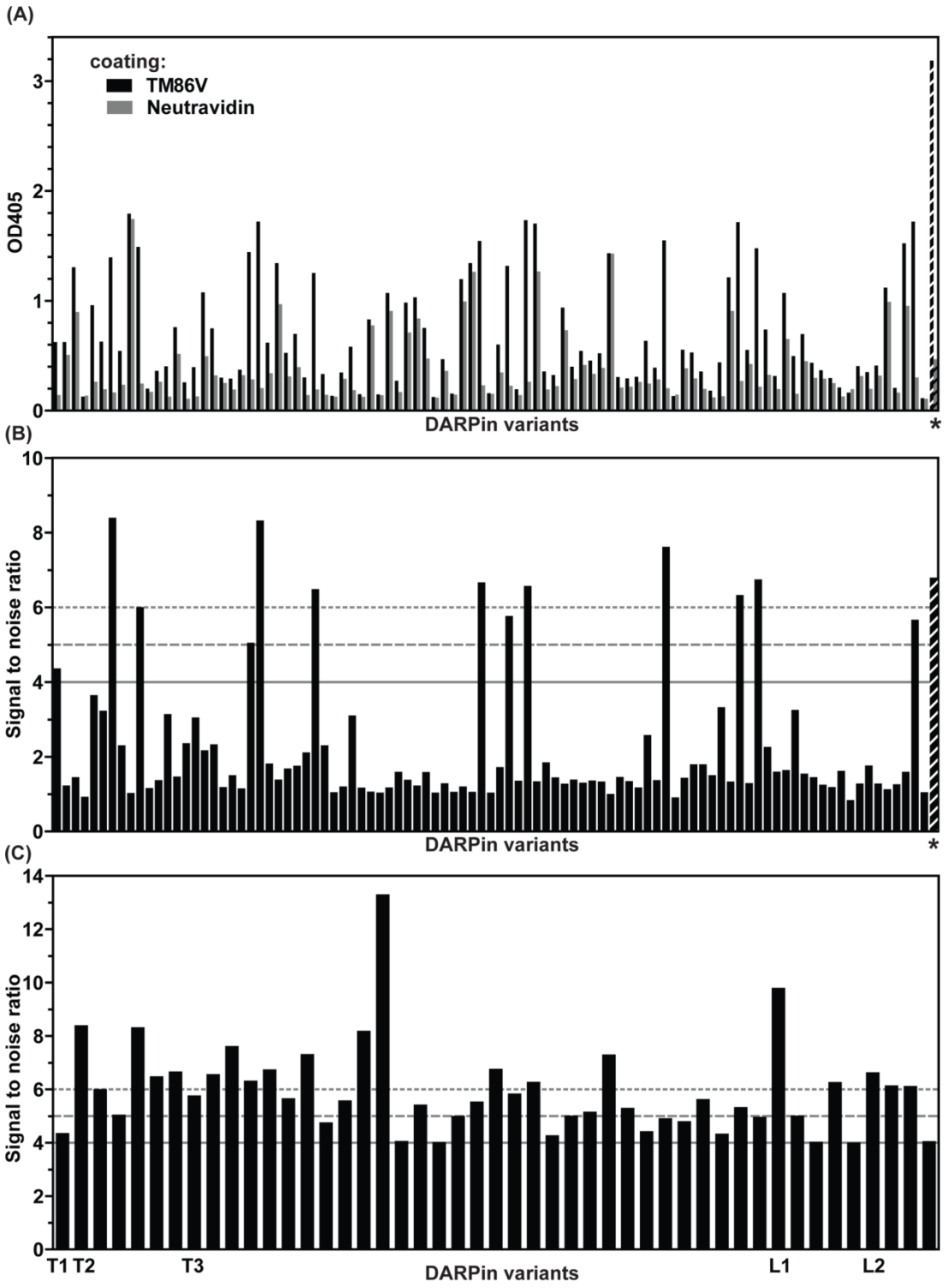

Figure 5-12. Overview of the screening of the final evolved DARPin library pools. (A) Representative raw data of a 96-well crude-extract ELISA screen for binders to b-TM86V. In total, 900 clones were analyzed, covering both selections against b-TM86V and b-L5X. Black bars, immobilization of b-TM86V via neutravidin; grey bars, neutravidin-coating only; *, MBP-off7 control. (B) Signal-to-noise ratio of the screened DARPins, calculated and replotted from (A). The signal-to-noise ratio is the ratio of the ELISA signal of DARPin binding to immobilized b-TM86V (black bars in (A)) to the ELISA signal of DARPin binding to neutravidin (grey bars in (A)). *, MBP-off7 control. (C) Signal-to-noise ratio of the 48 strongest binders among the 900 screened DARPin clones. The five binders that were further characterized are labeled by their name.

5.2.4 Sequence analysis

The strongest 40 DARPin clones were sequenced and their amino acid sequences in the variable library position were studied. From the 40 clones, only 12 showed a correct DARPin sequence (Figure 5-13).

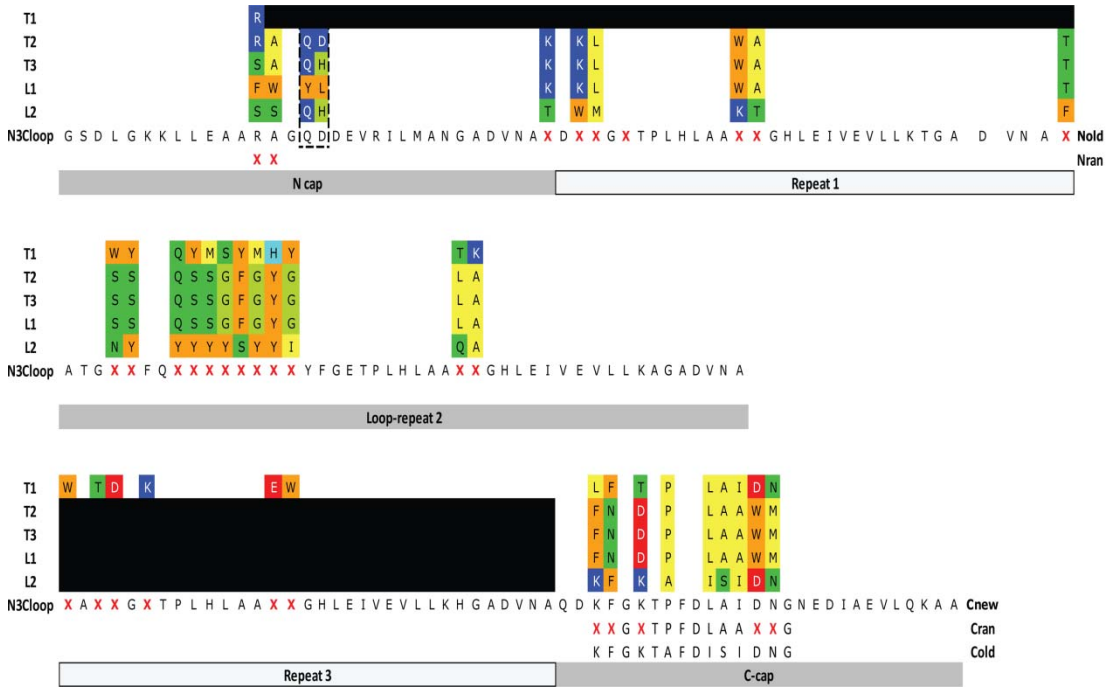

Figure 5-13. Sequences of the five DARPin binders. T1, T2 and T3 are identified to bind against TM86V, and L1 and L2 against L5X. The sequence of the N3Cloop library is given as reference. White areas indicate identity to the N3Cloop consensus. Individual mutations are colored with respect to their amino acid type. Deletions are highlighted in black.

All other sequences correspond to truncated DARPin sequences that, as a result of frameshifts in the sequence, did not extend beyond the N-terminal His_6-tag or the N-cap. The His_6-tag is used for ELISA detection, and can thus explain the signal for the truncated clones. However, it is not entirely clear why these clones have such a high signal-to-noise ratio. In case these are false-positive clones, the fraction of false-positives would be 75%. Such a high error rate is indicative of a non-robust selection.

Interestingly, the 12 remaining sequences revealed only 5 unique DARPin binders, with a dominant binder T2 that is retrieved seven times and a second binder that appears twice (T3, Table 5-4). All five binders are N2C-derived, with either an internal repeat module (T2, T3, L1, L2) or the N-cap (T1) deleted (Figure 5-13). The three binders T2, T3 and L1 have very similar sequences, and differ only in a few positions. Interestingly, all binders contain a loop sequence, and either a randomized or a new C-cap. The loop sequence is mostly hydrophobic, while basic amino acids are dominant in the randomized positions (Figure 5-13). These motifs are unusual, in comparison to selections on most soluble targets, where these properties are not selected, and might thus reflect a specific

property of DARPin binders to membrane proteins, or a technical issue within the selection (personal communication, J. Schilling).

Table 5-4. Characteristic values of the five identified DARPin binders.

			theoretical values				purified protein		
							yield	concentration	
DARPin	C-cap	# of sequences	aa	MW (kDa)	pI	ε	mg/L	mg/ ml	μM
T1	Cran/Cnew		133	14.7	5.89	23950	11.5	2.84	193
T2	Cran	12x	153	16.2	5.59	13980	8	1.96	121
T3	Cran	2x	153	16.1	5.68	13980	9.5	2.28	142
L1	Cran		153	16.3	5.58	20970	3	0.7	43
L2	Cold		153	16.7	5.82	17420	1.5	0.37	22

5.2.5 Analysis of DARPin binders by ELISA

The five DARPin binders T1, T2, T3, L1 and L2 were expressed in a 1 L- scale and purified via IMAC (Figure 5-14).

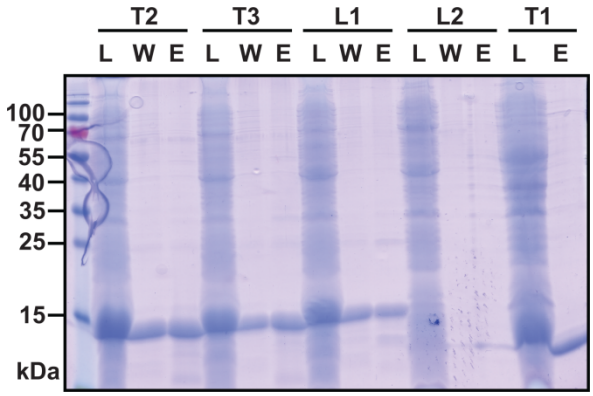

Figure 5-14. SDS-PAGE analysis of DARPin purification by IMAC. L= lysate, W= wash fraction, E= elution. L2 expresses at a low level compared to the other DARPins.

The purified protein was used for binding analysis to both targets b-TM86V and b-L5X by ELISA. Independent of the target that they were selected on, all five selected DARPins recognize both TM86V and L5X (Figure 5-15A). Hence, L5X and TM86V must display rather similar interaction surfaces. Different concentrations of DARPins were analyzed, and showed that for some binders, an equimolar ratio of target and DARPin (each 15 nM) is sufficient to obtain the full signal, indicating an affinity in the low nanomolar range. Apart from potential differences in DARPin-binding affinity, L2 gives the smallest ELISA signal which is close to background binding to neutravidin only (Figure 5-15A). L2 showed a very low purification yield, and the low ELISA signal might suffer from inaccurate determination of protein concentration.

Furthermore, we observe that the specific ELISA signal for binder T3 is stronger at lower DARPin concentrations. This can be an irrelevant observation, or could potentially point towards an inhomogeneous DARPin population, for which aggregation behavior is concentration-dependent. To further characterize the DARPin binders and narrow down the range of binding affinity, a competition ELISA was performed. In this setup, the binding of 15 nM DARPin to 15 nM biotinylated and immobilized target receptor was competed with 500 nM unbiotinylated and free receptor. However, the specific binding signal could not be competed with excess of free receptor, or only partially in the case of T2 (Figure 5-15B). This result is surprising regarding the specific DARPin binding observed under standard ELISA conditions, where the DARPins T1-T3 and L1-L2 do not bind empty micelles (Figure 5-15A). A possible explanation for this observation is that the DARPins bind to the interface of GPCR and detergent micelle, where the interactions with detergent micelles are strongly hydrophobic and dominant, and hence can not be competed.

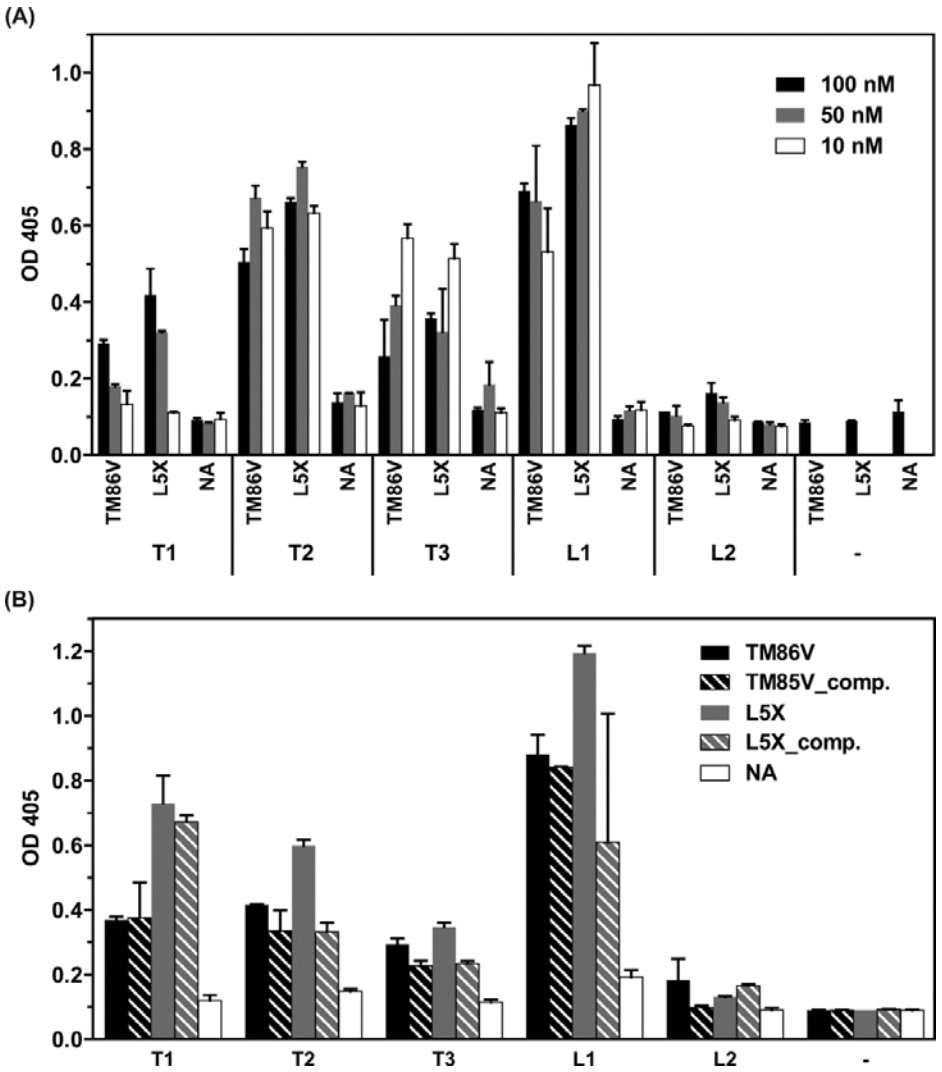

Figure 5-15. Analysis of DARPin-GPCR binding by ELISA. (A) Binding of purified DARPin (100 nM, black bars; 50 nM, grey bars; 10 nM, white bars) to 15 nM immobilized TM86V or L5X. Various DARPin-concentrations were tested. (B) Binding of 15 nM DARPin to 15 nM immobilized target in the presence of 500 nM non-biotinylated free target. Binding is poorly competed by soluble GPCR.

5.2.6 SEC analysis of DARPin binders

The DARPins were analyzed for their behavior in an analytical size exclusion chromatography with a separation of up to 200 kDa (SEC200).

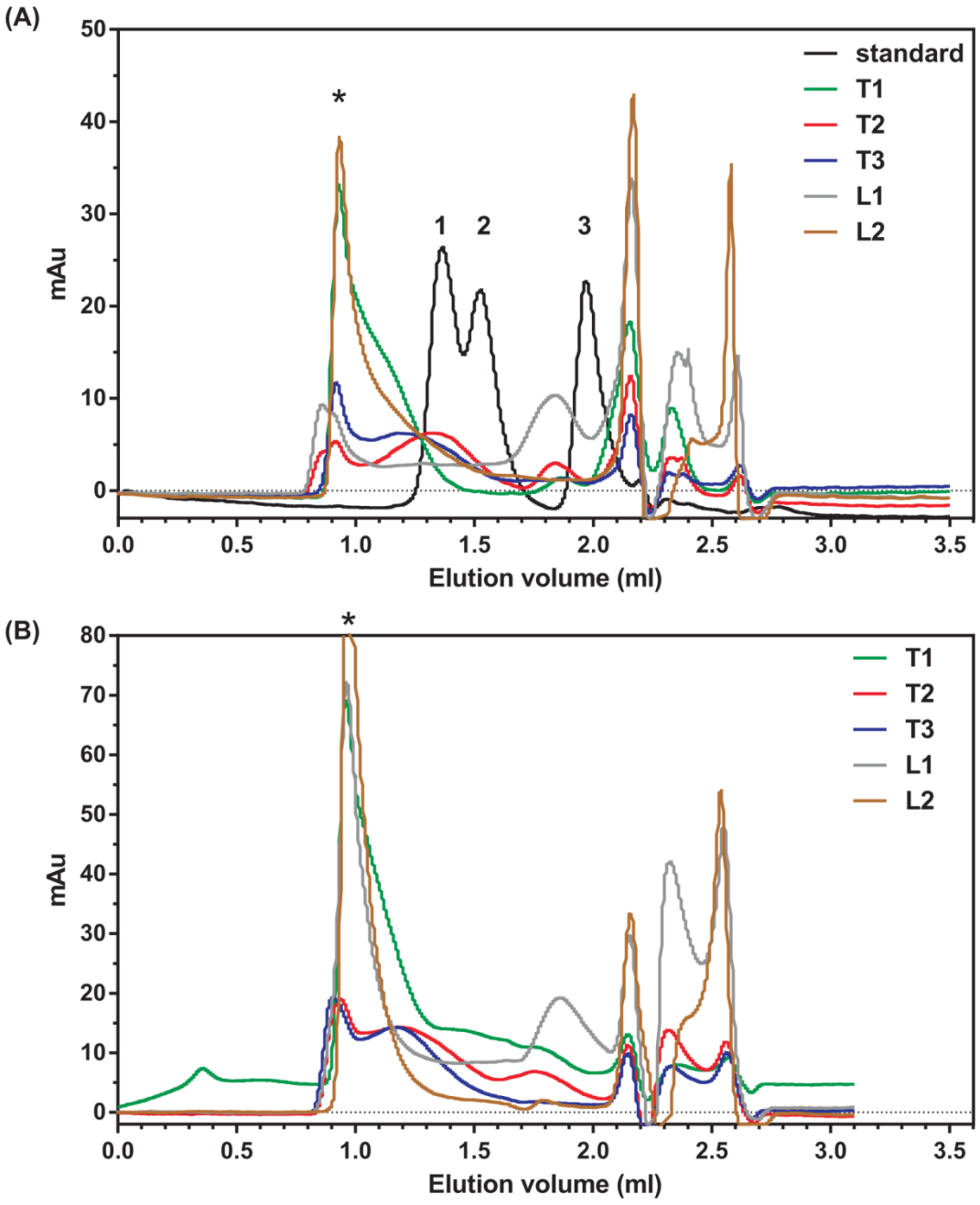

Figure 5-16. SEC200 analysis of the five selected DARPins T1, T2, T3, L1 and L2 in the absence of detergent (A) and presence of detergent (B). (A) 10 µM DARPin was analyzed on an analytical SEC200 (CV 2.4 ml) in 10 mM Tris·HCl pH 7.4 and 150 mM NaCl. (B) 20 µM DARPin was analyzed on an analytical SEC200 (CV 2.4 ml) in PBS/ 0.2% DM. (A) and (B) *, void peak; 1, standard peak β-amylase 200 kDa; 2, standard peak albumin 66 kDa; 3, standard peak cytochrome c, 12.4 kDa

Two different experimental conditions were used to assess the influence of detergent on protein behavior. In this study, DARPins were generated against membrane proteins in the presence of detergent, but the DARPins should be soluble and well-behaved also in the absence of detergent. In a buffer of 10 mM Tris pH 7.5 and 150 mM NaCl, all five DARPins showed multiple peaks up to the void volume (Figure 5-16). The actual DARPin would be expected at an elution volume of 1.8 to 2 ml. The small fraction of DARPin observed at this elution volume shows that most protein is oligomeric or aggregated. A similar result was obtained in the presence of detergent, here 0.2% DM, which was used throughout all selections. It thus appears that the protein properties of the selected DARPins are too poor for further studies.

5.3 Summary and discussion

Selections of DARPin binders against membrane proteins have been successfully performed for different proteins, such as the sodium symporter CitS (Huber *et al.*, 2007) or the membrane transporter AcrB (Monroe *et al.*, 2011). The latter protein has very large extracellular domains and thus behaves more like a soluble protein in selection experiments. The actual target proteins are well-behaved in their wild-type state and display high detergent stability that allowed crystal formation (Monroe *et al.*, 2011).

Here, we have performed selections with the receptor variants b-TM86V and b-L5X, which have been previously evolved for high detergent-stability. Specific DARPin binders to these evolved variants could facilitate structure determination of the receptor by cocrystallization approaches, and, depending of their mode of binding and action, might be of interest for functional studies such as activation or inhibition.

The specific enrichment of DARPin binders throughout selection was weak for the first two rounds and stronger in subsequent rounds. However, these selections were highly susceptible to changes in the washing stringency, and too strong washing steps abolished any enrichment. Individual selection rounds had to be repeated in order to optimize the washing stringency, and relatively short washing steps had to be used for selections against TM86V and L5X. Low washing stringencies do not necessarily indicate problematic selections, but rather result in binders with low affinity or in reduced discrimination between specific and unspecific binders. However, in this study, we could not identify specific DARPin binders. About 90% of all screened DARPin clones were characterized by high, but unspecific binding – defined as crossreactivity with neutravidin in the absence of GPCR – which is likely a result of binding to empty detergent micelles. The fact that so many false positives are observed is very unusual. Moreover, the five N2C-binders exhibit poor biophysical behavior, and display a non-competable ELISA signal. Repetition of selection round 4 produced a very similar result, with no better behaved DARPins among 1000 additional clones. Since enrichment of N2C vs. the original N3C library only occurred in the fourth round of selection (Figure 5-10), further 400 clones of the enriched pool after the third selection round were screened, also without success. While many positive signals were observed in the crude-extract ELISA, only five clones could be confirmed as a full-length N2C DARPins.

Taken together, selections against GPCRs might be hampered by presentation of the target protein in a detergent micelle, restricting the surface that is accessible for DARPin binding, as well as by the low degree of structure in the target protein region that is solvent-accessible. GPCRs that are embedded within a detergent micelle display their extra- and intracellular surface towards the solvent. These interfaces are mainly formed by helix-connecting loops, creating a conformationally flexible surface, which might not be suitable for DARPin binding. It is interesting to note that the five DARPin binders that were identified are all derived from the loop-DARPin library. The loop-DARPins were especially designed for binding of target-specific grooves. Even though the selected DARPins display poor biophysical properties, the loop sequence might nevertheless be crucial to allow binding to these targets at all. Most loop sequences are not only identical in their sequence, but are furthermore very hydrophobic, with high prevalence of tyrosine. Binding of the DARPin loop sequence between the interface of receptor and detergent would be a potential hypothesis to explain the observed results. Such binding would be mainly specific to the binding milieu, and hydrophobic binding to the detergent could explain the specific, but non-competitive binding, since such an interface would not be present in an empty detergent micelle.

Selection of DARPin binders to most soluble proteins by RD can be considered a very robust technique, and DARPins are versatile enough to generate binders that unambiguously distinguish the phosphorylation status of a target protein (Kummer *et al.*, 2012). Specific binders with high affinity to small soluble proteins such as the Bcl2-family have been successfully obtained within in a single selection round (J. Schilling, personal communication).

Hence, the failure to select DARPin binders to TM86V and L5X is likely attributed to the poor biophysical properties of the targets. Possible future approaches could be selections against GPCR fragments, such as loop fragments. Furthermore, purified receptors could be embedded into nanodisc particles (Leitz *et al.*, 2006). Nanodiscs are island-like particles composed of lipids, kept in a disc by the α-helical MSP protein surrounding the disc like a belt (Bayburt and Sligar, 2010). Nanodiscs better mimic the natural lipid bilayer than detergent micelles, and especially the protein-lipid interface would be more native-like. If binding between the detergent micelle and the protein is really the reason for the obtained results, selection against the target receptor embedded in nanodiscs could potentially resolve the issue.

Future selections could further address optimization of selection conditions. Possible “access points” would be the optimal ratio of streptavidin-binding sites to biotinylated target receptor and the washing stringency during the selection rounds. The presence of a detergent micelle largely increases the size of the target protein, and in case of target saturation, the detergent-micelles of immobilized target receptors could result in a continuous detergent layer that shields the G-protein interacting surface of the receptor from the actual selection (the biotinylated AviTag is located on the receptor C-terminus). To avoid this, the ratio of binding sites to target molecules should be increased, in order to separate individual receptor-containing micelles from each other. Along the same line, immobilization of the receptor via the N-terminus would preferentially present the G-protein interaction surface to the solvent, which might facilitate selection of DARPin binders to this interface. The washing stringency was carefully adjusted for each selection

round, but by performing selection on the King Fisher Flex (KFF), the duration of each washing step is necessarily longer than in manual selections: The King Fisher Flex is a platform that provides automated transfer of beads in a 24- or 96-well format and is routinely used for high numbers of parallel selections, where identical treatment of all samples is essential. However, individual steps such as bead collection via magnetic tips and transfer between individual plates are relatively slow, hence defining a minimum washing time of ~20 min. It cannot be excluded that this washing stringency was too harsh, and eliminated potential binders. To account for that, a manual selection of the naïve library would be recommendable, since it allows the washing stringency to be freely defined down to the second/minute time scale.

However, it is not clear from the above results whether such approaches are promising, or whether more profound target protein issues are encountered that cannot be easily alleviated. The receptor variants TM86V and L5X display the highest detergent stability reported for GPCRs so far, and L5X is furthermore preferentially stabilized in the agonist-bound state (Schlinkmann *et al.*, 2012 , chapter 4 of this work). If these receptors variants are not suitable for DARPin selections, it is quite likely that no rNTR1 variant will be.

5.4 Materials and Methods

5.4.1 Expression of pD-NT1 fusion protein

The plasmid pAT223-3C-NT1 (obtained from P. Egloff, Appendix page 190), encoding the fusion of the neurotensin peptide 8-13 and pD (phage λ head protein gpD, (Forrer and Jaussi, 1998)) connected by a linker and a 3C recognition site (termed pD-NT1), was transformed into *E. coli* BL21(DE3). A single colony was used to inoculate an overnight preculture (200 ml 2YT medium, 1% glucose, 100 μg/ml ampicillin). Five 1 L – expression cultures (2YT, 0.2% glucose, 100 μg/ml ampicillin in 5 L Erlenmeyer flask with baffles) were inoculated to OD_{600} = 0.1 and grown at 37°C to OD_{600} = 0.8 in a shaking incubator. Protein expression was induced by addition of 250 μM IPTG and continued for 5 h at 37°C. Cells were harvested by centrifugation, and the cell pellet stored at -80°C.

5.4.2 Purification of pD-NT1 fusion protein by IMAC

Cells (40 g wet cell weight) were homogenized in 100 ml buffer RB (50 mM HEPES pH 8, 500 mM NaCl, 25 mM imidazole, Complete Protease Inhibitor (Roche)). Cells were lysed by sonification (aliquots of 40 ml, 10x 30 s at duty cycle 6, output 50%; Branson sonifier 250) in the presence of 5 μg/ml DNase I (Roche), 5 mM $MgCl_2$ and 50 μg/ml lysozyme (Sigma-Aldrich). The soluble fraction was separated from cell debris by centrifugation at 11,000 g for 30 min, and applied by gravity flow to 12 ml Ni-NTA resin (Qiagen) equilibrated in buffer EQ (25 mM HEPES pH 8, 500 mM NaCl, 25 mM imidazole)

for immobilization of the His_6-tagged pD-NT1. The resin was washed with 10 CV of buffer EQ and 10 CV of buffer WB (0.2 M $NaHCO_3$ pH 8.3, 500 mM NaCl, 5 mM imidazole). The immobilized protein was subsequently eluted with 12 ml buffer EL (0.2 M $NaHCO_3$ pH 8.3, 500 mM NaCl, 300 mM imidazole). The eluate was concentrated to 15 mg/ml (if necessary) in an Amicon® Ultra 10,000 MWCO (Millipore) and dialyzed 3× against 1 L coupling buffer (0.2 M $NaHCO_3$, 500 mM NaCl). The purified and dialyzed protein fraction was stored at -80°C until further use.

5.4.3 Coupling of pD-NT1 to NHS-activated sepharose

The purified pD-NT1 fusion protein was covalently coupled to NHS-activated sepharose 4 Fast Flow (GE Healthcare 17-0906-01) for subsequent capturing of active rNTR1-variants by binding to the presented neurotensin peptide. 25 ml NHS resin was equally distributed into five empty PD10 columns (GE Healthcare), drained from the storage solution and washed by 60 ml ice-cold 1 mM HCl (given volumes apply per column). For the coupling reaction, 2.5 ml of 13 mg/ml pD-NT1 was added per column, and allowed to react for 2 h at room temperature (RT) under constant mixing. Remaining unreacted protein solution was drained, and the reaction was stopped by addition of 10 ml 0.1 M Tris·HCl pH 8.5 and incubation for 2 h at RT under constant mixing. The resin was subsequently washed by 12 ml each of 0.1 M NaOAc pH 4.5, 0.5 M NaCl and 0.1 M Tris·HCl pH 8.5. Subsequently, each column wash washed with 24 ml of 8 M GdmCl, H_2O and 20% ethanol, respectively. The resulting pD-NT1-resin was stored in a 1:1 dilution with 20% ethanol at 4°C.

5.4.4 Cloning of AviTag- receptor variants

The constructs pRG-RD_L5X and pRG-RD_L5X were generated for *in vivo* biotinylation in *E. coli* via the AviTag (GLNDIFEAQKIEWHE) in which the lysine is recognized by the *E. coli* biotin ligase (BirA). Starting from pRG-TM86V_P51-dW392_3C (obtained from P. Egloff), the 2724-bp fragment including the fusion protein sequence from MBP to thioredoxin plus the C-terminal His_{10}-tag and two stop codons was obtained by restriction digest with *Xba*I (see Figure 5-3B for illustration of the fusion protein sequence), and subcloned into pRGD03, for which the backbone *Eco*RI site was previously removed. The resulting construct pRG-xD_TM86V was used for expression of unbiotinylated receptor (Appendix page 191). Plasmid pRG-xD_L5X was obtained by replacing the TM86V-coding fragment of pRG-RD_TM86V with that of L5X via *Bam*HI/*Cfr*9I. pRG-RD_TM86V (plasmid ID 3370) was subsequently obtained by replacing the *Cfr*9I/*Eco*RI fragment covering the 3C-recognition site (LEVLFQGP) and the $N_4(G_3S)_2$-linker with the synthetically assembled $(G_4S)_6$-AviTag-3C_site-$N_4(G_3S)_2$ sequence (see Figure 5-3 for illustration of the fusion protein sequence, and Appendix page 191). pRG-RD_L5X (plasmid ID 3369) is obtained by replacing the TM86V-coding fragment with that of L5X via *Bam*HI/*Cfr*9I.

5.4.5 Expression of TM86V and L5X

rNTR1-receptor variants were expressed in large scale in a 50 L fermenter (Bioengineering). For *in vivo* biotinylation of L5X (b-L5X), pRG-RD_L5X was co-transformed with the plasmid pBirAcm (plasmid ID 212), encoding the *E. coli* biotin ligase BirA under control of the lac- promotor, into the *E. coli* strain BL21(DE3). For b-TM86V, overexpression of the BirA ligase interfered with 3C-cleavage of the fusion tags, and biotinylated TM86V was hence expressed in the absence of pBirAcm in BL21(DE3). Unbiotinylated receptor was expressed from the plasmids pRG-xD_L5X and pRG-xD_TM86V, respectively. A 50 ml pre-preculture (2YT medium, 1% glucose, 100 μg/ml ampicillin, 10 μg/ml chloramphenicol in the presence of pBirAcm) was inoculated with a single colony and grown overnight at 37°C in a shaking incubator. In the morning, a 1 L – preculture (5 L Erlenmeyer flask with baffles) was inoculated to an optical density OD_{600}= 0.1, and grown at 37°C for 8 hours. The actual expression in the fermenter (Bioengineering) was performed in 50 L 2YT medium supplemented with 0.6% glucose and 100 μg/ml ampicillin (no chloramphenicol during expression of BirA). Instrument settings were set to 37°C, 400 rpm, pH 6.5 ± 0.5 (adjusted by 5 M NaOH with 5 s on-time and 10 s off-time), 1 bar overpressure, and foam control with 1:10 diluted Antifoam Y30 (Sigma-Aldrich). Expression was inoculated with 1 L preculture. At OD_{600} = 3.5, the temperature was downregulated to 28°C and expression was induced by 250 μM IPTG (isopropyl-β-D-thiogalactoside). In case of BirA coexpression, 25 μM free biotin was added. Expression was continued for 12-15 hours, and the fermenter was then cooled to 18°C before harvesting by continuous centrifugation. The obtained wet cell pellet (500 – 600 g) was stored at -80°C until further use.

5.4.6 Purification of GPCR variants

100 g wet cell pellet was thawed at room temperature for 1 h, and homogenized in 200 ml 2× solubilization buffer (100 mM HEPES pH 8, 400 mM NaCl, 20% glycerol, complete protease inhibitor (Roche)). All subsequent steps are performed at 4°C. The cell suspension was supplemented with 2.5 mM $MgCl_2$, a few crystals of DNase I, 400 mg lysozyme, 0.6% CHAPS, 0.12% CHS and 1.7% DM in a total volume of 400 ml and stirred for 15 min. Cells were opened by sonification (Branson Sonifier 250) for 30 min (duty cycle 30%, output 5) under continuous stirring in an ice/water bath. After addition of 10 mM EDTA, solubilization was continued for 30 min. Solubilized material was separated from cell debris by centrifugation for 30 min at 15,000 g. The supernatant was mixed with 5 ml pD-NT1-resin previously equilibrated in buffer NTW1 (25 mM HEPES pH 8, 10% glycerol, 150 mM NaCl, 2 mM DTT, 0.3% DM) and incubated overnight to allow for receptor binding. The resin was collected by centrifugation at 600 g for 10 min, supernatant was partially removed and the resin was loaded into 2 empty PD10-columns. Each column (~2.5 ml column volume (CV)) was washed with 60 ml buffer NTW1 and subsequently with 40 ml buffer NTW2 (25 mM HEPES pH 7, 10% glycerol, 150 mM NaCl,

2 mM DTT, 0.3% DM). Resin was resuspended in 1 CV of buffer NTW2 each, and cleavage of the 3C-recognition sites performed in the presence of 125 µl 3C-protease (5.6 mg/ml) in buffer NTW2 for 3 h under continuous rotation. Cleaved receptor and fusion proteins were collected by elution with 10 ml buffer NTW2 per column. The salt concentration of the eluted fraction was adjusted by dilution with 2 volumes of buffer SP-B (10 mM HEPES pH 7.7, 10% glycerol, 2 mM DTT, 0.3% DM), loaded on a SP-sepharose column (5 ml CV, PD10 column, GE Healthcare) and washed with 10 ml buffer SP-B and 25 ml buffer SP-W (10 mM HEPES pH 7.7, 10% glycerol, 35 mM NaCl, 2 mM DTT, 0.3% DM). The pH was readjusted by washing with 3 ml buffer SP-W, and the bound protein was eluted with 12 ml buffer SP-E (10 mM HEPES pH 7, 10% glycerol, 350 mM NaCl, 2 mM DTT, 0.3% DM, 0.5 µM NT1-peptide) directly into a concentrator (Millipore Amicon® Ultra, 50,000 MWCO) and concentrated to less than 500 µl. The concentrated fraction was then applied to size exclusion chromatography on an S200-column (GE Healthcare Superdex 200, 24 ml CV) equilibrated in buffer SEC (10 mM HEPES pH 8, 150 mM NaCl, 2 mM DTT, 0.3% DM, 0.1 µM NT1-peptide). Fractions of 0.5 ml were collected at a flow rate of 0.4 ml/min. The relevant fractions were pooled, concentrated to 0.5 mg/ml (~10 µM) in an Amicon® Ultra 50,000 MWCO, supplemented with 30% glycerol, flash-frozen in liquid nitrogen and stored in 50 µl aliquots at -80°C.

5.4.7 Quantification of biotinylation efficiency

The degree of biotinylation for b-L5X and b-TM86V was analyzed according to Petris *et al*., 2011. Here, 11.5, 28.75, 57.5, 92 and 115 (and 138 pmol for b-TM86V) pmol receptor were incubated at 50°C for 10 min in SDS loading buffer (35 mM Tris·HCl pH 6.8, 10% glycerol, 2% SDS, 1% β-mercaptoethanol, 0.15% bromphenol blue). Samples were allowed to cool to room temperature before addition of 1 µg (71 pmol) streptavidin and incubation for 30 min at room temperature. Streptavidin-bound receptor was separated from free receptor on a 4-15% NuPAGE (Invitrogen) gradient SDS-PAGE. The binding of biotin-streptavidin is strong and retained also under denaturating SDS-PAGE conditions, provided that complex formation is allowed to proceed at room temperature. ImageJ (http://rsbweb.nih.gov/ij/) software was used to quantify the band intensity of free receptor. The band intensity of free receptor in the presence of streptavidin and free receptor in the absence of streptavidin was used to calculate the ratio of biotinylated receptor.

5.4.8 Expression of DARPins

The respective pDST67-derived clone encoding the DARPin was transformed into *E. coli* XL1blue. A single colony was used to start an overnight preculture (50 ml 2YT medium, 1% glucose, 100 µg/ml ampicillin). A 1 L – expression culture (5 L Erlenmeyer flask) was inoculated to OD_{600} = 0.1, and grown at 37°C to OD_{600} = 0.7. Protein expression was induced by addition of 1 mM IPTG and continued for 5 h at 37°C.

5.4.9 DARPin purification

Cells were solubilized in 10 ml buffer TBS_{400} (50 mM Tris·HCl pH 7.4, 400 mM NaCl) and lysed by sonification (3x 30 s, duty cycle 50%, output 6). Soluble material was separated from cell debris by centrifugation at 13,000 g for 20 min at 4°C and subsequently applied to 3 ml Ni-NTA resin (Qiagen) equilibrated with 10 CV buffer TBS-W (50 mM Tris·HCl pH 7.4, 400 mM NaCl, 20 mM imidazole, 10% glycerol). The resin was allowed to clear by gravity flow and washed with 20 CV buffer TBS-W. The bound DARPin was eluted stepwise (fraction e0: 1 ml, e1: 1.5 ml, e2: 1.5 ml, e3: 1.5 ml) with buffer TBS-E (50 mM Tris·HCl pH 7.4, 400 mM NaCl, 250 mM imidazole, 10% glycerol). Fractions were analyzed for their protein content by SDS-PAGE, and relevant fractions were pooled. Absorption at 280 nm (NanoDrop 1000, Thermo Scientific) was measured to determine the final protein concentration using the specific extinction coefficients (Table 5-4).

5.4.10 Analytical size exclusion chromatography

The behavior of the selected DARPins was analyzed on an analytical size exclusion chromatography (Superdex 200, 2.4 ml CV, GE Healthcare). DARPins were diluted to 10 μM/ 20 μM in the buffer of interest (PBS/0.2% DM to analyze protein behavior in the presence of detergent, as during selection; 10 mM Tris·HCl/ 150 mM NaCl to analyze protein behavior in the absence of detergent). The column was equilibrated in the assay buffer, and 100 μl DARPin sample was injected via the autoloader of the AEKTAMicro (GE Healthcare).

5.4.11 Ribosome display selections

All ribosome display (RD) selections were performed according to the detailed ribosome display manual version 01.2 (March 17th, 2011), and the manual “ribosome display in 96 well format” (see protocol database) and employing the King Fisher Flex (KFF) for automated selections in solution. Selections were performed in the presence of 250 nM target receptor on 50 μl MyOne Streptividin beads T1 (Invitrogen) per reaction, with a target to binding site ratio of 1 to 4.4. The low ratio was chosen to account for the large radius of the detergent micelle, which might shield neighboring streptavidin molecules. The standard detergent Tween 20 was consequently replaced by 0.2% DM throughout all selection with the target proteins b-TM86V and b-L5X. The S30-extract without DTT was used to retain the target disulfide bridge. Throughout all PCR reactions, the primer WTC4 was replaced by JSDRDir4 (designed by J.Schilling, ATCTGCTTCG GCCTTCGCTT TAGCATCTGC CGCCGCTTTCG) and the primer EWT5short by JSCRDif2 (designed by J. Schilling, AGAGGATCGC ATCACCATCA CCATCACGGA TCCGACCTGGG). VentR® Polymerase (NEB) was replaced by Herculase® II (Stratagene). The outline of a typical selection round on KFF, here round 3, is given in

Table 5-5 and Table 5-6. All other rounds were performed accordingly with adjustment of the washing times (Table 5-7).

Table 5-5. Protocol of RD selection round 3 performed on King Fisher Flex.

			release	mix (min)			collect (min)	
step	substep	plate	(min)	slow	medium	cycle (#)	count	time
start	pick up tip	pp-p-pd						
	collect beads	wash 1			02:00		00:05	00:10
prepanning	prepanning	pp-p-pd	02:00	04:00	01:00	6	00:05	00:10
	removal of prepanning beads	trash	01:00					
pause	add target	pp-p-pd						
panning	mix	pp-p-pd		04:00	01:00	12		
pause	add beads to wash 1	wash 1						
pulldown	collect new beads	wash 1					00:05	00:10
	pulldown	pp-p-pd	00:30	04:00	01:00	6	00:05	00:10
wash 1		wash 1	00:30	01:00	01:00	1	00:05	00:10
wash 2		wash 2	00:30	04:00	01:00	1	00:05	00:10
wash 3		wash 3	00:30	03:00	01:00	2	00:05	00:10
wash 4		wash 4	00:30	03:00	01:00	2	00:05	00:10
wash 5		wash 5	00:30	04:00	01:00	1	00:05	00:10
elution		elution	03:00	04:00	01:00	2	00:05	00:10
release beads		trash	01:00					
end	leave plate	pp-p-pd						

Table 5-6. Plate setup on RD selections using King Fisher Flex.

plate	reagent	volume (µl)
pp-p-pd	stop buffer	250
	translation mix	250
	target	12.5
wash 1	buffer WB-DM	800
	beads	100
wash 2	buffer WB-DM	1000
wash 3	buffer WB-DM	1000
wash 4	buffer WB-DM	1000
wash 5	buffer WB-DM	1000
elution	buffer EB	200
trash	buffer WB-DM	500

Table 5-7. Washing conditions used in RD selections.

		RD selection round			
		1	2	3	4
wash step (min)	1	-	1	2	2
	2	-	5	5	5
	3	-	5	8	10
	4	-	5	8	10
	5	-	1	5	15
Σ wash time*		20	38	48	62

* the total wash time is the sum of the actual duration plus the transfer times between individual steps.

5.4.12 ELISA methods

High throughput crude-extract ELISA

The screening of DARPin binders by crude-extract ELISA was performed according to the HT_ELISA manual (ht_elisa_protocol_09.11.11.pdf; T. Looser) with the following modifications: The detergent Tween-20 was replaced by 0.2% DM to ensure target protein activity. For the same reason, cell lysis was not performed with the detergent mix B-PER II (Pierce), but instead achieved by incubation with DNase I and lysozyme. The cell pellet was resuspended in 250 µl buffer DESOL (1× PBS, 1 mM EDTA, 50 µg/ml DNase I (Roche), 0.5 mg/ml lysozyme, 10 mM $MgCl_2$) and incubated on a horizontal plate shaker (Titramax 1000) for 1 h at RT. The crude extracts were diluted with PBS to a final volume of 1 ml, and frozen at -80°C until further use.

ELISA

A 96-well MaxiSorp ImmunoPlate (Nunc) was washed twice with 250 µl PBS and subsequently coated with 100 µl of 66 nM neutravidin solution per well overnight at 4°C. All incubation steps were performed on a horizontal plate shaker (Titramax 1000). Remaining binding sites were blocked with 250 µl PBS-DB (PBS, 0.2% DM, 0.5% BSA) for 1 h at RT. Each well was washed 3x with 250 µl PBS-D (PBS, 0.2% DM) before immobilization of 100 µl 15 nM TM86V or L5X, respectively, for 1 h at 4°C. Each well was again washed three times, followed by incubation with 100 µl DARPin solution of a defined concentration for 1 h at 4°C. Each reaction was performed in duplicates. After the next wash step, bound DARPin was detected by 100 µl αRGSHis$_6$-antibody in PBS-DB (diluted 1:5000; internal ID 24) for 1 h at 4°C and the secondary αmouse IgG - antibody conjugated with alkaline phosphatase (1:10,000 in PBS-DB, internal ID 38). Subsequently, 100 µl of 3 mM 4-pNPP substrate (4-nitrophenyl phosphate disodium salt) in buffer pNPP (50 mM $NaHCO_3$, 50 mM $MgCl_2$) was added to each washed well for reaction with alkaline phosphatase and the signal was allowed to develop for 30 min to several hours. OD_{405} was measured for readout (Tecan Infinite M1000 plate reader).

Competition ELISA

The competition ELISA was essentially performed according to the above protocol. To assess if the DARPin binding to immobilized target receptor is competitive, the following reaction setup was chosen: In one reaction, 50 nM DARPin were allowed to bind to immobilized target, and in a second reaction, 50 nM DARPin were mixed with 500 nM unbiotinylated target receptor before addition to the immobilized biotinylated receptor.

References

Alder, M.N., Rogozin, I.B., Iyer, L.M., Glazko, G.V., Cooper, M.D., Pancer, Z. (2005). Diversity and function of adaptive immune receptors in a jawless vertebrate. *Science* **310**, 1970-1973.

Bayburt, T.H., Sligar, S.G. (2010). Membrane protein assembly into Nanodiscs. *FEBS Lett.* **584**, 1721-1727.

Binz, H.K., Amstutz, P., Kohl, A., Stumpp, M.T., Briand, C., Forrer, P., Grütter, M.G., Plückthun, A. (2004). High-affinity binders selected from designed ankyrin repeat protein libraries. *Nat. Biotechnol.* **22**, 575-582.

Binz, H.K., Stumpp, M.T., Forrer, P., Amstutz, P., Plückthun, A. (2003). Designing repeat proteins: well-expressed, soluble and stable proteins from combinatorial libraries of consensus ankyrin repeat proteins. *J. Mol. Biol.* **332**, 489-503.

Chapman-Smith, A., Cronan, J.E., Jr. (1999). *In vivo* enzymatic protein biotinylation. *Biomol. Eng.* **16**, 119-125.

Cull, M.G., Schatz, P.J. (2000). Biotinylation of proteins *in vivo* and *in vitro* using small peptide tags. *Methods Enzymol.* **326**, 430-440.

Dreier, B., Plückthun, A. (2011). Ribosome display: a technology for selecting and evolving proteins from large libraries. *Methods Mol. Biol.* **687**, 283-306.

Forrer, P., Binz, H.K., Stumpp, M.T., Plückthun, A. (2004). Consensus design of repeat proteins. *ChemBioChem* **5**, 183-189.

Forrer, P., Jaussi, R. (1998). High-level expression of soluble heterologous proteins in the cytoplasm of *Escherichia coli* by fusion to the bacteriophage lambda head protein D. *Gene* **224**, 45-52.

Forrer, P., Stumpp, M.T., Binz, H.K., Plückthun, A. (2003). A novel strategy to design binding molecules harnessing the modular nature of repeat proteins. *FEBS Lett.* **539**, 2-6.

Hanes, J., Plückthun, A. (1997). *In vitro* selection and evolution of functional proteins by using ribosome display. *Proc. Natl. Acad. Sci. USA* **94**, 4937-4942.

Huber, T., Steiner, D., Röthlisberger, D., Plückthun, A. (2007). *In vitro* selection and characterization of DARPins and Fab fragments for the co-crystallization of membrane proteins: The Na(+)-citrate symporter CitS as an example. *J. Struct. Biol.* **159**, 206-221.

Interlandi, G., Wetzel, S.K., Settanni, G., Plückthun, A., Caflisch, A. (2008). Characterization and further stabilization of designed ankyrin repeat proteins by combining molecular dynamics simulations and experiments. *J. Mol. Biol.* **375**, 837-854.

Kohl, A., Binz, H.K., Forrer, P., Stumpp, M.T., Plückthun, A., Grütter, M.G. (2003). Designed to be stable: crystal structure of a consensus ankyrin repeat protein. *Proc. Natl. Acad. Sci. USA* **100**, 1700-1705.

Kummer, L., Parizek, P., Rube, P., Millgramm, B., Prinz, A., Mittl, P.R., Kaufholz, M., Zimmermann, B., Herberg, F.W., Pluckthun, A. (2012). Structural and functional analysis of phosphorylation-specific binders of the kinase ERK from designed ankyrin repeat protein libraries. *Proc. Natl. Acad. Sci. USA* **109**, E2248-2257.

Leitz, A.J., Bayburt, T.H., Barnakov, A.N., Springer, B.A., Sligar, S.G. (2006). Functional reconstitution of β_2-adrenergic receptors utilizing self-assembling Nanodisc technology. *BioTechniques* **40**, 601-602, 604, 606, passim.

Monroe, N., Sennhauser, G., Seeger, M.A., Briand, C., Grütter, M.G. (2011). Designed ankyrin repeat protein binders for the crystallization of AcrB: plasticity of the dominant interface. *J. Struct. Biol.* **174**, 269-281.

Petris, G., Vecchi, L., Bestagno, M., Burrone, O.R. (2011). Efficient detection of proteins retro-translocated from the ER to the cytosol by *in vivo* biotinylation. *PloS one* **6**, e23712.

Plückthun, A. (2012). Ribosome display: a perspective. *Methods Mol. Biol.* **805**, 3-28.

Rosenbaum, D.M., Cherezov, V., Hanson, M.A., Rasmussen, S.G., Thian, F.S., Kobilka, T.S., Choi, H.J., Yao, X.J., Weis, W.I., Stevens, R.C., Kobilka, B.K. (2007). GPCR engineering yields high-resolution structural insights into β_2-adrenergic receptor function. *Science* **318**, 1266-1273.

Schatz, P.J. (1993). Use of peptide libraries to map the substrate specificity of a peptide-modifying enzyme: a 13 residue consensus peptide specifies biotinylation in *Escherichia coli*. *Biotechnology. (N. Y).* **11**, 1138-1143.

Schlinkmann, K.M., Hillenbrand, M., Rittner, A., Künz, M., Strohner, R., Plückthun, A. (2012). Maximizing detergent stability and functional expression of a GPCR by exhaustive recombination and evolution. *J. Mol. Biol.*, DOI: 10.1016/j.jmb.2012.1005.1039.

Spirin, A.S., Swartz, J.R., (2007). Cell-free Protein Synthesis. Methods and Protocols, ed 1 ed. Wiley-VCH, Weinheim.

Chapter 6

Summary and Future Perspectives

Saturating Mutagenesis

Despite enormous effort, the pace and progress of GPCR research has not caught up with that of soluble proteins. While brute-force approaches have been successful in some cases, it was clear that the crucial limitations that are intrinsic to GPCRs had not been addressed yet, and that innovative approaches were necessary to break new ground. Many mutagenic studies have been performed on GPCRs, but they were never exhaustive in their coverage, leaving open questions regarding the potential still hidden within GPCR sequences.

Instead of searching manually for the needle in the haystick, we have systematically dissected the contribution of every side chain to expression and function of the rNTR1-D03 by saturating mutagenesis of every receptor position. Alanine-scanning mutagenesis has been applied to several targets and also to some GPCRs (Magnani *et al.*, 2008; Serrano-Vega *et al.*, 2008; Shibata *et al.*, 2009), but saturating mutagenesis was previously only selectively applied to relevant positions of a target protein (Tan *et al.*, 2008), or to ensembles of several positions (Delagrave and Youvan, 1993; Huang *et al.*, 1996). Such a comprehensive saturating scanning approach as performed here was the first of its kind, and will likely remain so. The main argument for this assumption is that generation of hundreds of individually randomized libraries is laborious and cost-intensive, and requires stringent quality control measures to ensure library diversity, the most critical factor of this study. About a third of all position-specific libraries had to be re-synthesized due to early quality control issues. With the final ultra-deep sequencing analysis of the evolved library pools, we could confirm that, except at about 10 positions, those issues had been resolved. Selection and sequencing analysis of about 400 libraries with the handling of more than 25,000 individual clones was certainly worth the effort, but is too time-consuming to be performed for every receptor of interest.

Among many possible implications, we expected that the analysis of the position-specific libraries would reveal something about the tolerance of each receptor position towards mutagenesis and identify the positions with obvious constraints. More than that, thirty shift positions were found that increased expression levels, and some also affected detergent stability. With the subsequent generation of combinatorial libraries, the full potential of the identified shifts was revealed, highlighting that pivotal positions had been identified, and that the shift mutations alleviated previous constraints. Notably, these shift mutations target receptor-specific constraints, as shown by high expression of the evolved variants in *Sf9* cells, and are by no means a result of host adaptation. The creation of evolved receptor variants with unprecedented expression and detergent stability represents the key finding of this study.

Coevolution of expression levels and detergent stability

The strong coevolution of expression and detergent stability observed for the combinatorial variants was surprising, as the latter was never under direct selection pressure. This observation is in agreement with the results of previous studies applying random mutagenesis and selection to evolve GPCRs *in vitro* (Dodevski and Plückthun, 2011; Sarkar et al., 2008). Obviously, selection for functionally expressed GPCR indirectly selects for stability. Such a correlation could arise from effects on protein folding and packing, thus improving the efficiency of correct insertion into the membrane. Preliminary data suggest that for the evolved receptor variants, the total fraction of active receptor in the membrane is increased, but the total amount of protein is still similar to wild type. This observation supports the above hypothesis that protein folding and insertion of the evolved variants is improved. In this respect, it is interesting to note that highest functional expression of the evolved receptor variants is observed at 30°C, which is not the case for the less-evolved D03 or for wild-type rNTR1. This shows that the *E. coli* protein synthesis machinery can actually accommodate higher expression levels, and that the toxicity of GPCR overexpression is a result of its primary amino acid sequence and poor biophysical properties. Usually, GPCRs such as the wild-type rNTR1 are expressed in *E. coli* at low temperatures to decrease the rate of protein synthesis, providing sufficient time for protein folding and insertion.

An interesting hypothesis is that expression and selection in *E. coli* exerts a strong selective pressure for fast synthesis and folding of membrane proteins (Tate, 2010). Mammalian cells divide approximately every 24 h, providing ample time for a GPCR to reach the surface, while in *E. coli*, the short generation time of approximately 20 min provides a much smaller time window to do so, hence exerting selective pressure. In mammalian cells, it is less relevant how long the process of folding and membrane insertion takes, as long as enough functional molecules are presented at the cell surface. Hence, the enforced selection pressure could explain the coevolution of expression and detergent stability as observed here.

In a perfect world, the evolved variants would be functionally identical to the wild type, while displaying increased expression and stability. With respect to ligand binding, the evolved variants behave as wild type, with the only exception of reduced antagonist affinity for L5X. The evolved variants also display signaling activity after restoration of the functionally important DRY motif, but similar to D03, are characterized by increased basal activity of the receptor. Other than C7E02 and TM86V, the L5X variant does not respond to agonist stimulation, and is assumed to be preferentially stabilized in the active conformation R*. The slight decrease in signaling ability is not desired, but tolerable, since especially for L5X, it indicates conformational stabilization of the active receptor, which in turn is advantageous for structural studies. Furthermore, all variants do still bind the heterotrimeric G protein, and cocrystallization of evolved GPCR variant with its cognate G protein is surely a relevant approach, restraining the flexible intracellular loops of the GPCR and providing a large hydrophilic surface for crystal contact formation.

Implications for the directed evolution of further GPCRs

The high potential of D03 for directed evolution without compromising the receptor phenotype is striking. Together with results with other receptors, it can be assumed that this feature is common to all GPCRs. Future studies should therefore address if and how the identified shifts are transferrable to other GPCRs. As discussed above, it is not feasible to apply saturating mutagenesis as a standard tool for directed evolution to every GPCR. Rather, a combination of targeted mutagenesis, full randomization of some "hot spots" together with random mutagenesis of the receptor sequence could prove successful. Some effects identified here are likely hot spots of general relevance, allowing specific targeting of these positions in other GPCRs: First and foremost, avoidance of any free cysteine in the extracellular space is relevant for high expression of D03 (mutants L5X and MT1), and is likely of general interest, since it facilitates correct disulfide formation. Notably, mutation of C332$^{6.59}$ on rNTR1 wild type does not increase functional expression of the wild-type receptor (Grisshammer *et al.*, 1993). The fact that proper formation of the one disulfide bridge becomes relevant only at very high expression levels suggests that this is a limitation imposed by the *E. coli* host rather than by the GPCR. High GPCR expression levels could lead to oversaturation of the periplasmatic *E. coli* Dsb-protein family responsible for disulfide formation, or the respective cysteines may be inaccessible, thus causing other, unspecific intramolecular or intermolecular reactions, which is in both cases alleviated by mutation of C332$^{6.59}$. A further striking observation is that many shifts hit highly conserved helical positions, denoted as x.50 by the Ballesteros-Weinstein numbering. These positions are highly conserved throughout GPCR evolution, and are characteristic for each transmembrane helix. Apparently, these positions are highly relevant for regulation of receptor expression levels. Since these residues are also often involved in receptor functionality, such as R167$^{3.50}$ in D03, targeted mutagenesis at these positions should include full randomization to include also the wild type, and demands further analysis to assess the effect on receptor functionality.

Implications and questions for additional studies

An interesting continuation of this study would be to analyze *how* the evolved variants achieve high expression and stability. Mutagenic studies on TM86V and L5X have already highlighted crucial residues for high detergent stability and functional expression levels. However, the molecular basis for these effects is not yet elucidated. Structure determination of individual variants could highlight differences in helix packing, side chain interactions and conformational state of the receptor, to decipher the molecular details of how expression and detergent-stability is achieved. However, despite ongoing efforts, crystallization of GPCRs is still a cumbersome undertaking, with no guarantee of success. L5X could be a first promising candidate, since it is stabilized in the active state, thus reducing the conformational heterogeneity of the receptor population, which is advantageous for crystallization. TM86V is another interesting candidate, since it is a

minimal mutant with respect to detergent stability. Surely, structure determination of these variants would mark a new milestone in our understanding of the mutants' phenotype, and will simultaneously give rise to new questions and hypotheses.

Equally interesting is the question of how the evolved variants differ from the wild type receptor, or other GPCRs, in terms of membrane insertion and folding to give an active receptor. Functional studies assaying the process of membrane targeting and integration via the SecYEG translocon pore in *E. coli* (or Sec61 in eukaryotes) could unravel whether the evolved variants have been adapted for efficient insertion into the membrane. The process of membrane insertion might represent a crucial bottleneck, eventually imposing an upper limit to GPCR expression by saturation of the translocon machinery. In light of the hypothesis that expression and selection in *E. coli* could have fostered selection for efficient protein folding, it would be interesting to analyze protein folding *in vitro*, and to compare these results to the *in vivo* efficiency of GPCR folding and integration into the lipid bilayer, both in *E. coli* and in mammalian cells.

Summary

Taken together, this work has successfully addressed the main bottlenecks in *in vitro* GPCR research, namely low expression and detergent-stability. The evolved variants overcome these restraints without affecting function, and hence hold great promise as targets for structural, functional and drug screening studies. The knowledge gained from the saturating mutagenesis will eventually help to more rationally engineer further GPCR targets, and so to expand the spectrum of GPCRs that are available for drug screening approaches.

References

Delagrave, S., Youvan, D.C. (1993). Searching sequence space to engineer proteins: exponential ensemble mutagenesis. *Biotechnology. (N. Y).* **11**, 1548-1552.

Dodevski, I., Plückthun, A. (2011). Evolution of three human GPCRs for higher expression and stability. *J. Mol. Biol.* **408**, 599-615.

Grisshammer, R., Duckworth, R., Henderson, R. (1993). Expression of a rat neurotensin receptor in *Escherichia coli*. *Biochem. J.* **295** 571-576.

Huang, W., Petrosino, J., Hirsch, M., Shenkin, P.S., Palzkill, T. (1996). Amino acid sequence determinants of beta-lactamase structure and activity. *J. Mol. Biol.* **258**, 688-703.

Magnani, F., Shibata, Y., Serrano-Vega, M.J., Tate, C.G. (2008). Co-evolving stability and conformational homogeneity of the human adenosine A_{2A} receptor. *Proc. Natl. Acad. Sci. USA* **105**, 10744-10749.

Sarkar, C.A., Dodevski, I., Kenig, M., Dudli, S., Mohr, A., Hermans, E., Plückthun, A. (2008). Directed evolution of a G protein-coupled receptor for expression, stability, and binding selectivity. *Proc. Natl. Acad. Sci. USA* **105**, 14808-14813.

Serrano-Vega, M.J., Magnani, F., Shibata, Y., Tate, C.G. (2008). Conformational thermostabilization of the β_1-adrenergic receptor in a detergent-resistant form. *Proc. Natl. Acad. Sci. USA* **105**, 877-882.

Shibata, Y., White, J.F., Serrano-Vega, M.J., Magnani, F., Aloia, A.L., Grisshammer, R., Tate, C.G. (2009). Thermostabilization of the neurotensin receptor NTS1. *J. Mol. Biol.* **390**, 262-277.

Tan, L., Wiesler, S., Trzaska, D., Carney, H.C., Weinzierl, R.O. (2008). Bridge helix and trigger loop perturbations generate superactive RNA polymerases. *J. Biol.* **7**, 40.

Tate, C.G. (2010). Practical considerations of membrane protein instability during purification and crystallisation. *Methods Mol. Biol.* **601**, 187-203.

Appendix

1. Relevant plasmids
2. Cell strains
3. Detergents
4. Abbreviations

1. Relevant plasmids

1.1 pRGD03 and pRGD03_Avi

The plasmid pRGD03 (Plasmid ID 2438) was used as the basis for expression and selection of all position-specific libraries (chapter 3), as well as for expression and selection of the single StEP-libraries (chapter 4). Sloning library L1 was also expressed from this plasmid, and Sloning libraries L2-L4 (Chapter 4) were expressed from pRGD03 in a modified form (see Figure A-3B-D). Any library is subcloned into pRGD03 via *Bam*HI and *Cfr*9I restriction sites.

The plasmid pRGD03_Avi (Plasmid ID 2433) is identical to pRGD03 except for the C-terminal His_{10}-tag, which is replaced by the AviTag sequence GLNDIFEAQKIEWHE. Expression from pRGD03-Avi leads to *in vivo* biotinylation of the fusion protein at the C-terminus, and is used for all detergent-stability assays requiring immobilization of the fusion protein.

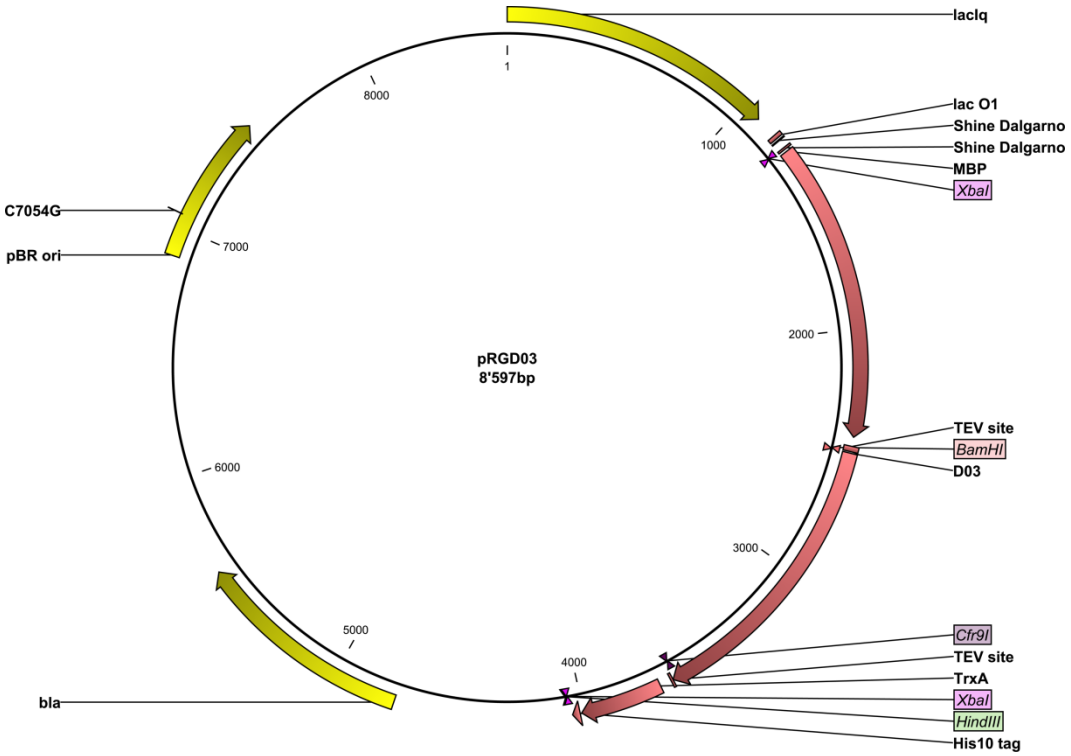

Figure A-1. Circular presentation of plasmid pRGD03. The GPCR coding fragment, here D03, can be replaced using *Bam*HI and *Cfr*9I restriction sites. The linker between MBP and before the TEV-site and D03 is a $GS(N)_{10}$-sequence, and the linker between TEV site and thioredoxin (TrxA) is a $N_5(G_3S)_2$-EF sequence.

1.2 eLIC47D03 and eLIC47patD03

eLIC47D03 and eLIC47patD03 were cloned to express D03 or any GPCR variant as fusion with N-terminal MBP and C-terminal thioredoxin (as in pRGD03, plasmid ID 2438) from plasmids with higher copy number (Chapter 4). eLIC47D03 (plasmid ID 3254) was obtained from eLIC_047 (plasmid ID 3041, alternative name HT_369) harboring a ColE1-origin by replacing the SacB cassette of eLIC_047 with the MBP-GPCR-trx-H_{10}-2×stop fragment from pRGD03 using ligase-independent cloning. eLIC47patD03 (plasmid ID 3361) was subsequently obtained from eLIC47D03 by replacing the ColE1- origin of replication with a mutagenized ColE1-sequence ((Bayer *et al.*, 2007))

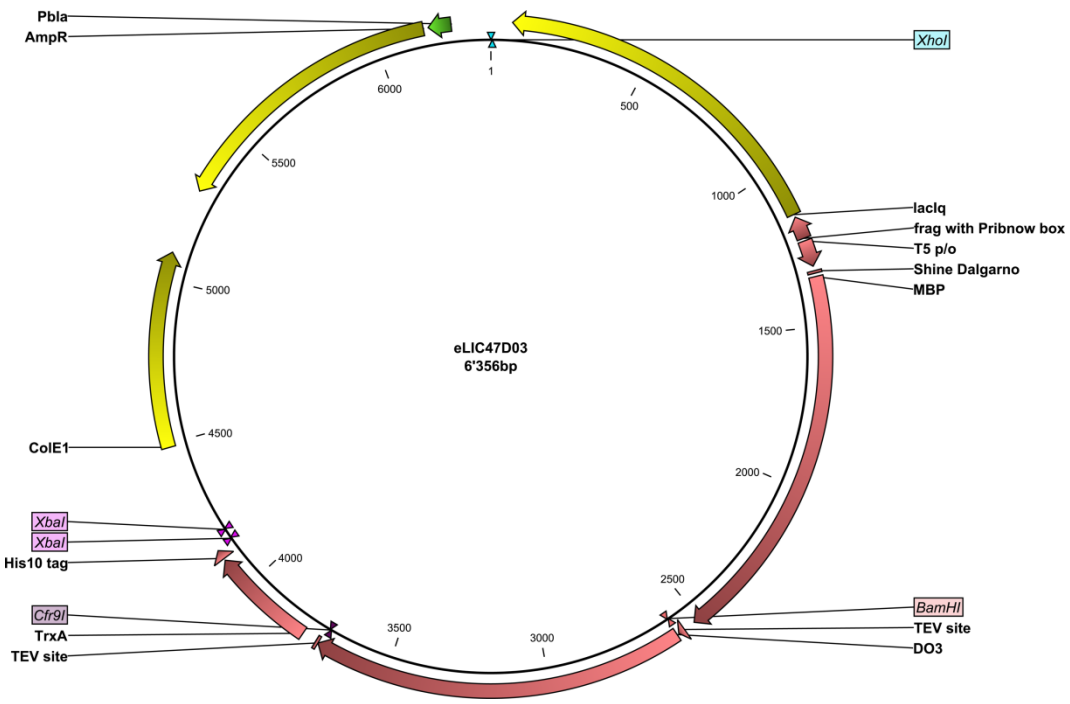

Figure A-2. Circular presentation of eLIC47D03 (ID 3254). eLIC47patD03 (ID 3361) is identical to eLIC47D03 except for ColE1, which carries additional base changes that increase plasmid copy number further.

1.3 Sloning library constructs

Sloning library L1 (ID 3493), L5 (ID 3501) and L6 (ID 3503) were expressed as conventional fusion protein constructs as in pRGD03 (Figure A-3A) from vectors with different plasmid copy numbers. Library L1 (Figure A-4A) was cloned into vector pRGD03 (plasmid ID 2438), whereas Library L5 was cloned into eLIC47D03 (plasmid ID 3254) and library L6 (Figure A-4B) into eLIC47patD03 (plasmid ID 3361). L5 and L6 are identical except for point mutations in the vector origin of replication. Libraries L2 (ID 3495), L3

(3497) and L4 (ID 3499) are characterized by truncation of the receptor C-terminus and absence of the thioredoxin fusion protein (L3-L4, Figure A-3B-D).

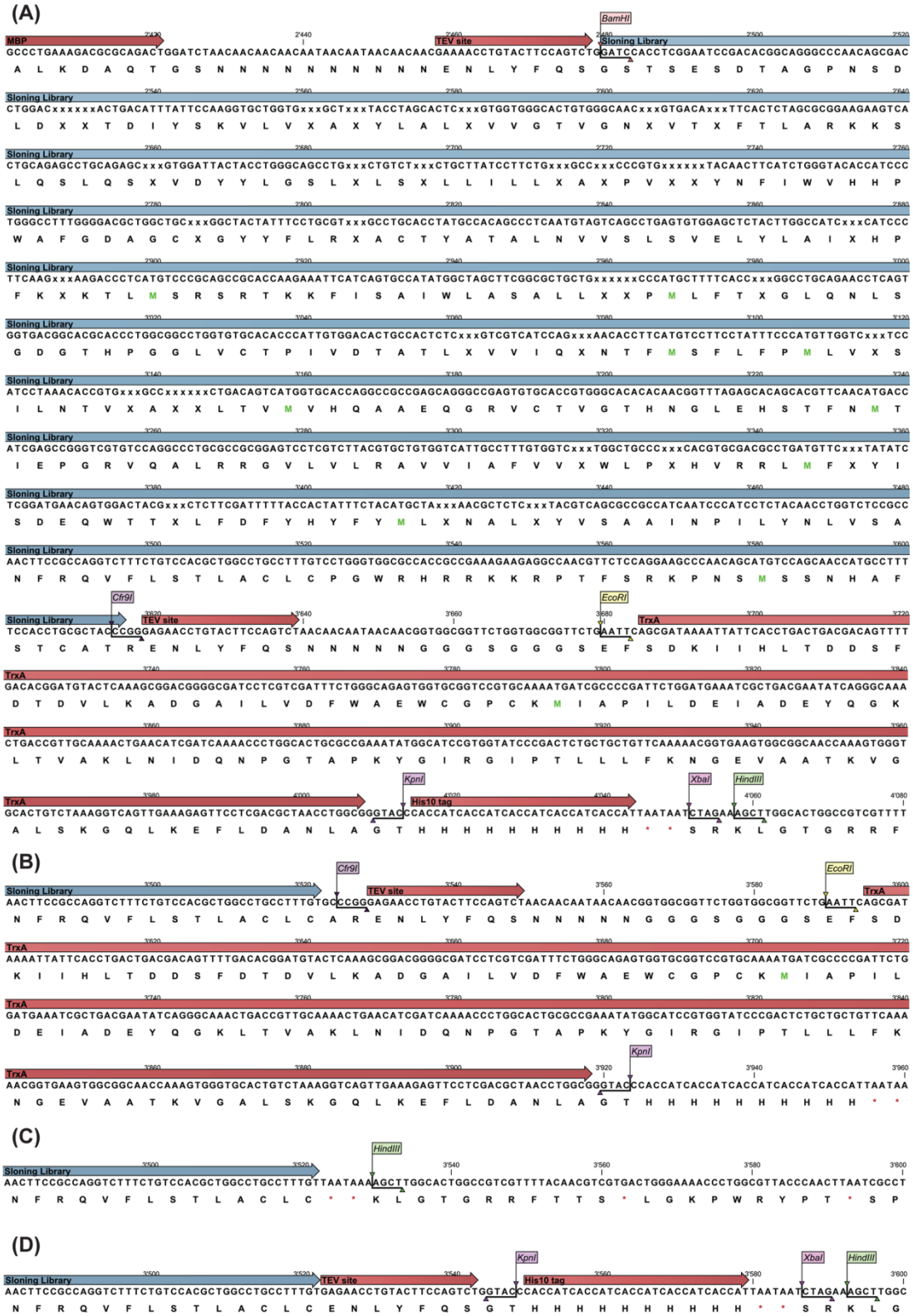

Figure A-3. Sloning library constructs used in selection. (A) Conventional fusion protein sequence of library L1. (B) Library L2 is truncated after helix 8 of the GPCR (incl. C389) in contrast to L1, L5 and L6 (A). (C) Library L3 is truncated after helix 8 (incl. C389) and expressed without any C-terminal tag. (D) Library L4 carries a TEV site and His_{10}-tag after helix 8 (incl. C389).

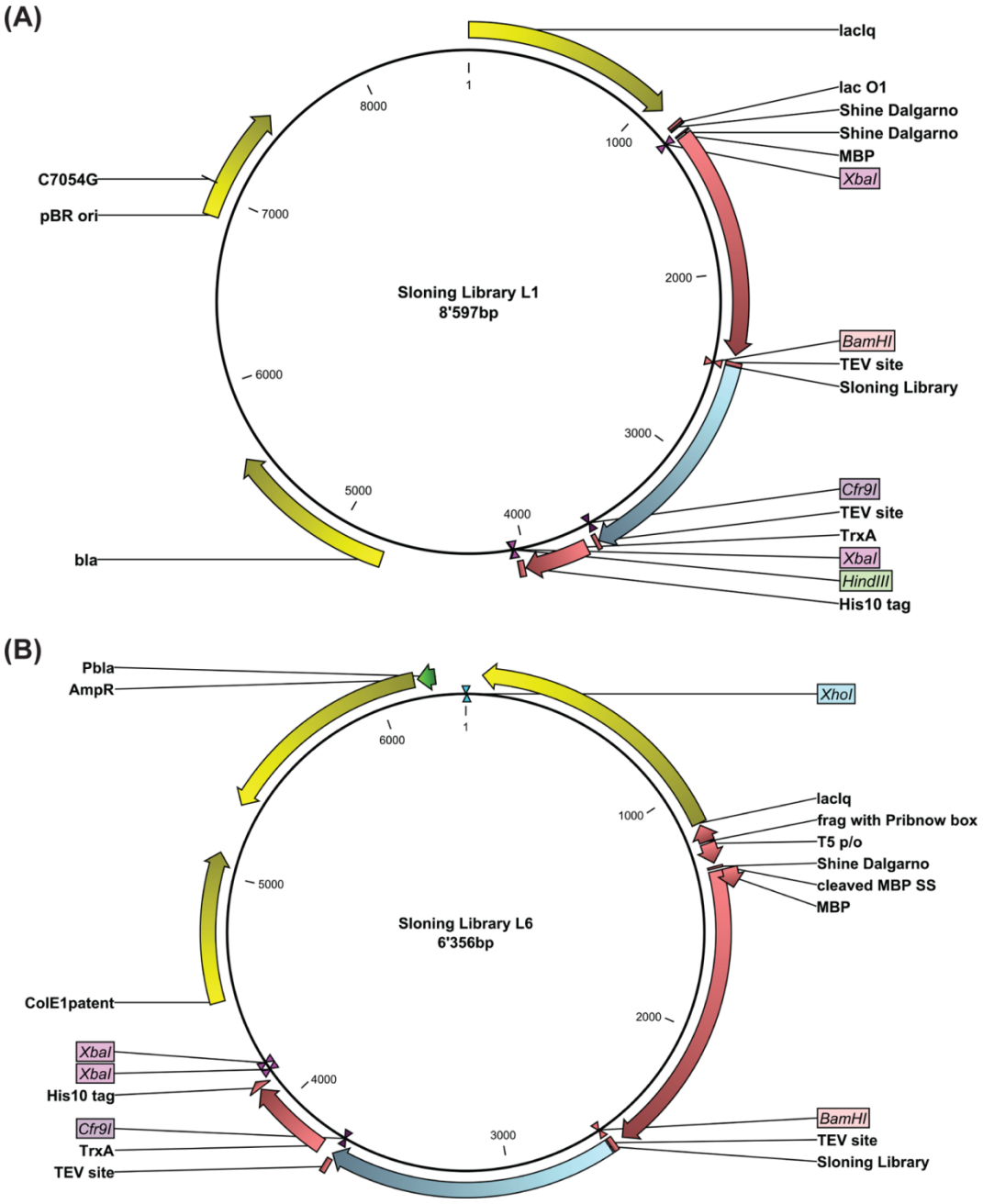

Figure A-4. Comparison of vector constructs used for Sloning library selections. Vector L1 is derived from pRGD03, and vector L6 from eLIC47patD03. The fusion protein sequence is identical, but the vector and importantly, origin of replication are different. L5 differs from L6 only by point mutations in the vector origin of replication.

1.4 Constructs for ribosome display selections

Plasmid pAT223-pD-NT1 for expression of pD-NT1 was obtained from P. Egloff. The NT(8-13) peptide sequence is C-terminally fused to pD via a linker sequence.

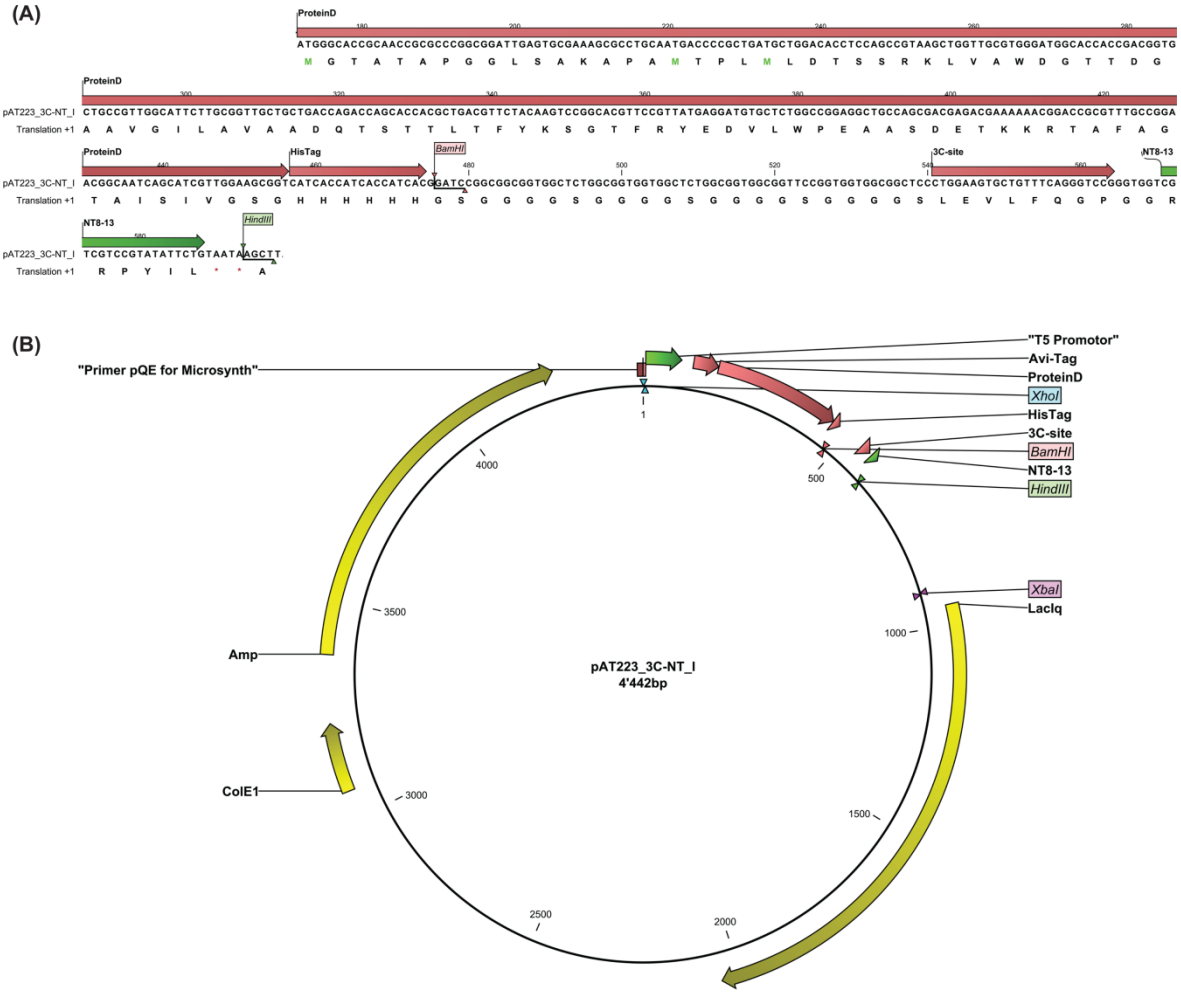

Figure A-5. Plasmid pAT223_3C-NT1 for expression of pD-NT1. (A) Sequence of the pD-NT1 fusion protein. (B) Circular presentation of plasmid pAT223_3C-NT1.

The cloning of pRG-RD_TM86V and pRG-RD_L5X is described in chapter 5, paragraph 5.5.4. The plasmid pRG-TM86V_P51-dWC392_3C, used for crystallization trials, was previously generated by P. Egloff, starting from pRGD03_TM86V. The unstructured N- and C-termini of the receptor were truncated and the recognition sites for TEV protease cleavage were replaced by 3C-recognition sites. pRG-xD_TM86V (and pRG-xD_L5X) is identical except for an *Eco*RI restriction enzyme site in the vector (Figure A-6). pRG-RD_TM86V (plasmid ID 3370) and pRG-RD_L5X (plasmid ID 3369) are derived from this construct, fusing a $(G_4S)_6$-AviTag linker to the C-terminus of the receptor (Figure A-7).

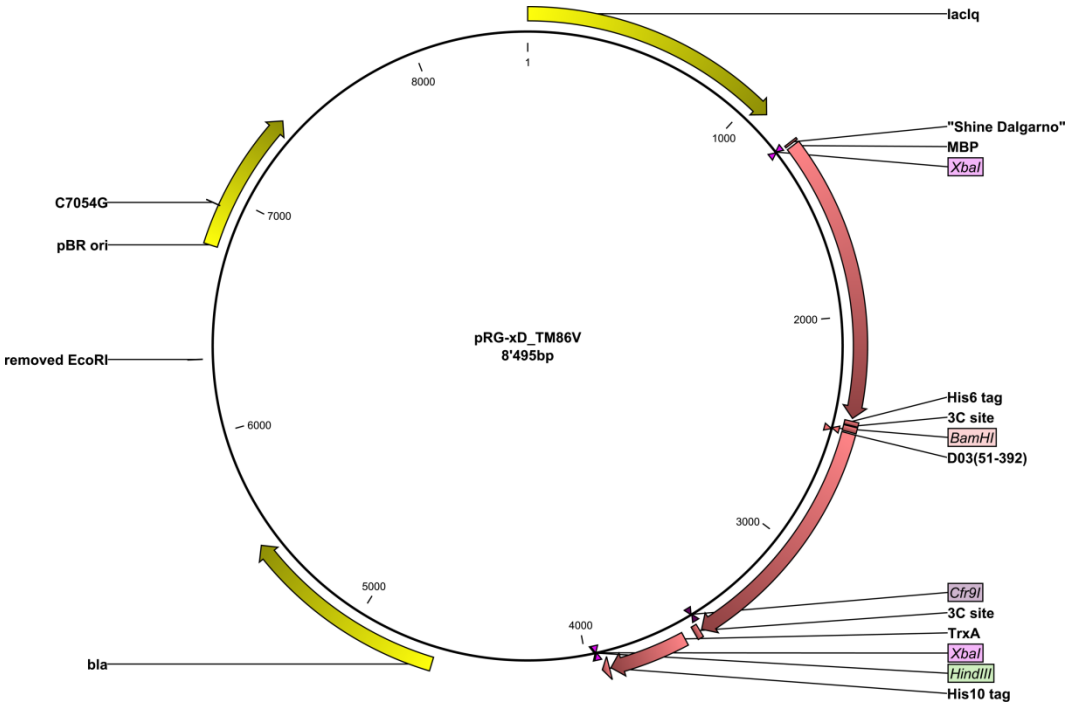

Figure A-6. Circular presentation of plasmid pRG-xD_TM86V as used for expression of unbiotinylated receptor for ELISA experiments (and crystallization trials). Plasmid pRG-xD_L5X is identical except for the receptor-coding sequence.

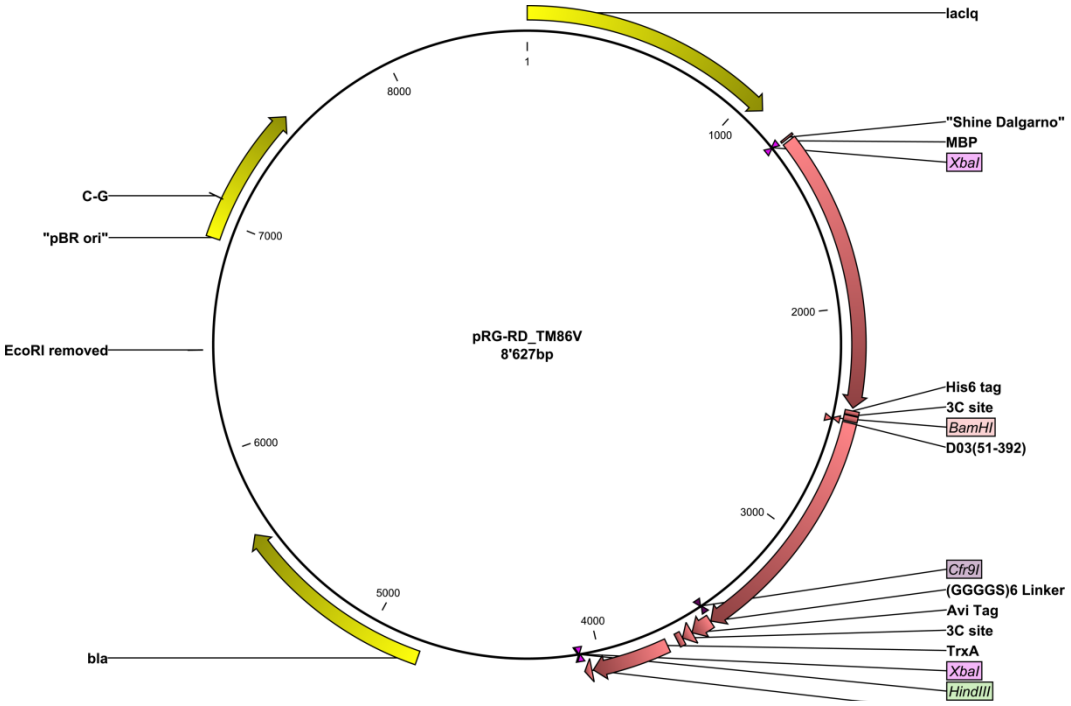

Figure A-7. Circular presentation of pRG-RD_TM86V (plasmid ID 3370). TM86V is extended by a flexible $(G_4S)_6$-linker and the AviTag-sequence (GLNDIFEAQKIEWHE). pRG-RD_L5X (plasmid ID 3369) is identical except for the receptor-coding sequence.

The previously constructed plasmid pRDVLDnew (plasmid ID 2228; adapted from pRDV by J. Schilling) was used throughout ribosome display selection rounds. Plasmid pDST67 (plasmid ID 827; by D. Steiner) was used for expression of selected DARPins.

2. Cell strains

2.1 *E. coli* DH5α

The *E. coli* strain DH5α was used throughout all cloning procedures, and for expression of rNTR1-variants for selection and detergent-stability measurements. Chemocompetent cells were prepared according to a modified Inoue protocol (Inoue *et al.*, 1990). Electrocompetent cells were prepared according to (Dower *et al.*, 1988).

Genotype: *F^- endA1 glnV44 thi-1 recA1 relA1 gyrA96 deoR nupG Φ80dlacZΔM15 Δ(lacZYA-argF)U169, hsdR17(r_K^- m_K^+), λ-*

2.2 *E. coli* XL1blue

The *E. coli* strain XL1blue was used for expression of DARPins. XL1blue provides $lacI^q$ *in trans*, and is thus suitable to express DARPins from pDST67 that does not have $lacI^q$ *in cis*. Chemocompetent cells were prepared according to a modified Inoue protocol (Inoue *et al.*, 1990).

Genotype: *endA1 gyrA96(nal^R) thi-1 recA1 relA1 lac glnV44 F'[::Tn10 $proAB^+$ $lacI^q$ Δ(lacZ)M15] hsdR17(r_K^- m_K^+)*

2.3 *E. coli* BL21(DE3)

The *E. coli* BL21(DE3) strain was used for large-scale fermenter-expression of rNTR1-variants. Chemocompetent cells were prepared according to a modified Inoue protocol (Inoue *et al.*, 1990).

Genotype: *F^- ompT gal dcm lon $hsdS_B$(r_B^- m_B^-) λ(DE3 [lacI lacUV5-T7 gene 1 ind1 sam7 nin5])*

3. Detergents

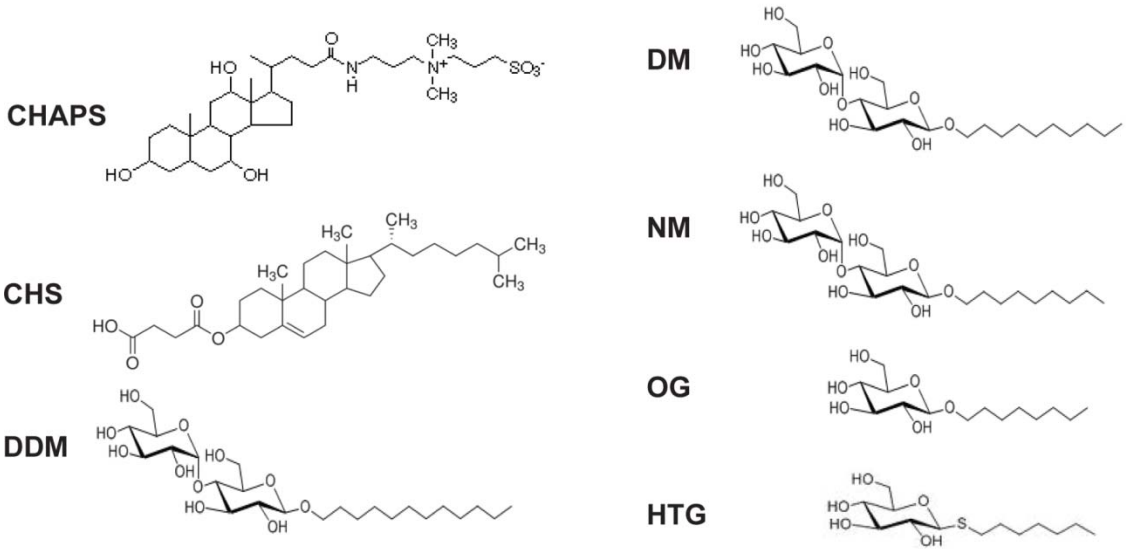

Figure A-6. Chemical structure of the detergents used in this study.

The detergents CHAPS (3-[(3-cholamidopropyl)dimethylammonio]-1-propane-sulfonate) and CHS (cholesterol hemisuccinate) in combination with DM (n-decyl-β-D-maltopyranoside) were used for solubilization of the receptor variants from the *E. coli* membrane. DDM (n-dodecyl-β-D-maltopyranoside), DM, NM (n-nonyl-β-D-maltopyranoside), OG (n-octyl-β-D-glucopyranoside) and HTG (n-heptyl-β-D-thioglucopyranoside) were used during detergent stability assays, to assess the influence of the detergent on receptor stability. The size of the detergent micelle depends on the detergent, with decreasing radius in the following order: DDM > DM > NM > OG > HTG.

4. Abbreviations

2YT	2x concentrated yeast tryptone medium
3C	recombinant protease from human rhinovirus
aa	amino acid
AviTag	avidin-tag, a polypeptide sequence for in vivo biotinylation (sequence: GLNDIFEAQKIEWHE)
b-L5X, b-TM86V	biotinylated L5X or TM86V
BirA	*E. coli* Biotin Ligase BirA
BODIPY	boron-dipyrromethene
bp	base pairs
BP-NT	BODIPY-neurotensin
BSA	bovine serum albumin
C7E02	evolved variant of rNTR1
cDNA	complementary DNA/ mRNA-copy
ceELISA	crude-extract ELISA
CHAPS	3-[(3-cholamidopropyl)-dimethylammonio]-1-propane sulfonate
CHS	cholesteryl hemisuccinate
CV	column volumne
DARPin	designed ankyrin repeat protein
DDM	n-dodecyl-β-D-maltopyranoside
DM	n-decyl-β-D-maltopyranoside
DMSO	dimethylsulfoxide
DTT	dithiothreitol
E. coli	*Escherichia coli*
EDTA	ethylenediaminetetraacetic acid
EL1/ECL1	extracellular loop 1
ELISA	enzyme-linked immunosorbent assay
FACS	fluorescence activated cell sorting
GDP	guanosine diphosphate
GPCR	G protein-coupled receptor
GTP	guanosine triphosphate
GTPγS	non-hydrolyzable GTP analog; thioester bond
HEPES	4-(2-hydroxyethyl)-1-piperazineethanesulfonic acid
HTG	n-heptyl-β-D-thioglucopyranoside
ID/plasmid ID	plasmid collection identification number for the described plasmid
IEX	ion exchange chromatography
IL1/ ICL1	intracellular loop 1
IMAC	immobilized metal ion affinity chromatography
IMP	integral membrane protein
IPTG	isopropyl-β-D-thiogalactoside
kDa	kiloDalton
KFF	King Fisher Flex
L5X	evolved variant of rNTR1
LB	Luria Broth
LCP	lipidic cubic phase

MBP	maltose binding protein
MFI	mean fluorescence intensity
mRNA	messenger RNA
MW	molecular weight
MWCO	molecular weight cutoff
N2C	DARPin library with N-cap, C-cap and 2 internal repeats
NHS	N-hydroxysuccinimide
Ni-NTA	nickel-nitrilotriacetic acid
NM	n-nonyl-β-D-maltopyranoside
NT	neurotensin
OD_{600}	optical density at 600 nm
off7	DARPin binder to MBP
OG	n-octyl-β-D-glucopyranoside
PAGE	polyacrylamide gel electrophoresis
PCR	polymerase chain reaction
pD/ gpD	capsid-stabilizing protein from bacteriophage λ
PDB	Protein Data Bank
PDB ID	Protein Data Bank identification number
pI	isoelectrical point
Plasmid ID/ ID	plasmid collection identification number for the described plasmid
pNPP	4-nitrophenyl phosphate disodium salt
R	Inactive conformational state of a GPCR
R*	active conformational state of a GPCR
RBS	ribosomal binding site
RD	ribosome display
RLBA	radioligand binding assay
RNC	ribosome-nascent-chain complex
rNTR1	rat neurotensin receptor 1
RT	room temperature
scRNA	*Sacharomyces cerevisiae* RNA
SDS	sodium dodecylsulfate
SEC	size exclusion chromatography
Sf9	*Spodoptera frugiperda*
SPR	surface plasmon resonance
StEP	staggered extension process
T4L	T4 lysozyme
TEV	tobacco etch virus
TM	transmembrane helix
TM86V	evolved variant of rNTR1
trx/ TrxA	thioredoxin

References

Bayer, K., Grabherr, R., Nilsson, E., Striedner, G. (2007). Expression vectors with modified ColE1 origin of replication for control of plasmid copy number. **EP 1 326 989 B1**.

Dower, W.J., Miller, J.F., Ragsdale, C.W. (1988). High efficiency transformation of *E. coli* by high voltage electroporation. *Nucleic Acids Res.* **16**, 6127-6145.

Inoue, H., Nojima, H., Okayama, H. (1990). High efficiency transformation of *Escherichia coli* with plasmids. *Gene* **96**, 23-28.

Curriculum Vitae

Name	Karola Schlinkmann
Date of Birth	February 22nd, 1983
Place of Birth	Hannover
Nationality	German
Address	Funkackerstrasse 16 CH-8050 Zürich

Dec 2007 – Oct 2012	PhD thesis with Prof. Andreas Plückthun Dept. of Biochemistry, University of Zurich, Switzerland *Title*: Maximizing expression and detergent stability of a GPCR by directed evolution.
Juli 2007 – Nov 2007	Research project with Prof. Bernhard Dichtl Inst. of Molecular Life Sciences, University of Zurich, Switzerland *Title*: Regulation of transcription termination in *S. cerevisiae*.
Sept 2006 – June 2007	Diploma thesis with Prof. Wolfgang Wintermeyer Inst. of Molecular Biology, Witten/Herdecke University, Germany *Title*: Regulation of the SRP-FtsY GTPase by interactions with ribosome-nascent chain complexes and SecYEG.
Oct 2004 – Aug 2006	Diploma studies in Biochemistry Witten/Herdecke University, Germany *Final grade 1.0*
Oct 2002 – Sept 2004	Pre-diploma studies in Biotechnology University of Münster, Germany
1993 – 2002	Theodor-Heuss-Gymnasium Waltrop, Germany Allgemeine Hochschulreife Final grade 1.0

Acknowledgements

First of all, I would like to thank Prof. Andreas Plückthun for giving me the opportunity to conduct my PhD project under his supervision, and for his support throughout the project. I am thankful to Profs. Raimund Dutzler, Donald Hilvert and Wolfram Welte for accepting to be a member of my thesis committee, and for their feedback and support.

My great thanks go to my colleagues that were directly involved in the project, namely Annemarie Honegger for the detailed analysis of the 454-sequencing data and further Matthias Hillenbrand, Alexander Rittner and Madeleine Künz for their contribution to the signaling state of the evolved receptor variants. I would also like to acknowledge Dasa Lipovsek from Codon Devices and Ralf Strohner from Sloning Biotechnology for the fruitful collaboration on library generation. Further, I am thankful to Malgorzata Kisielow and Anette Schütz for their expert technical support with FACS sorting.

To all former and present members of the Plückthun group, I want to say thank you for your support throughout all stages of the project, for your motivation, for interesting discussions and suggestions, for a helping hand and very importantly, for creating a stimulating work atmosphere, especially Mark Schmitz, Marc-Simon Schwer, Jakob Stüber, Igor Dodevski, Christian Jost, Johannes Schilling, Anja Mohr, Ykelien Boersma.

For their valuable support in all administrative and IT-issues I would like to thank Peter Lindner, Petra Vogt and Steve Rast, representative for the IT-team.

A very special thank you goes to my dear friends, for listening, for their understanding and motivation during the last years, especially Nicole Grosse and Sonja Tattermusch – your support was indispensable.

I am very grateful to S. Bischoff, C. Borer and Melanie Seite, for their valuable help, which I appreciated very much, and which enabled me to literally stand through the last years.

To my family, my parents and siblings, for your sympathy, for your continuous support, especially in hard times, for being there, and for your believe in me, and that all will be fine – herzlichsten Dank!